MEFYQUE

Forest and timber quality in Europe

Modelling and forecasting yield and quality in Europe

FINAL REPORT
Main Document

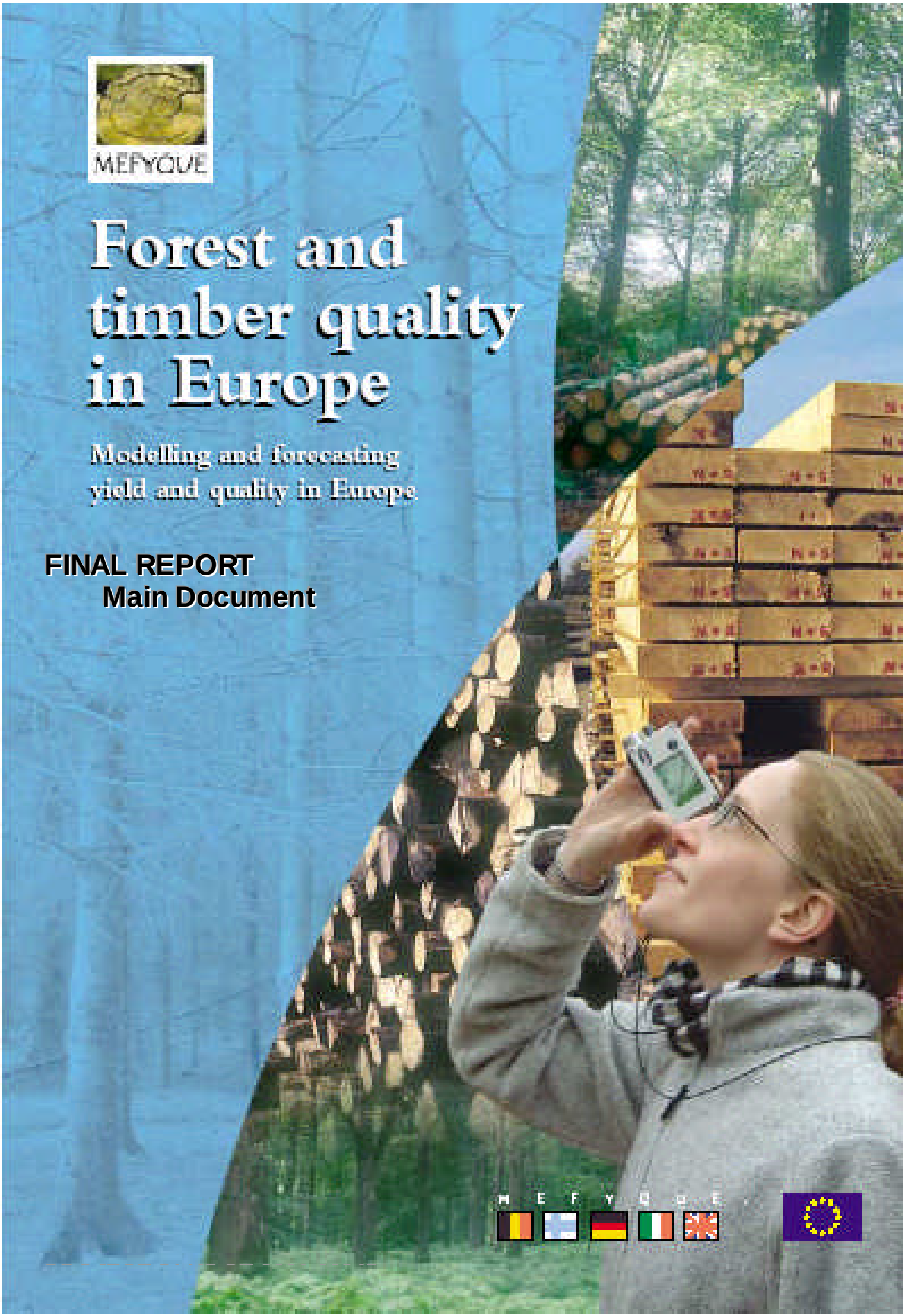

Forest and timber quality in Europe: modelling and forecasting yield and quality in Europe

Final Report

Main Contributors (alphabetical):
Bascietto M., Calfapietra C., Ceulemans R., Chase T., Craig I., Curiel-Yuste J., DeCinti B., Deckmyn, G., De Boever L., Eggers T., Evans S., Henshall P., Houston T., Matteucci G., Maun K., Meyer J., Lindner M., Liski J, Overdieck D, Randle T., Scarascia-Mugnozza G., Van Acker J, Vansteenkiste D, Ziche D., Zudin, S.

Edited: T. Randle

Biometrics, Surveys and Statistics Division, Forest Research, Alice Holt Lodge, Farnham, Surrey, UK GU10 4LH
email: Tim.Randle@forestry.gsi.gov.uk

Mefyque Final Report Main Table of Contents

Co-ordinator's Overview

Sam Evans

Biometrics, Surveys and Statistics Division, Forest Research, Alice Holt Lodge, Farnham, Surrey, UK GU10 4LH
email: Sam.Evans@forestry.gsi.gov.uk

The principal deliverable of this project is:

A prototype integrated modelling system that will assist forest managers, the timber industry and policy makers to decide whether management of forests should be primarily for production, conservation of amenity outputs, within the context of multipurpose forest management.

In presenting this final report, I am highlighting a number of considerations that have shaped the final outcomes achieved by the programme of research.

This project is characterised by:

1. Its breadth of disciplines.
2. Single focus on developing a unified approach cross-cutting traditional discipline boundaries.
3. The requirement to develop of common understanding between individuals working in traditionally distant disciplines, and ultimately;
4. The complexity of the research objectives proposed, sometimes in the absence of prior background or foreground knowledge in critical areas.

As stated from the outset by both the consortium team and the moderating panels, this was an ambitious project. It is so given the theoretical and practical complexities involved in demonstrating concept proof of:

(a) Harmonised data collection of complex biological, biochemical and technological data.

(b) Developing a complex knowledge-based model of the forestry woodchain, underpinning;

(c) Demonstration through simulation, the potential effects on the forestry woodchain of current and future climate conditions.

For the project to have been successful in its entirety, it required all project components to effectively integrate over time and through the new and shared knowledge base. This as proved largely successful: yet where unforeseen difficulties have arisen, and accounting for complexities in the different working parts, their relative impacts have proved of some significant.

The project has largely achieved its stated aims of:

- Collecting new fundamental data through a unified sampling approach, in so doing ensuring harmonisation across the range of information collected. These data will continue to be of significant value beyond the immediate needs of this project, and will become available to a wide research and industrial communities.

- Demonstrating the feasibility of bringing together a large and diverse research team, in so doing developing a unifying conceptual paradigm that has successfully approached a complex research task at the science-policy-industrial interface.

- Developing nested mechanistic and data-driven models of the forestry woodchain, the interactions between the quality and quantity of the timber supply and the potential capacity of the timber industry to process forest outturn of variable quality.

- Of greatest overall significance, demonstrating the feasibility of the theoretical approach, in so doing indicating the future possibility for further developing unified, predictive systems describing the forestry woodchain. The prototype system of the complete forestry woodchain, that constitutes the major, but by no means sole project outcome, indicates that it is tractable to account, through modelling, for variable quality in wood source material. It also highlights the potential for demonstrating its impact on the capacity for a representation of the industrial base to process it, while accounting for future interactions with environmental and climate changes.

- Transferring the new knowledge base to the wider communities through a variety of knowledge transfer approaches.

As with every major research project of an international nature, it has not been without its own difficulties. The delay in submitting the final report can be justified primarily by the complexities involved in:

1. Developing a common lexicon among a disparate and geographically diverse multidisciplinary project team.
2. Providing a context for new knowledge derived from the diverse experimental and monitoring components of the project, into the broader base of understanding. Of particular note has been the collection of extensive harmonised fundamental data on the interactions between climate change processed (e.g. enhanced CO_2) and its impacts on tree physiology, anatomy and biochemistry.
3. Developing a singularly large modelling framework of the forestry woodchain, with development undertaken across a number of sites, incorporating the larger part of the emerging and current mechanistic knowledge base.
4. Coupling new understanding with the existing knowledge base, and then expressing this in the modelling framework.

The project has clearly shaped the research directions of a number of project participants, and through research publications has, and will continue to inform the broader communities engaged in this arena of investigation.

In conclusion, primacy of outcomes rests in demonstrating the feasibility of coupling existing and new basic and applied knowledge, held by a range of disciplines, to improve current understanding of an issue central to the long-term, sustainable viability of the forestry sector and wood industry in Europe. This issue is wood and timber quality in standing trees, and its potential effects on the wood processing industry, and its long-term viability when faced with the challenges posed by environmental and climate change, alongside those economic and social strands that together form multipurpose forestry.

1 Mefyque Introduction

Main Contributors:
Joris Van Acker, Tim Randle

1.1 Forestry – wood industry in Europe: opportunities and constraints

Joris Van Acker

Far more than generally perceived the forestry – wood industry chain is nowadays based on the changing societal and economical elements in Europe. Increased knowledge on this is required to be able to define options and to stimulate discussion on issues related to forestry and the wood industry. A wood processing strategy should be based on opportunities and constraints in order to match the goals and requirements of long-term forestry with the initiatives from the forest products industry.

Geographically the forestry – wood industry chain is not uniform over the European continent. Major tree species differ based on the natural forest types established since the last glacial period. From these differences, *e.g.* between coniferous and broadleaved species, an adapted processing industry has evolved. Additionally the wood industry has been influenced by the evolution in wood processing technology used.

1.1.1 Total usage wood industry

There is clearly a shift towards wood processing with lower requirements for to specific species or tree quality. Increased importance of the pulp and paper sector in the overall picture includes considering strategies of full forest utilisation for one product type. Biomass for energy clearly evolves from the usage of wood residues and recovered wood towards direct impact on forest management. As such this use for energy will induce competition for resources by the pulp and paper sector as well as the wood based panel sector. Production methods for wood based panels like chipboard and to a certain extent also MDF and OSB, are nowadays lower in specificity than a few decades ago. This evolution is clearly also influenced by renewed interest in bio-energy (new biomass-based electricity plants in Germany) and new developments like the production of wood plastic composites (products now showing important market potential in North America). The wood industry is becoming increasingly independent from the local forestry species and is now mainly located where consumption is high. The impact of material recovering and recycling activities on the geographical distribution of biomass based electricity plants, chipboard plants and paper mills focussed on recycled fibre is relevant in this respect.

1.1.2 Changing forests

New forest strategy approaches lead to the higher usage of local tree species and more mixed stands. Increasingly, important forest areas are dedicated to landscape development, nature reserves and protected species. The increased emphasis on hardwood species creates extra opportunities but will inevitably also require more skills and management to obtain sufficient tree quality for the production of suitable sawn wood (defect free for many applications) and veneer production. Higher costs of both investments and salaries may not be compatible with the need for additional selective thinning, pruning and forest friendly exploitation techniques. Increasingly mixed forests combined with low level of tree quality management could limit the usage to solely primary conversion based on chipping. This strategy is suitable for some parts of the wood industry but could decrease the potential of future forestry in Europe.

The current forest distribution in Europe is ranging from the Nordic countries with extended forest areas up to scarcely forested areas in western Europe, e.g. England, the Netherlands, Flanders and some Mediterranean regions like central Spain and Greece (Figure 1.1).

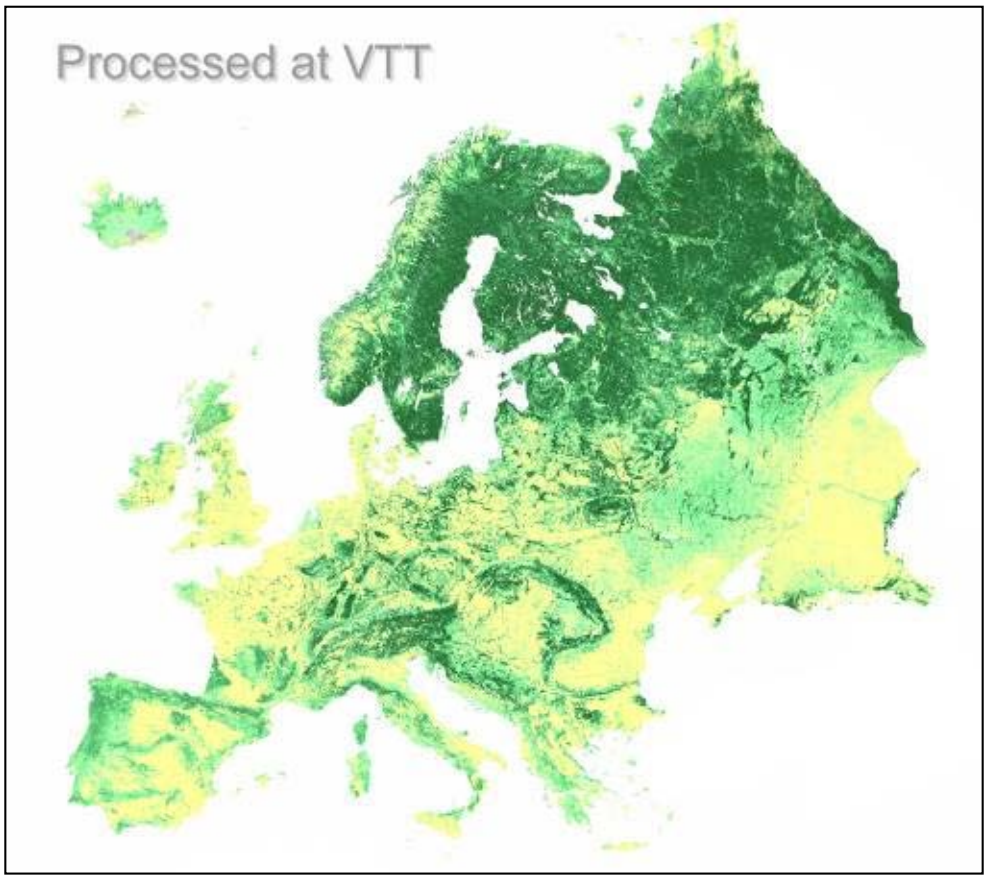

Figure 1.1: Distribution of forests in Europe**.**

The forest is inevitably also different depending on the tree species and growth conditions specific to certain regions in Europe. As can be seen from Figure 1.2 the main forest types are: boreal forest, cool temperate forest and Mediterranean forest.

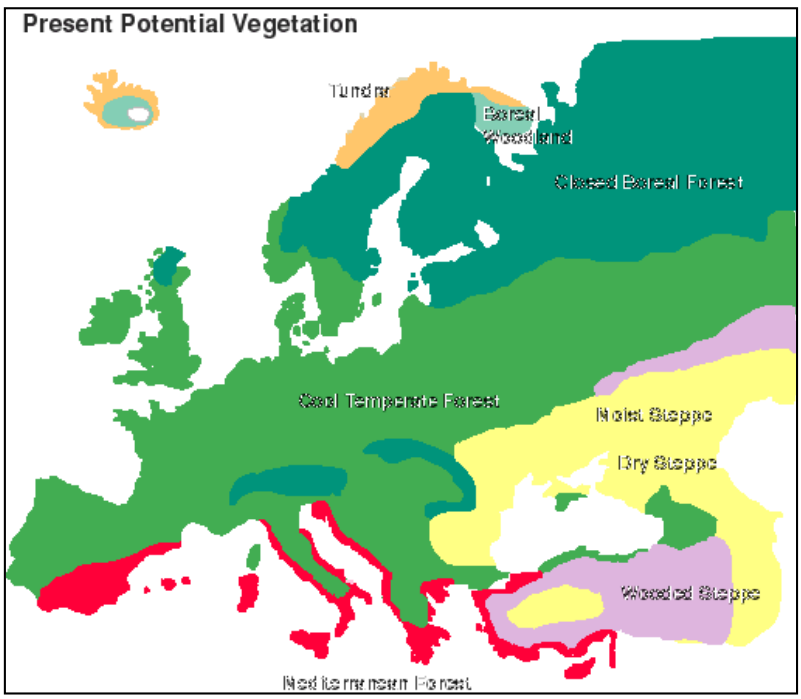

Figure 1.2: Main forest types as typical potential vegetation.

Often vision for future forest is based on the concerns to re-establish zonal vegetation as was considered present after the last glacial period. Such approach leads to mixed wood species distributions in forests that are different from the ones currently present in some areas (Figure 1.3).

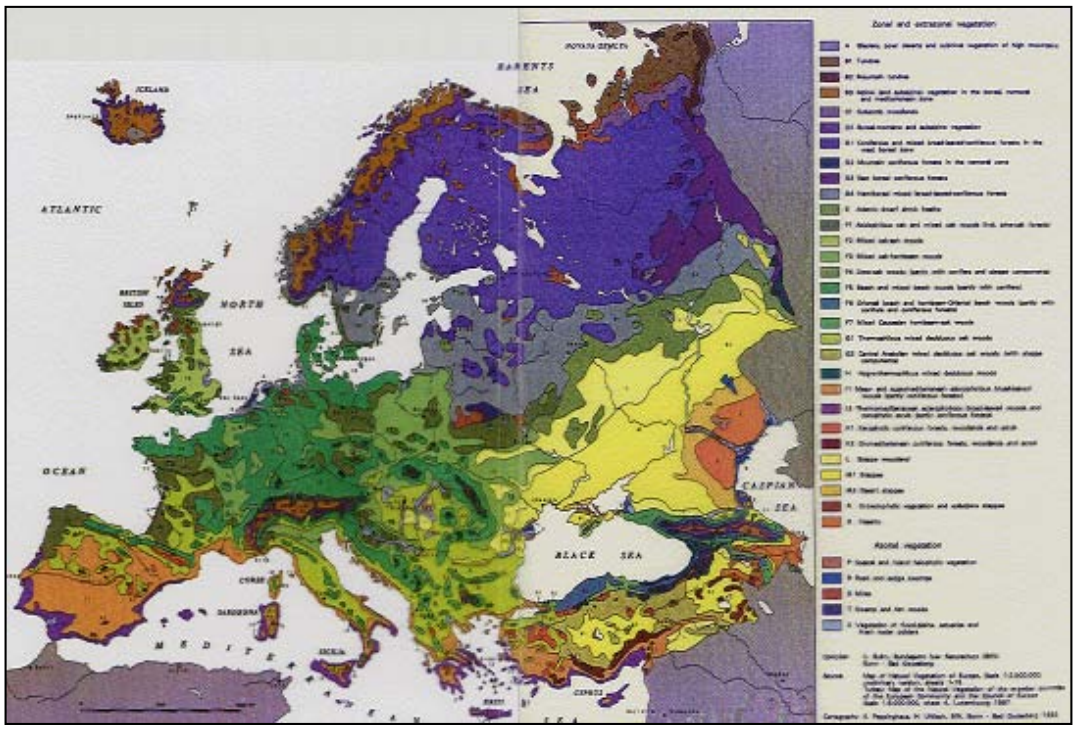

Figure 1.3: Vegetation as considered present after the last glacial period.

1.1.3 Local industry linked to forest types

Contrary to the primary wood conversion processes mentioned in the previous paragraph which are based on chipping of particles, the milling for solid timber and peeling or slicing for veneers is directly linked to the forest types present. In general, sawn wood products for construction are based on softwoods while many furniture, exterior joinery and decking applications involve the use of local or imported hardwood species from temperate and tropical forests. Higher quality requirements not only relate to specific wood species but also focus on quality trees coming from fully developed 'climax' forests. The primary wood conversion process can be simple, *e.g.* for utility poles, posts, railway sleepers or require low overall quality, *e.g.* for packaging or fencing products, but can however also involve a very selective grading of trees and logs for *e.g.* veneer based products. Rotary cut veneer for plywood and sliced decorative veneer have always created extra opportunities for quality based management of specific tree species or even of individual trees in local forests. Besides veneer production another typical example of a high quality application is the oak forestry – wood industry chain for the production of wine barrels in France using merrain quality.

Looking for regional forest complexes that clearly influence the forestry-wood industry chain 3 examples are given below. First the Sonian Forest near Brussels is a typical beech 'cathedral' forest where social functions are important besides ecological and economic functions. The beech trees are mostly containing large amounts of red heartwood and as such specific end uses for technical applications are envisaged. A second example is the 'Forêt des Landes de Gascognes' with approximately 1 million ha mainly consisting of maritime pine in Aquitane – France. This forest has links to a complete wood industry chain comprising pulp and paper,

sawmilling and plywood. A third example is the 'Forêt de Tronçais', a high quality Oak Forest in center of France where the link to the production of wine barrels is of major importance.

The fact that local industry can be linked to forests present is far more obvious when looking at the distribution of plywood plants than when considering the productions sites of MDF plants (Figure 1.4). Plywood mill are clearly linked to the presence of birch and spruce in Finland and eastern Baltic, poplar regions like the Po-valley and the pin maritime region in France. MDF plants are far more linked to the areas with higher population density and hence higher consumption of wood products like furniture and laminated flooring.

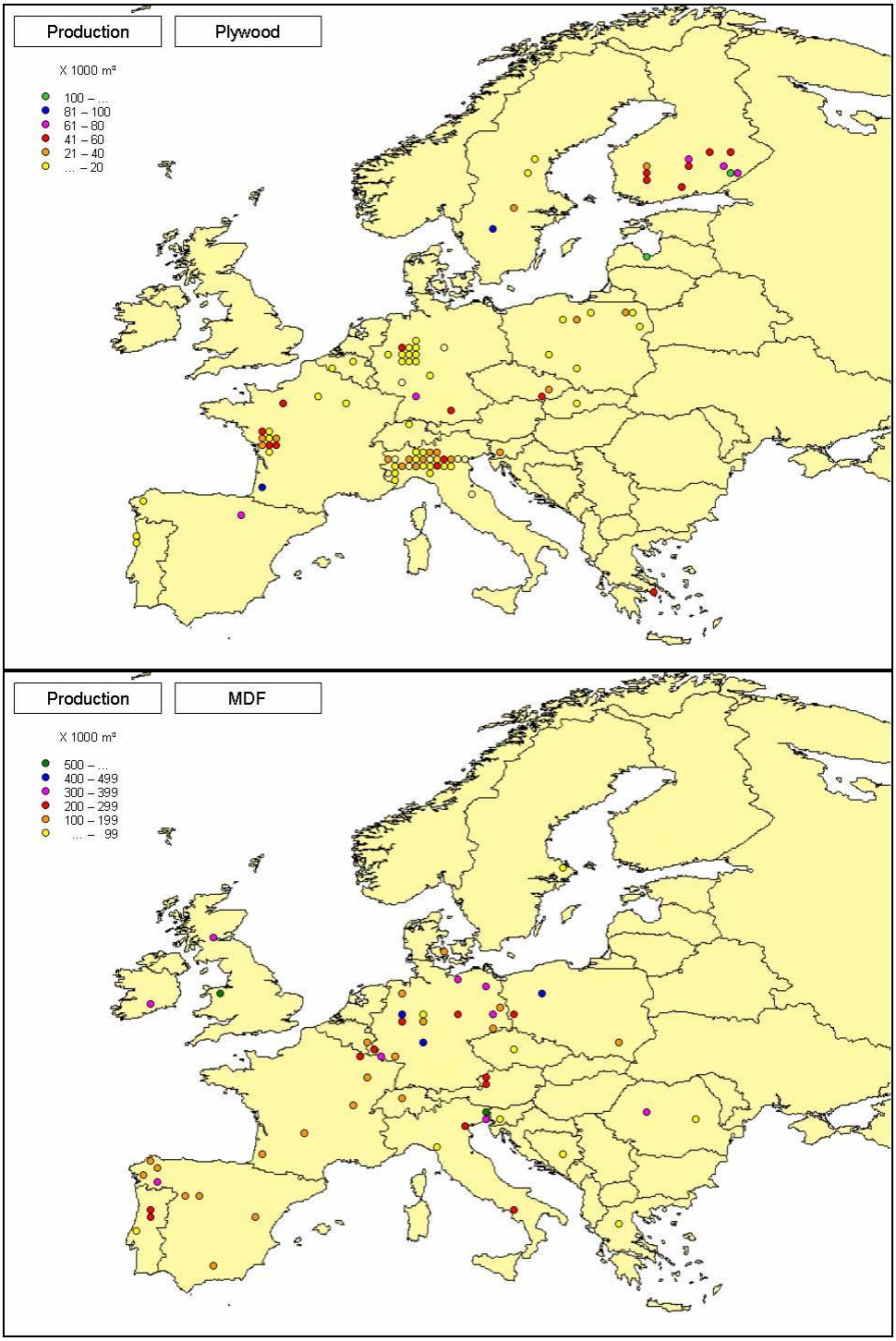

Figure 1.4: Production plants for plywood and MDF production at the beginning of the 21st century.

1.1.4 Alternative lignocellulosic materials

Wood production is no longer the prime objective in several European forests. However, the increased need for lignocelluclosic material for the production of pulp and paper, wood based panels and bio-energy is present. A wood processing strategy might require a closer look at raw material not only coming from 'natural' forests. In addition to sustainable forest management based on principles respecting ecosystem development, there is a possibility to lower the pressure in wood volume production by these forests by allocating this functionality to man-made forests and additional input from the agricultural sector. The basic idea to create a sustainable production of lignocelluclosic material can partly relate to plantation timber from poplar, eucalyptus and robinia (black locust) or highly volume based coniferous forest products *e.g.* based on Sitka spruce. From the agricultural sector sustainable production of miscanthus, willow coppice, wheat straw or even bamboo are potential options. Focus should not only be on *e.g.* energy crops, as recycling and recovering of all lignocelluclosic material also needs to be addressed.

In conclusion, it can be stated that forestry should work towards more quality trees in order to guarantee sustainability both based on a larger scale ecosystem linked approach as well as on the local societal and economical background. The conversion of wood by means of chipping into particles should continue to focus on the use of secondary forest products like thinnings or top end logs. However an increased support for the use of recovered and recycled products as well as promoting man-made forests (tree plantations), partly based on the potential of the agricultural sector, might contribute to the development of a sustainable forestry – wood industry chain in Europe.

1.2 Context of the Mefyque Project

Tim Randle

It is against this background that the Mefyque project explores the development of the forestry woodchain from growth to an end-use carbon budget. The project was divided into 5 major components:

- **The Monitoring Component** – designed to characterise the relationships between site conditions, growth, yield prediction and timber quality. Together with how these vary as a function of multi-purpose forest management practices. It combines field measurement of site conditions, forest growth and quality of standing timber. Where possible the sites build upon past and present monitoring or order to maximise information collected. Three categories of observation level site are identified.

  Primary – sites where extensive data can be collected, and destructive samples from the forests taken. Where possible building upon existing data e.g. Level II sites.

  Secondary – Located at existing monitoring sites, where data has, and is being collected as part of other EU projects (eg. POPFACE, flux sites).

  Tertiary – Located at or close to established centres, where manipulation of CO_2, temperature, irrigation and fertilisation may be possible.
- The Manipulative Component – at tertiary sites, uses growth chambers to produce plant material at various treatment levels. This plant material was analysed for differences in physical structure and biochemical content. These data were then used to formulate theories to further understanding climate change impacts and the development, parameterisation and validation of process-based models.
- The Laboratory Component - Uses laboratory techniques to assess the anatomy, biochemical composition, and mechanical properties of the wood and whether they vary as a result of growth conditions (climate and CO_2 concentration). Material examined is from; new plant material from the monitoring and manipulative experiments; existing material from previous experiments (eg FACE); and over-mature standing timber from both ambient and elevated CO_2 conditions.

- The Modelling Component – based on existing state of the art empirical and process models available within the project, developed new modules to create a new model. This is to produce: (i) a model capable of simulating some of the characteristics involved in determining wood quality in addition to mensurational values, and (ii) to produce an integrated model capable of following the forestry woodchain through growth, logging, saw-milling and final utilisation.
- The Database – The database, developed to hold the data collected within the project, designed in such a way as to allow both raw and metadata to be easily accessed, and is broadly based around three levels of information; site, tree and sub-tree.
- Technical Transfer –The dissemination and sharing of results, developments, data and information amongst the partners, other European scientific groups and the world-wide scientific community. This takes the form of presentations, scientific papers models, databases etc.

The Technical Annex for the project (Appendix K) refers to these aspects in greater detail.

2 The Monitoring Component

Main Contributors:
Bruno DeCinti, Tim Randle, Tracy Houston, Dieter Overdieck

2.1 Introduction

The **MONITORING COMPONENT** is designed to characterise the relationships between site conditions, growth, yield prediction and timber quality and how this varies as a function of multi-purpose forest management practices. It combines field measurements of site conditions, forest growth, and of quality for standing timber, together with an assessment of forest product usage.

2.2 Primary, secondary and tertiary sites.

A total of 17 primary, 4 secondary and three tertiary sites have been established. Comprehensive data have been collected for non-destructive and destructive assessment of growth and quality.

Some pictures of the sites are provided below (Figure 2.1 and Figure 2.2):

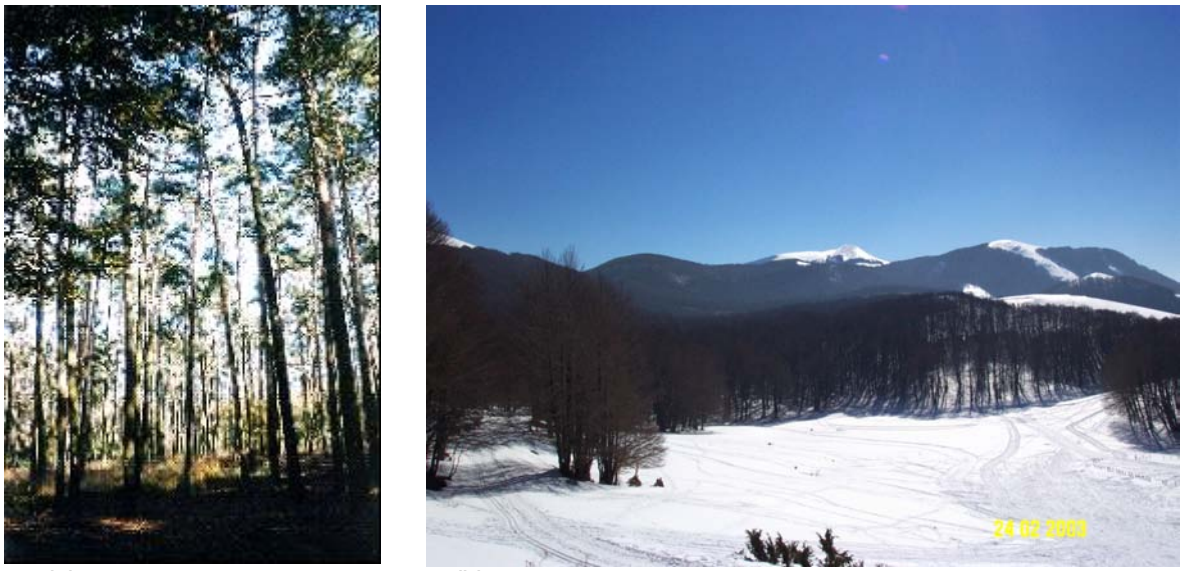

(a) (b)

Figure 2.1: (a) the Brasschaat site (Belgium), and (b) Collelongo (Italy) primary-secondary site

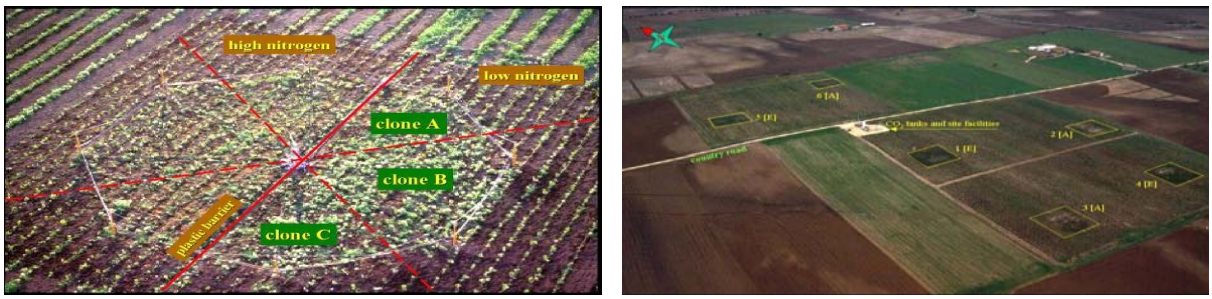

Figure 2.2: Tertiary site Tuscania (italy)

A detailed description of each site has been provided including: altitude, slope, surface form (e.g. convex or concave) and topographical features within the plot such as streams (Figure 2.3), gullies, rock outcrops *etc.*

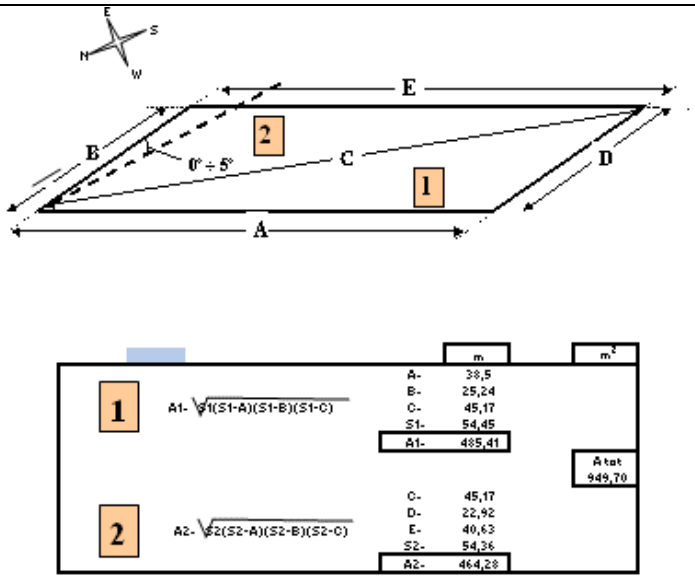

Figure 2.3: Example of plot surface description (Collelongo, Italy)

Climatic data like mean annual rainfall, maximum and minimum temperatures, meteorological station or other source from which records was obtained, period to which they refer, *etc* have been also provided (Figure 2.4).

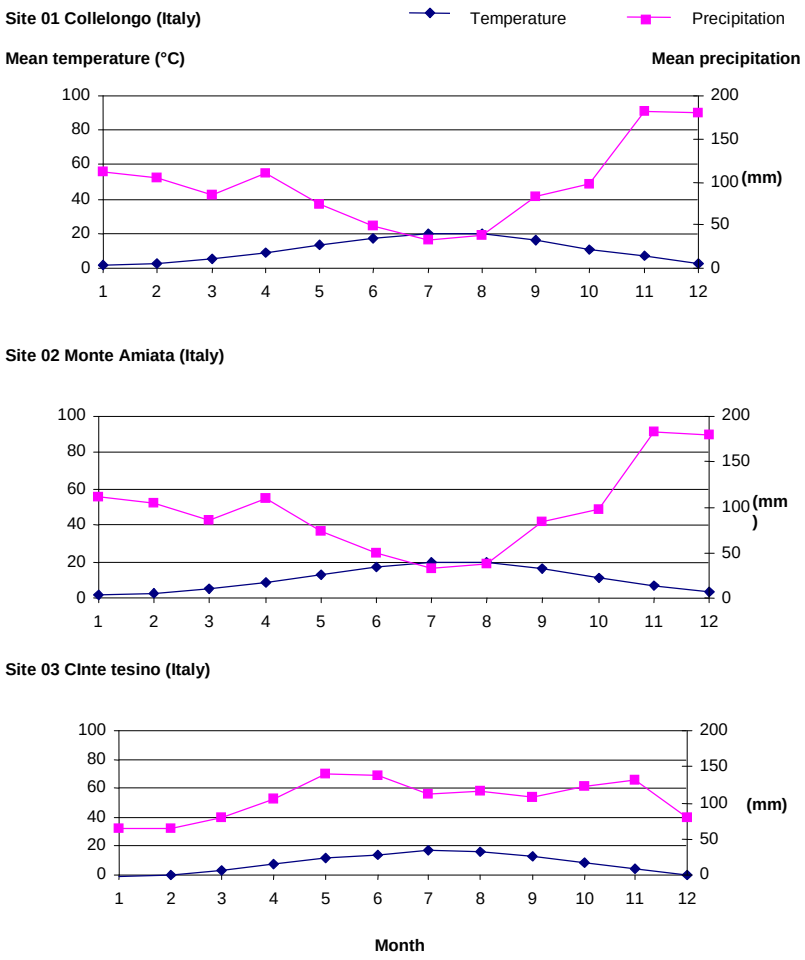

Figure 2.4: Summary climatic data

2.2.1 Sampling levels

Three sampling levels have been carried out in the sites and for each level has been used a different selection criteria.

At the 1st sampling level the operations have been carried out on all the trees of the plot, the 2nd one on 10 standing trees at existing Pan-European Monitoring Programme sites and 30 standing trees at new sites. The 3rd one is divided into above and below ground sampling and is carried out on a number of nine trees (3 trees per dominance class) that have been felled for more accurate measurement.

At a number of sites the trees selected for the 3rd sampling level have been transferred to a mill for 3-D scanning and subsequent milling.

At the 1st sampling level the following measurements were carried out: diameter at breast height; classification into quality and dominance classes (in accordance with the MEFYQUE in sampling protocol, appendix E) of all the stand trees; top height evaluation and stem lean measurement (Figure 2.5, Figure 2.6); number of dead trees.

Figure 2.5: Measurement of stem lean**.**

Figure 2.6: Measurement of height. All heights measured using a hyposmeter or clinometer (eg Vertex, Blume, Leiss, Sunnto)

At the 2nd sampling level were measured:

- total height (
- Figure 2.6)
- timber height;
- stem taper;
- lower crown;
- upper crown;
- crown diameter;

Where the harvest was not allowed the trees were climbed to take the

measurements requested (Figure 2.5)

Figure 2.7: Taper and timber height measurement by Tree climbing.

At the 3rd sampling level destructive and non destructive sampling have been carried out.
In the non-destructive sampling procedure, for each individual has been measured:

- height of 1st live branch/whorl
- height of 1st dead branch
- bark thickness

In the destructive sampling procedure the following operations were carried out:

- total canopy biomass and length measurement
- fine coarse root biomass estimation
- Discs collection
- Logs collection

Some of the felled trees were shipped to the UK for 3-dimensional laser scanning.

Figure 2.8: N-S orientation on logs

Figure 2.9: Colour marking of logs prior to scanning

Figure 2.10: Example of three-dimensional scanning of logs at a sawmill

Figure 2.11: Root sampling; cores, stumps and extractions

In the secondary sites eddy-covariance measurements are routinely performed: fluxes of water, carbon and energy exchanges above the forest canopy in real time, and metereological data at sub-hourly intervals (Figure 2.12).

A comprehensive suite of physiological parameters is available for all sites, whilst individual studies of hydrological and carbon balance are available at most of them. These data have been collated into the project database and used to inform and validate the process level sub-models (photosynthesis, respiration and transpiration) of the integrated modelling system.

Figure 2.12: Meteorological monitoring in Grunewald forest (Germany)

Due to the delay in the project start date, some sites originally proposed for use in this project (see Technical Annex) were no longer available for research purposes. Abandoned sites have been replaced with new sites and key changes to the monitoring network are described below.

At the majority of sites monitoring is also carried as prescribed in the relevant technical manual of the EC/ICP Pan-European Monitoring Programme On Forest Ecosystems (Level II sites). Authority has been granted for data from Level II sites to be made available to MEFYQUE by the EC data holding centre (FIMCI, Herenveen, The Netherlands) and data are currently being requested for inclusion in the project database.

The tertiary sites

The tertiary sites include experimental plots provided with open top chambers (OTC) or Free Air CO_2 Enrichment (FACE) equipment.

The FACE infrastructure is installed on short rotation plantations of various poplar species, that were grown for the second year after coppicing, during summer and fall 2003, that is the reporting period. The main experimental objectives of this period concerned (i) the continuous updating of the CO_2 fumigation plant to keep the pace of the growing trees, (ii) the correct functioning of the plantation infrastructure (irrigation, differential fertilization), (iii) the measurement of carbon uptake; (iv) monitoring of tree growth and stand dynamics; (v) investigations on water relations; (vi) assessment of energy balance, respiration and organic matter decomposition; (vii) investigation on below-ground processes; (viii) wood quality evaluation.

2.3 Data collection at MEFYQUE sites and example results

The main results achieved for the monitoring component at primary and secondary sites are provided in tables 2.1 to table 2.3 below. These tables summarise the key characteristics of the MEFYQUE project sites where monitoring plots have been established.

Table 2.1: Primary Site details.

Level II #r	MEFYQUE Site #	Site location	Country	Plot area (m^2)	Forest area (ha)	Elevation (m)	Mean precipitation (mm)	Soil characteristics	MEFYQUE plot established and measured	Co-located with Secondary site
06-512	1	Straits Enclosure	UK	2916	70	80	780	Pelo-stagnogley	ü	ü
06-919	2	Coalburn	UK	2988		300	1200	Cambic stagnohumic gley	ü	
06-920	3	Tummel	UK	3051		400	1500	Ferric podzol	ü	
06-717	4	Rannoch	UK	3052		470	1500	Humo-ferric gley podzol	ü	
06-517	5	Grizedale	UK	2954		115	1800	Brown podzol	ü	
06-715	6	Thetford	UK	3030		20	600	Calcareous sand	ü	
not Level II	7a	Clunes	UK	991		76	1780	Brown soil		
not Level II	7b	Clunes	UK	996		76	1780	Surface water gley		
not Level II	7c	Clunes	UK	1085		76	1780	Brown soil		
not Level II	7d	Clunes	UK	1012		76	1780	Brown soil		
not Level II	8a	Sawley	UK	973		225	1000	Brown soil	ü	
not Level II	8b	Sawley	UK	1041		225	1000	Podzol	ü	
not Level II	8c	Sawley	UK	1131		225	1000	Brown soil	ü	
06-716	9	Hope (Sherwood)	UK	3081		265	960	Podzol (sandy)	ü	
02-015	10	Brasschaat	Belgium		150		750		ü	ü
1101	11	Grünewald	Germany	1600				Ferric cambisol	ü	
1102	12	Grünewald	Germany						ü	
	13	Grünewald	Germany						ü	
	14	Collelongo	Italy	950	3000	1500	1148	Calcareous brown soil	ü	ü
	15	Monte Amiata	Italy	1130	7500	1250	800	Vulcaniti-soil	ü	
	16	Pieve Tesino	Italy	1261	10000	800	1258	Brown soil generated on limestone cliffs	ü	
	17	Renon	Italy	1055	15000	1700	1300	Haplic podsol	ü	ü

Table 2.2: Tree details at Primary Sites.

Level II #	Site location	Planting y. (average)	Dominant species	Other tree species	Understorey species and ground vegetation	Date of last Measurement /	trees/ha	Mean height (m)	Dominant DBH (cm)	Mean DBH (cm)
06-512	Straits Enclosure	1935	OK	*Fraxinus excelsior*	*Corylus avellana, Cratagus monogyna, rubus spp*	Mar-2001	495	19.9	29	24.5
06-919	Coalburn	1974	SS		Mosses, Lichens	Mar-2000	1850	14.5	32.6	20.7
06-920	Tummel	1969	SS		None	Nov-1999	2082	15.2	31.2	19.3
06-717	Rannoch	1965	SP		Grasses, Mosses	Nov-1999	2270	10.4	21.4	14.4
06-517	Grizedale	1920	OK		Grasses, Bilberry, Bracken, Mosses	Feb-2000	230	17.4	43.7	34.9
06-715	Thetford	1967	SP		Grasses, Bracken, Mosses, Nettles	Mar-2000	978	14.9	28.5	20.4
	Clunes	1935	NS			Feb-1996	1463	25	41.4	26.5
	Clunes	1935	NS			Feb-1996	1145	26.2	44.2	30.4
	Clunes	1935	NS			Feb-1996	1143	25.6	45.7	30.5
	Clunes	1935	NS			Feb-1996	1146	23.6	43.4	29.4
	Sawley	1943	SS		*Deschampsia*, Mosses, Ferns	Apr-2002	154	30.8	65.1	59.8
	Sawley	1943	SS		None	Apr-2002	893	26.7	43.5	30.7
	Sawley	1943	SS		*Rhododendron ponticum, Prunus serotina, Molinia caerulea*	Apr-2002	239	29.5	52.6	46.8
06-716	Hope (Sherwood)	1952	SP	*Fagus sylvatica, Quercus petreae*	*Prunus serotina, Sorbus aucuparia*	Feb-2000	1125	16.4	29.3	21.9
02-015	Brasschaat	1929	SP/OK/BE			2001		23		
1101	Grünewald	1900	SP/OK/BE			2001				
1102	Grünewald	post-1945	ESF/SP			2001				
	Grünewald	post-1945	ESF			2001				

Level II #	Site location	Planting y. (average)	Dominant species	Other tree species	Understorey species and ground vegetation	Date of last assessment	trees/ha	Mean height (m)	Dominant DBH (cm)	Mean DBH (cm)
	Collelongo	Natural forest	BE	*Acer pseudoplatanus Acer platanoides Taxus baccata Sorbus aucuparia Sorbus aria Laburnum anagyroides*	*Stellaria nemorum*, *Galium odoratum* , *Cardamine bulbifera*, *Cardamine enneaphyllos*, *Cardamine chelidonia*, *Anemone apenina*, *Anemone nemorosa Corydalis cava*	May-03	640		27	26.2
	Monte Amiata	Natural forest	BE	*Fraxinus excelsior Acer pseudoplatanusOstrya carpinifolia., Carpinus betulus*	*Geraneum reflexum, Epipactis parviflora, Gallium aparine Epilobium montanum*, *Calamintha grandiflora*	Oct-02	610		32.7	31.15
	CinteTesino	Natural forest	NS/ESF	*Fagus sylvatica, Larix decidua*	*Vaccinium myrtillus Fragaria vesca, Melampaum sylvaticum, Homogyne alpina, Hieracium sylvaticum*	Lug-2003	540			25.9
	Renon	Natural forest	NS	*Pinus cembra, Larix decidua*	*Rhododendron ferrugineum Vaccinium vitis-idaea Vaccinium myrtillus Arnica montana Melampyrum sylvaticum Oxalis acetosella*	oct-2003	710	24.8		

Species key: OK: Oak
SS: Sitka spruce
SP: Scots pine
NS: Norway spruce
BE: Beech
ESF: European silver fir

Dominant and mean DBH are quadratic means:

$$\sqrt{\frac{\left(\sum x^2\right)}{n}}$$

Table 2.3: Secondary Site details

MEFYQUE Site n°	**1**	**10**	**14**	**17**
Site location	Straits	Brasschaat	Collelongo	Renon
Country	UK (south)	Belgium (north)	Italy (central)	Italy (north)
Elevation		16 m	1500 m	
Mean temp.	10.6 °C	10.0 °C	6.2 °C	
Mean precipitation	780 mm	750 mm	1100 m	
Forest area	70 ha	150 ha		
Stand age	72 yrs	73 yrs	100 yrs	Unevenaged
Dominant species	Oak (*Quercus robur*) + ash (*Fraxinus excelsior*)	Scots pine (*Pinus sylvestris*)	Beech (*Fagus sylvatica)*	
Other species	Hazel (*Corylus avellana*), hawthorn (*Crataegus monogyna*) & *Rubus spp*	Oak (*Quercus robur*); beech (*Fagus sylvatica*); *Rhododendron spp*, *Prunus serotina*		
Tree height	19.3 m (1995)	23 m (2001)	25 m	
Soil characteristics	Pelo-stagnogley; 80 cm deep, pH 4.7	Wet sandy soil to podsol; pH	Brown earth; 80 cm deep	
Meteorological data	Since 1955, and at the site since 1994	Since 1996		
Eddy flux data	Since 1999(?)	Since 1996	Since 1994 (?)	Since 2001 (?)
Other programmes	UN/ECE ICP Level I and Level II	UN/ECE ICP Level II EU CarboEuroflux project	UN/ECE ICP Level II	
Other information	Continuous pollution records (7.4 kg/ha N in 1997)	Continuous pollution records since 1996	GPP, NPP, NEP and other carbon budget terms	

Tree and stand characteristics are measured and wood material sampled, according to the project Sample Plot Protocol. A total of 17 project plots have been established. Data collection at the primary sites has been carried out. Data for these sites are included in the project database (chapter 8).

For illustrative purposes, and using the data collected at primary and secondary sites, some results of 1st and 2nd sampling level are provided in the figures below:

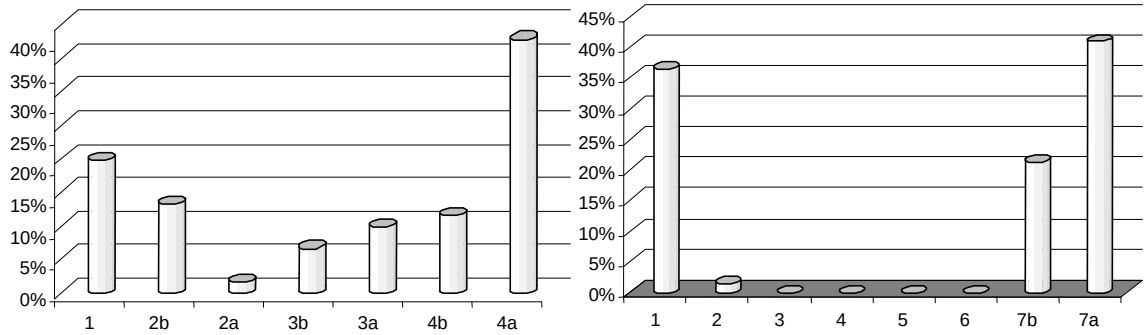

Figure 2.13: Frequency of each quality class in a softwood (Cinte Tesino site) and a hardwood (Monte Amiata) site.

Some other additional studies have been undertaken at primary sites. At the Grünewald site stem circumferences at breast height were continued in the older mixed pine-oak stand (1101, 120-year-old pines) and in the 50-year-old pine stand (1102).

Figure 2.14 below shows the development of the DBH of *Pinus sylvestris* on the plot 1102; the reduction of stem circumference in winter 2002/2003 is due to stem shrinking. In addition, samples were taken every two weeks with a special small corer to sample the last 4 tree rings at the 50-year-old pine-stand (1002). Samples were stored for further anatomical analyses.

At the same site, results from the measurements at the very beginning of the project were evaluated and compared with data from 1986 obtained in the same stands. Although 15 years are only a short moment in tree life span and in forest succession, some slight changes are visible. In the older stand growth limit of Scots pine is reached. Oak could only slightly expand its stand wood volume at the cost of its high mortality. It can be assumed that at this stand strong competitive power maintained equilibrium between the species. In the younger Scots pine stand that is still in its fast growing phase, oak could fill gaps and provide a gene resource for natural regeneration. Nevertheless, it was found that the portion of oak in the dominant layer is decreasing. We, therefore, postulate that in both stands pedunculate oak might become a dominant tree species after senescence of the pine layer only.

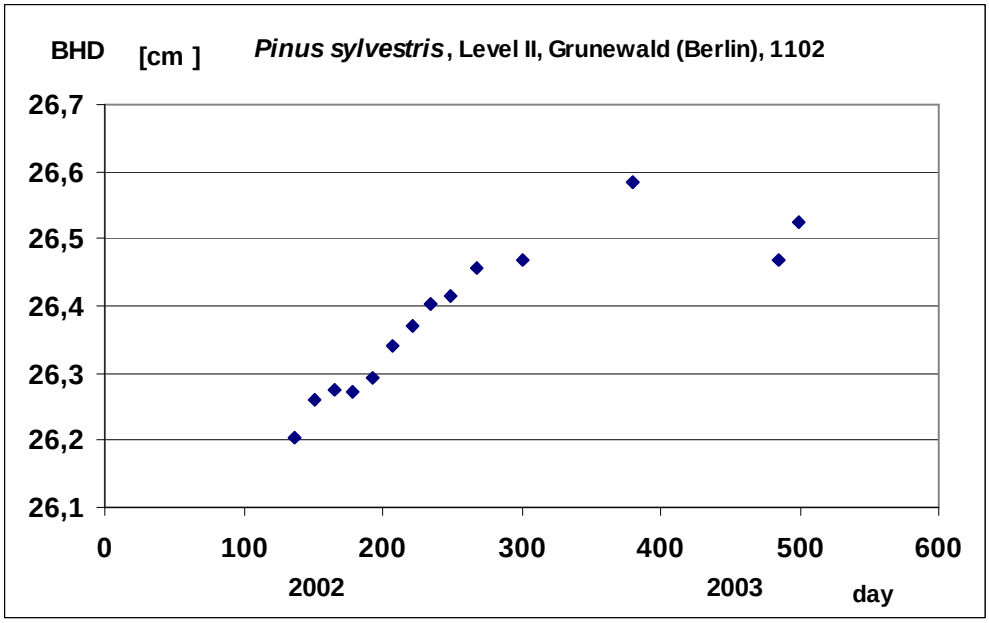

Figure 2.14: Monthly course of stem diameter at breast height at the primary site with ~50-year-old Scots pines during the previous and the current year in Grünewald forest, Berlin, Germany.

For the plots located in Grünewald forest, crown projections can be schematically represented in Figure 2.15 . Diameter class distribution is shown in Figure 2.16 while Figure 2.17 shows the increment of diameter at breast height for the period 1986-2000, and outlines the biomass increments per tree compartment for ICP/ECE plot 1102 over the same period (data supplied by ICP/ECE FIMCI Data Co-ordination Centre).

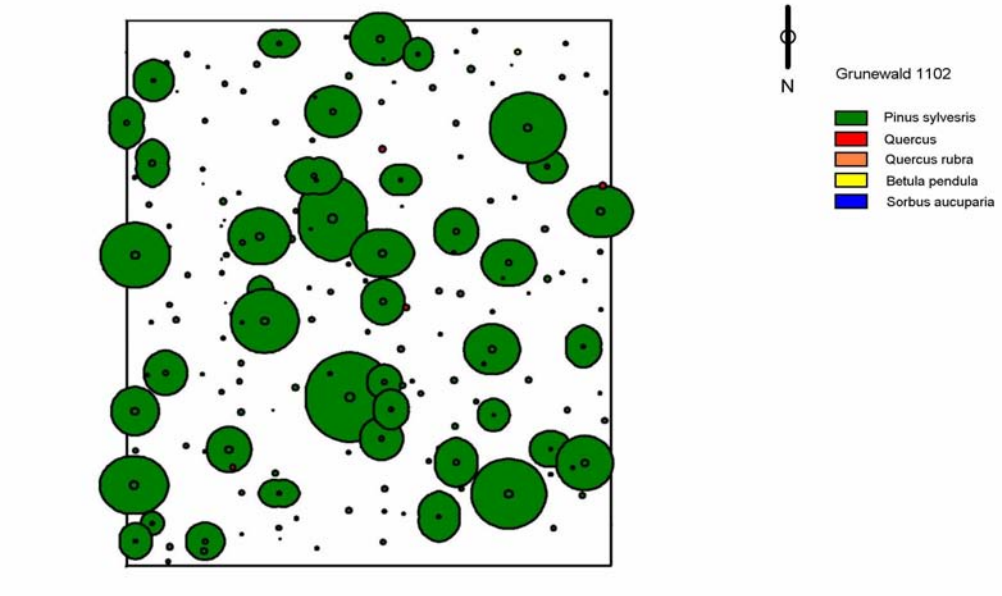

Figure 2.15: Crown cover at the MEFYQUE monitoring plots in the Grünewald forest.

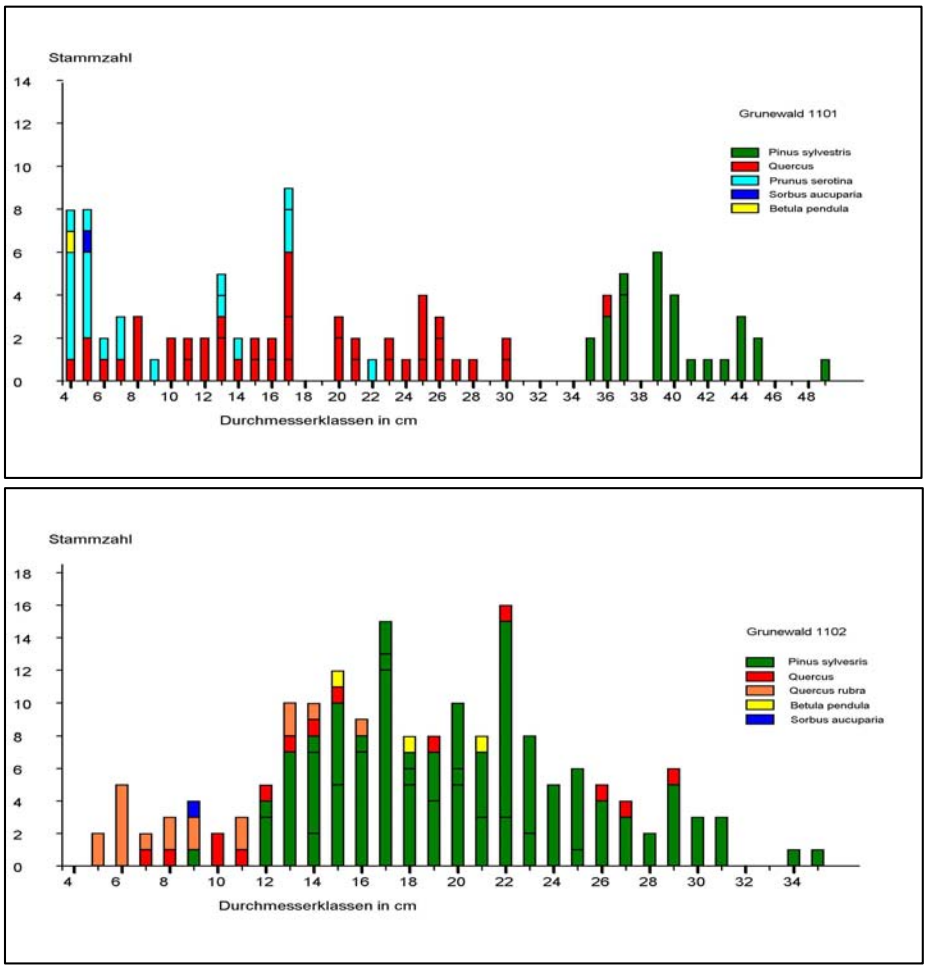

Figure 2.16: number of trees in each diameter class at the MEFYQUE monitoring plots in the Grünewald forest

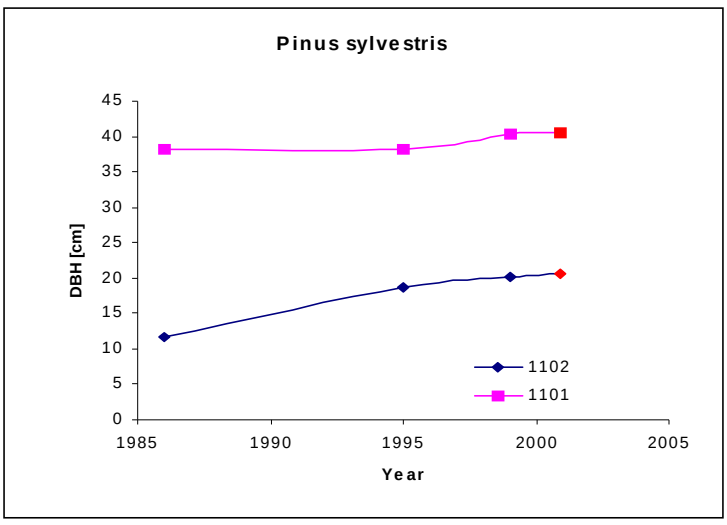

Figure 2.17: DBH increments at the MEFYQUE monitoring plots in the Grünewald forest in the period 1986-2000

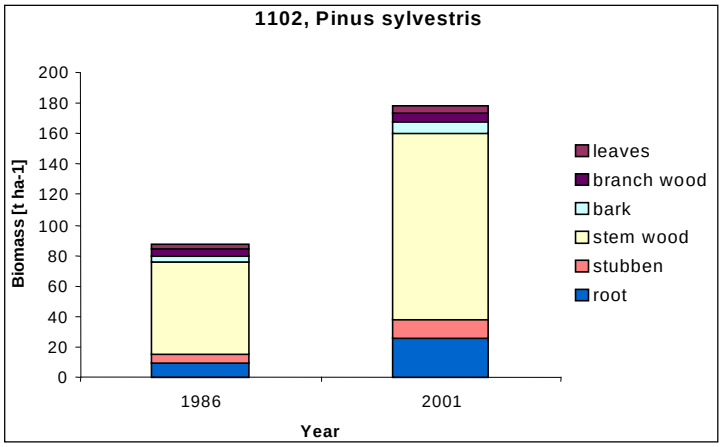

Figure 2.18: biomass increments in tree biomass compartments in Plot 1102 at the MEFYQUE monitoring plots in the Grünewald forest for 1986 and 2000.

By stem analysis (from the discs collected each 2.5 m on the stem) and wood density of the nine trees per plot harvested, standing biomass of past years and productivity have been estimated (Figure 2.19).

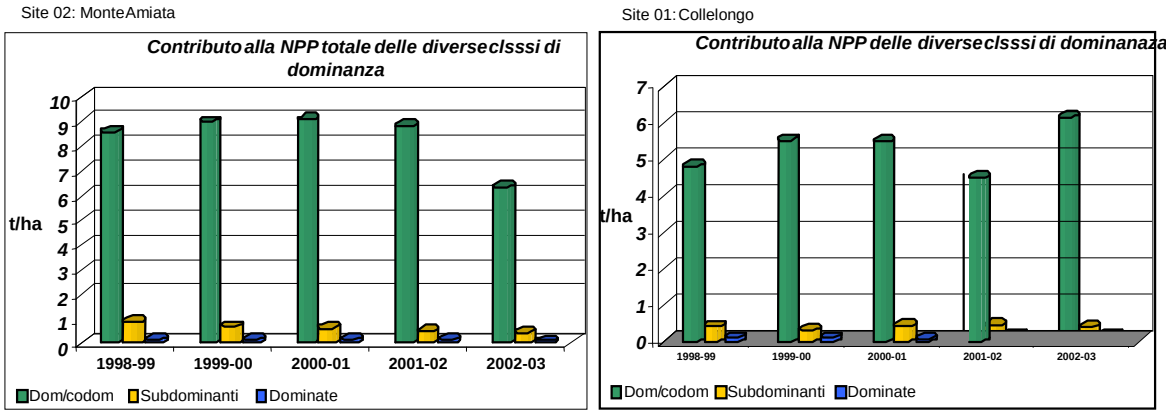

Figure 2.19: Contribution of each dominance class to determine the stand NPP

Other examples of data collection (roots) undertaken are illustrated in Figure 2.20 and Figure 2.21 below, outlining the data from one Italian primary site.

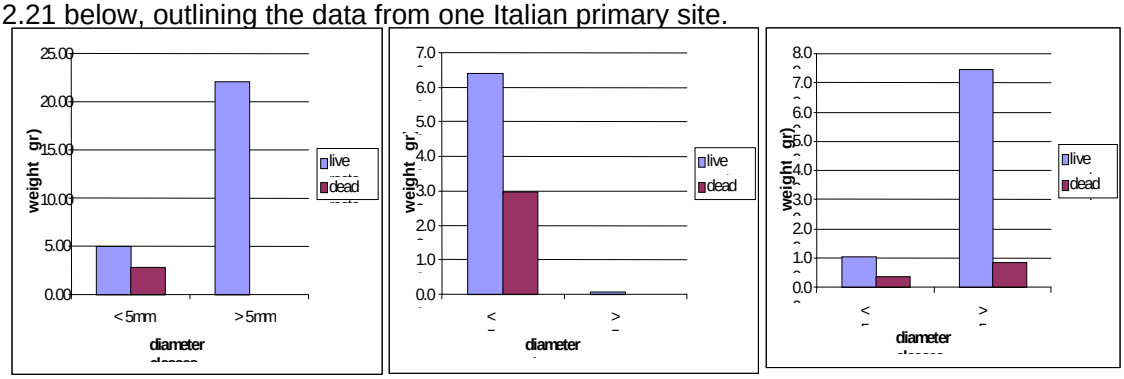

Figure 2.20: Root weight (g) per diameter class of three samples

Sample A1 (10 cm from tree) Sample A2 (50 cm from tree) Sample A3 (100 cm from tree)

Roots weight of sample A1:				Roots of sample A2:				Roots weight (g):			
Live roots		Dead roots		Live roots		Dead roots		Live roots		Dead roots	
<5mm	>5mm	<5mm	>5mm	<5mm	>5mm	<5mm	>5mm	<5mm	>5mm	<5mm	>5mm
5.00	21.97	2.83	0.00	6.40	0.07	2.97	0.00	1.06	7.44	0.37	0.88

Detailed evaluation of the log quality scores has been carried out at Italian sites, as an example, the Collelongo site study is shown in Figure 2.21 below.

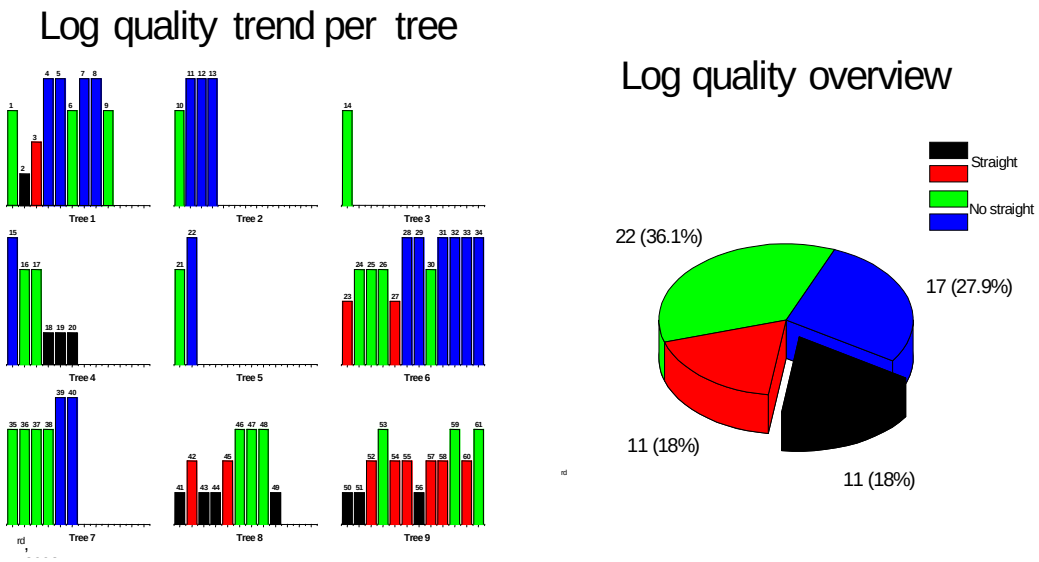

Figure 2.21: trend on log quality score and overview of log quality scores

Data collected in the tertiary sites gives important information about growth in simulated condition. The large stimulation observed of the volume index induced by the FACE treatment, progressively decreased during the second growing season (Figure 2.22) converging for all genotypes to a common value of approximately 20%. This was of course related to the larger values intrinsically causing smaller percentage differences. Nevertheless, absolute differences of D^2H between FACE and Control treatments considerably increased at the end of the second growing season as compared to the first growing season.

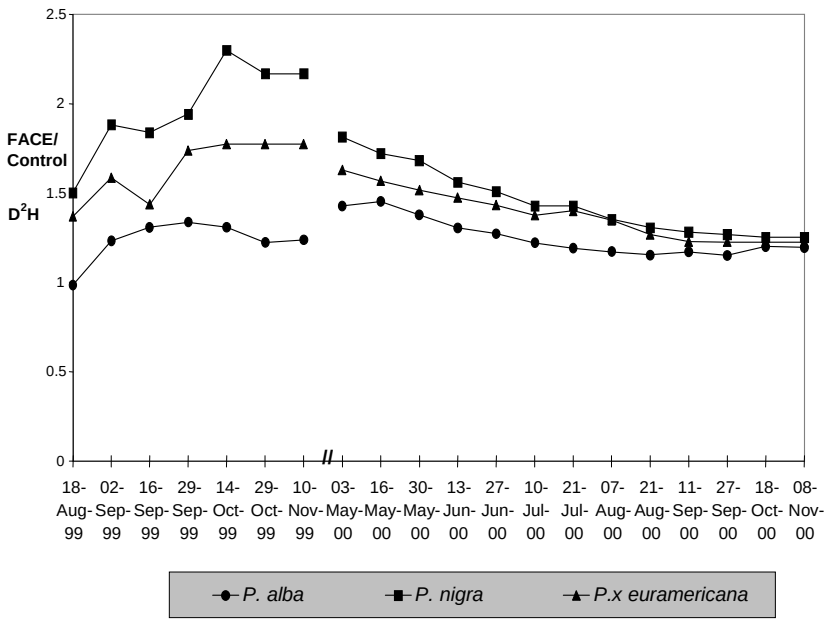

Figure 2.22: effect of the FACE treatment on stem volume index (D^2H) for three *Populus* genotypes ±SE grown for two growing seasons under FACE and Control treatments. Symbols represent the ratio between mean values in FACE and Control treatments

A strong treatment effect was observed at the end of the first growing season both on sylleptic branches BA and on total BA (Figure 2.23). This was significant for *P. nigra* ($p<0.001$) but not for *P. x euramericana* ($p<0.1$), whereas for *P. alba* only a small stimulating effect was observed. These differences persisted at the end of the second growing season.

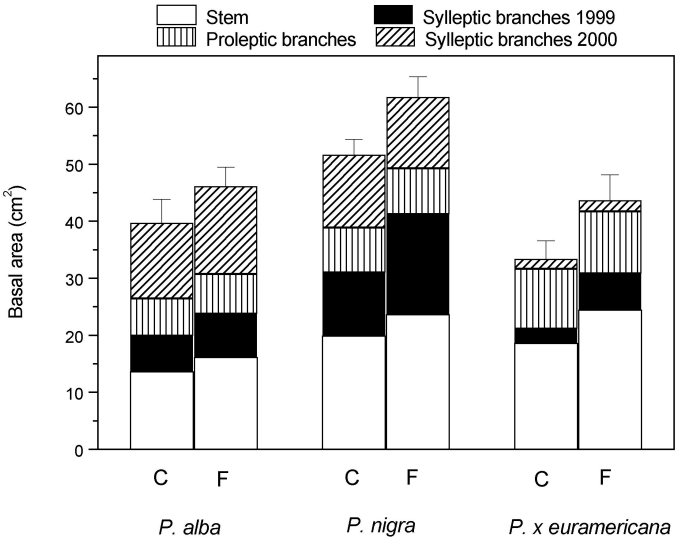

Figure 2.23: Distribution of basal area (BA) over stem and branches at the end of the second growing season in FACE (F) and Control (C) treatments for three *Populus* genotypes. Each value represents the mean ±SE (of total value) of 12 trees

Wood density was not influenced by the FACE treatment in all species, but a significant difference was observed among species. Mean values for whole stem wood density ranged from 0.348 g cm^{-3} in *P. x euramericana* to 0.409 g cm^{-3} in *P. nigra*. Differences were evident among the three portions of the stem corresponding with the HGIs. Wood density was always highest in HGI 3, with values ranging from 0.422 g cm^{-3} to 0.470 g cm^{-3}.

Inorganic soil nitrogen content was similar among species and between treatments in the spring of the third growing season, whereas a significant treatment effect emerged in the fall. A depletion of soil nitrogen was evident for all species in both treatments, except for *P. nigra* in the control treatment.

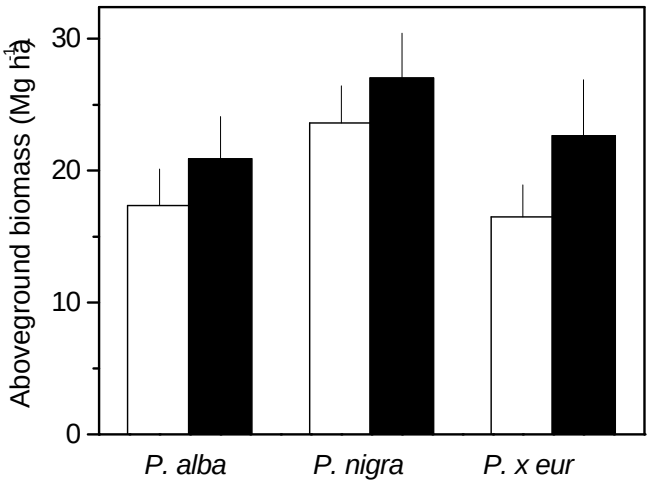

Figure 2.24: Total above-ground biomass (Mg ha^{-1}) observed after two growing seasons for three *Populus* species under control and FACE treatments. Mean values (+ standard error) of the control

(open bars) and FACE (closed bars) treatments are presented. Each bar represents the mean of 144 trees for which biomass was determined using allometric relationships
Collection of eddy covariance data collection on the meteorological tower was made. These data have been processed (gap-filled and corrected). Furthermore the data have been fully analysed resulting in the publication of one paper and a second paper recently submitted (see Chapter 9).

The data is held in the project database (Chapter 8).

2.4 3-Dimensional scanning of logs from felled trees and example results.

Logs resulting from harvesting of softwood trees selected for destructive sampling have been scanned using 3-D scanners in industrial sawmills based in Scotland, and at the Building Research Establishment, Watford. The sawmill industry also assisted with the conversion of the sawlogs that are large enough to produce structural battens. Logs were marked with a colour spray system on both ends of the logs (Figure 2.9). As the sawmilling system is automatic (Figure 2.10) and can process 10 logs per minute, this is a necessary procedure to allow identification of individual logs during 3D scanning and conversion.
The marking system adopted by MEFYQUE is as follows:

Top end of log -
- A background colour linking a particular group of trees to a known stand.
- A number stencil colour for all the logs of a particular tree
- A numbered stencil identifying the logs and their order in the tree from the butt end
- The north point was marked to record the orientation of the log during scanning

Butt end of log -
- 4 quadrants of different colours (same for all logs) with same colour quadrant starting at the north point. This is necessary for the log saw operator to attempt to cut all logs with their north point vertical. Where this does not prove possible the colour quadrant system will give the information necessary to reconstruct the orientation of cut battens.

Logs have been scanned to output the true log shape (Figure 2.25 to Figure 2.27). This required an up-grading of software at the mills in order to produce scans at 10 cm intervals (Figure 2.27).

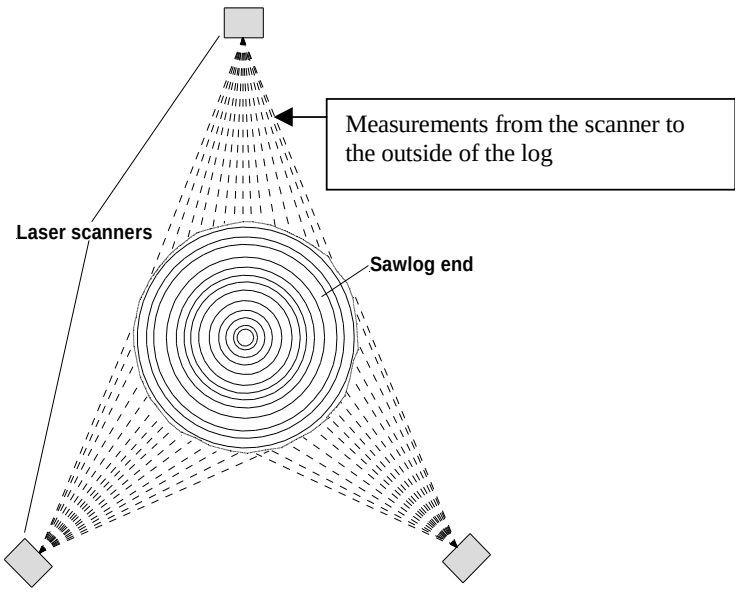

Figure 2.25: 3D Laser Scanner

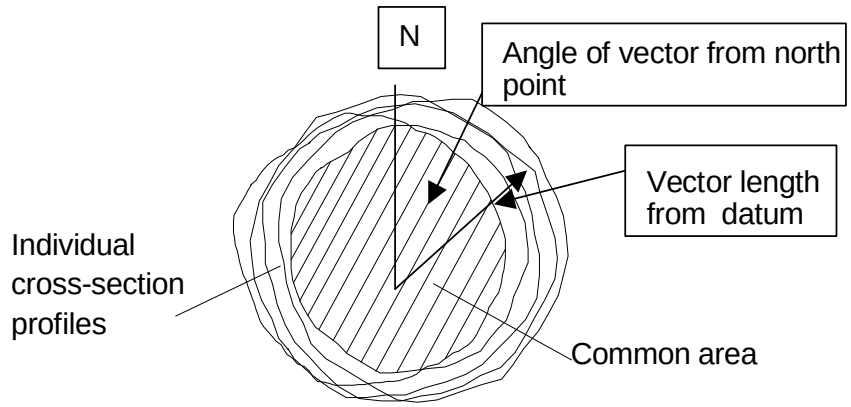

Figure 2.26: Stacked scans

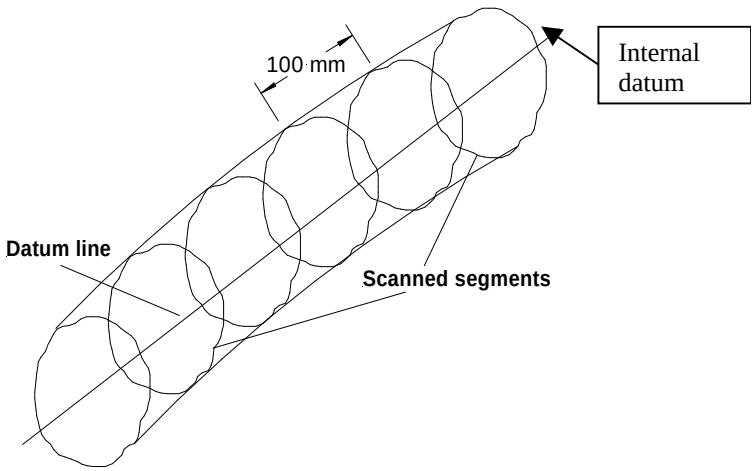

Figure 2.27: Complete 3D log picture.

The industrial scanning system described above cannot cope with stems < 75mm diameter, nor can it deal with hardwood logs. Stems portions < 75 mm in diameter, the tops of trees from the primary and secondary sites, all sampled material from tertiary sites and all hardwood logs have been scanned at BRE, Watford (UK). At this location accurate log stem measurement and conversion has been carried out. To this end a new low cost system, using of 'off the shelf' components has been developed. Financial support for this equipment has been provided jointly by MEFYQUE, another EU project (COMPRESSION WOOD) and a UK national programme. As the new device has patent possibilities, no further details will be provided here. Following scanning of logs, small material was milled to produce small strength and stiffness assessment samples for use in laboratory analysis (Chapter 4).

2.4.1 –Example Scans

Logs were scanned at James Jones and Son (JJ), the 2nd biggest saw-millers of the UK. The sawmill scanned and cut the logs large enough for their system; badly twisted and small logs, some of which were from Belgium, were put to one side to return to BRE for further assessment. Unfortunately a significant amount of time elapsed after which (JJ), on cleaning up the sawmill yard, were destroyed the project's remaining small distorted logs, though clearly marked. James Jones (JJ) have since apologised but the event has caused a loss of some entity to the project.

Due to pressure of business (JJ) could not scan or cut all of the project logs; some were therefore cut at Adam Wilson and Son Ltd [1], and the remaining logs dealt with at BRE, where a scanner has been developed and built. The scanner is a shared cost development but has been mainly used by the MEFYQUE project. The scanner is a low cost device using off-the-shelf components that has required considerable additional programming effort.

The theory of 3-D scanning has been reported in previous annual reports. Some practical results of the new scanner are reported below.

A camera, as shown in Figure 2.25, with the image processed to give the result shown in Figure 2.29, views a laser line round a log.

Figure 2.28: straight line laser view at an angle

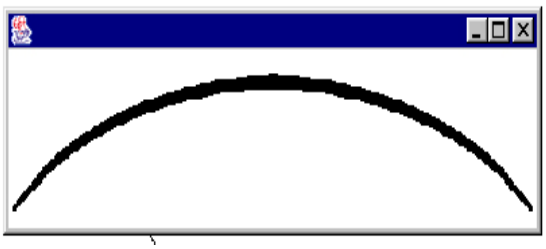

Figure 2.29: Processed image in rectangular coordinates.

The true shape is then derived by geometric equations, as shown in Figure 2.30

Figure 2.30: True shape of arc of log**.**

The scanner uses three laser lines and three cameras to see round the log. and show the scans and 3 arcs of one cross-section.

Figure 2.31: three laser scans**.**

[1] This was a special favour to BRE. BRE are indeed grateful to both sawmills for making their facilities available on Saturday mornings. This is an industry showing a real interest in the project.

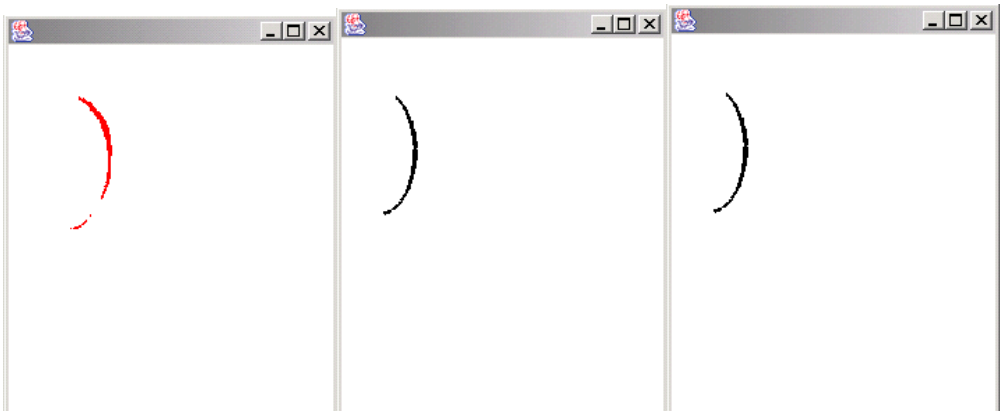

Figure 2.32: Scans converted into arcs by the computer software

Images are then processed to give the cross-section, as shown in Figure 2.33 below

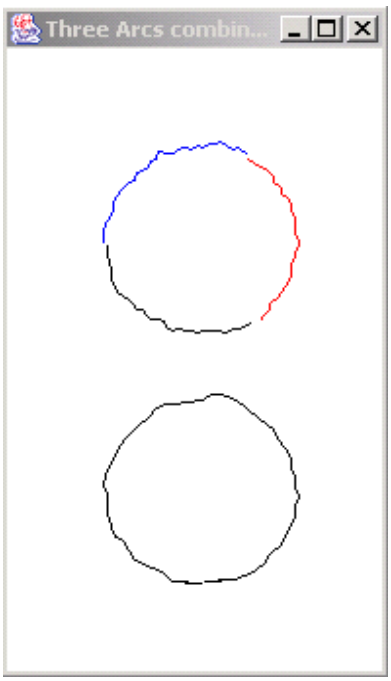

Figure 2.33: The 3 scans are processed and combined to give log cross-section.

Software has been developed to read both the output from the industrial and BRE scanners to view and analyse the scans and build them into logs. The industrial data was very noisy and special software had to be developed to clean up the output. Figure 2.34 shows scans of a log stacked to give the common area. The significance of the common area is discussed below.

Figure 2.34: Stacked clean spans to give the common area.

The developed software not only reads all the scans and cleans up the data, it also allows the log to be turned through 360 degrees, in 10 degree intervals, increment and it calculates maximum log bow and it rotational position. Also, it outputs the data in mm strip rectangular co-ordinates for the common area and each cross-section for 36 rotations. Simulation programmes to derive optimum cutting patterns outlined in chapter 5 use these data as input.

3 Tree Tissue properties under ambient and elevated CO_2

Main Contributors:
Dieter Overdieck, Daniel Ziche

3.1 Analyses of wood anatomical properties and tree ring analyses in laboratory conditions

3.1.1 Role in model parametrisation and validation

The growth data from the manipulative experiments are important both for the parametrisation and for the validation of the plot scale MEFYQUE model. For the parametrisation the values of SLA and root/shoot allocation were used (see chapter 6 on parametrisation and validation). Furthermore, the data are being used for validation of the allocation module (between stems, roots, branches and leaves), including the effects of T and CO_2 on allocation, and the effects on height growth. Since the allocation module (see chapter 5) is the core in simulating environmental effects on wood quality, this validation is of great importance to the value of the model in simulating the effects of global change. The budbreak values are used for validating the budbreak module, where the effect of T is of special importance. The growth rate is being used to validate the overall output from the stand model.

The gas-exchange data from the manipulative experiments are used both for the parametrisation and for the initial validation of the plot scale model. For the parametrisation the values of maximal photosynthesis and respiration were of particular importance (see chapter 6 on parametrisation and validation). Furthermore, the data are being used for validation of the stomatal conductance calculations, and the derived transpiration. For an improved simulation of the effects of T and CO_2 on gas-exchange, the experimental data from these well-controlled experiments are of particular interest, since many parameters that interact were measured on the same material and during the same period, while the trees were under optimal conditions of water and nutrients. Data from field experiments are often more complicated, since many effects interact, and such data are therefore less ideal for initial parametrisation and validation.

3.1.2 Analyses of softwoods

Scots pine (Pinus sylvestris L.) is the most widely distributed pine species in Eurasia and one of the important timber species. Therefore, Scots pine forests could play a major role in mitigating the global elevation of atmospheric CO2 concentration that is apparently accompanied by temperature increase.

Wood quality is of major importance in the forestry industry. Although it is difficult to link wood anatomical properties directly to wood quality an understanding of micro-allocation patterns is crucial for the understanding and prediction of wood formation and the resultant wood quality. The CO_2 and the temperature effect on wood formation and micro-allocation patterns are not necessarily synchronised. If due to CO_2 enhancement more assimilates are transferred from leaves to stem, a ‘better’ supply of cambial cells and their derivates should lead to higher production of cells and higher carbon allocation to cell wall. On the other hand, an increase in temperature can lead to faster rates of cell division, cell growth and cell maturation and consequently shorten the time in which the assimilates can be used by the cells (Morison and Lawlor, 1999).

A number of experiments have been conducted to evaluate the effects of CO_2 enhancement alone on growth of juvenile softwoods, but the wood properties of only a small porportion of the resultant plant material have been analysed (Telewski et al., 1999; Ceulemans et al., 2002). Consequently the amount of studies of the interaction effects of temperature and CO_2 on wood (anatomical) properties of softwoods is even smaller (Kilpeläinen et al., 2003). Due to their major importance in forest industry, species of the genera, Pinus are represented well in the small group of studies which examine the CO_2 effect on wood anatomical properties (Donaldson et al., 1987, Telewski et al., 1987; Conroy et al.1990; Telewski et al., 1999), and in particular, Pinus sylvestris: Ceulemans et al., 2002, Kilpeläinen et al., 2003. Nevertheless, linkage of growth and biomass partitioning to cell growth and cell wall formation has been

rarely described. Therefore, we followed the hypothesis that clear results of the interaction between CO_2 and temperature as environmental factors are to be expected and can be quantified not only on the overall plant level but also on the cell level.

3.1.2.1 Material and methods

The objective of this sub-task is to obtain detailed data on cell structure. Up to now, quantitative wood anatomical measurements have always been done manually, on thin microtome sections using a microscope. In recent years, digital image processing has offered faster means for performing such analyses but methods are still lacking for automating and speeding up the data collection. New sample preparation methods and automated image analysis procedures are required, customised for every species, since the preparation of microtome sections is very time-consuming, the sections and the images can be of poor quality in spite of careful preparations, and because manual computer-aided measurements are also time-consuming and labour-intensive.

To speeding up the process of quantitative measurements in wood anatomy often measurements on surfaces were performed (Schnell and Sell, 1989; Evans 1994; Saß and Eckstein, 1994). The resolution and surface smoothness limits the accuracy of these measurements (Saß and Eckstein, 1994, Spieker et al. 2000). Therefore in this work measurements were performed with conventional transmission light microscopy and at high magnification.

In digital imaging the segmentation is the crucial step, in case of wood anatomy it means the separation between lumen and cell wall pixels. Automatic segmentation methods are beneficial to reduce the operator bias and the working time (Park and Telewski, 1993). In a detailed analysis Moell and Donaldson, 2000 have tested different methods of segmentation for its use in wood anatomical applications.

The aim of this study was to establish methods for automated image analysis on wood anatomical samples and to assess the quality of these results.

3.1.2.1.1 Sampling

In this work juvenile Scots pine material was analysed from CO_2 x temperature experiment in Berlin.

Additionally, on four of the MEFYOUE sites in Western Europe, six trees in Scots pine stands were felled (N=24). The sites are part of the UN/ECE ICP Forests Level II Forest Health Monitoring Network. The age of the stands ranged from ~34 to ~70 years (Table 3.1). The trees were representative for their stand and taken from three classes: dominant, subdominant and suppressed.

Table 3.1: Characteristics of the four sites in United Kingdom and Belgium.

Site	Age	Trees ha^{-1}	DBH	Mean Height	Basal Area
Brasschaart (B)	70	377	29.7	21.4	28.5
Rannoch (UK)	36	2270	13.8	10.4	37.0
Thetford (UK)	34	978	19.6	14.9	31.9
Sherwood (UK)	50	1125	21.0	16.4	42.5

3.1.2.1.2 Measurement protocol

- Sample preparation

Before cutting sections the samples were infiltrated with PEG 1500 in order to obtain more stability (Saß and Eckstein, 1994). This method consists of a pre-infiltration in a solution of 20% PEG 1500 and 80% water for three days at 60°C followed by one day in 100% PEG 1500. Then, 20µm thick cross sections were cut with a sliding microtome (SM2000R, Leica). The sections were stained with Safranin one day and Astrablue one minute and mounted on glass slides with Euparal.

- Equipment

A transmitted light microscope (Laborlux S, Leitz) was used for the estimation of cell features at a magnification of 400. The microscope was equipped with a video camera (15/3, Kappa) which was connected to an image capture board (Meteor II, Matrox) on a PC. QWin 2.8 software (Leica Microsystems) was used for grabbing the images. This combination of microscope and digital imaging system resulted in a resolution of 0.34 µm per pixel. In case of the juvenile material 8 bit grey level pictures were taken every 200µm in radial line from the last two growth rings on two opposite radii. In case of the old Scots pine trees images were taken from the last 10 years (1992-2001). The pictures covered a surface area of 254 x 195µm.

- Digital Imaging:
  - Grey level imaging
    The grey level pictures were processed by removing noise by averaging five frames for segmentation between cell wall and lumen. The grey level of each pixel was recalculated with a logarithmical (look-up) table.

  - Segmentation
    The automatic segmentation methods used by Moell and Donaldson, 2000 were taken over for the analyses. It was a histogram based thresholding, previously used by Lee and Rosen, 1985 in wood anatomy, a shape based (p2a) method (Ranefall et al., 1998) and two texture based methods, the l-method and the h-method (Panda and Rosenfeld, 1978). The parameters of the algorithm in the methods were adjusted to the needs of this analysis. The calculations of the thresholds with the different methods were performed with Visual Basic Macros in Excel (Microsoft) via dynamic data exchange with QWin (Leica Microsystems). Further the threshold was set manually and by the automatic method of the imaging software QWin. Together 6 methods were tested. All these methods are common that by setting a threshold they use a global segmentation method.

  - Binary imaging
    In order to eliminate small groups of erroneously classified pixels from the cell wall area layer, binary pictures were processed by removing twice a one pixel thick layer from the borders of each group of detected (=lumen) pixels. Then, a one pixel thick layer was doubly added again (opening procedure). Groups of non-detected pixels within the lumen pixels were detected with a geodesic dilation. In addition, the individual cells were separated by calculating an artificial middle lamella with the ultimate skeleton procedure followed by a pruning procedure (Leica Microsystems). By these procedures, a one-pixel thick middle lamella was set at half the distance of two lumen borders (Figure 3.1).

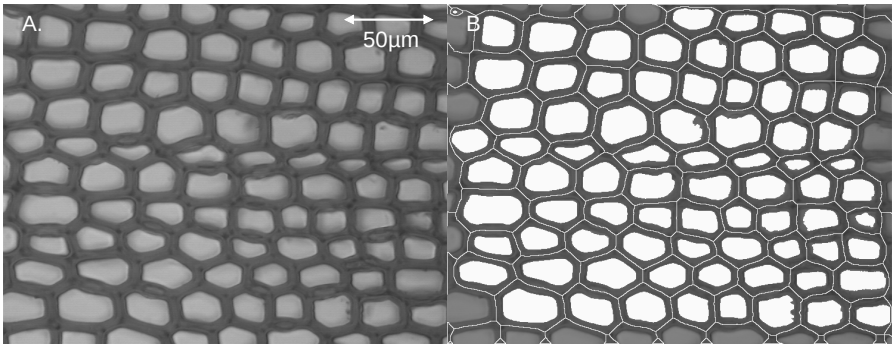

Figure 3.1: A) Original grey-level, B) processed image with a binary layer, (254 x 195µm) of juvenile Scots pine wood.

The main problem is the shadowing within the lumen area caused by the cell walls. It leads to a gradual decrease in grey level value between lumen and cell wall. The solution for this problem was performing dilation with two cycles on the binary image. The dilation was restricted to pixels with grey level values > Ts – 6, where Ts is the threshold estimated by the segmentation method. This added in areas with a gradual lumen – wall grey level transition two rows of pixels to each lumen.

The success of the segmentation of lumen and cell wall pixels was manually controlled by visual assessment and pictures in which the segmentation was not satisfactory were deleted.

- Measurements
  On a single cell basis, the width and area of cell, cell wall and lumen was measured (Figure 3.2). The ratio of double cell wall width to lumen width (Mork's index) was derived from these variables and, in addition, the ratio of cell wall to total cell area. In the measurements, only cells were included within a rectangular window with a size of 130 x 98 µm in case of juvenile wood. The window was centred in the picture.

  The relative position of each picture within the tree ring was determined. Then the descriptive statistical parameters of the measured variables for the cells in each picture were calculated. In the subsequent evaluation the mean values for the variables of each picture were used.

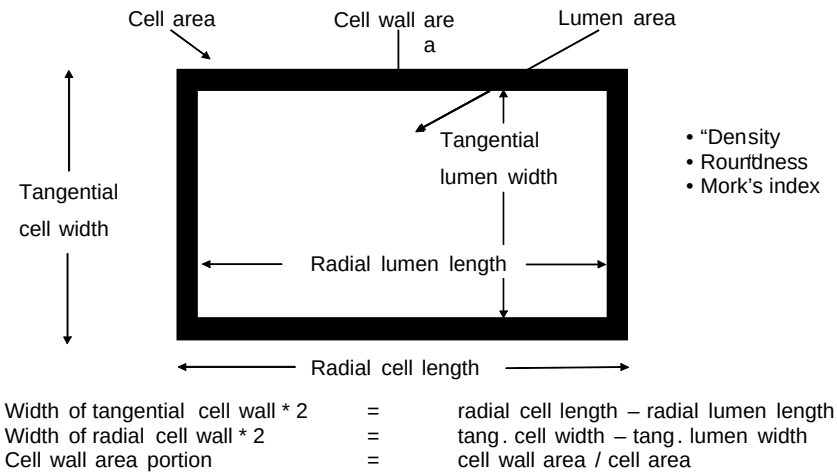

Figure 3.2: Variables measured for single cells

- Automation
  With the macro-programming facility of the software QWin runs were programmed which did all steps of digital imaging automatically with exception of the image acquisition. The results of the measurements were outputted and filed in Excel sheets (Figure 3.3). This had the advantage that the images which had been taken during daytime by an operator could be processed during the night automatically.

  The second step in the automation of the method used macros programmed for SAS 8.02 (SAS Institute). These were for sorting and fitting data and further statistical evaluation.

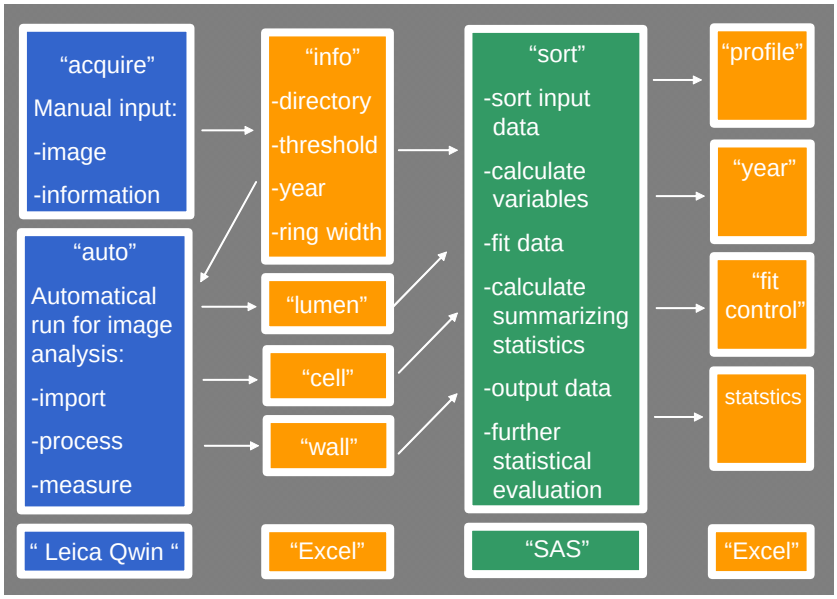

Figure 3.3: Data flow of automated image analysis, with orange = Excel-sheets, blue = QWin-routines and green = SAS-routines

- Data evaluation
  Mork's index was used to distinguish between latewood and earlywood. In cases were the detection of latewood by Mork's index failed, in latewood only measurements from the last 10% of the growth ring were included.
  Furthermore the weighted mean values of the variables were calculated separately for earlywood and latewood cells by using the distance of each measurement (image) to the neighbour measurements within an intraanual profile as weighting factor

- Quality assessment of the methods
  To estimate the influence of the quality of the input image 4 quality classes were visually assessed for the images:
  – Quality class I: good images with a high contrast between lumen and cell wall and undamaged cell wall
  – Quality class II: satisfying quality with a partly gradual grey level transition between lumen and cell wall but undamaged cell walls
  – Quality class III: main parts of the image are of quality class II but in some parts the quality class is IV
  – Quality class IV: poor quality with a low contrast between lumen and cell wall leading either to large groups wrongly classified lumen pixel or cell wall pixels. Further cell walls were damaged. Images of this quality were rejected.

  A set of 36 images of the quality classes' I - III was selected: 12 per quality class and within each quality class 4 images contained earlywood and latewood of adult trees,

respective, and 4 the wood of juvenile trees. On these images measurements were repeated differing in the methods of thresholding.

Then, on the images the cell lumina were masked manually with the aid of the digital imaging system and a graphic tablet (SummaSketch III, GTCO CalComp). The grey level of the lumen pixels was set to 255 (=white). Approximately 30 minutes was needed to work on each image. Measurements of the cell features were performed on the images with the same methods. The results were regarded to represent the “true” values and they were used to estimate the bias of each segmentation method.

On images with the quality class I the content of wrongly classified pixels was 1.5% performing the manual segmentation method of QWin (Figure 3.4). The automatic segmentation method caused a standard error of 2.2 % pixels, the histogram based method 2.5%, the shape based p2a method 4.8% and the texture based methods 2.4% for the l_method and 2.5% for the h_method.

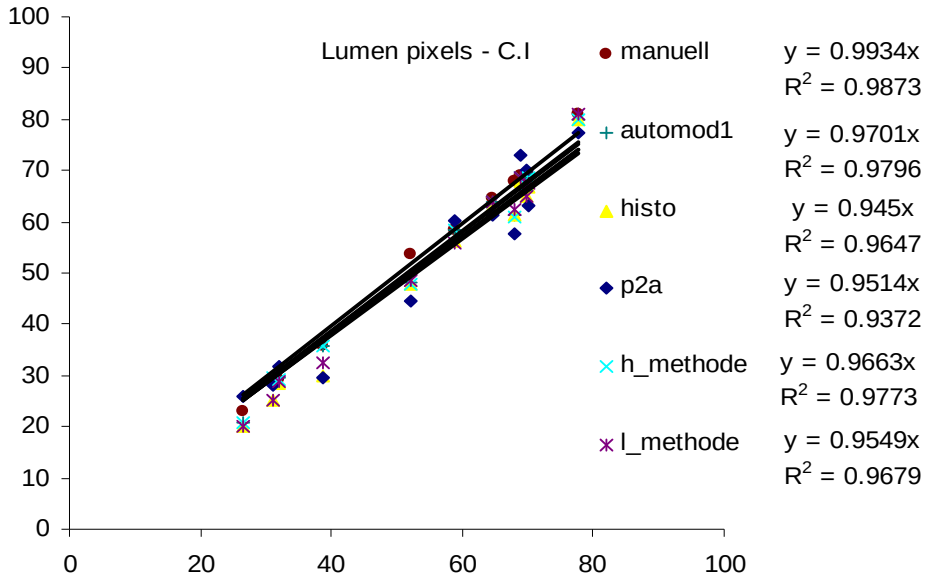

Figure 3.4: Correlation between the percentages of detected lumen pixels performing the different segmentation methods (y-axis) against the percentage of detected lumen pixels in the control set (x-axis). The results of measurements on 12 images of quality class I are shown.

The standard error of wrongly classified pixels increased with decreasing image quality. On the set of images with the quality class I-II the manual segmentation method leaded to an error of 2.5%. The automatic segmentation method of QWin caused an error of 2.7%. The shape based method caused an error of 4.6% and the histogram based method had an error of 2.4%. The standard error of the texture based methods was for the l_method 2.4% and for the h_method 4.5%.

On images with the quality class I-III manual setting of the threshold caused an error of 3.7%. The automatic segmentation method of QWin caused an error of 3.5%. The p2a method had an error of 5.7% and the histogram based method had an error of 3.6%. Performing the l_method and the h_method leaded to an error of 3.3% and 5.0% respective.

The results indicate that the impact of the image quality is higher than the impact of the segmentation method. The six methods of segmentation deviate only slightly in their accuracy. On measurements including images of all three quality classes only the

shape based p2a method has a standard error higher than 5%. Nevertheless it has to be recognised that for the double cell wall width the resolution of the used imaging system leads to a bias of ~5% at a width of 6µm in case of an earlywood cell and of ~2% in case of a latewood cell with a width of 15µm.

Automated digital imaging provides a sufficient method for quantitative measurements in wood anatomy. For accurate measurements a high resolution and a high image quality is needed. Both had a significant impact on the accuracy of the measurements. This shows that a big potential is located in the search of new methods for sample preparation and microscopy to enhance the image quality.

The main advantage of the automation is the saving of working time by speeding the process by the factor 5. Performing the main steps of digital imaging automatically over night saves approximately 8 minutes per images (inclusive image acquisition) and reduced the operator working time to approximately two minutes per image.

- Wood rays and resin canals
  Wood rays were counted at the end of the growth ring under a transmitted light microscope (Laborlux S, Leitz) at a magnification of 200, and its number was divided by the perimeter derived from the tree ring width. Under a magnification of 40, all resin canals were counted per tree ring and their number was divided by tree ring area.

- Tree ring width and wood density
  A standard linetable (Frank Rinn Engineering) was used to measure the tree ring width on the sections from the stem base on four radii at right angles. The cross sectional area was calculated for each tree ring. Relative growth rate based on cross sectional area (RGRcsa) per year was calculated according to:

  RGR = (ln x2 – ln x1)/(t2-t1),
  where x2 is the value of variable at time 2 (t2) and x1 is the value of variable at time 1 (t1).

  Wood density was measured as ratio of dry mass (85 °C) to volume, estimated at debarked ca. 1cm long stem sections from the lowest stem section. Volume was calculated by means of height and diameter of these sections.

3.1.2.1.3 Statistical methods

All statistical analyses were performed with the SAS 8.02 software package (SAS Institute). Differences between the CO_2 concentrations, temperature treatments and their interaction effects were tested for significance with a two-factorial analysis of variance (ANOVA) for fixed effects by using the single plants as replicates.

The last two years of growth were included for the wood anatomical properties as a within-object-factor, and differences between the treatments and years were tested for significance with a two-factorial repeated measure ANOVA. Then, the relative growth rate of cross-sectional area (RGRCSA) was introduced as covariate in the model to estimate the effects independently from the individual growth rate, and ANOVA was repeated.

The homogeneity of variance between the experimental groups was tested with an F-test, and the distribution within the groups was tested for normality with a Shapiro Wilk-test. Differences between groups were tested with a Bonferroni t-test. Differences between the treatment and the control groups were tested with the Dunnett's test for unequal sample sizes.

Furthermore, a linear regression was fitted between the variables and the temperature in the different treatments as regressor by using the single plants as replicates. It was tested whether the assumption of linearity was significant and whether the slope deviated significantly from zero.

In case of the old Scots pine trees, differences between dominance classes and sites were tested with a two-factorial ANOVA for significance. Furthermore, an analysis of covariance was performed with the DBH at the beginning of the 10 years period (1991) as covariate.

3.1.2.2 Results

3.1.2.3 CO_2 and temperature effects on stem wood anatomy of juvenile Scots pine (Pinus sylvestris L.)

Tree ring width and wood density

CO2 concentration had a significant impact on the tree ring width (Figure 3.5). Whilst the difference in the 2nd year of the experiment was < 5%, in the 3rd year tree rings were 10% wider at elevated CO_2. No significant temperature effect on tree ring width occurred and there was no combinational effect of CO_2 and temperature on tree ring width, but a significant increase was determined from the 2nd to the 3rd year of 26%. No differences were found between the experimental groups and the field control.

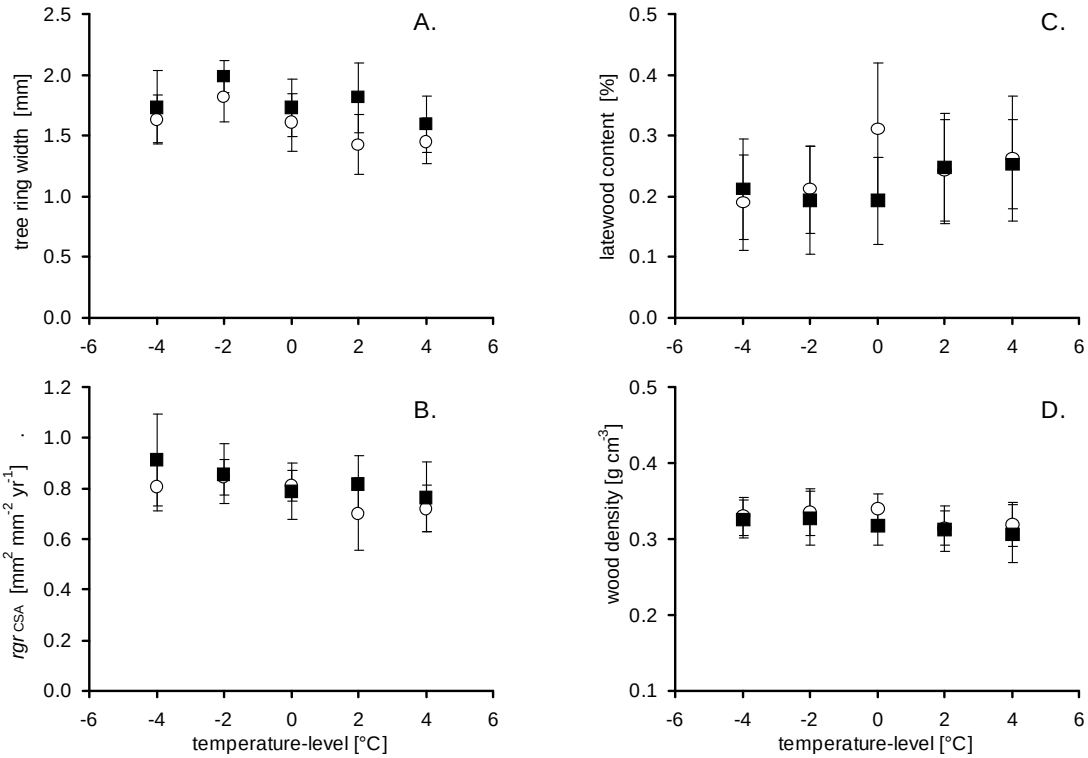

Figure 3.5: Tree ring width (A.), relative growth rate of cross sectional area (B.), latewood content (C.) and wood density (D.) in relation to the temperature differences of the treatments; with • : ambient CO_2 concentration, • : elevated CO_2 concentration. A. and C. show the results of the 3rd growth year.

The ratio of latewood to earlywood was not different between the treatments (Figure 3.5). In the 2nd year it was 14% higher compared to the 3rd year. There were also no differences between the combined treatment groups and the control group.

RGRCSA was also not significantly affected by the treatments (Figure 3.5); although there was a tendency for it to decline with increasing temperature levels. At the lowest temperature level, RGRCSA was 19% higher compared to RGRCSA at the uppermost temperature level in the 3rd season. Furthermore, the lowest temperature treatment was the only treatment in which the RGRCSA remained constant in the 3rd year. In the other treatments RGRCSA declined.

There were no significant differences in wood density between the experimental groups (Figure 3.5), but the wood density in the control group was 13% lower than in the experimental groups.

Table 3.2: Probability classes of statistics for anatomical characteristics and wood properties. Results of the two-factorial repeated ANOVA are shown, with the sum the effects of the last two experimental years. Columns headlined with COV show the results for the inclusion of RGRCSA as covariate. n.s.: not significant; * : p < 0.05; ** : p < 0.01; *** : p < 0.001; X : effect was not estimated.

	Repeated 2-factor ANOVA										Regression
	CO2		temperature		CO2 x temperature		time		control (Dunnett's -test)		Slope > 0
		COV		COV		COV		COV	2ndyr.	3rdyr.	
EW. Cell area	n.s.	n.s.	n.s.	n.s.	*	*	***	n.s.	n.s.	*	n.s.
EW. Cell width	0.06	*	n.s.	*	**	**	***	n.s.	n.s.	*	*
EW. Cell wall width	n.s.	n.s.	*	*	n.s.	n.s.	***	n.s.	*	*	***
EW. Cell/total area	n.s.	n.s.	n.s.	n.s.	n.s.	n.s.	n.s.	n.s.	*	n.s.	n.s.
LW. Cell area	n.s.	n.s.	0.08	n.s.	n.s.	n.s.	***	*	*	n.s.	**
LW. Cell width	n.s.	n.s.	***	**	n.s.	n.s.	***	*	*	n.s.	***
LW. Cell wall width	n.s.	n.s.	0.05	*	n.s.	n.s.	***	n.s.	*	n.s.	**
LW. Cell/total area	n.s.	n.s.	0.08	0.08	n.s.	n.s.	***	n.s.	n.s.	n.s.	n.s.
Wood ray density	n.s.	n.s.	n.s.	n.s.	n.s.	n.s.	***	n.s.	*	n.s.	*
Resin can. density	*	**	**	***	n.s.	n.s.	***	n.s.	*	n.s.	**
Tree ring width	*	X	0.07	X	n.s.	X	***	X	n.s.	n.s.	n.s.
RGRCSA	n.s.	X	0.07	X	n.s.	X	***	X	n.s.	n.s.	*
Latewood content	n.s.	n.s.	n.s.	n.s.	n.s.	n.s.	*	n.s.	n.s.	n.s.	n.s.
Wood density	n.s.	X	n.s.	X	n.s.	X	X	X	*		***

There were no significant differences in wood density between the experimental groups (Figure 3.5), but the wood density in the control group was 13% lower than in the experimental groups.

Anatomical features
Cell features (cell area, cell wall width, ratio of cell wall area /total area) were not significantly affected by CO_2 (Figures 3.6, 3.7 and Table 3.2). Cell growth was only slightly enhanced by elevated CO_2 (Figure 3.6). In the 2nd year of the experiment differences between the CO_2 treatments were < 5% in all variables. In the 3rd year cells tended to become larger; on average, latewood cell area increased by 6% and 8% in earlywood at elevated CO_2 concentration (statistically not significant). At ambient CO_2, resin canal density had been 29 % higher in the 2nd year and 43% higher in the 3rd experimental year than at elevated CO_2 (Figure 3.8). Wood ray density was not significantly affected.

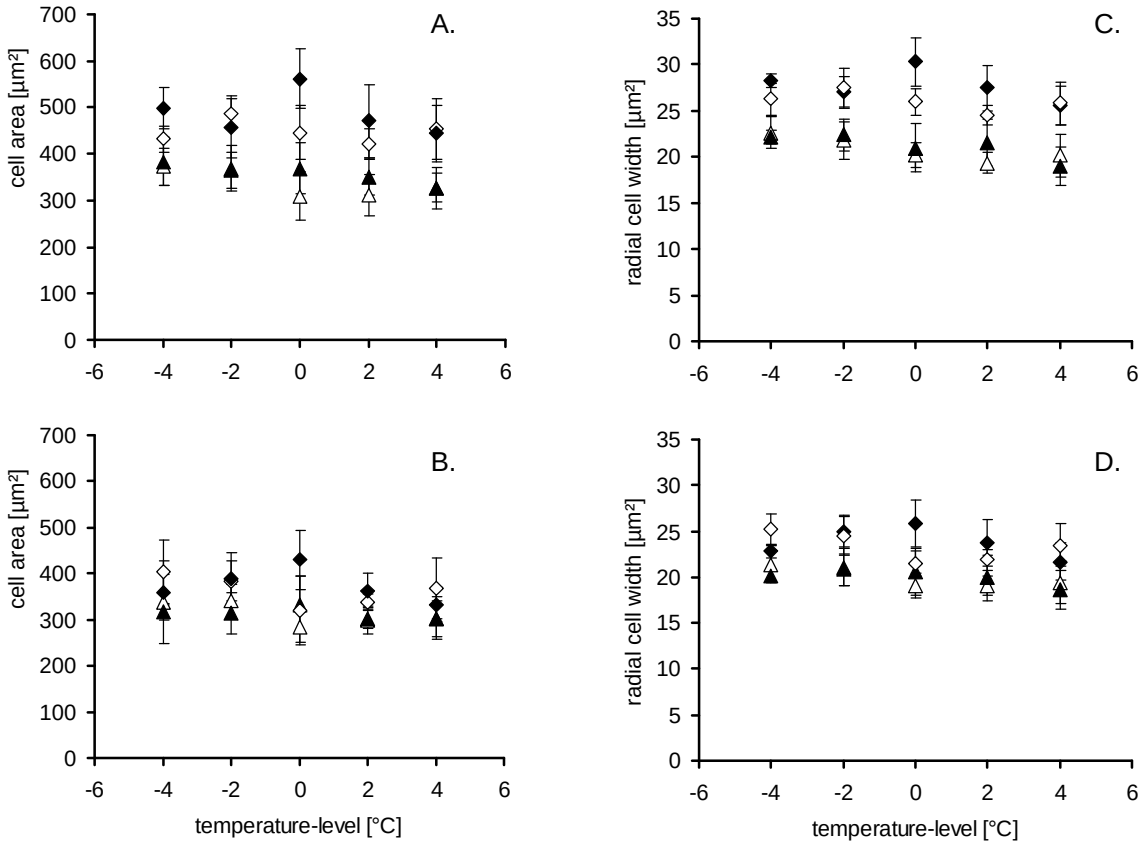

Figure 3.6: Cell area (A. and B.) and radial cell width (C. and D.) of earlywood and latewood cells in relation to the temperature-levels of the treatments. A. and C. show the results of the 3rd year and B. and D. of the 2nd year; with • : earlywood/ambient, • : earlywood/elevated, • : latewood/ambient, • : latewood/elevated.

Cell features tended to decrease with increasing temperature, with a few exceptions (Table 3.2): The decrease was more evident in latewood cells. In both years, cell wall width of latewood cells declined by 11% with temperature increasing to +4 °C above the local long-term mean (Figure 3.7, Table 3.2). Also cell area was affected by temperature in latewood, as a tendency (Figure 3.6). In the 2nd year, area was 8% and in the 3rd year 16% greater at lowest temperature. In earlywood, cell walls grown in the last two years of the experiment were 13% thinner at high temperature compared to low temperature levels (Figure 3.7). Ratio of cell wall area to total cell area and the cell area of earlywood showed no significant

differences between the temperature levels. Resin canal density increased significantly at higher temperature levels (Table 3.2). Comparing the groups '+4°C' and '-4°C', resin canal density was about 29% higher in the 2nd and 16% higher in the 3rd year (Figure 3.8). There were no statistically significant differences in wood ray density between the temperature treatments. Nevertheless, on average, wood ray density tended to increase with increasing temperature (Figure 3.8, Table. 3.2).

The Combination of temperature and CO_2 affected earlywood. At base temperature regime and at elevated CO_2 concentration cells were 21% larger (Figure 3.6).

Comparing the data from the 3rd with data from the 2nd year, a clear time effect on all variables could be found (Table 3.2); with the exception of the ratio cell area/total area in earlywood all cell features increased significantly in the course of time. In earlywood, cell area increased about 27% and the cell wall width 9%. In latewood, there was an increase in cell area of 11% and in cell wall width of 16%. The ratio of cell wall area/total area increased 7% in latewood. In contrast, resin canal density declined by 29% and the wood ray density declined by 9%.

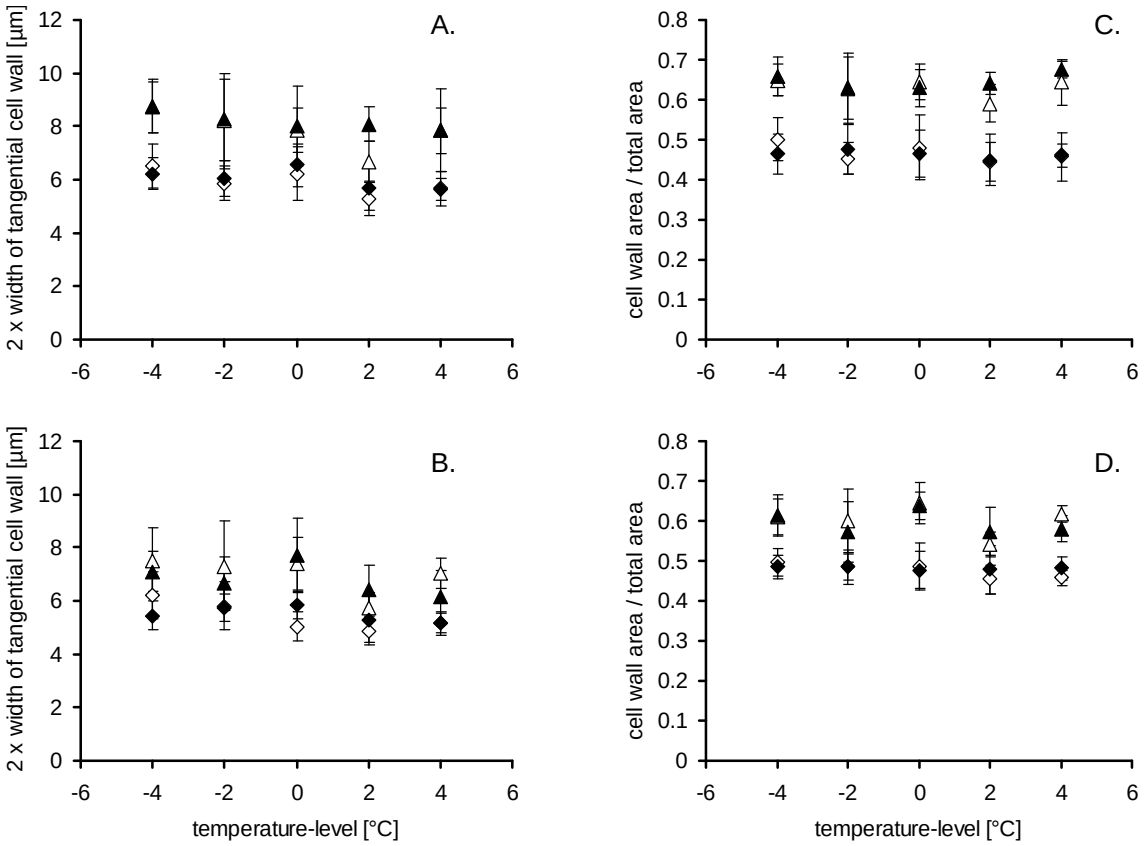

Figure 3.7: Width of tangential cell wall x 2 (A. and B.) and ratio of cell wall area to total cell area (C. and D.) of earlywood and latewood cells in relation to the temperature-levels of the treatments. A. and C. show the results of the 3rd year and B. and D. of the 2nd year; with • : earlywood/ambient, • : earlywood/elevated, • : latewood/ambient, • : latewood/elevated.

In the 2nd year of the experiment, groups in the chambers showed significant differences to the control group in the field (Table 3.2). Latewood cell area was about 13% smaller than in the control plants. In earlywood, cell walls were 9% thinner and in latewood 12%. The ratio of cell wall area/total cell area of earlywood cells was 4% lower. Cell wall width in earlywood was 6% smaller in the free growing control group than in the experimental groups in the 3rd year under exposure. In the same year, earlywood cell area was about 14% smaller in the control

group compared to the other groups. In the control group, the resin canal density was 25% higher and the wood ray density was 11% higher in the 2nd year than in all the in the experimental plants.

Introduction of the RGRCSA as a covariate in the statistical model eliminated, in most cases, the time effect.

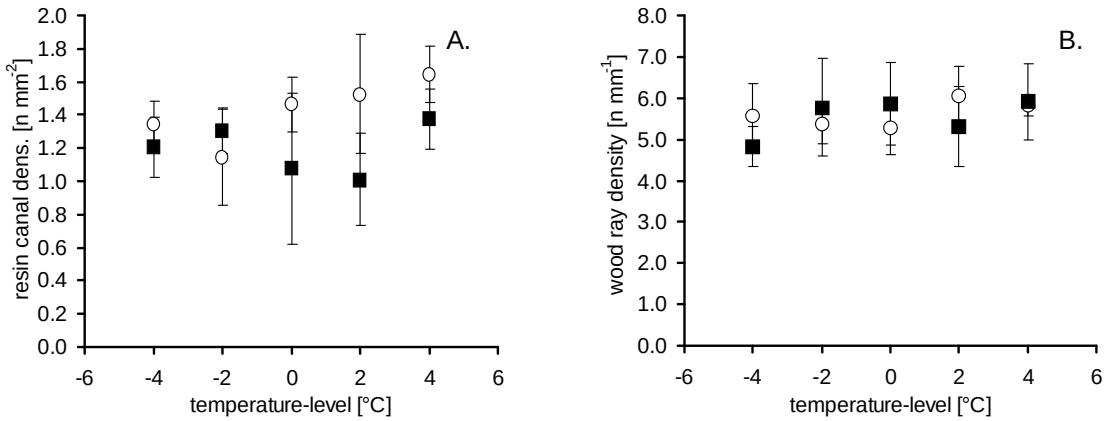

Figure 3.8: Resin canal density (A.) and wood ray density (B.) in relation to the temperature-levels of the treatments in the 3rd year of the experiment; with • : ambient CO2 concentration, • : elevated CO2 concentration**.**

3.1.2.4 Influence of tree dominance on wood anatomical properties of Scots pine

Dominant trees had a higher ratio of cell wall area to total cell area in latewood (Figure 3.9). This was due to the significantly thicker cell walls, whilst the cell area did not differ significantly between the dominance classes. In earlywood tree dominance caused thicker cell walls but no differences in ratio of cell wall area to total areablesell ell wall widthth (b & e) and ratio of cell wall area to total cell area (c & f) of earlywood.

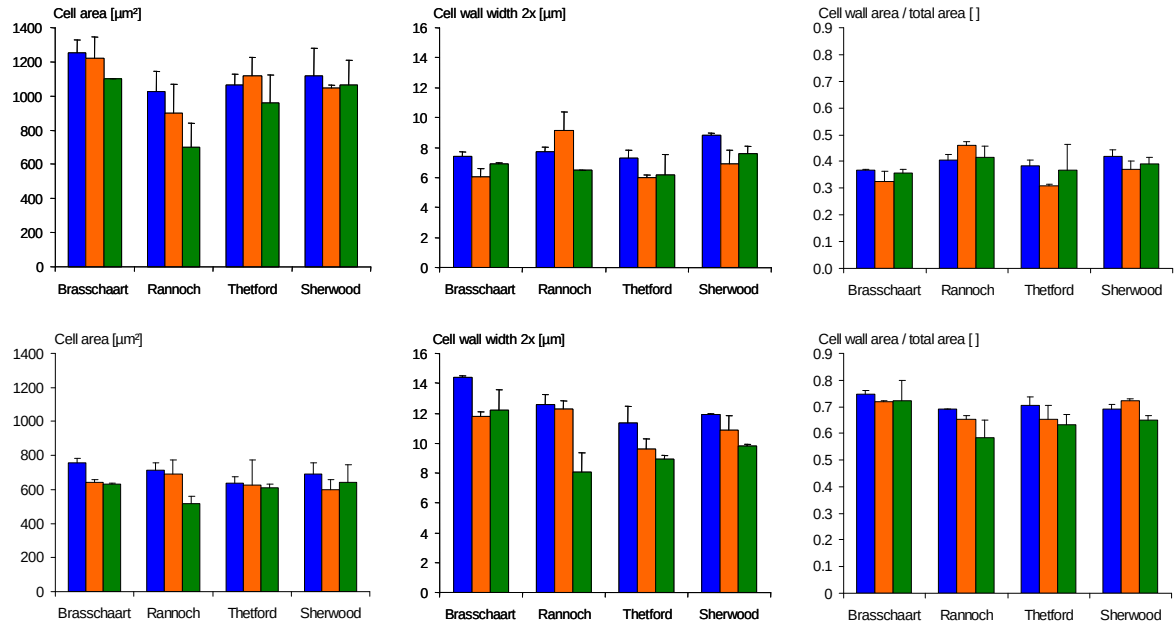

Figure 3.9: Effects of tree dominance class and site on cell area (a & d), cell wall width (b & e) and ratio of cell wall area to total cell area (c & f) of earlywood cells (a – c) and latewood cells (d – f); with blue = dominant, orange = subdominant and green = suppressed trees.

Differences between the sites were caused in latewood by higher cell wall width in the oldest stand (Brasschaart) while in earlywood the densest stand had the highest ratio of cell wall area to total cell area (Rannoch; Figure 3.9). Furthermore, in earlywood the effect of tree dominance on cell wall width was influenced by the site effect.

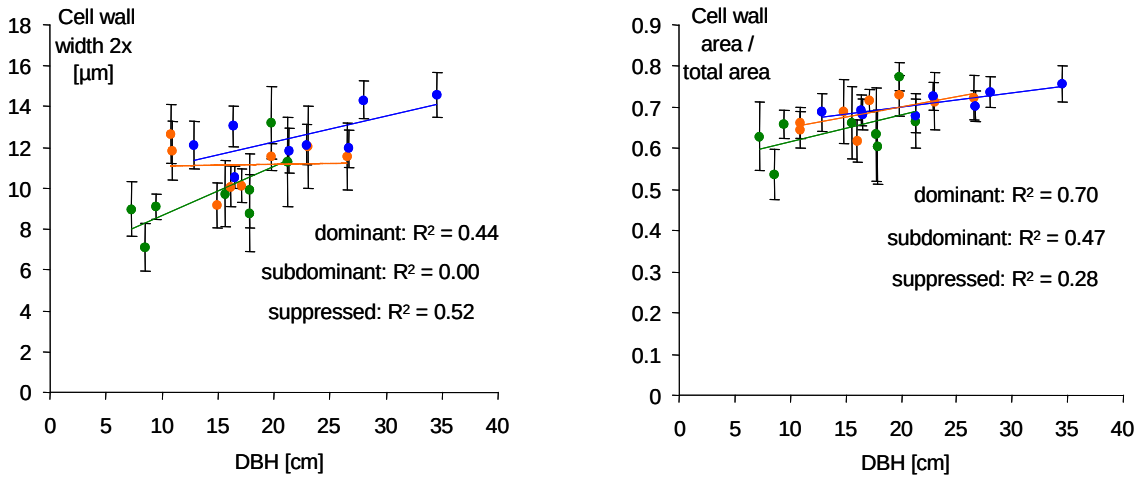

Figure 3.10: Effects of tree dominance class and site on resin canal density (a) and correlation between resin canal density and tree ring width (b); with blue = dominant, orange = subdominant and green = suppressed trees.

There was no effect on parenchyma content, but suppressed trees had a higher resin canal density, which correlated with tree ring width (Figure 3.11)

Using the DBH at the beginning of the 10 years period as covariant eliminates the dominance effect on cell wall width and ratio of cell wall area to total area in latewood and earlywood. A regression shows a dependency of both variables to DBH in dominant and suppressed trees (Figure 3.10).

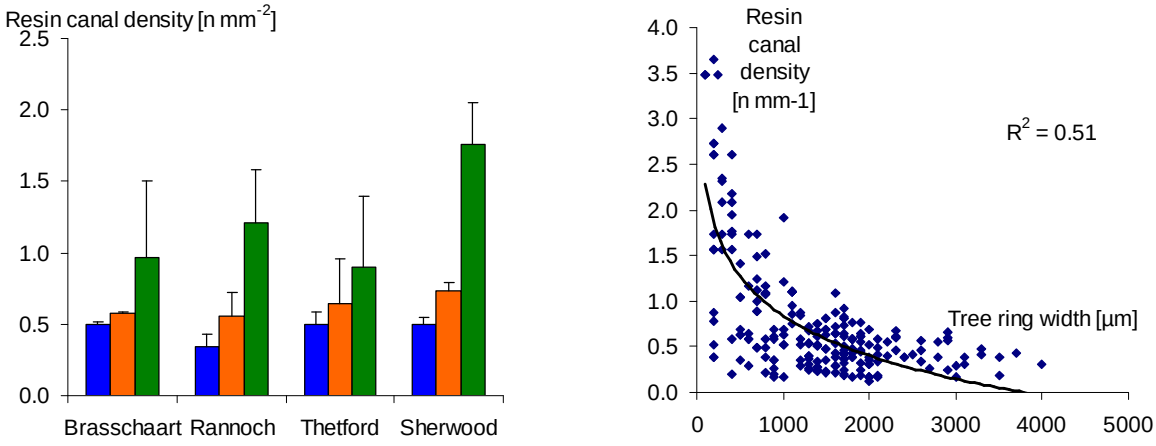

Figure 3.11: Regression within the three dominance classes between mean cell wall width (a) and ratio of cell wall area to total cell area (b) of 1992-2001 with DBH of 1991; with blue = dominant, orange = subdominant and green = suppressed trees.

3.1.2.5 Discussion

CO_2 affects plant growth mainly as substrate of photosynthesis; temperature has a general impact on plant metabolism, including photosynthesis, respiration and meristematic activity. The combination of both environmental factors leads to a variety of theoretically possible changes in assimilation, source-sink relationships and allocation patterns.

Wood structure was hardly affected by CO_2 qualitatively but it responded to temperature in our experiment. Former experiments of the effects of CO_2 on the wood anatomy of softwoods can be split in two sets: One with no CO_2 effect on wood anatomical properties (Donaldson et al. 1987; Telewski et al., 1999, our study). and the other set in which the anatomical properties are changed by CO_2 enrichment (Conroy et al., 1990; Ceulemans et al., 2002). In the second set of experiments analysed variables differ. In a study on Scots pine, a significant positive effect on tracheid width (Ceulemans et al., 2002) and on tracheid wall thickness of Pinus radiata was reported (Conroy et al., 1990). No CO_2 effect but rather a temperature effect could be measured on tracheid length in Scots pine (Kilpeläinen et al., 2003).

The pattern of earlywood cell formation is often regarded to be influenced mainly by temperature whilst latewood formation is mainly considered as a product of assimilate supply. Our results contradict this view because of the lacking CO_2 effect on latewood in our trees. Uggla et al. (2001) reported constant carbohydrate levels in the cambial zone during earlywood / latewood transition and could support the theory that the duration and not the rate of wall material deposition causes variation in cell wall thickness (Whitmore and Zahner, 1966; Skene, 1969; Wodzicki, 1971: Horacek et al., 1999). The lack of a clear CO_2 effect on cell wall thickness in our study is in agreement with this theory. Wood formation can be divided in three processes: cell division, cell enlargement and cell maturation. At higher temperature the duration of organ growth (expansion) is shorter. Therefore, at higher temperature faster rates of cell division, cell enlargement and cell maturation can be expected for cambial cells and their derivates (Bannan, 1962; Fritts, 1976; Horacek et al., 1999). On a single cell basis, faster rates of cell production may cause an opposite trend to the effect of a 'better' substrate supply of the cambium by elevated CO_2. If at higher temperature levels the cells undergo higher rates of cell enlargement and cell maturation, then the duration in which the assimilates can be used is shortened. This explains why the cell walls tended to become thinner at higher temperature in our experiment.

Table 3.3: Ratio of tree ring width of trees grown at elevated CO_2 concentration (~700 µmol mol-1) to tree ring width of trees grown at unchanged ambient CO_2 conditions (E/A-ratio) and the response of anatomical variables. Ratios were derived from published data. RD : radial diameter; FL : fibre length; LD : lumen diameter; WT : wall thickness; CA : Cell area; CWA/CA (or LA) : ratio of cell wall area/cell area (or lumen area); * : at least one variable differs significantly between the CO_2-concentrations, n.s. : not significant ; 1: E/A-ratio calculated using total stem diameters.

	Cell feature	Species	E/A	Anatomical response
Ceulemans et al., 2002	RD	Pinus sylvestris	1.42	*
Conroy et al., 19901	LD, WT , FL	Pinus radiata	1.20	*
Telewski et al., 1999	CWA/CL	Pinus taeda	1.15	n.s.
Ziche and Overdieck (this study)	CWA/CA, CA, WT, RD	Pinus sylvestris	1.11	n.s.

On the other hand, faster growth rates of juvenile trees may lead to a faster aging of the cambial initials. The cell length and tangential diameter of tracheids is mainly determined by the size of the cambial initials which increase with time during the first 20-30 years. It was previously pointed out that differences in growth rate can lead, with time, to different development stages between different CO_2 treatments (Bruhn et al., 2000). Sorting the results

of the studies in order of their response of tree ring growth rate to CO_2 enrichment support this assumption (Table 3.3): In experiments, in which the elevated/ambient ratio of tree ring width was high, a significant response of wood anatomical properties to CO_2 could be measured.

The response of radial cell width to temperature change and CO_2 enrichment in latewood is similar to the response of cell wall thickness. Therefore, the ratio of cell wall area to total area was not different between our treatments. Ratio of cell wall area to total cell area is one of the main components of wood density; consequently, also wood density did not differ between our treatments. In the field control plants wood density, earlywood cell area and the ratio of cell wall area were lower. Since radial cell width is affected by soil water supply during cell enlargement (Antonova et al., 1995; Horacek et al., 1999), It can be assumed that the soil water supply of the free rooting controls differed from that of the potted plants in the growth chambers. Thus at least partly causing the lower earlywood cell area.

A negative effect of CO_2 on resin canal density was already measured for Scots pine (Ceulemans et al. 2002) whilst in another experiment with Pinus taeda resin canal density showed no significant differences between different CO_2 treatments (Telewski et al., 1999). Resin canal density can be regarded in two ways: as a function of growth rate and a reaction to physiological stressors (Larson, 1994). The number of resin canals was positively and linearly correlated with tree ring width in our study. This is also known from studies on adult Scots pines (Stephan, 1967; Rigling et al., 2003). The use of RGRCSA as covariate did not eliminate the CO_2 effect on resin canal density. Nevertheless, it can be assumed that if - in general - more growth has a negative effect on resin canal density this is also true for CO_2 enhanced growth. In accordance with our results, a positive response of resin canal density to increasing temperature was shown by several authors for adult (Wimmer et al., 1999; Rigling et al., 2003) and juvenile trees (Zamski, 1972).

Generalising our results, one can conclude that clear effects not only on growth parameters and biomass allocation of Scots pine but also combinational effects on cell growth and cell wall formation can be expected if atmospheric CO_2 concentration will increase further and air temperature will continue to rise.

3.1.3 Analyses of hardwoods

3.1.4 CO_2 and temperature effects on the parenchyma content – A case study on European beech

3.1.4.1.1 Material and methods

In this study juvenile beech material was used, which derived from the CO_2 x temperature experiment in Berlin.

- Measurement of parenchyma and vessel content

From the basal stem part of each tree 20µm thick cross sections were cut with a sliding microtome (SM2000R, Leica). The sections were stained with Safranin and Astrablue and mounted on glass slides with Euparal.

The measurements of the tissue types were performed on the last growth ring. A transmitted light microscope (Laborlux S, Leitz) equipped with a video camera (15/3, Kappa) and a digital imaging software (QWin 2.8, Leica Microsystems) was used to estimate the tissue content of parenchyma and vessels. The tissue content was estimated in terms of cross sectional area covered by the different tissue types. The segmentation of the tissue types was done manually on images. On two opposite radii images with a magnification of 40 were used to detect wood rays which were wider than 5 cell rows (Fig. 3.12). Under a magnification of 200 six images per radius were taken to measure the content of wood rays with a width of one to five cell rows, of the axial parenchyma and of the xylem. At this magnification the combination of microscope and digital imaging system resulted in a resolution of 0.68 µm per pixel. The tree

ring area of the last growth ring was used to calculate the absolute values of the content of the tissue types.

- Statistical methods

All statistical analyses were performed with the SAS 8.02 software package (SAS Institute). Differences between the CO_2 concentrations, temperature treatments and their combinational effects were tested for significance with a two-factorial analysis of variance (ANOVA) for fixed effects by using the single plants as replicates.

The homogeneity of variance between the experimental groups was tested with the Levene's-test, and the distribution within the groups was tested for normality with a Shapiro Wilk-test.

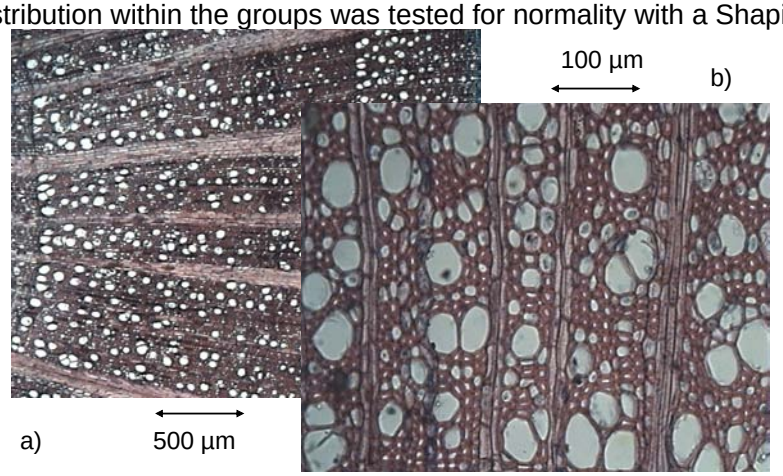

Figure 3.12: Cross sections of wood from European beech, stained with Safranin and Astrablue.

The parenchyma and vessel content was estimated on cross sections.

Differences between groups were tested with a Bonferroni t-test in cases of significant differences between the groups.

Furthermore, a linear regression was fitted between the variables and the temperature in the different treatments as regressor by using the single plants as replicates. It was tested whether the assumption of linearity was significant and whether the slope deviated significantly from zero.

Table 3.4: Statistics of a 2-factorial ANOVA and a regression of the variables against temperature level. If the 2-factorial ANOVA did not indicated a CO_2 or a combined temperature x CO2 effect, then the regression of the variables against temperature was performed with all samples per temperature level regardless of the CO_2 level; with -: not significant; ( ): $p < 0.1$; +: $p < 0.05$; ++: $p < 0.01$; +++: $p < 0.001$

	2-factorial ANOVA (p)			Regression ~T	
	CO_2	temperature	CO_2 * temperature	r^2	A > 0 (p)
Cross sectional area	-	(0.09)	-	0.85	++
Tree ring area	-	-	-	0.39	-
Leaf area	-	+	-	0.88	+++
Leaf area / Tree ring area	-	(0.06)	-	0.87	++

3.1.4.1.2 Results

While there were no differences between the CO_2 regimes in total cross sectional area it increased with increasing temperature (Table 3.4). At the highest temperature regime the cross sectional area was 32% larger (Figure 3.13). The tree ring area of the last year didn't show that tendency (Table 3.4). In the last year more leaf area per unit tree ring area was produced with increasing temperature. The increase amounted to 67% comparing the highest with the lowest temperature regime (Figure 3.13).

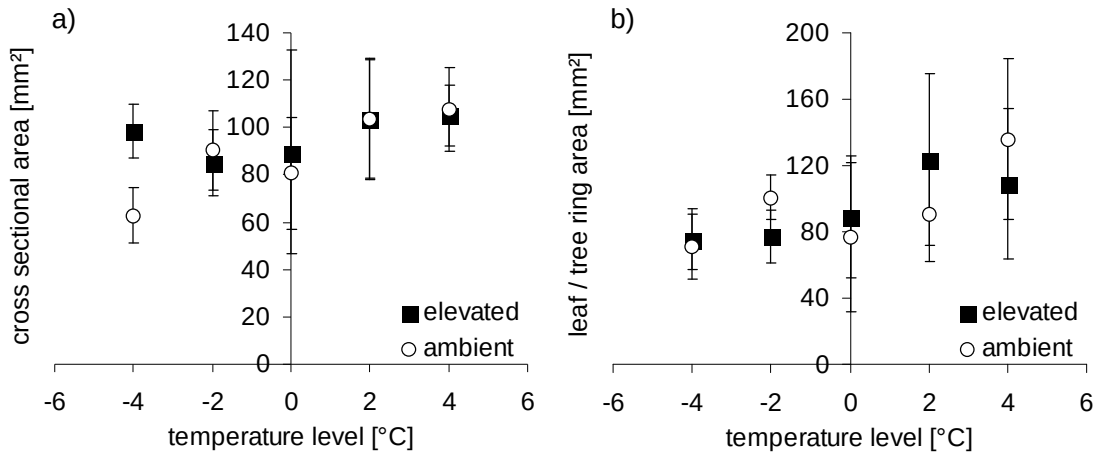

Figure 3.13: Cross sectional area (a.) and the ratio of leaf area to tree ring area (b.) in relation to the temperature differences of the treatments; with •: ambient CO_2 concentration, •: elevated CO_2 concentration.

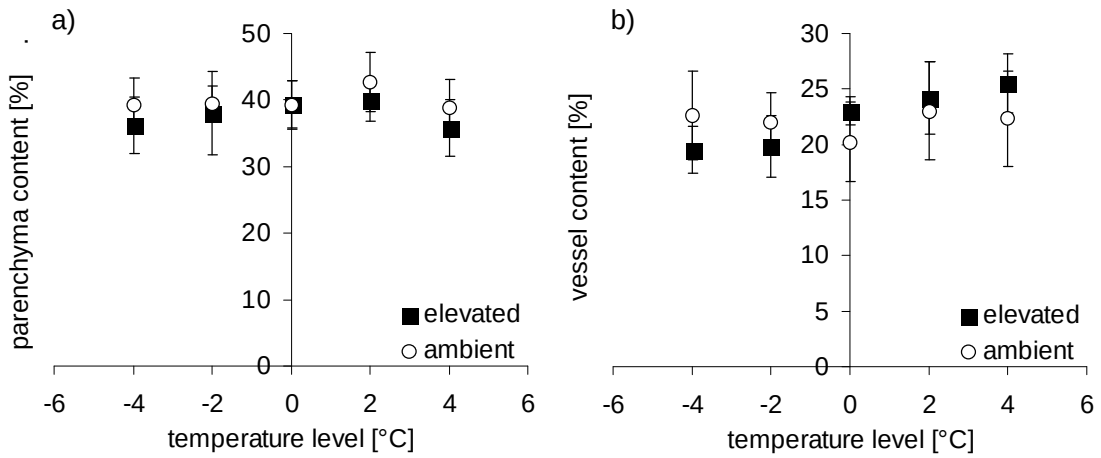

Figure 3.14: Parenchyma a) and vessel b) content of the last growth ring in relation to the temperature differences of the treatments; with •: ambient CO_2 concentration, •: elevated CO_2 concentration.

Using the tree ring area for scaling up the relative parenchyma content of the last tree ring the results do not indicate significant differences between the treatments (Table 3.5). The up scaled absolute values of vessel area show the tendency to increase with increasing temperature.

There were no differences in the ratios of tissue types between the treatments. The mean parenchyma content was 39%, the mean vessel content was 22% (Figure 3.14). The vessel content at elevated CO_2 tended to increase with increasing temperature (Table 3.4); it was 38% higher at the highest temperature regime compared to the lowest. At ambient CO_2 the vessel content didn't show that tendency.

Table 3.5: Statistics for the microscopical wood properties. If the 2-factorial ANOVA indicated no combined temperature x CO_2 effect, a regression of variables against temperature was performed with all samples per temperature level regardless of CO_2 level. With e. = regression was performed only for samples at elevated CO_2 levels. (-) not significant; +: $p < 0.05$; ++: $p < 0.01$; +++: $p < 0.001$

	2-factorial ANOVA (p)			Regression ~T	
	CO_2	temperature	CO_2 * temperature	r^2	A > 0 (p)
Rel. vessel content	-	(0.09)	(0.09)	0.95 (e.)	+++ (e.)
Rel. parenchyma content	-	-	-	0.02	-
Abs. vessel content	-	-	-	0.84	-
Abs. parenchyma content	-	-	-	0.16	-

3.1.4.1.3 Discussion

The constant parenchyma content could be due to the ontogenetic stage. It can be assumed that the high content of medullar rays overshadows environmental effects on secondary ray content and axial parenchyma content. An increase in vessel area with temperature (found in former studies) is lacking. Constant air humidity levels in the experimental setup may have caused this.

3.1.4.2 CO_2 effects on the fibre length - A case study on three Poplar species

3.1.4.2.1 Material and methods

In this study wood from the poplar species P. x euramericana, P. nigra and P. alba was analysed. 3-year old stems taken from the first rotation cycle at the POP-EUROFACE experiment (see chapter 2, monitoring) were used for the analyses. All the above-ground components were dried for 5 days at 70° C before being weighed. Each stem was divided into three parts according to the three height growth increments (HGIs).

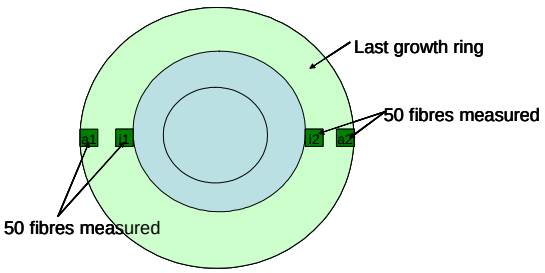

Figure 3.15: Sampling of wood for the analyses. Four sub-samples per tree (N=70) were taken: At two opposite sites one from the beginning and one from the end of the last growth ring.

Samples were taken at two opposite sides of 70 stems from the third tree ring of the lowest HGI for measurements of fibre length. On each side, one piece of wood was cut from the beginning of the tree ring (Figure 3.15); from the other side, one was cut from the ending of the tree ring (together four pieces per sample). The four sub-samples were separately macerated, stained and mounted on glass-slides with conventional methods. The length of 50 fibres, which were straight, fully macerated and non-damaged, was measured in each sub-sample (together 200 fibres per tree) with the aid of transmitted light microscopy and the use of a digital imaging system.

3.1.4.2.2 Results

Fibres were significantly longer at elevated CO_2; also differences between species were statistically significant (Figure 3.16; Table 3.6). Mean fibre length increased with increasing CO_2 for P. alba from 877 µm to 939 µm (7%); for P. nigra from 804 to 834 µm (5%) and for P. x euramericana from 834 to 855 µm (3%). P. alba, the species which had the longest fibres, produced less biomass and smaller basal area (Figure 3.16) than the others. In P. alba and P. x euramericana fibre length at the ending of the growth ring tended to increase with increasing basal area (r2: 0.37-0.74) within species and treatment. Fibres at the beginning of the growth ring did not show that tendency.

Table 3.6: Statistics from repeated two-factorial analysis of variance; (-) not significant; + : $p < 0.05$.

	fibre length				growth		
2-factorial ANOVA	egs	lgs	total	egs/ lgs	heigth	basal area	bio-mass
species	+	+	+	+	-	+	(0.07)
treatment	+	+	+	-	+	+	+
species * treatment	-	(0.07)	-	-	-	-	-

Fibres at the end of the growth ring were approximately 11% longer than fibres at the start of the ring. The ratio between fibre lengths from start and end of the tree ring showed no significant differences between treatments, but it was higher in *P. x euramericana* compared to *P. nigra* .

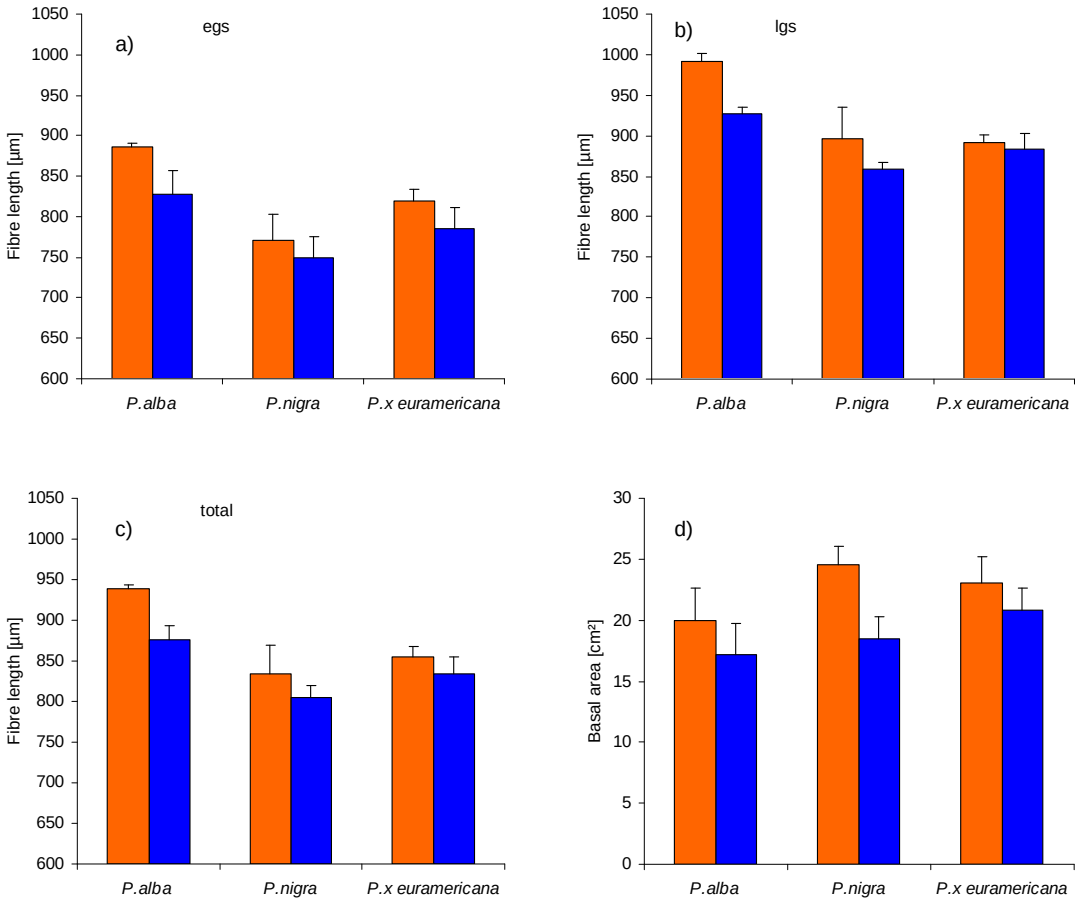

Figure 3.16: Fibre length of the wood from a) the beginning of the growth ring (egs), b) the ending of the growth ring (lgs) and c) total mean (lgs + egs) fibre length of the wood and d) basal area of the stems of the three poplar clones and the two CO_2 treatments. Blue = ambient CO_2 air concentrations, red = elevated CO_2 air concentrations (550 µmol mol-1).

3.1.4.3 Discussion

Fast growing tree species usually show the greatest response to increased CO2 air concentrations. Consequently short rotation cultures (SRC) with Populus-species could increase their productivity under global change.

Earlier studies on the same plants have shown that future CO2 concentrations enhance growth of juvenile poplars in short rotation cultures. This will be accompanied by an increase in fibre length. The quality of pulp is related to fibre length and thus will increase under elevated CO2 concentrations. Nevertheless the increase in fibre length is low compared to the enhancement of tree growth.

3.1.4.4 References

Antonova, G., Cherkassin, V.P., Stasova, V.V., and Varkasina, T.N. (1995). Daily dynamics in xylem cell radial growth of Scots pine (Pinus sylvestris L.) *Trees - Structure and Function* **10:** 24-30.

Bannan, M.W., (1962) 3-21. In: Tree Growth, (ed T.T. Koszlowki), Ronald Press, New York.

Bruhn, D., Leverenz, J.W., and Saxe, H. (2000). Effects of tree size and temperature on relative growth rate and its components of Fagus sylvatica seedlings exposed to two partial pressures of atmospheric CO2. *New Phytologist* **146:** 415-425.

Ceulemans, R., Jach, M.E., Van De Velde, R., Lin, J.X., and Stevens, M. (2002). Elevated atmospheric CO2 alters wood production, wood quality and wood strength of Scots pine (Pinus sylvestris L) after three years of enrichment. *Global Change Biology* **8:** 153-162.

Conroy, J.P., Milham, P.J., Mazur, M., and Barlow, E.W.R. (1990) Growth, dry matter partitioning and wood properties of Pinus radiata D. Don. after 2 years of CO2 enrichment. *Plant, Cell and Environment* **13**: 329-337.

Donaldson, L.A., Hollinger, D., Middleton, T.M., and Souter, E.D. (1987) Effect of CO2 enrichment on wood structure in Pinus radiata D. Don. *IAWA Bulletin* **8:** 285-295.

Evans, R., 1994: Rapid measurement of the transverse dimensions of tracheids in radial wood sections from Pinus radiata. *Holzforschung* **48:** 168-172.

Fritts, H.C., (1976). Tree rings and climate. Academic press, London.

Horacek, P., Slezingerova, J., Gandelova, L., 1999: Effects of Environmant on the Xylogenesis of Norway spruce. In: *Tree-ring analysis. Biological, methodological and environmental aspects* eds. R. Wimmer and R.E. Vetter, CABI Publishing, Wallingford, UK. pp 33-54

Kilpeläinen, A., Peltola, H., Ryyppo, A., Sauvala, K., Laitinen, K. and Kellomäki, S. (2003). Wood properties of Scots pines (Pinus sylvestris) grown at elevated temperature and carbon dioxide concentration. *Tree Physiology* **23:** 889-897.

Larson, P.R. (1994). The vascular cambium. Development and structure. Springer-Verlag, Berlin.

Lee, J., and Rosen, D. (1985). On the use of automated microscopy in wood research. *Holzforschung* **39**: 1-6.

Möell, M.K., and Donaldson, L.A. (2001). Comparison of Segmentation Methods for Digital Image Analysis of Confocal Microscope Images to Measure Tracheid Cell Dimensions. *IAWA Journal* **22:** 267-288.

Morison, J.I.L. and Lawlor, D.W. (1999). Interactions between increased CO2 and temperature on plant growth. [Commissioned Review] for *Plant, Cell and Environment* **22:** 659-682.

Panda, D. P., and Rosenfeld, A. (1978). Image Segmentation by Pixel Classification in (Gray Level, Edge Value) Space. *IEEE transactions on computers* **27:** 875-879.

Park, W.K. and Telewski, F.W. (1993). Measuring Maximum Latewood Density by Image analysis at the Celluar Level. *Wood and Fibre Science* **25:** 326-332.

Ranefall, P.K., Wester, K., and Bengtsson, E. (1998) Automatic quantification of immunohistochemically stained cellnuclei using unsupervised image analysis. *Analytical Cellular Pathology* **16:** 29-43.

Rigling, A., Bruhlhart, H., Braker, O.U., Forster, T. and Schweingruber, F.H. (2003). Effects of irrigation on diameter growth and vertical resin duct production in Pinus sylvestris L. on dry sites in the central Alps, Switzerland. *Forest Ecology and Management* **175:** 285-296.

Sass, U. and Eckstein, D. (1994). Preparation of large thin sections and surfaces of wood for automatic image analysis. *Holzforschung* **48:** 117-118.

Schnell, G.R., and Sell, J., 1989: *Holzforschung* **47:** 351-354.

Skene, D.S. (1969). The period of time taken by cambial derivatives to grow and differentiate into tracheids in Pinus radiata. *Annals of Botany* **33:** 253-262.

Spieker, H., Schinker, M., Hansen, J., Park, Y, Ebding, T. and Döll, W. (2000). Cell structure in tree-rings: Novel methods for preparation and image analysis of large cross section. *IAWA Journal* **21:** 361-373.

Stephan, G., 1967: Untersuchungen uber die Anzahl der Karzkanäle in Kiefern (Pinus sylvestris) *Archiv Forstwesen* **16:** 461-470.

Telewski, F.W. and Strain, B.R., 1987: 726-732. In: *Proceedings of the International Symposium on Ecological Aspects of Tree Ring Analysis*, eds. G.C. Jacoby and J.W. Hornbeck. Nat Tech Inf Ser, Springfield.

Telewski, F.W., Swanson, R.T., Strain, B.R., Burns, J.M. (1999). Wood properties and ring width responses to long-term atmospheric carbon dioxide enrichment in field-grown loblolly pine (Pinus taeda L.). *Plant, Cell and Environment* **22**: 213-219.

Uggla, C., Magel, E., Moritz, T., and Sundberg, B. (2001). Function and Dynamics of Auxin and Carbohydrates during Earlywood/Latewood Transition in Scots Pine. *Plant Physiology 125:* 2029-2039.

Wimmer, R., Grabner, M., Strumia, G., and Sheppard, P.R. (1999). Significance of vertical resin ducts in tree rings of spruce. In: *Tree-ring analysis. Biological, methodological and environmental aspects*. eds, R. Wimmer and R.E. Vetter. CABI Publishing, Wallingford, UK pp 33-54

Whitmore, F.W. and Zahner, R. (1966). Development of the xylem ring in stems of young red pine trees. *Forest Science* **12:** 198-210.

Wodzicki, T.J. (1971). Mechanisms of xylem differentiation in Pinus silvestris L. *Journal of Experimental Botany* **22:** 670-687.

Zamski, E. (1972). Temperature and photoperiod effects on xylem and vertical resin duct formation in Pinus halepensis Mill. *Israel Journal of Botany* **21:** 99-107.

3.2 Analyses of wood biochemical properties in laboratory conditions

3.2.1 Overview

The main objective was to analyse a selected number of biochemical components of wood material from the monitoring sites and from all main plant compartments harvested in the experiments (Appendix K). This included total carbon and total nitrogen analyses as well as quantitative analytical determination of **glucose, fructose, sucrose and starch ('non-structural carbohydrates')** and of cell wall components ('structural carbohydrates').

Biochemical analyses
total C/N content of wood (also for other compartments e.g. leaf, branch, stem, fine and coarse roots)
'non-structural' and 'structural carbohydrate content'

'Structural carbohydrates':
cellobiose*
rhamnose,mannose,
arabinose,galactose,
xylose, cellulose (as glucose units), total lignin (flavone-lignin).

*: cellobiose in a few cases only.

List of tree species:

Juvenile trees (from experiments, mostly all plant compartments)*:

Pinus sylvestris Scots pine
Fagus sylvatica European beech

Adult trees from stands (mostly disks from stems)*:

Pinus sylvestris (Belgium, England, Germany)
Picea sitchensis (England)
Quercus robur et *petraea* (England)**
Picea abies (England)**
Fagus sylvatica (Italy)**

* ordered according to the number of chemical analyses; ** data were stored but not interpreted by partner 4.

3.2.2 Nitrogen

3.2.2.1 Method

Dry mass (85 °C) from harvests at the experimental sites as well as from the disks taken at the forest stands was powdered. Total C- and N- contents of this material [% of dry mass] were determined thermo-conductometrically (Leco-Instruments). Data were stored and documented in the data base (FR). Juvenile *Pinus sylvestris* of the experimental site in Berlin were all harvested in September 2001 C and N-contents of powdered fine roots, coarse roots and all four stem sections and three stem sections of the juvenile Scots pines were determined. The three annual needles sets of these trees were analysed separately. Mass from harvests of *Fagus sylvatica*- roots saplings, collected in 1999, 2000 and 2001 (final harvest) at the Berlin tertiary site, were separately dried and analysed. Data that were obtained from this experiment in Berlin were evaluated by partner 4. Wood samples were taken by means of a corer from bark (partly), sapwood, transition zone between sapwood and heartwood (bigger disks only) and from heartwood of the disks of the adult trees. This material was also homogenized before the chemical analyses. All data were sent to the data base (FR).

3.2.2.2 Results (juvenile trees)

Pinus sylvestris

It is planned to publish the results of the juvenile trees together with data from the carbohydrate analysis in a peer-reviewed journal 2005/06.

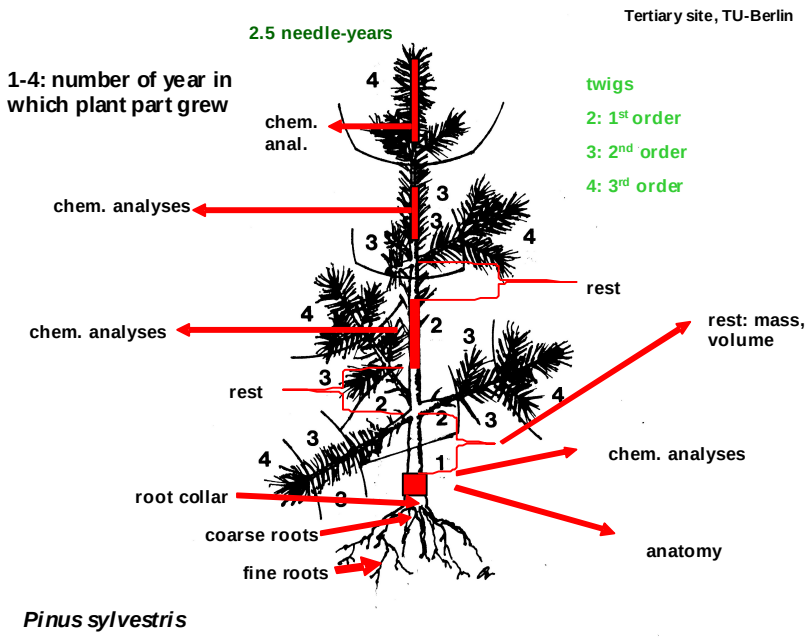

Figure 3.17: Scheme of the samples taken from four-year-old Scots pines grown for three years at two different CO_2 concentration and five different temperature levels in phytotron chambers at the TU-Berlin.

Nitrogen concentrations [%] of all needles were decreased at elevated CO_2 on the average. This was statistically significant in the needles of the last year and those from the year before the last one. In twigs no CO_2 influence on N concentrations could be detected. Whereas, with the exception of the oldest stem part, concentration was also lower in the stems.

By calculating the total amounts of nitrogen in the plant organs it could be shown that relative differences in percent are equalized in most cases because of positive CO_2 effect on biomass accumulation (enhancement)..

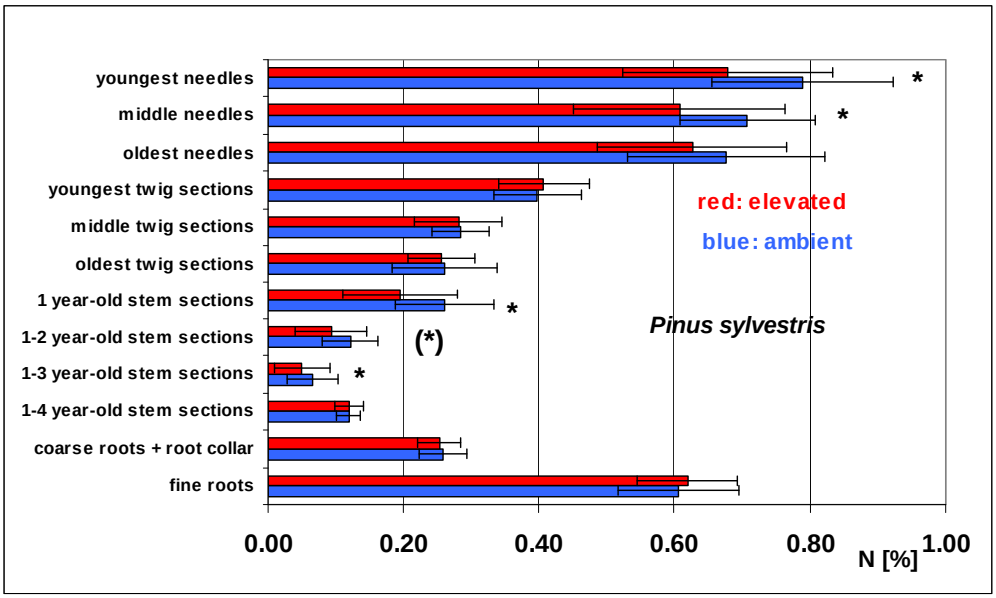

Figure 3.18: N concentration in different organs of juvenile *Pinus sylvestris* at ambient air and at elevated (700 µmol mol^{-1}) CO_2; *: p <0.05, (*): p: 0.05 – 0.1 after tthree years; data pooled for the factor CO_2 alone.

Table 3.7: Table 1: Absolute N-amounts in different compartments of juvenile *Pinus sylvestris* at temperature levels lowered (low: -4 and -2 °C)) and elevated (high: +4 and +2 °C) relative to the mean temperature levels at Berlin-Dahlem after three years; data pooled for the factor temperature alone.

N [g]/tree									
	temperature								
Plant compartment	low		high						
	mean	standard dev.	mean	standard dev.	p	n	significance	• in [g]	• in %
fine roots	**0.1813**	0.1516	**0.2351**	0.1047	0.0801	24	(n.s.)	**0.0538**	29.7
coarse roots	**0.0269**	0.0157	**0.0205**	0.0056	0.0396	23,22	*	**-0.0064**	-23.7
coarse roots with root collar	**0.0393**	0.0265	**0.0280**	0.0064	0.0265	24,22	*	**-0.0113**	-28.7
1-4- year-old stem sections	**0.0029**	0.0020	**0.0022**	0.0013	0.0941	24	(n.s.)	**-0.0006**	-22.4
1-3- year-old stem sections	**0.0029**	0.0017	**0.0023**	0.0017	0.1913	12	n.s.	**-0.0006**	-21.1
1-2 year-old stem sections	**0.0048**	0.0028	**0.0040**	0.0020	0.2135	12	n.s.	**-0.0008**	-16.8
1- year-old stem sections	**0.0054**	0.0031	**0.0051**	0.0030	0.4061	12	n.s.	**-0.0003**	-5.6
total stems (sum)	**0.0160**		**0.0136**					**-0.0024**	-14.8
oldest twig sections	**0.0059**	0.0028	**0.0048**	0.0033	0.1133	24	n.s.	**-0.0011**	-18.4
middle twig sections	**0.0103**	0.0058	**0.0111**	0.0043	0.3075	24	n.s.	**0.0007**	7.2
youngest twig sections	**0.0253**	0.0104	**0.0211**	0.0060	0.0500	24	*	**-0.0041**	-16.4
total twigs (sum)	**0.0415**		**0.0370**					**-0.0045**	-10.8
oldest needles	**0.0310**	0.0156	**0.0131**	0.0140	0.0001	24	***	**-0.0179**	-57.6
middle needles	**0.1180**	0.0403	**0.1263**	0.0312	0.2148	24	n.s.	**0.0083**	7.0
youngest needles	**0.2297**	0.0676	**0.2176**	0.0374	0.2236	24	n.s.	**-0.0121**	-5.3
total needles (sum)	**0.3787**		**0.3571**					**-0.0217**	-5.7
means of total N amounts	**0.6568**		**0.6708**					**0.0140**	**2.1**

Total nitrogen amounts which were accumulated in dependence of temperature elevation were also tested statistically. In youngest and oldest needle, in coarse roots with root collar and coarse roots alone significantly less nitrogen was found. The only organ which contented absolutely more nitrogen at higher temperatures was the fine root.

Fagus sylvatica

At elevated CO_2 concentration N-contents [% of dry mass] were smaller in leaves of the juvenile *Fagus sylvatica* only but not in fine roots, coarse roots and the older (4 years) part of stem. As an example figure 3 only shows the timely course for the N-concentration in stems. In the long-run (over 3 years) N-contents decreased in all plant compartments, most evidently in stems and coarse roots and less in leaves. In general there was no clear temperature effect of N-uptake of fine roots, coarse roots and stems within the temperature range of 8 °C given by the experimental set-up (minus 4 – local mean – plus 4 °C, Figure 3.19).

Whereas a possible slight negative effect of lower temperature regimes on the N-uptake of leaves was diminished by the additional CO_2 supply in tendency.

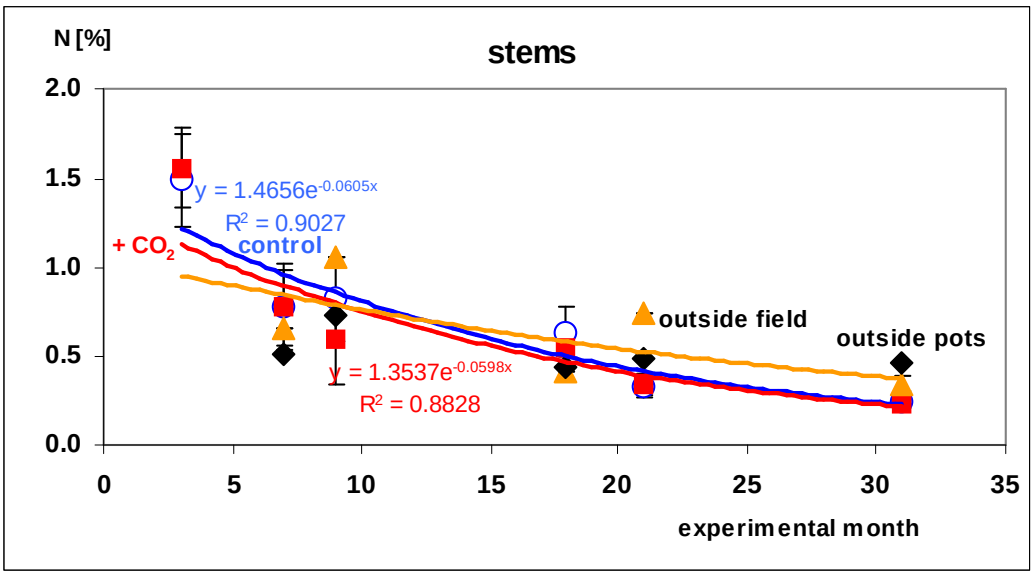

Figure 3.19: N-concentration of stem dry mass of beech saplings grown at elevated CO_2 (~700 µmol mol^{-1}, filled squares) and ambient air CO_2 concentration (open circles: control chambers with ambient CO_2 concentration) in comparison with outside pots and saplings growing in the field; data pooled for the CO_2 factor alone.

3.2.2.3 Results (adult trees)

The vertical pattern of nitrogen distribution in the 50-year-pold *Pinus sylvestris* from the primary site in Grunewald was clearly different from that of the juvenile trees (Figure 3.20). Most evident were the high percentages of nitrogen in the branches and the decrease in concentration in the needles from the bottom to the top of the crown.

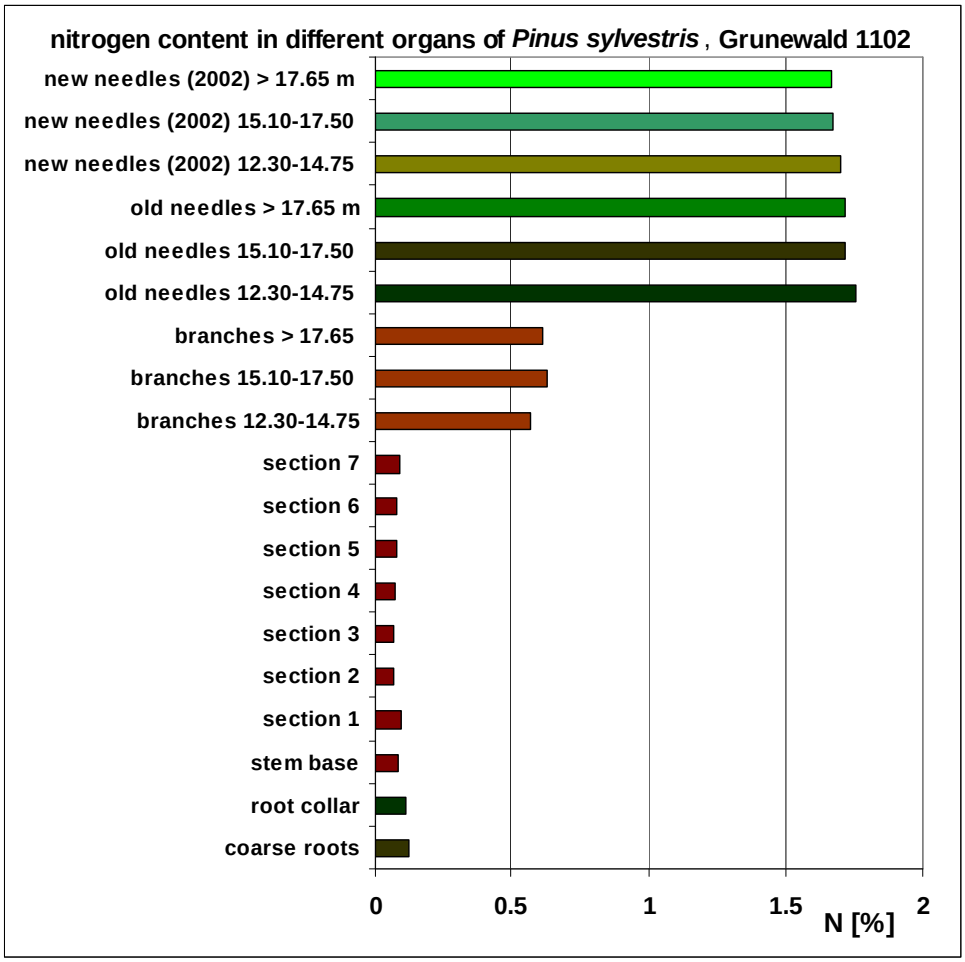

Figure 3.20 : Nitrogen distribution in one representative 50-year-old *Pinus sylvestris* from the primary site 1102 in Berlin /Grunewald.

In the disks from England, Belgium and Germany nitrogen contents decreased horizontally from the periphery of the stem towards the centre (compare the example in Figure 3.21).

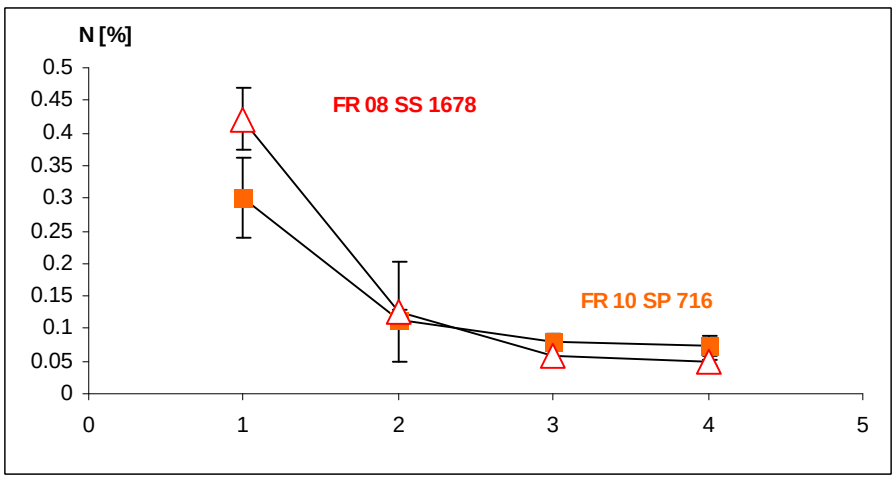

Figure 3.21: Horizontal distribution of Nitrogen [%] in stem base disks; bark (1), youngest sapwood (2), transition zone (3), to heartwood (central wood, 4) of *Pinus sitchensis* (SS) and *Pinus sylvestris* (SP) from primary sites in England.

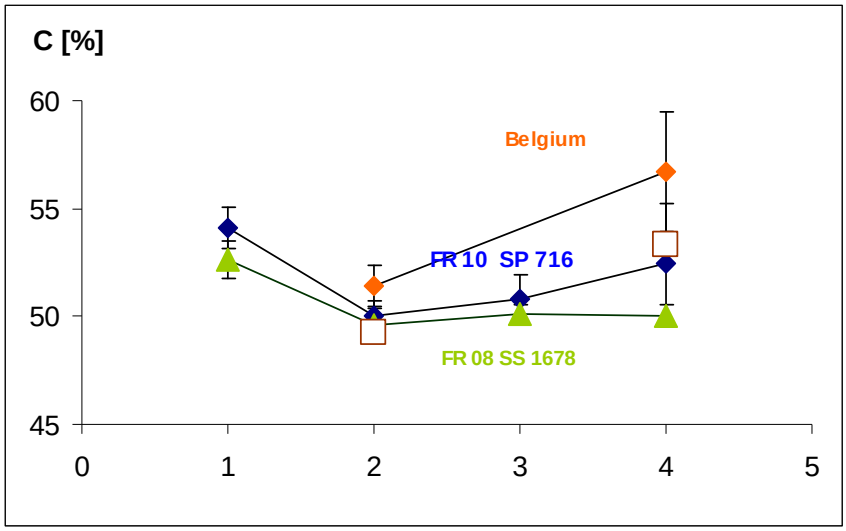

Figure 3.22: Total carbon concentrations [%] in base disks from bark (1), to youngest sapwood (2), to transition zone (3), to heart wood (centre wood, 4) of Scots pine (SP) , Sitka Spruce (SS) in England and Scots pine from Belgium (on top) and Germany, •: Scots pine from Grunewald/Berlin.

3.2.2.4 Results (Carbon concentration, juvenile trees)

Carbon concentrations remained almost unchanged horizontally from the periphery towards the central wood of Sitka spruce basal stem disks (SS, England) whereas carbon concentrations increased slightly but significantly from outside to inside in basal stem disks of all Scots pine disks (England, Germany and Belgium (Figure 3.22)). Carbon concentrations of the oldest pines of this study from Belgium were the highest and their horizontal increase was the most obvious of this study.

3.2.3 Non-structural carbohydrates

3.2.3.1 Methods

Glucose, fructose, sucrose and starch contents of the Scots pine powdered samples from the monitoring sites in England, Belgium and Germany and the same substances in the needles and stems of the juvenile Scots pine at the CO_2 x temperature experiment in Berlin (phytotron) were determined with enzymes (Boehringer-Corporation methods) after fractionated extraction. The mono-saccharides glucose, fructose and the disaccharide sucrose were extracted with methanol for this procedure and glucose subunits of starch were obtained by enzymatic hydrolysis with • -amylase and amylo-glucosidase for the enzymatic determination.

The three needle groups (1-3- year-old) of the experimental plants were analysed separately.

In order to get enough material from the disks of the adult trees for the analyses, wood powder left over from the C/N-analyses had to be combined and mixed from all disks of suppressed trees in one pool, subdominant together and dominant trees together, in order to get enough material for the analyses.

8.2.2 Results, juvenile trees

At first all data were pooled for the CO_2 factor only (regardless of the temperature level of the CO_2 x temperature experiment in Berlin). It is planned to publish these data together with the outcome of the C/N analyses in 2006.

Stem wood

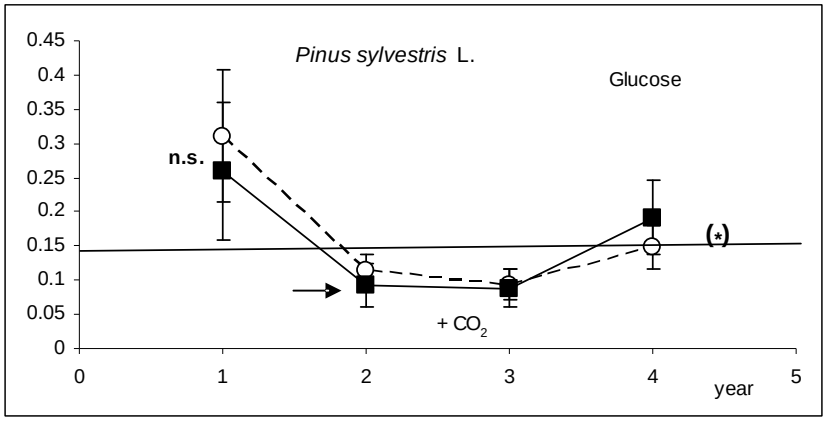

Figure 3.23: Glucose concentrations in 4- year-old Scots pine stems (experiment, Berlin) grown at elevated (~700 µmol mol^{-1}, •) and ambient air CO_2 concentration (~390 µmol mol^{-1}, •); number 1 - 4: year in which the stem section was developed; n = 16; 1: oldest section; n.s.: not significant, (*): $p < 0.1$; the horizontal line in fig. 7 marks the sensitivity limit of the biochemical method.

No statistically significant differences could be found in response to the two different CO_2 concentration levels of the experiment. At the top of the stems (year 4) there was a certain tendency ($p < 0.1$) for a positive CO_2 effect on glucose contents (Figure 3.23). Fructose and sucrose showed a similar accumulation in the stem section at the bottom of the sapling but no tendency of being increased by the elevated CO_2 supply. Therefore,, data are not presented here. All relative contents of those three soluble non-structural carbohydrates were not influenced by the temperature levels of the experiment.

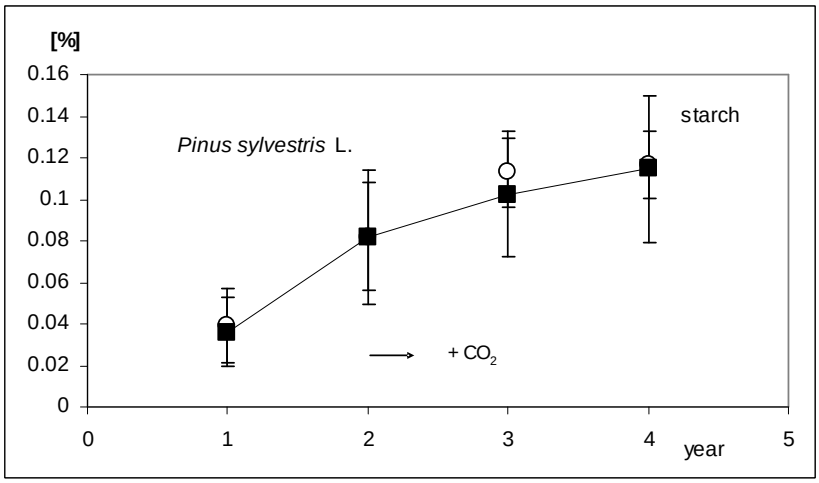

Figure 3.24: Starch concentrations in 4- year-old Scots pine stems grown for 3 years at elevated (~700 µmol mol l^{-1}, •) and ambient air CO_2 concentration (~390 µmol mol^{-1}, •); number 1 -4: year in which the stem section was developed; n = 16 (1: oldest section: four-year-old); data pooled for the CO_2 factor alone.

Methodical limits were also tested for starch analyses and it was found that reliability started with contents above 0.08%.

The traces of starch of stem wood material (Figure 3.24) showed an opposite trend along the stem in comparison with the soluble carbohydrate contents (Figure 3.23). It increased from the bottom to the top of the stem. Means - calculated for the two different CO_2 concentration levels (not regarding the temperature factor) – were almost identical. These results indicated that there was a small starch accumulation in the top shoot in September which could be retrenched in autumn and winter or used for the new flush in the coming spring. In contrast to

the soluble no-structural carbohydrates, starch also showed a certain tendency to decrease slightly with increasing temperature (Figure 3.25, all data pooled for the 5 different temperature levels, regardless of the CO_2 concentration).

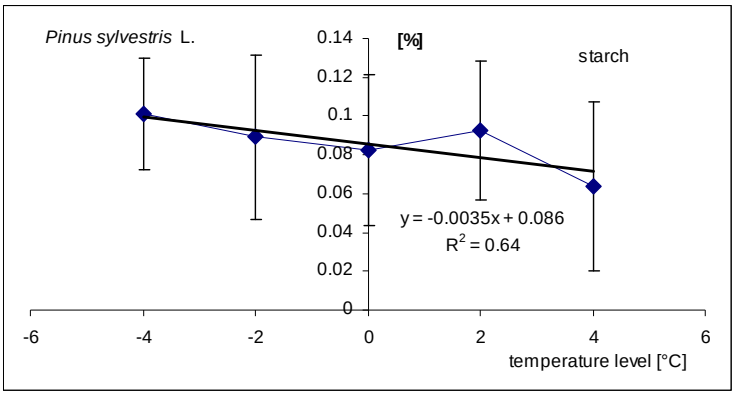

Figure 3.25: Starch concentration of stem wood of juvenile Scots pine at final harvest grown for 3 years at five different temperature levels (- 4, -2, 0 = base, +2, +4 °C); zero-line: temperature reference base = long-term local annual monthly mean temperature (day and night) in Berlin-Dahlem (Germany).

Needles

All values of glucose, sucrose, fructose and starch of the needle samples from *Pinus sylvestris* (experiment, Berlin) were clearly above the sensitivity limit of the analytical method.

There was neither a clear CO_2 nor any evident temperature effect on glucose-, sucrose- and fructose-content (soluble carbohydrates) of the three annual needle sets of the juvenile Scots pine in that CO_2 x temperature experiment. Also the contents of these soluble non-structural carbohydrates were not affected by (needle) age. Therefore, these results are not presented in figures or tables here.

In contrast to the three soluble carbohydrates, starch showed a clear response to CO_2 and the combination of elevated CO_2 and temperature (Figure 3.26). Temperatures around the long-term annual mean showed the most evident CO_2 enhancement of starch accumulation of the used German provenance of Scots pine. In addition, there was a clear effect of the age at both the CO_2 concentration levels (Figure 3.27, independent from temperature and CO_2). On the average, starch contents were the lowest in the oldest annual needle set and the highest in the new needles from the last year of the experiment.

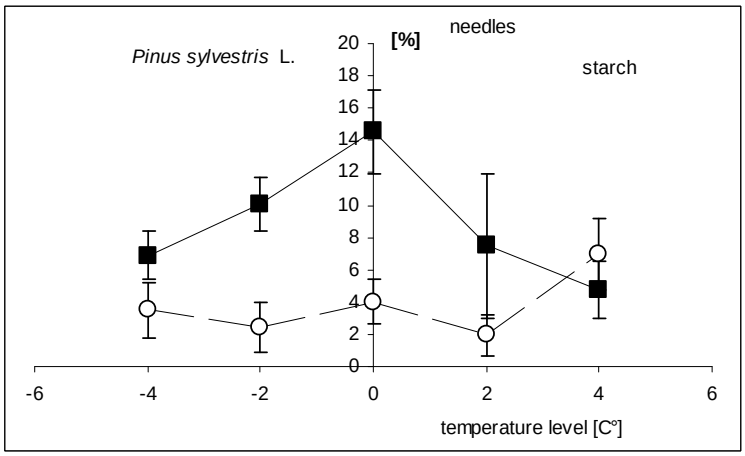

Figure 3.26: Starch content of Scots pine needles grown for 3 years at five different temperature levels(- 4, -2, 0 = base, +2, +4 °C; zero-line: temperature reference–base = long-term local annual monthly mean temperature (day and night) in Berlin- Dahlem) at elevated (~700 µmol mol-1, •) and at ambient CO_2 concentration (~390 µmol mol^{-1}, •).

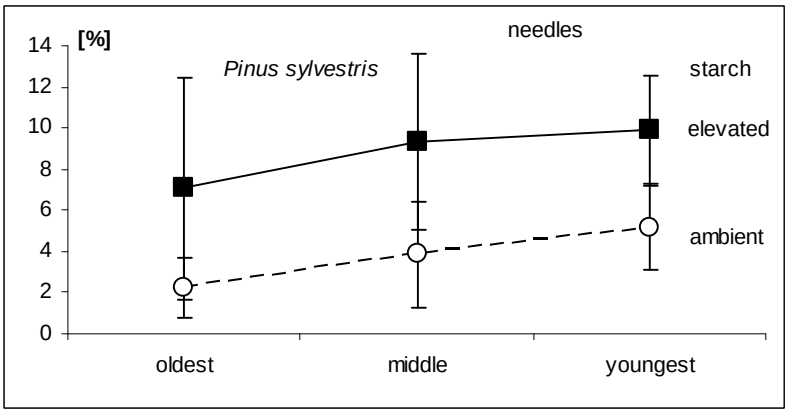

Figure 3.27: Starch content of the three annual needles sets (oldest, middle and youngest) on juvenile Scots pine grown for three years at elevated (~700 µmol mol-1, •) and at ambient CO_2 concentration (~390 µmol mol^{-1}, •); data pooled for the factor CO_2.

3.2.3.2 Results, adult trees

Soluble carbohydrates

All values below 0.1% of non-structural carbohydrates from the basal stem wood of adult trees were considered as traces like with the juvenile trees because they also could not be determined exactly enough (methodical limitation).

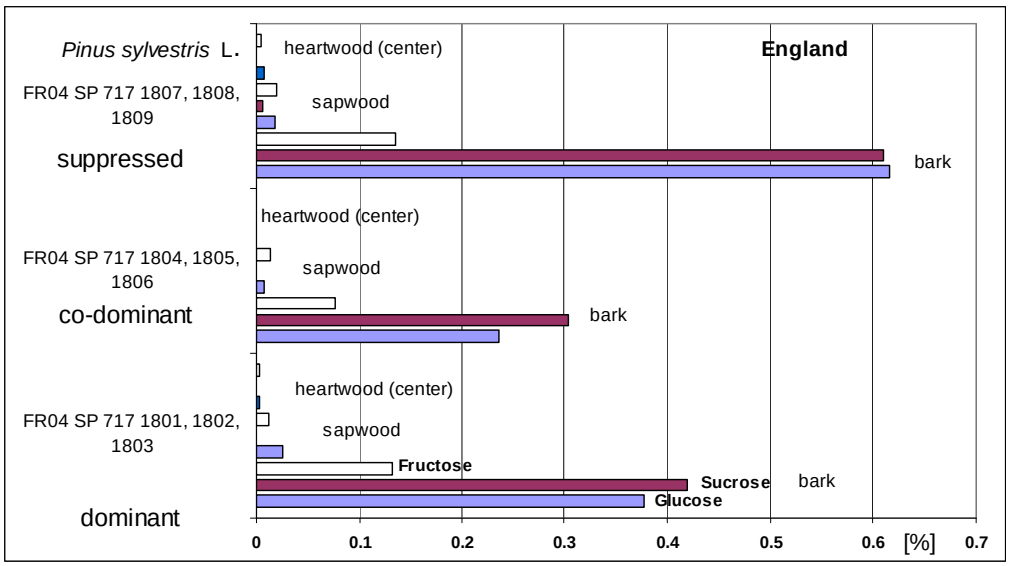

Figure 3.28: Glucose, sucrose and fructose contents in wood and bark from the basal stem log of dominant (1801, 1802, 1803), co-dominant (1804, 1805, 1806) and suppressed (1807, 1808, 1809) Scots pine (*Pinus sylvestris*, FR 04, Rannoch-UK).

Figure 12 stands as one example of the results which were obtained for the primary sites in the UK. Really measurable amounts could only be detected in the barks reaching the highest values in suppressed individuals. There was also a trend of increasing fructose contents from suppressed trees to dominant trees.

Contents of those soluble carbohydrates in the Scots pines of Brasschaat (Belgium) were the lowest in comparison with all other sites. There, only in the bark traces, slightly below the sensitivity limit of the method, were found. Therefore, these data are not presented here.

Starch

Differences in starch contents between the trees from the 3 different dominance classes could only be shown for the bark material again (example: FR 04, Rannock, UK, Figure 3.29). In the most dominant trees also in the periphery of the stem disk (youngest sapwood) a little more starch was accumulated than in the two other classes. However, there only traces of starch could be detected.

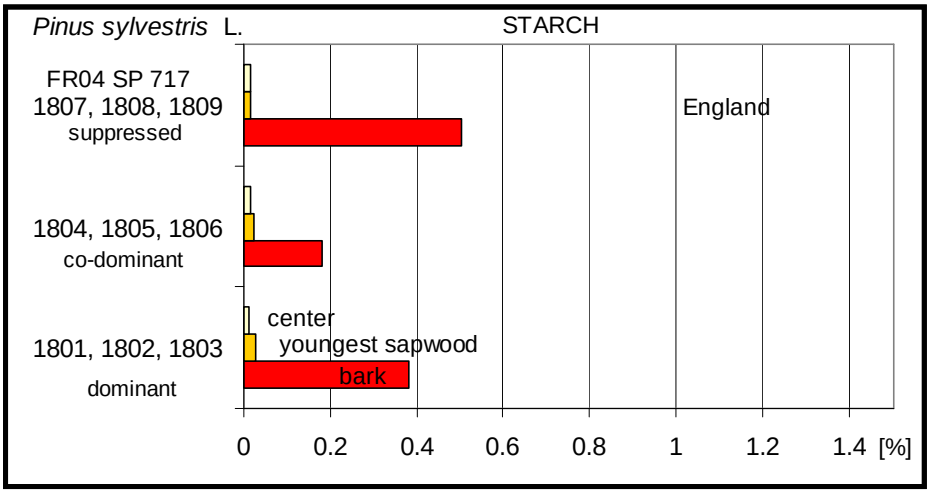

Figure 3.29: Starch contents in wood and bark from the basal stem log of dominant (1801, 1802, 1803), co-dominant (1804, 1805, 1806) and suppressed (1807, 1808, 1809) Scots pine (FR 04, Rannoch-UK).

Exceptionally high concentrations of starch were found in the bark and the youngest sapwood of Scots pine disks from the Belgian forest site in comparison with the other sites. And there was an increase of the starch traces in the youngest sapwood from dominant to suppressed trees.

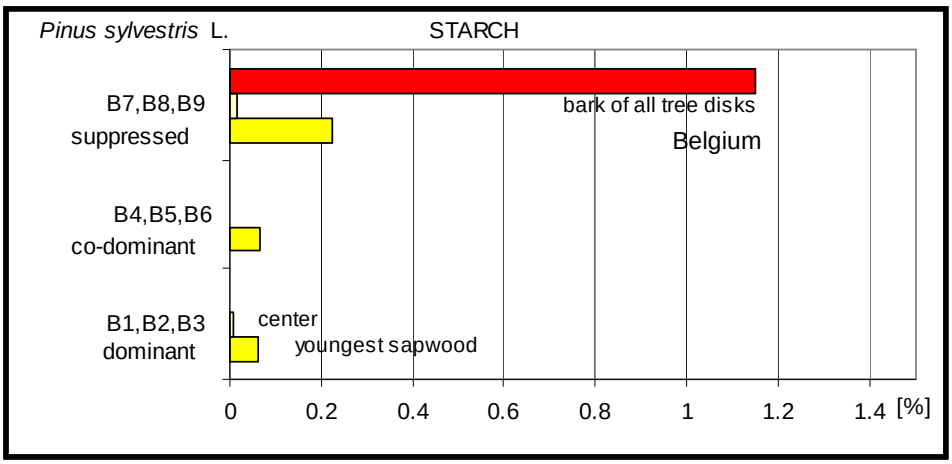

Figure 3.30: Starch contents in wood and bark from the basal stem log of dominant (B1, B2,B3), co-dominant (B4,B5,B6) and suppressed (B7,B8,B9) Scots pine in Brasschaat (Belgium).

The powdered samples from Grunewald (Berlin, Germany), taken at different stem heights (2-7), had to be mixed up together in order to get enough material for the analyses. (C/N and structural carbohydrate contents had been already determined before from the same material.)

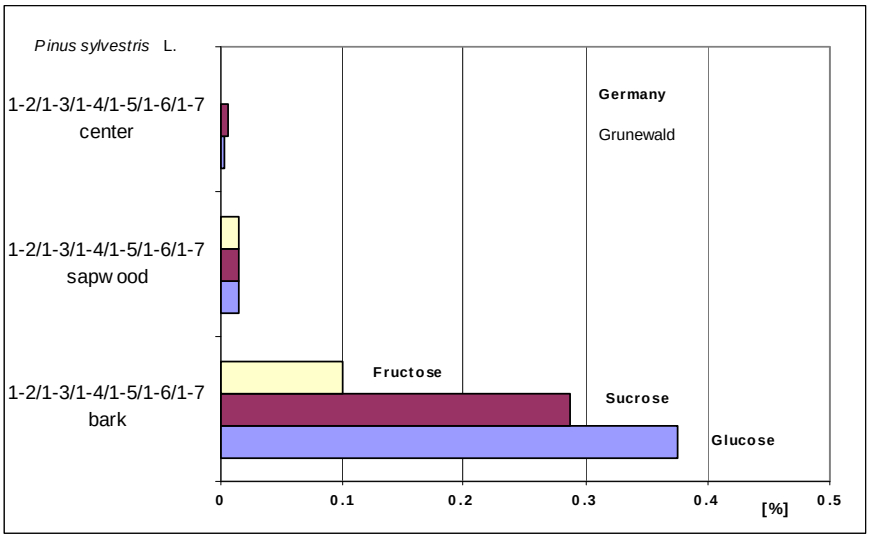

Figure 3.31: Glucose, sucrose and fructose contents in wood and bark of one Scots pine (*Pinus sylvestris*) in Grunewald , Berlin (Germany); lowest disk: 1-2 and highest disk: 1-7 (material from all five disks was homogenized).

The clear difference between sapwood and heartwood (centre) was as obvious as in the material from the other sites. Only a little sucrose was found in the central wood. Starch contents of the Grunewald pine was the lowest of all MEYFYQUE samples from *Pinus sylvestris* L. Therefore, those data are not presented here.

3.2.4 Structural carbohydrates

3.2.4.1 Methods

Structural carbohydrates of the solid material (wood from stems, so-called solid material) in cooperation with the Institute of Wood Chemistry of University of Hamburg (BFH, Dr. J. Puls) and the Institute of Food Chemistry of the TU-Berlin (a few samples in ring analyses). Samples were pre-prepared in the laboratory of partner 4 (Berlin) and components were quantified by means of a special HPLC-equipment for wood analyses in Hamburg except total lignin (flavone-lignin) which was determined gravimetrically in Berlin.

3.2.4.2 Results, juvenile trees

Rhamnose concentrations (Figure 3.32) increased evidently from the oldest (1-4th year) up to the youngest stem part (4th year). On the average, contents were higher in the youngest parts of the stems grown at ambient air than at air with CO_2 enrichment (700 µmol mol^{-1}). In contrast to rhamnose, mannose decreased from the bottom part of the stem towards the top reaching 10% of the dry mass in the oldest, basal stem section (Figure 3.32). At each stem height mean contents were higher at elevated CO_2 concentration. The higher the contents were the more significant the positive CO_2 effect became in the case of mannose. Arabinose increased from ~2% in the bottom stem part up to ~6% in the top shoot reaching significantly higher values in the stem sections from the trees which had been exposed to ambient atmospheric CO_2 concentration. Xylose decreased from the basal stem section towards the top shoot (~9 • ~6%) without significant differences between the two CO_2 levels. 4-O-methyl-glucuron-acid also decreased towards the top (~0.8 • ~0.4%) without clear CO_2 effects. Figure 3.32-Figure 3.36 represent (as examples) five of the eight components which were analysed in the solid material of the stems.

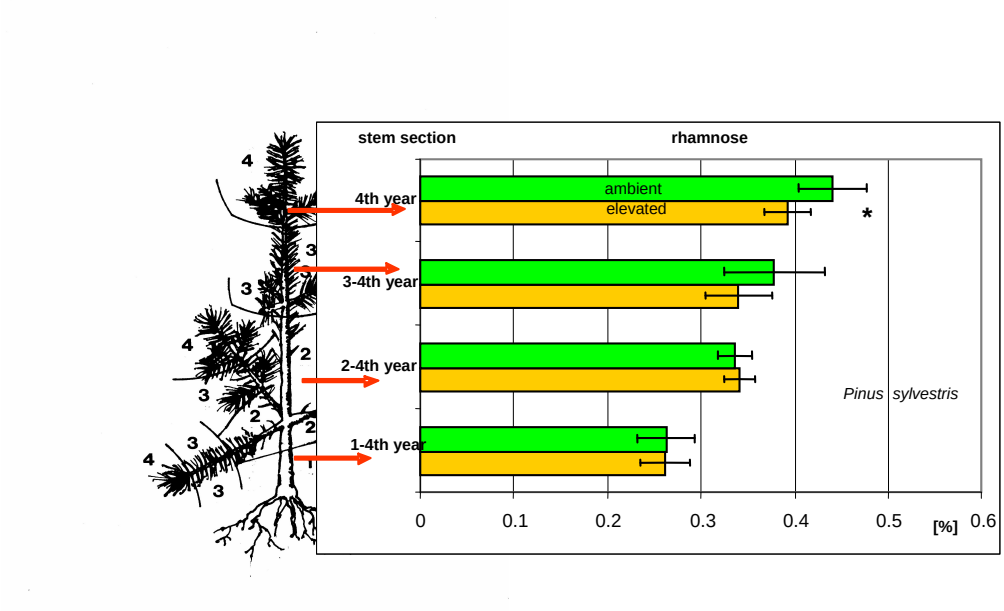

Figure 3.32: Rhamnose contents [%] from bottom to the top of juvenile *Pinus sylvestris* stems grown at ambient air and at air with elevated CO_2 concentration at the tertiary site in Berlin; *: $p<0.05$; data pooled for the CO_2 factor alone.

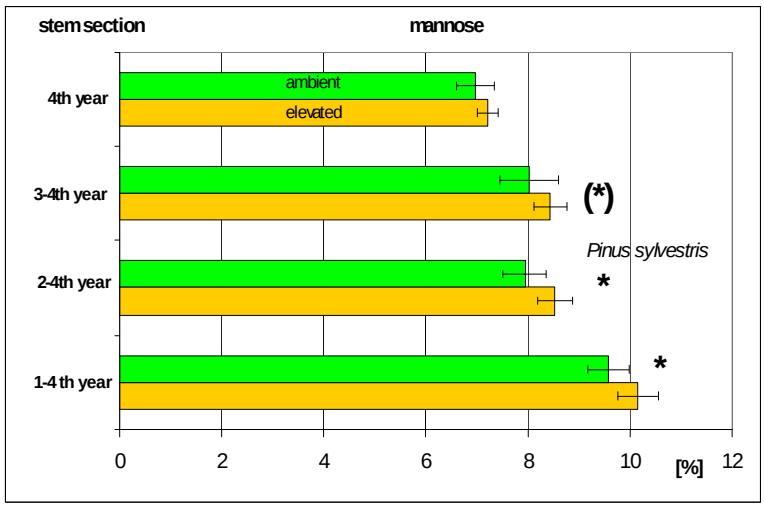

Figure 3.33: Mannose contents [%] from the bottom to the top of juvenile *Pinus sylvestris* stems grown at ambient air and at air with elevated CO_2 concentration (~700 µmol mol^{-1}) at the experimental site in Berlin; (*): $p< 0.1$, *: $p<0.05$; data pooled for the CO_2 factor alone.

Cellulose contents decreased from the oldest towards the youngest stem sections (~38% • 29%) of the four-year-old Scots pine in the experiment at the experimental site in Berlin. In tendency cellulose contents were slightly higher at elevated CO_2 concentration, at least in the younger stem parts: CO_2 enhancement was significant on the $p < 0.1$-level in the three-year-old stem sections as well as in the youngest shoots on top (Figure 3.34). Two-factorial analysis of variance (temperature, CO_2-concentration) indicated an overall CO_2 enhancement, with significance on the $p < 0.05$ level and no clear temperature effect. Difference between the total means of the CO_2 levels amounted to ~ 1.7%.

Results from analyses of total lignin (flavone-lignin) showed no distinct tendency either from bottom to the top of stems or in comparison of stems from the two different CO_2 treatments (Figure 3.35).

Temperature effects on most of the structural carbohydrates were separately tested statistically but no clear significances could be found with the e.

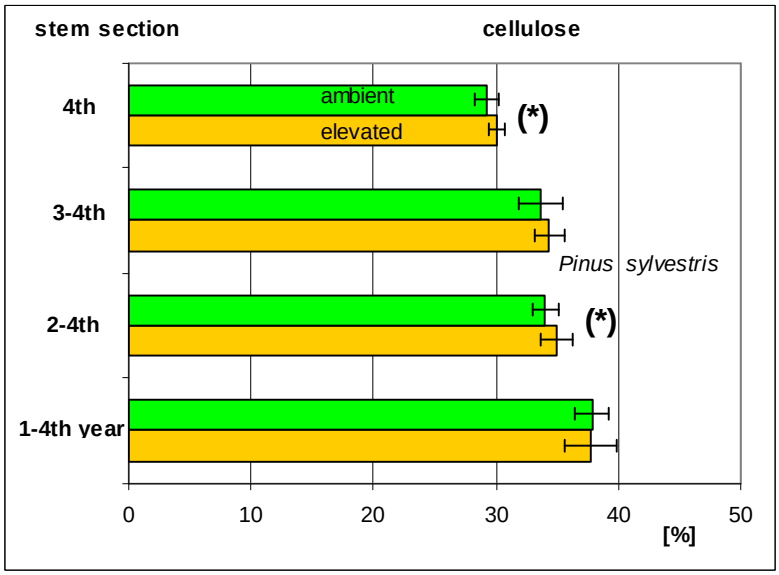

Figure 3.34: Cellulose content from the bottom to the top of juvenile *Pinus sylvestris* stems grown for three years at ambient air and air with elevated CO_2 concentration; (*): p: 0.05-0.1; data pooled for the CO_2 factor alone.

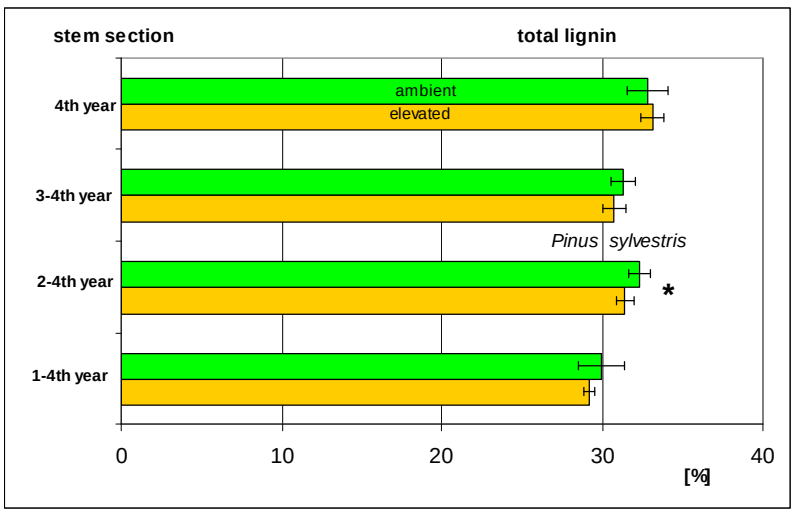

Figure 3.35: Total lignin (flavone-lignin) content from the bottom to the top of juvenile *Pinus sylvestris* stems grown for three years at ambient air and air with elevated CO_2 concentration; *: $p<0.05$; data pooled for the CO_2 factor alone.

Temperature effects on most of the structural carbohydrates were separately tested statistically but no clear significances could be found with the exception of galactose (Figure 3.36).

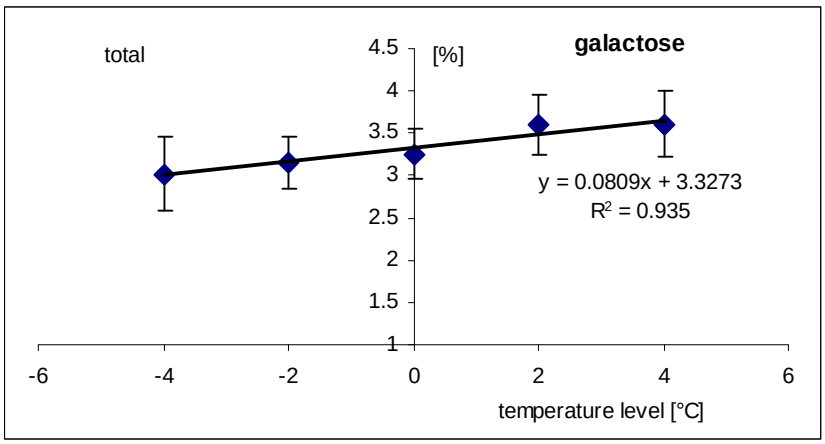

Figure 3.36: Galactose content of juvenile Scots pine stems grown for three years at five different temperature levels (-4, -2, 0 = base, +2, +4 °C); zero-line: temperature reference-base = long-term local annual monthly mean temperature (day and night) in Berlin-Dahlem; data pooled for the factor temperature alone (neglecting the difference in CO_2 concentration).

3.2.4.3 Results, adult trees

Pinus sylvestris

A part of wood powder left over from the C/N-analyses had to be combined and mixed from all disks of suppressed trees in one pool, subdominant together and dominant trees together in order to get enough material also for the structural carbohydrate analyses.

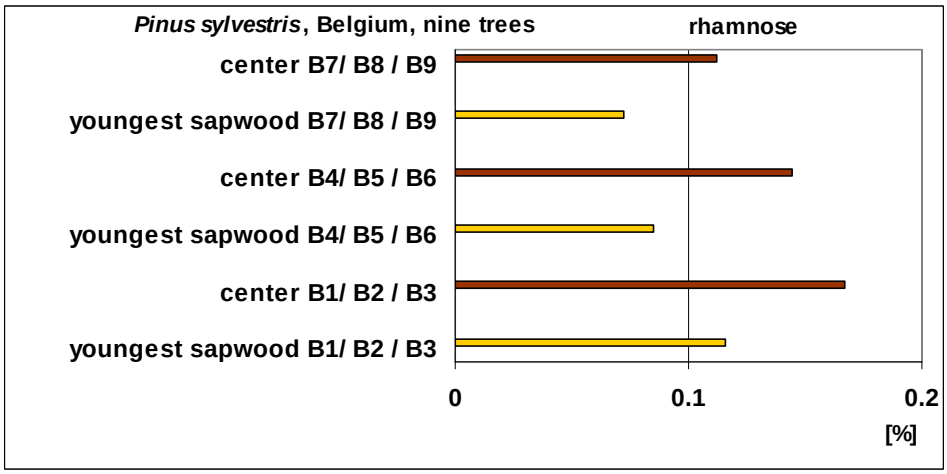

Figure 3.37: Rhamnose concentrations in disks from the stem base of dominant (B1, B2, B3), subdominant (B4, B5, B6) and suppressed (B7, B8, B9) *Pinus sylvestris* in Brasschaat /Belgium.

Concentration of rhamnose in the heartwood was by approximately 30% higher in the centre of the stems than in the periphery in the suppressed trees and in the co-dominant and dominant trees. And the concentration of this component decreased from dominant towards suppressed trees in the youngest sapwood as well as in the heartwood of *Pinus sylvestris* at the Belgian primary site.

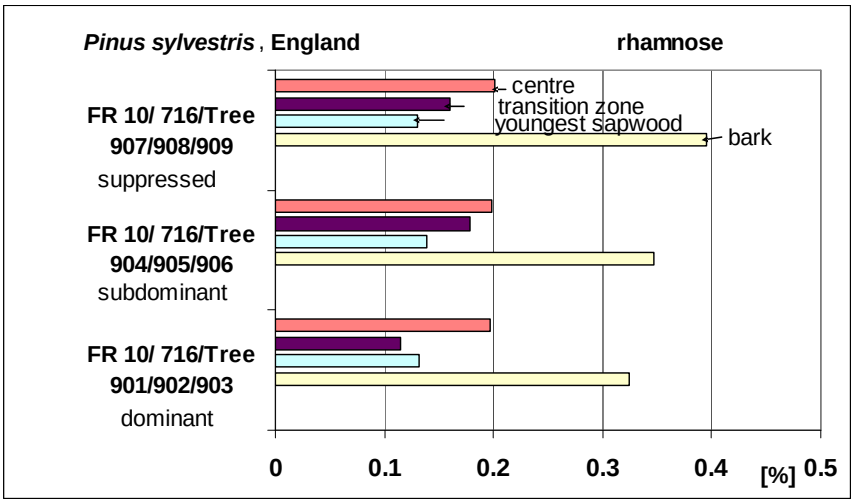

Figure 3.38: Rhamnose concentration in *Pinus sylvestris* stem-bases from a stand in England (FR).

In contrast to the pines in Belgium the example from the stand in England showed no clear trend in rhamnose concentration or less content of this carbohydrate in the dominant trees, respectively. Again the horizontal increase from the youngest sapwood towards the centre of the stem was obvious. Contents of rhamnose clearly increased from the dominant to the suppressed trees. The other substances showed no clear dependence on the tree's status in competition.in a first rough and preliminary data evaluation.

The main component cellulose decreased from the *Pinus sylvestris* stem periphery towards the centre as is shown in Figure 3.39. Again, there was no clear difference between the dominance classes. Differences between youngest sapwood, transition zone and stem centre were greater in the classes 'dominant' and 'co-dominant' than in the wood of the suppressed trees.

Pinus sylvestris wood from the English stands (mean) and from the German stand (Berlin/Grunewald) had lower cellulose contents in the youngest sapwood at the stem base than wood from the Belgian pine-site. Cellulose contents of the heartwood were slightly lower (~2%) in the Belgian sample than in the samples from England and Germany which were very similar.

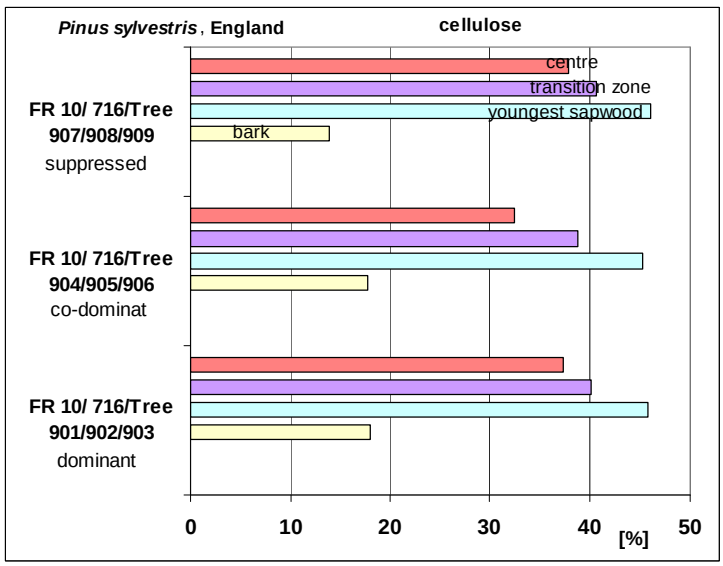

Figure 3.39: Cellulose concentration at the base of *Pinus sylvestris* stems at a stand in England (FR) in three different dominance classes.

Picea sitchensis

Mannose contents were the highest with the co-dominant trees and the lowest with the suppressed trees (Figure 3.40). Sapwood had by ~0.5% more mannose than heartwood, on the average.

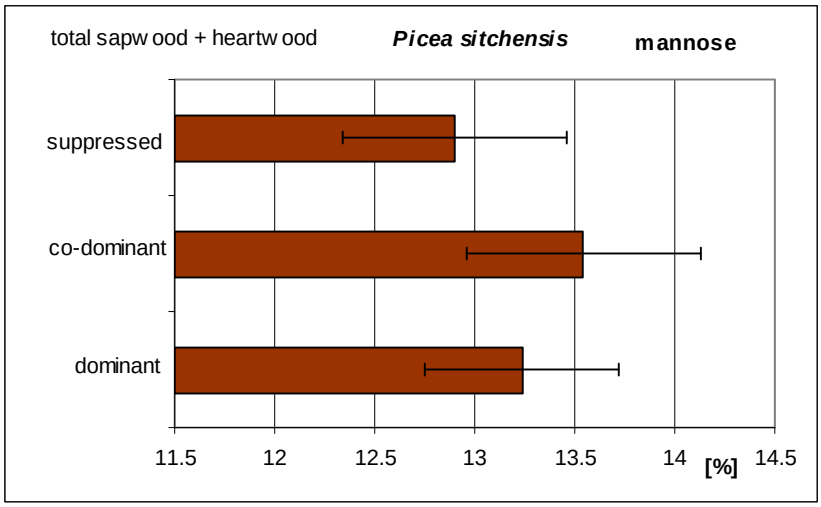

Figure 3.40: Overall mean of mannose content in the basal stem wood of dominant, co-dominant and suppressed *Picea sitchensis* from three different stands in England (homogenized heartwood and sapwood material).

The component galactose had the lowest concentration in the dominant trees and the highest in the suppressed Sitka spruces, on the average of all trees and samples (central and peripheral wood) from FR 02 (Coalburn - UK), FR 03 (Tummel - UK) and FR 08 (Sawley - UK). Figure 3.41 shows the mean differences between the dominant classes at the bottom and the difference between peripheral (blue columns) and central wood (violet columns) on the top. Dominant and co-dominant had higher contents in the centre of the stems, and in the suppressed trees mean contents were almost equal. The great standard deviations are mainly due to differences between the 3 stands. Data have still to be submitted to statistical tests.

Sitka spruce

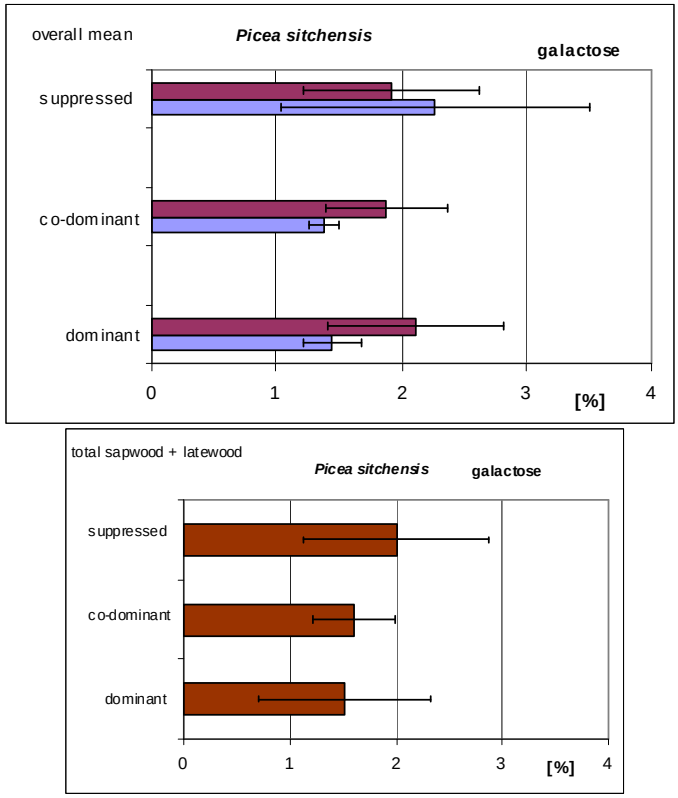

Figure 3.41: Galactose contents in wood from the basal stem log of dominant, co-dominant and suppressed Sitka spruce (FR 02, 03, 08 - UK); at the bottom overall means and at the top, differences between peripheral (blue) and central wood (dark violet).

Rhamnose-, mannose-, arabinose-, and xylose-contents were also determined quantitatively. Cellobiose occurred in traces only. All data were sent to FR (UK) for further interpretation.

Less **cellulose** could be found in the central wood (3-4% less). This decrease from peripheral to central wood was obvious in the discs from the all the three sites. Cellulose concentrations were almost identical in the dominant and co-dominant tree class, on average. suppressed trees had less cellulose in the peripheral as well as in the central wood Figure 3.42).

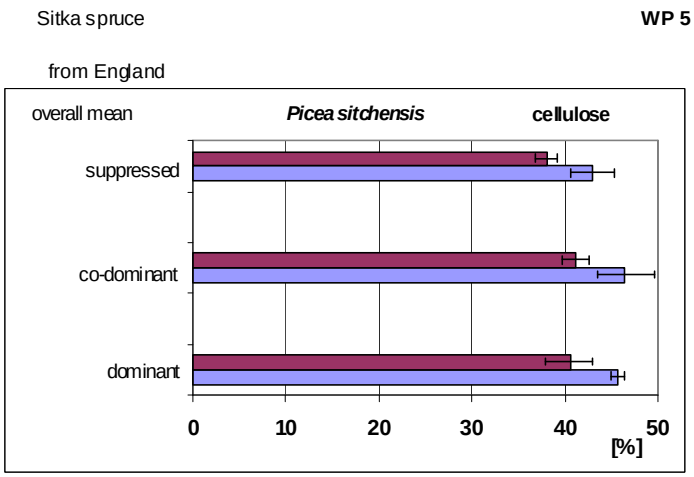

Figure 3.42: Means of cellulose contents in wood from the basal stem log of dominant, co-dominant and suppressed Sitka spruce (three sites, UK); peripheral wood (blue) and central wood (dark violet).

Lignin behaved the opposite way to cellulose. In general, contents were slightly higher in the centre of the stem disks than in samples from the periphery (Figure 3.43).

Figure 3.43: Means of lignin (flavone-lignin) content (in wood from the basal stem log of dominant, co-dominant and suppressed Sitka spruce (three sites, UK); peripheral wood (blue) and central wood (dark violet).

And in contrast to cellulose, on the average, lignin reached the highest values in suppressed trees and approximately the same mean contents in co-dominant and dominant trees. In all tree classes maximum of lignin concentration occurred in the transition zone between the central and the peripheral wood of the disk (Figure 3.44: example stand FR 08 SS).

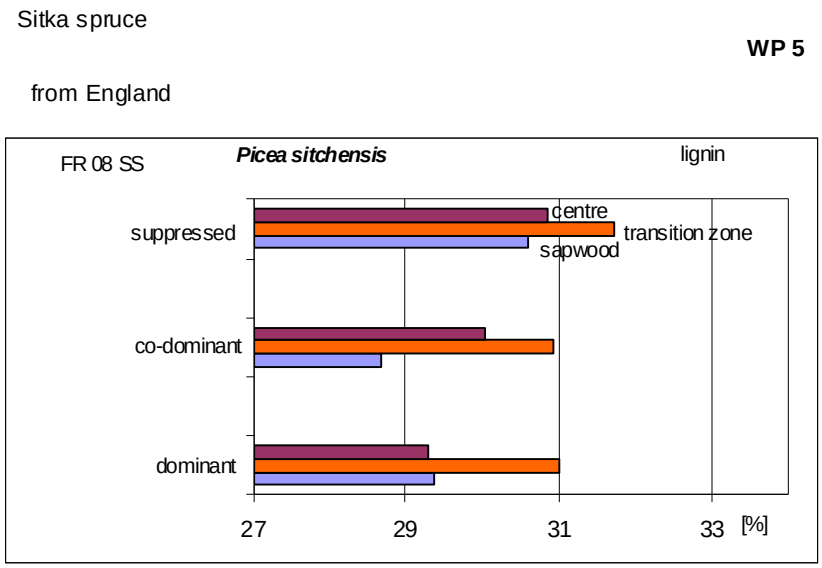

Figure 3.44: Lignin contents (flavone-lignin) in wood from the basal stem log of dominant, co-dominant and suppressed Sitka spruce (site FR 08 - UK); peripheral wood (blue), transition between sapwood and heartwood (orange), and central (heartwood) wood (dark violet).

3.2.5 Discussion and conclusions

Nitrogen

The significantly lower nitrogen concentrations (Figure 3.18) in the needles of the juvenile Scots pines at elevated CO_2 correspond with the results of many older studies (Overdieck, 1990; Murray 1996; Linder and Murray 1998) indicating a negative effect of elevated CO_2 on the N-concentrations of the main photosynthetic active organs. Although the difference between the means of the oldest annual needle set pointed to the same trend, in this case, difference was not significant. This detail could be taken as a hint that this special CO2-nitrogen-effect diminishes in aging needles (and leaves, respectively). A new aspect is that this decrease in nitrogen concentration could not only be found for needles but also in the youngest stem sections of juvenile pines. This shows that this CO_2 effect is of greater importance than expected because it has far-reaching consequences for the nitrogen supply of other plant organs than needles (or leaves). It is interesting to see that this effect could not be revealed in the oldest basal stem section of the pines in our experiment (Figure 3.18). Possibly, in general the very small differences of nitrogen amounts are equalized in older wood. After comparing the nitrogen concentrations of the 50-year-old pine from Grunewald with those from the juvenile trees (Figure 3.18 and Figure 3.20) one can postulate a rather similar distribution pattern starting from the stem base upwards to the branches and needles for both developmental stages. On the other hand, the juvenile trees had relatively higher nitrogen concentrations in the below ground parts as far as the upper root parts and the coarse roots are concerned. Unfortunately, in the forest fine roots could not be harvested as exactly as in the pot experiment and therefore, N-concentrations of fine roots are not presented in this report.

It was often concluded (Linder and Murray, 1998) that the slightly lower nitrogen concentrations at elevated CO_2 are caused by dilution in more carbon. This conclusion seems to be logical if one assumes that at a greater CO_2 supply CO_2 net uptake rates always increase, i.e. the carbon influx is always greater in this case and this could lead to certain small shift in the equilibrium between N and C. Therefore, one could speculate that total carbon concentration should increase to same extend as nitrogen decreases. In our case – as in many other cases – that was not found. Nevertheless, we do not conclude that the decrease in nitrogen concentration had been due to dilution. Because in this chain of arguments one has to take into account that nitrogen contents are very low compared to carbon contents in the plant tissues, and differences in nitrogen concentrations (caused by elevated CO_2) amount to a few tenth of a percent. Total carbon concentrations can only be determined with accuracies around the 1% level using a C/N-analyzer. Therefore, it could still be a dilution phenomenon which could not be detected by means of this method.

The juvenile trees had approximately the same concentrations of nitrogen as the adult forest tree from Grunewald (Berlin) in the stem, whereas the concentrations in branches and needles of the adult tree were twice as high as in the same organs of the juvenile trees. Although only one tree from a homogeneous forest stand was completely analyzed one can conclude that N-limitation of a positive CO_2 effect on photosynthesis and growth would more likely occur in a pot experiment than in Grunewald. In other words, limitation of the CO_2-effect by a lack of nitrogen in pine forests around Berlin – and certainly in most regions of Central Europe – is not probable because the positive CO_2 effect was still evident at much lower N-concentrations in the plant tissues (as was shown by our experiment).

Elevation of temperature (Table 3.1) had negative effects on absolute nitrogen concentrations of most organs with the exception of fine roots, the middle twig sections and two-year-old needles. This negative effect was statistically highly significant in some cases. Therefore, one can conclude that the possible enhancement of growth by temperature increase is not followed by a higher absolute uptake rate and accumulation of nitrogen. One clear effect of increasing temperature was the comparatively low N-concentration in the oldest annual needle

set. This can be taken as a sign for earlier aging at higher temperature levels. (Considerable amounts of nitrogen must have been already exported from the old needles.)

The continuous decrease of nitrogen concentrations in the juvenile beech stems down to very low percentages in all groups after 30 experimental months (Figure 3.19) show, on the one hand that at final harvest the young trees had reached the concentration level of an adult wood. On the other hand, it also shows that the experimental factors CO_2 and temperature had no clear effect on nitrogen concentrations of the woody parts of this species. Less nitrogen was found at elevated CO_2 only in case of leaves. This corroborates the interpretation of this study on the juvenile pines. Thus, lowered nitrogen percentages in the photosynthetic active organs seem to be very common and wide spread as an effect of elevated troposheric CO_2 concentration.

It was expected to find the highest nitrogen concentrations in the bark of adult Scots pine and Sitka spruce (Figure 3.21) and only traces in the central wood. This assumption could be verified by our analyses. A new aspect is that this low level is already reached in the youngest sapwood directly behind the bark of both the species. Carbon concentrations were almost identical in the Scots pine wood from Grunewald and from England. In both cases they clearly increased from the youngest sapwood towards the central wood by about 2.5%, on the average. This increase cannot be explained by a decrease of nitrogen. Or in other words, possibly, this is possibly not a sign of decreasing amounts of protein-rich parenchyma alone but probably also a hint to more carbon-rich substances in the central wood. This increase was especially evident in the disks from Brasschaat (Belgium, Figure 3.22). The wood from this stand was the most resinous of this study and therefore, one could suppose that resin formation was the reason for that elevated concentration of total carbon in the central wood.
In contrast to Scots pine the mean carbon concentration of the Sitka spruce was approximately equal from the periphery of the stem disk to its centre indicating a rather homogeneous wood consistence (Figure 3.22).

Non-structural carbohydrates

The very low concentrations of ‘soluble carbohydrates’(glucose, fructose, sucrose, (Figure 3.23) and starch (Figure 3.24) in the basal stem wood of the juvenile Scots pine clearly show that at the harvest time in September these substances were not activated and transported to a considerable extend. Although many of the values scattered around the sensitivity limit of the analytical method it could clearly be shown that the largest amount of glucose and fructose occurred in the basal stem part and also that a certain probability of a positive CO_2 effect on glucose accumulation in the top shoot of the young pines can be assumed. In consequence, one could argue that some of the additional net carbon uptake by photosynthesis at elevated CO_2 concentration is going to the glucose pool in the youngest shoot, whereas starch concentrations behaved oppositely to the ‘soluble carbohydrates’. Its concentration increased from the bottom to the top of the stems (Figure 3.24), and CO_2 concentration had no influence. Therefore, it can be concluded that in stems of juvenile pines starch is not the pool for the additional amount of carbon which is taken up at elevated atmospheric CO_2 concentration.

On the other hand, increasing temperature had a clear negative effect on starch concentration (Figure 3.25) at the end of the experiment (decrease with increasing temperature). In general, this finding also clearly indicates that starch accumulation in the lowest stem part is a function of temperature within a realistic temperature range around the local means in Central Europe.

In the needles only starch seems to be the pool which takes additional amounts of carbon (Figure 3.26 and Figure 3.27) at elevated CO_2 concentration This enlargement of the starch pool in the needles without clear effects on other pools further down in the plant body might hint to a bottle neck for the transport of carbohydrates downwards. It is also possible that greater amounts glucose are activated from this starch pool with a certain delay and then transported basipetally. Significantly more starch was accumulated at the lower temperature levels and some interaction between temperature and CO_2 can be presumed because

temperature effect was only evident with trees grown at elevated CO_2 concentration (Figure 3.26). An aging effect on starch concentrations could also be shown (Figure 3.27): The older the needles were the less starch was found.

As expected, in general, concentrations of the soluble carbohydrates were the highest in the bark of the adult Scots pines (England) and the suppressed trees had the most glucose and sucrose in their bark in comparison with the two other dominance classes (Figure 3.28). In the co-dominant tree class the lowest concentrations of all substances were found in the periphery of the basal stems as well as in the central wood. The horizontal decrease of 'soluble carbohydrates' from the bark towards the central wood was also obvious in the Grunewald individual.

Not a bit of sucrose was found in the wood of dominant and co-dominant trees and very small amounts of this substance in the suppressed ones. Therefore, one can conclude that at harvest time of the disks the most prominent transport carbohydrate of plants, namely sucrose, was not available in considerable amounts in the basal stem wood. All these results support the general conclusion that dominant trees in a pine stand differ evidently from suppressed trees in the carbohydrate composition of wood.

The pine trees from Brasschaat (Belgium) were by far the oldest of our study and had the lowest 'soluble carbohydrate' concentrations of all analyzed trees. If harvest time had been the same as in England age might be taken as a reason for this phenomenon. On the other hand, starch concentrations were by far the highest in Scots pine bark from Belgium (Figure 3.30) and occurred also – in contrast to the results from English pines – almost exclusively in the youngest sapwood without a difference between the co-dominant and the dominant tree class and reached the highest level in the suppressed trees. It can be, therefore summarized that - for some still unknown reason – the pines from Brasschaat (Belgium) differed from all the other analyzed pines also with regard to their starch concentrations in the basal stem wood.

Structural carbohydrates

Because rhamnose, mannose, arabinose, galactose and xylose are components of the woody material and were determined as mono-saccharides by means of the HPLC-technique as substances of the so-called solid material, they are considered under the head-line 'structural carbohydrates' together with cellulose and lignin in this report.
As it was expected these substances occurred in much greater amounts in the stem wood material than starch and 'soluble carbohydrates' and therefore, could have had a much greater potential to offer pools for the via photosynthesis additionally up-taken carbon amounts at elevated atmospheric CO_2 concentration.

Data of the rhamnose, mannose, galactose, cellulose and favone-lignin determinations were evaluated in detail and plotted into diagrams by partner 4 within the time-frame of the MEFYQUE project. Therefore, only these results are discussed here.

An interesting new aspect is the quite opposite distribution pattern of rhamnose and mannose (Figure 3.32 and Figure 3.33) in juvenile stems of Scots pine. Higher concentrations of rhamnose seem to be typical for younger and mannose for older Scots pine wood. But only mannose can apparently perform as a sink for the additional carbon that is offered via enhanced CO_2 net uptake at elevated atmospheric CO_2 concentration because significantly higher amounts were found in the basal stem section.

Temperature effects on the concentrations of all the substances analyzed in this study could not be detected with the exception of galactose (Figure 3.36). Nevertheless, the possibility that temperature effect could have had occurred in our experiment cannot be fully excluded and therefore, this aspect warrants further investigations.

Cellulose and flavone-lignin of course were qualitatively and quantitatively the most important components of the juvenile Scots pine wood (Figure 3.34 and
Figure 3.35). It can also be concluded from cellulose determinations that elevated CO_2 concentration causes an increasing size of the cellulose pool at least in the younger stem parts, whereas lignin concentrations were not clearly altered by elevated CO_2. There was a certain opposite trend in the concentrations of these two components: Cellulose amounts increased towards the bottom parts, lignin decreased slightly or remained unchanged.

Galactose – as mentioned above – seems to be a temperature dependent wood component (Figure 3.37). Interpretation of this phenomenon is not yet possible on the basis of our results.

Rhamnose concentrations in the disks from the adult Scots pine trees show the exceptional performance of the adult Scots pines from Belgium again (Figure 3.37). In contrast to the pines from England Figure 3.38) the decrease of rhamnose concentration from dominant over co-dominant to suppressed trees is quite obvious. On the other hand, results from all pine stands show that concentration of this component increases from the periphery of stem wood of Scots pine towards the centre (Figure 3.37 and Figure 3.38).

Cellulose concentrations decreased towards the centre of the stem disks of pines from England (Figure 3.39) and are possibly replaced by other substances like lignin. However, lignin data have still to be evaluated.

Sitka spruce stem wood was very different from that of Scots pine, also as far as the components of the 'solid material' are concerned (Figure 3.40 and Figure 3.41). Mannose concentrations were evidently higher as in the juvenile pines and surprisingly reached the highest level in the co-dominant trees, on the average (Figure 3.40). The reason for this phenomenon is still unknown. Galactose is a component of pectin and therefore, takes essentially part in the formation of the middle lamellae. If one considers the suppressed trees as individuals being in a 'younger' stage of ripening these higher amounts of galactose seem to be plausible (Figure 3.41). This assumption corresponds with the finding, that - in contrast to the dominant and co-dominant trees - galactose concentrations were higher in the periphery of stem disks (younger wood) than in the central wood (older wood).

In total, cellulose concentrations were slightly lower in the suppressed trees quite opposite to the flavone-lignin concentrations which reached higher levels in the suppressed trees on the average (Figure 3.42 and Figure 3.43). This seems to be a rather general trend in coniferous wood, because - as mentioned above – also in the stem wood of Scots pines this reversed behaviour of the two main components could be suggested.

Cellulose and lignin also behaved conversely if one compares peripheral and central wood: Cellulose concentrations were lower in the centre of the stem and there lignin concentrations were higher and vice-versa. This again is a clear hint to a distinct antagonism of cellulose and lignin in Sitka spruce. In one case (FR 08 SS, Figure 3.44) we were able to take an additional wood sample for analyses at equal distance between the centre and the periphery of the disk. There the highest lignin concentrations were reached. Therefore, one could argue that the increase of lignin concentrations [%] towards the central wood is not linear in Sitka spruce stems but is better described by an optimum curve and optimum is located somewhere in the middle between central and peripheral wood.

3.2.6 References

Overdieck, D., 1990. In: The greenhouse effect and primary productivity in European agro-ecosystems, eds, Goudriaan, J., van Keulen, H. and HH. van Laar , pp. 31-37.

Murray, M. B., Leith, I.D. and P.G. Jarvis, 1996. *Trees* **10**, 393-402.

Linder, S. and M.B. Murray, 1998. In: European forests and global change, ed, Jarvis, P.G., pp.215-235.

4 Wood Quality Under Normal and Elevated CO_2 Conditions

Main Contributors:
Dries Vansteenkiste, Lieven De Boever, Joris Van Acker

4.1 Introduction

In order to maximise the value of results, much of the work described was carried out alongside other funded work, both prior and during the time of this project. Appropriate recognition is therefore given to the EC's Fourth Framework Environment and Climate RTD programme as research project POPFACE (contract no. ENV4-CT97-0657, the Italian Natural Environment Research Council and Department of Environment, Food and Rural Affairs (grant nos. GR9/04077 and NFO410 to GT) within the Terrestrial Ecosystems Research Initiative (TERI).

Draft versions of papers are presented in this chapter (data analysis, data integration and interpretation of results have been more complicated than expected. For instance, for the analysis of the effects of elevated [CO_2] on cell element length, nearly 500 distributions representing several millionlength measurements).

4.2 Role in model parameterisation and validation

The parallel development of the growth model, with the laboratory anatomical, biochemical and strength properties analysis was intended to provide both data for parameterisation and validation. The model had not produced such detailed break-down of the constituent parts of the wood (earlywood, latewood, trachids etc.)

4.3 Elevated CO2 effects on wood properties

The project undertook research on wood quality under conditions of elevated [CO_2]. Because the dimensions of pine, beech or oak are still small after three years of CO_2-elevated growth, assessment of wood quality is difficult. To be able to point out differences in structure and wood properties between non-elevated and CO_2-elevated grown wood, in order to make best use of additional knowledge, data and facilities POPFACE material was primarily used to evaluate potential wood quality effects in hardwoods. These topics will be treated separately in three papers on microscopic effects on fibre length, vessel anatomy and physical-mechanical properties of juvenile poplars, currently under preparation. The work and results are summarised in these papers; Vansteenkiste, D. *et al.* (in prep, a) , Vansteenkiste, D. *et al.* (in prep, b) , De Boever, L. *et al*. (in prep) which are entitled respectively:

- Cell length distributions of juvenile poplars (*Populus nigra* L.) are modified by Free-Air Carbondioxide Enrichment (FACE)
- Does free-air with elevated CO_2-concentrations (FACE) alter vessel anatomy in juvenile poplars (*Populus nigra* L.)?
- Effects of Free-Air Carbondioxide Enrichment (FACE) on intra-ring microdensity variations and micromechanical properties of juvenile poplar trees (*Populus nigra* L.).

4.3.1 *Draft paper*: Cell length distributions of juvenile poplars (*Populus nigra* L.) are modified by Free-Air Carbondioxide Enrichment (FACE)

Vansteenkiste[a], D., De Boever[a], L., Van Acker[a], J., Ziche[b], D., Overdieck[b], D., Evans[c], S., Ceulemans[d], R., Scarascia-Mugnozza[e] , G. and Calfapietra[e], C.

[a] Ghent University, Belgium (corresponding E-mail: Dries.Vansteenkiste@UGent.be); [b] Technical University of Berlin, Germany; [c] Forestry Commission Research Agency, Farnham, UK; [d] University of Antwerpen, Belgium. ; [e] Università degli Studi della Tuscia, Viterbo, Italy.

4.3.1.1 Abstract

The main objective of this study was to investigate the influence of elevated CO_2 concentrations ([CO_2]) on spatial and statistical distributions of fibre length and fibre proportion within growth rings of juvenile Poplar (*Populus nigra* 'Jean Pourtet'), within the framework of the EU-funded research projects POPFACE and MEFYQUE.

Defect-free material was extracted from the second annual ring (*year 2001*) of 22 three-year-old trees, 10 of which had been subjected to air with enhanced [CO_2]. The radial changes of cell element length and fibre proportion were analysed on macerates of groups of five thin (150 µm) tangential sections (TL) within each annual ring, hence at 0.75 mm intervals. The cell

length distributions were assessed automatically by means of a Kajaani fibre analyser. Using maximum likelihood estimation, bimodal distributions were fitted to each cell length histogram, by deconvolution into three distinct gaussian curves. Characteristic variables were extracted from each deconvoluted distribution allowing comparisons between trees and to evaluate the influence of enhanced [CO_2]. Fibre length generally decreased from the beginning towards the end of the growth ring, especially in CO_2 enhanced trees. Results therefore need to be interpreted as a function of intra-ring position. Principal component analysis (PCA) revealed that fibre length increases significantly with about 10 to 15% under the influence of enhanced [CO_2]. Furthermore, the shape of the element length distribution changes as a result of CO_2-enhancement. Effects of [CO_2] enhancement appeared to be most pronounced at the beginning and towards the end of the annual ring. The changes are likely to be paralleled by changes in wood porosity and may, thus, affect microdensity variations and micromechanical wood properties.

4.3.1.2 Materials and methods

Site description and plantation layout

The FACE study is located in central Italy, near Viterbo (Tuscania; 42°22• N, 11°48• E, altitude 150 m) on 9 ha of former agricultural land. Following detailed soil analyses, six 30 × 30-m experimental plots (120 m apart) were selected, and a FACE design was established in three of the plots. The remaining three plots were left under natural conditions and designated control plots. In late-spring 1999, the 9-ha plantation was established with poplar cuttings at a planting density of 10,000 trees ha^{-1} (1 × 1 m spacing) within the six experimental plots, and 5,000 trees ha^{-1} (2 × 1 m spacing) in the non-experimental surrounding plantation. The experimental plots were planted with three *Populus* genotypes (clones), *i.e. P.* × *euramericana* 'I-214', *P. nigra* 'Jean Pourtet' and a local selection of *P. alba* L. ('2AS-11'), whereas the non-experimental part of the plantation was planted with *P.* × *euramericana* 'I-214'. Each 314 m^2 plot contained 350 plants, and was divided into six triangular sectors, with two sectors per genotype. The plantation was designed and managed as a short-rotation forest with typical high plant densities (Mitchell *et al.* 1999). For plantation details see Scarascia-Mugnozza *et al.* (2000).

Carbon dioxide enrichment is provided through a polyethylene octagonal ring (22 m diameter) mounted on 12-m telescopic poles. Pure CO_2 is injected through laser-drilled holes in the ring (target CO_2 concentration of 550 µmol mol^{-1}). The CO_2 concentration was 544 ± 48 $\mu mol.mol^{-1}$ during the first year of treatment and 532 ± 83 $\mu mol.mol^{-1}$ during the second year. Daytime CO_2 enrichment was provided from bud burst to leaf fall. For a detailed description of the FACE setup is referred to Gielen *et al*. 2001 and Miglietta *et al.* 2001.

Tree sampling, subsampling and experimental methods

In total, 22 plants of the clone *P. nigra 'Jean Pourtet'* were sampled, 12 plants from the three ambient plots (2, 3 and 6) and 10 plants from the plots with elevated [CO_2] (1, 4 and 5). These are referred to as respectively Ambient-1 to Ambient-12, and Elevated-1 to Elevated-10. From clear internode samples taken at ± 1 m height in these 22 plants, specimens including ring number 2 (year 2000) were isolated from the stem so that the dimensions were about 6 cm longitudinally and 8 mm tangentially. These tree-ring samples were saturated with de-ionised water prior to microtome sectioning. Using a specially adapted microtome, a radial intra-ring subsampling was carried out in each ring at 150 µm intervals. This yielded sets of successive strips of equal thickness covering the entire ring-width. Subsequently, each thin strip was subjected to mechanical tensile testing, up to rupture (results not presented here). After this mechanical testing, the remains of the strips were grouped into clusters consisting of five subsequent strips, and macerated. The macerates were analysed with a Kajaani Fiber Analyser at the BioComposites Centre in Bangor, Wales, UK. This equipment allows measuring cell lengths up to 7 mm. Cell element length histograms were provided for at least 15000 elements out of each macerate, with length class width being 50 µm.

Using a Matlab script, based on maximum likelihood estimation (mle), a bimodal frequency distribution consisting of three symmetrical normal distributions was fitted to each histogram.

4.3.1.3 Results and Discussion

The fitted distributions gave accurate estimates of the measured histograms (R^2 0.965 to 0.998). First results indicate a significant increase in fibre-length of 10 to 15% as a result of CO_2 enhancement. However, results will have to be interpreted taking into account intra-ring position, inter-tree and inter-plot variations and possible effects induced by intra-tree variations (sleeping buds, knots), presence of tension wood, sample imperfections, auto-correlation, chemical differences, breakage in mechanical testing. Some examples of result graphs are given below:

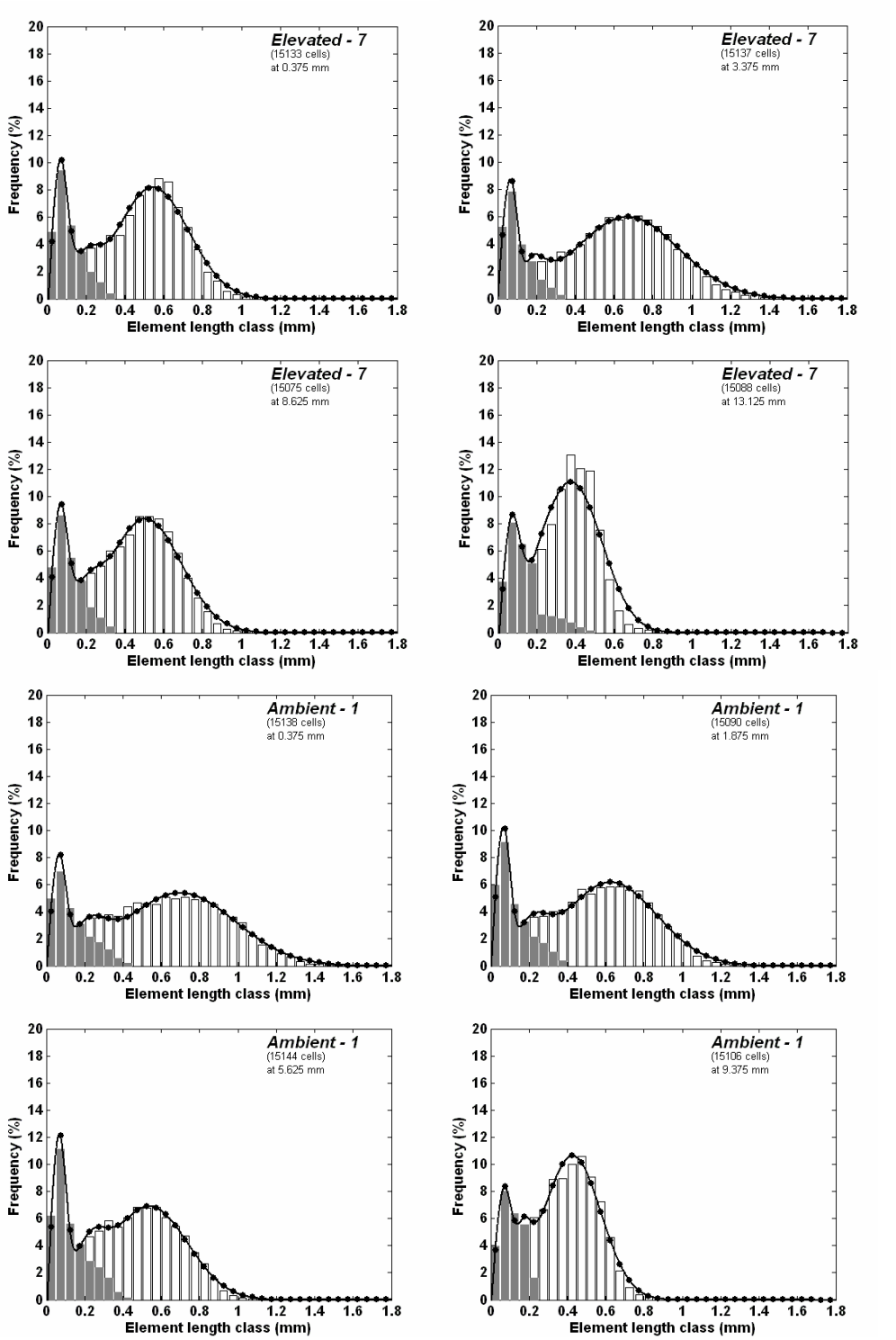

Figure 4.1: Element length distributions (histograms with classes of 50 µm) and fitted distributions (black curve, •) at different radial positions in the 2001 ring of tree 'Elevated-7'. Grey bars in

histogram represent fines proportion, white bars represent fibres proportion in each element length class. In total, 287226 cells have been analysed in this ring.

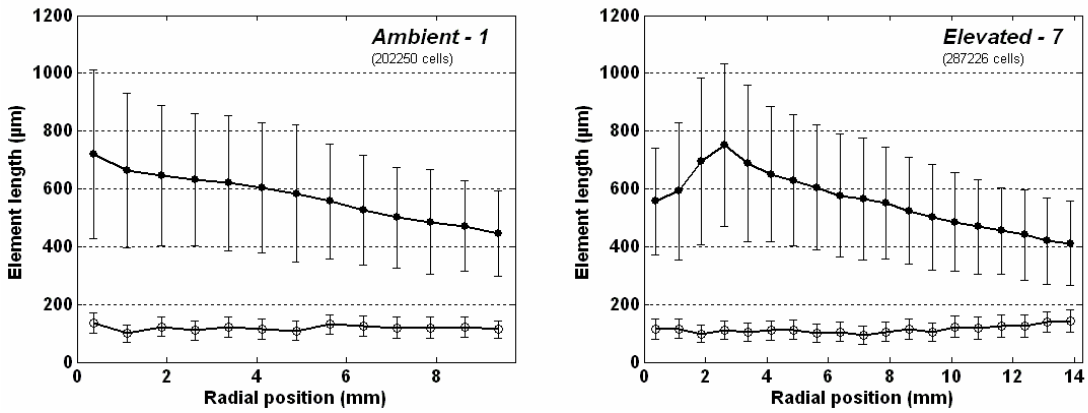

Figure 4.2: Course of mean element length (in µm) in the 2001-ring of trees 'Ambiant-1' (left) and 'Elevated-7' (right): mean fibre length (top curve, •) and vessel element length (bottom curve, •). The error bars represent the standard deviation of the element length measurements at each radial position. Note the larger ring width in the tree grown under elevated [CO_2].

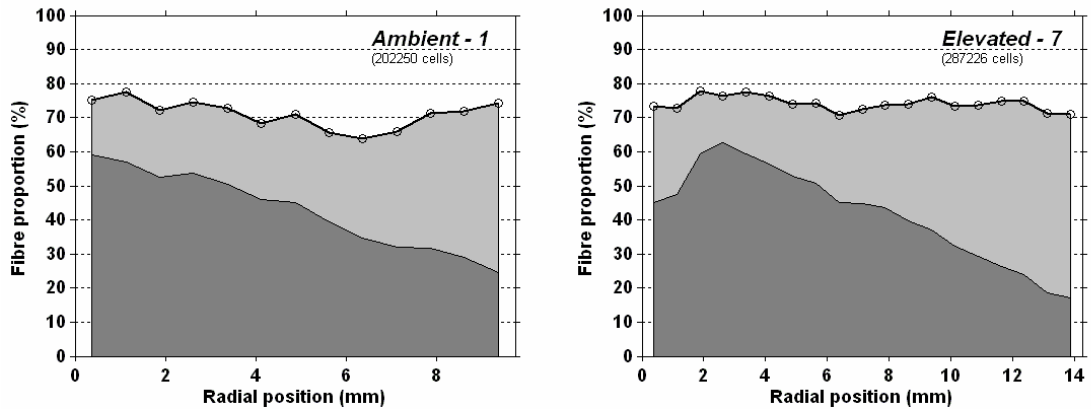

Figure 4.3: Cumulative proportion (in %) of fibres that are shorter than 500 µm (light grey area) and longer than 500 µm (dark grey area) within the 2001-ring of trees 'Ambiant-1' (left) and 'Elevated-7' (right). Total proportion of fibres is represented by the top outline curve (•).

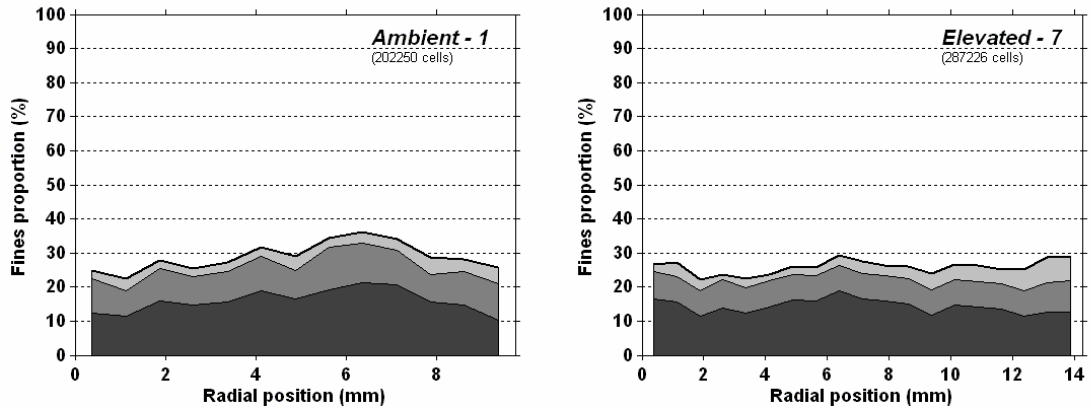

Figure 4.4: The proportion of fines (in %) in the 2001-ring of trees 'Ambiant-1' (left) and 'Elevated-7' (right). The fines are located in the left peak of the element length histogram; their distribution consists of two overlapping sub-distributions with length ranges of respectively 0 - 200 µm (black area) and 0 - 500 µm (dark grey). Class proportions in the left tail of the fibre length distribution, *i.e.* for length classes • 200 µm, are represented by the light grey area**.**

These findings could be compared with preliminary results obtained at TUB (by Daniel Ziche), derived from a comparative study performed on samples from the outer growth-ring in three-year-old stems taken from the first rotation cycle of all three clones (*P. x euramericana* 'I214', *P. nigra* 'Jean Pourtet' and *P. alba* '2AS-11'):

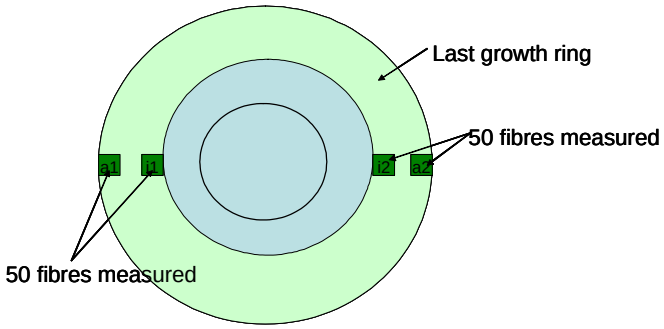

Figure 4.5: Position of samples taken for fibre length analyses, at the beginning and at the end of the outer growth ring, at two opposite positions in the stem.

In each of the four sub-samples, the length of 50 straight, fully macerated and non-damaged fibres was measured (*i.e.* totalling 200 fibres per tree), using transmitted light microscopy and digital image analysis. Fibres were found to be significantly longer at elevated [CO_2]. Differences between species were statistically significant (Table 4.1). Mean fibre length increased with increasing [CO_2] from 877 to 939 µm (+ 7 %) in *P. alba*, from 804 to 834 µm (+ 5 %) in *P. nigra* and from 834 to 855 µm (+ 3 %) in *P. x euramericana*. *P. alba*, the species which had the longest fibres, produced less biomass and, hence, had a smaller basal area (Fig.) than the others. In *P. alba* and *P. x euramericana*, fibre length at the end of the growth-ring tended to increase with increasing basal area (R^2 respectively 0.37 and 0.74) within species and treatment. Fibres at the beginning of the growth ring did not show that tendency.

Table 4.1: Statistics from repeated two-factorial analysis of variance (- not significant, and + significant at $p < 0.05$).

	fibre length				growth		
2-factorial ANOVA	egs	lgs	total	egs/ lgs	heigth	basal area	bio-mass
species	+	+	+	+	-	+	(0.07)
treatment	+	+	+	-	+	+	+
species * treatment	-	(0.07)	-	-	-	-	-

Fibres at the ending of the growth ring were approximately 11% longer than fibres at the beginning of the ring (contradictory to our results). The ratio between fibre lengths from beginning and end of the tree ring showed no significant differences between treatments, but it was higher in *P. x euramericana* than in *P. nigra*.

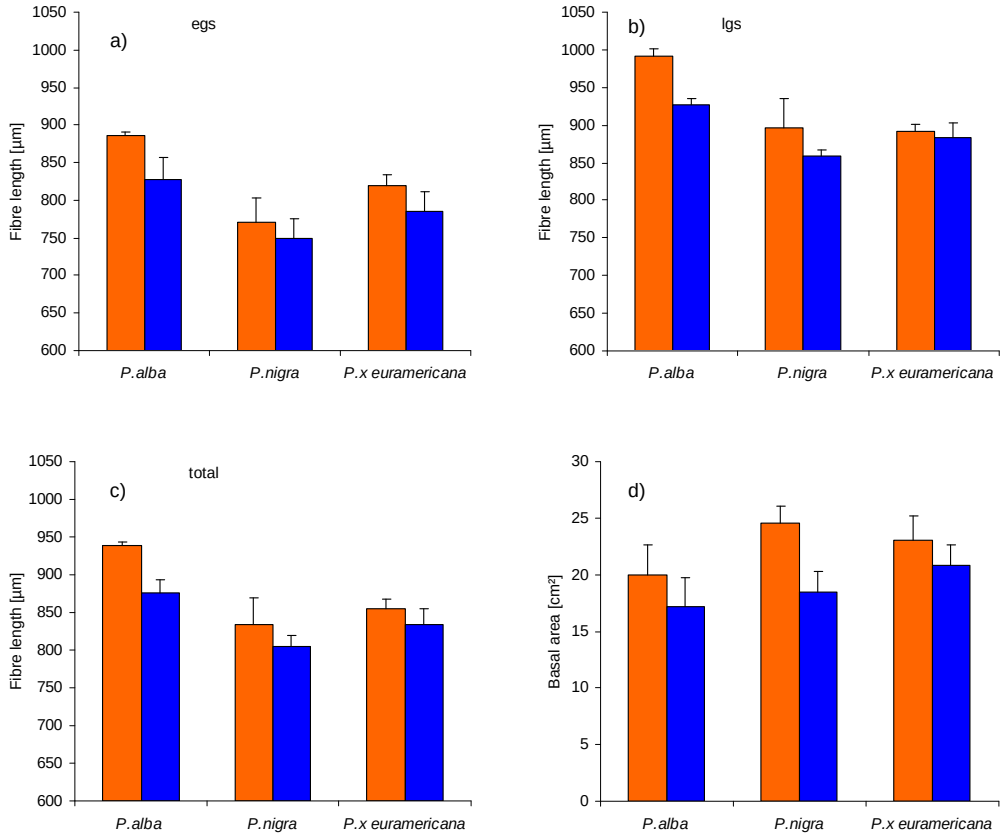

Figure 4.6: Fibre length in wood tissue from a) the beginning of the growth ring (egs), b) the end of the growth ring (lgs), and c) total mean fibre length (lgs + egs), and d) basal area of the stems of the three poplar clones and the two CO_2 treatments. Blue = ambient [CO_2], red = elevated [CO_2] of approximately 550 µmol mol^{-1}.

Caution should be taken when comparing UGent results with TUB results, considering the sizeable difference in number of cells analysed (50 fibres *versus* 15000 cells). Even though TUB measured 'perfect', intact fibres, the reduced number might not be sufficient to obtain a reliable estimate of fibre length. In fact, the means derived from measurements on a limited number of 'perfect' fibres, 800-950 µm (n=50) are likely to be over-estimates of true fibre length. Moreover, the 'random' selection of intact fibres may be strongly biased by subjectivity of the operator and produce anomalous results. Our results show that individual fibre lengths may be anywhere between 250 and 1500 µm, which is consistent with literature data (Wagenführ and Scheiber 1994, Ilvesaalo-Pfäffli 2000). The mean fibre lengths we obtained are in the order of 450 to 750 µm (n=10000). Hence, even though mean fibre lengths derived from fibre length histograms might yield under-estimations of true values, due to presence of broken fibres or long vessel elements, the results may be considered to be more reliable. The TUB mean values can be situated in the higher range of our histograms and, thus, results might be comparable only by considering only the higher length classes (L > 750 µm). The increase of mean fibre length as a result of increased [CO_2] is consistent with our results. However, the higher fibre length found by TUB at the end of the growth-ring compared to that at the beginning contradicts the general tendencies we found for mean fibre length, *i.e.* fibre length generally decreases in an almost linear fashion over the course of a single growing season.

4.3.1.4 References

Butterfield BG (2003) Wood anatomy in relation to wood quality. In*: Wood quality and its biological basis*, (eds. JR Barnett and G Jeronimidis), Blackwell Publishing, CRC Press, 30-52.

Cruiziat P, Cochard H, Améglio T (2002). Hydraulic architecture of trees: main concepts and results. *Ann. For. Sci*. **59,** 723-752.

Gielen B, Calfapietra C, Sabatti M, Ceulemans R (2001). Leaf area dynamics in a closed poplar plantation under free-air carbon dioxide enrichment, *Tree Physiology* **21,** 1245–1255.

Lev-Yadun S (2000). Cellular patterns dicotyledonous woods: their regulation, In: *Cell and molecular biology of wood formation* (Eds. RA Savidge, JR Barnett and R Napier), BIOS Scientific Publishers Ltd., Oxford, 315-324.

Pereira H, Graça J, Rodrigues JC (2003) Wood chemistry in relation to wood quality. In*: Wood quality and its biological basis*, (eds. JR Barnett and G Jeronimidis), Blackwell Publishing, CRC Press, 53-86.

Savidge RA (2003) Tree growth and wood quality. In: *Wood quality and its biological basis*, (eds. JR Barnett and G Jeronimidis), Blackwell Publishing, CRC Press, 1-29.

Taylor G, Tricker PJ, Zhang FZ, Alston VJ, Miglietta F and Kuzminsky E (2003). Spatial and Temporal Effects of Free-Air CO2 Enrichment (POPFACE) on Leaf Growth, Cell Expansion, and Cell Production in a Closed Canopy of Poplar. *Plant Physiology* **131,** 177–185.

4.1.2 *Draft paper*: Does free-air with elevated CO_2-concentrations (FACE) alter vessel anatomy in juvenile poplars (*Populus nigra* L.)?

Vansteenkiste[a], D., De Boever[a], L., Van Acker[a], J., Evans[b], S., Ceulemans[c], R., Scarascia-Mugnozza[d], G. and Calfapietra[d], C.

[a] Ghent University, Belgium. (corresponding E-mail: Dries.Vansteenkiste@UGent.be); [b] Forestry Commission Research Agency, Farnham UK.; [c] University of Antwerpen, Belgium.; [d] Università degli Studi della Tuscia, Viterbo, Italy.

4.3.1.5 Abstract

The main objective of this study was to investigate the influence of elevated CO_2 concentrations ([CO_2]) on spatial and temporal variations in vessel anatomy in cross-sections of juvenile Poplar growth-rings, within the framework of the EU-funded research projects POPFACE and MEFYQUE. Defect-free material was extracted from the second annual ring (*year 2001*) of 22 three-year-old poplar trees (*Populus nigra* 'Jean Pourtet'), 10 of which had been subjected to air with enhanced [CO_2]. Using thin microtomed cross-sections and high-resolution digital image analysis, vessel anatomy has been quantified in terms of intra-ring position (radial and tangential coordinates), vessel lumen diameter, circumference and surface together with vessel frequency. Quantitative data on vessel anatomy were then converted to a physiologically relevant parameter, *i.e.* hydraulic conductivity based on the Poiseuille-Hagen equation. Cross-sectional vessel dimensions generally decreased while vessel frequency initially decreased and then increased from beginning to end of the annual ring. However, intra-ring fluctuations were observed in both the dimension and the frequency parameters, which resulted in a highly variable annual development of hydraulic conductivity. These radial variations coincide with temporal fluctuations of climatic conditions. Mean vessel diameter was found to increase as a result of CO_2-enhancement, while vessel frequency decreased. This produced a net stimulating effect on hydraulic conductivity. Intra-ring changes in vessel anatomy and hydraulic conductivity have been compared to radial profiles describing the evolution of fibre length during the growing season.

4.3.1.6 Materials and methods

Site description and plantation layout

The FACE study is located in central Italy, near Viterbo (Tuscania; 42°22• N, 11°48• E, altitude 150 m) on 9 ha of former agricultural land. Following detailed soil analyses, six 30 × 30-m experimental plots (120 m apart) were selected, and a FACE design was established in three of the plots. The remaining three plots were left under natural conditions and designated.

control plots. In late-spring 1999, the 9-ha plantation was established with poplar cuttings at a planting density of 10,000 trees ha^{-1} (1 × 1 m spacing) within the six experimental plots, and 5,000 trees ha^{-1} (2 × 1 m spacing) in the non-experimental surrounding plantation. The experimental plots were planted with three *Populus* genotypes (clones), *i.e. P.* × *euramericana*

'I-214', *P. nigra* 'Jean Pourtet' and a local selection of *P. alba* L. ('2AS-11'), whereas the non-experimental part of the plantation was planted with *P.* × *euramericana* 'I-214'. Each 314 m^2 plot contained 350 plants, and was divided into six triangular sectors, with two sectors per genotype. The plantation was designed and managed as a short-rotation forest with typical high plant densities (Mitchell *et al.* 1999). For plantation details see Scarascia-Mugnozza *et al.* (2000).
Carbon dioxide enrichment is provided through a polyethylene octagonal ring (22 m diameter) mounted on 12-m telescopic poles. Pure CO_2 is injected through laser-drilled holes in the ring (target CO_2 concentration of 550 µmol mol^{-1}). The CO_2 concentration was 544 ± 48 µmol.mol^{-1} during the first year of treatment and 532 ± 83 µmol.mol^{-1} during the second year. Daytime irrigation and CO_2 enrichment was provided from bud burst to leaf fall. Water supply to roots may therefore be considered to be close to optimal. Climate was monitored continuously, *i.e.* with a 15 minute interval; temperature, insolation, precipitation and relative humidity were recorded. For a more detailed description of the FACE setup refer to Gielen *et al*. 2001 and Miglietta *et al.* 2001.

Tree sampling, subsampling and quantitative wood anatomical methods
In total, 22 plants of the clone *P. nigra 'Jean Pourtet'* were sampled, 12 plants from the three ambient plots (2, 3 and 6) and 10 plants from the plots with elevated [CO_2] (1, 4 and 5). These are referred to as respectively Ambient-1 to Ambient-12, and Elevated-1 to Elevated-10. From clear internode samples taken at ± 1 m height in these 22 plants, small specimens including ring number 2 (year 2000) were isolated. These tree-ring samples were saturated with de-ionised water prior to microtome sectioning of 15 µm thin transversal cuts (RT) that covered the entire ring-width in each of the sampled trees. These crosscuts were stained with safranin, permanently mounted and, subjected to a specially adapted interactive image analysis programme (user scripts developed with TimWin software), using a light microscope and a digital camera at high magnification. The maximum, radial and tangential diameters, lumen circumference, surface area and local vessel frequency were quantified for every complete vessel present in radially sequenced overlapping image frames having a tangential width of nearly 1 mm. The Linear accuracy of image analysis measurements was around 1.7 µm horizontally and 1.4 µm vertically, coinciding respectively with tangential and radial directions.

Using a customized Matlab script, the data allowed mapping and the cross-sectional vessel anatomy in each ring studied, in detail and in 2D. Based on the Hagen-Poiseuille equation which describes the relationship existing between hydraulic efficiency and vessel diameter, and taking into account the differences in CO_2 regime, an attempt was made to link spatial variations in anatomical features of vessels to daily climate data in order to date characteristic fluctuations in the hydraulic conductivity curve.

4.1.2.5 Results and Discussion

First interpretations suggest that, as a result of CO_2-enhancement, the number of vessels per unit area (vessel frequency) is decreasing, while the surface of the individual vessel lumen is increasing. Also the number of vessels per vessel grouping is decreasing. (Figures 4.8 and 4.9).

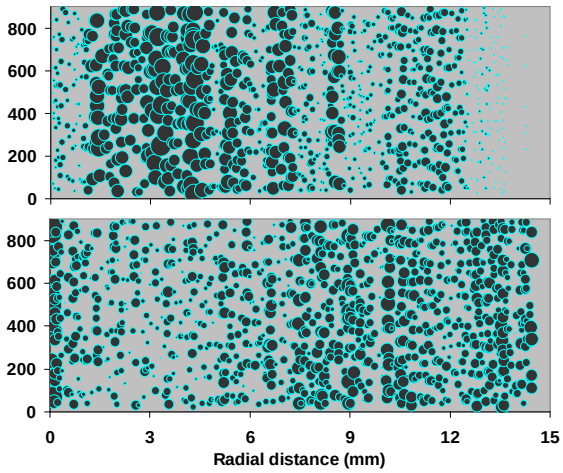

Figure 4.7: Example of 2-D bubblemaps of vessel anatomy (tree 'Elevated-7'): vessel conductivity (top) and vessel frequency (bottom) - Y-axis gives tangential distance in microns. Bubble size is proportional to the highest value of the selected variable.

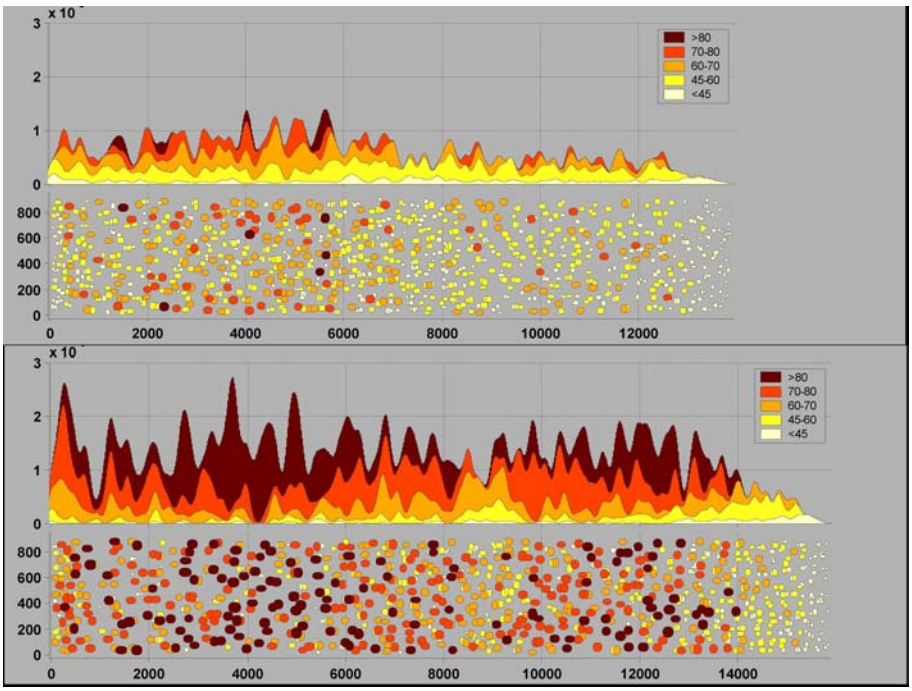

Figure 4.8: Two examples of 2-D distributions of vessels and derived radial distributions of hydraulic conductivity in the 2001-ring of trees 'Ambient-10' (top graphs) and 'Elevated-1' (bottom graphs). Vessel size is scaled proportional to highest value and colours correspond to five vessel diameter classes. X-axis gives radial distance (in µm) and Y-axis gives respectively tangential distance (in µm) and conductivity (in mm^4).

Wood formation can be divided in three processes: cell division, cell enlargement and cell maturation. At higher temperature the duration of organ growth (expansion) is shorter. Therefore, at higher temperature faster rates of cell division, cell enlargement and cell maturation can be expected for cambial cells and their derivates (Bannan 1962; Fritts 1976; Horacek *et al.* 1999). On a single cell basis, faster rates of cell production may cause an opposite trend to the effect of a 'better' substrate supply of the cambium by elevated CO_2. If at higher temperature levels the cells undergo higher rates of cell enlargement and cell maturation, then the duration in which the assimilates can be used is shortened. This explains why the cell walls tended to become thinner at higher temperature. On the other hand, faster growth rates of juvenile trees may lead to a faster aging of the cambial initials. The cell length

and tangential diameter of tracheids is mainly determined by the size of the cambial initials which increase with time during the first 20-30 years. It was previously pointed out that differences in growth rate can lead, with time, to different development stages between different CO_2 treatments (Bruhn *et al.* 2000). In experiments in which the elevated/ambient ratio of tree ring width was high, a significant response of wood anatomical properties to CO_2 could be measured.

Interpretation of results will depend on considerations which take into account the presence of microdomains (senso Savidge 2003). Trees of one clone having received the same treatment may produce very different anatomical structures. The control mechanisms underlying microdomain formation could be at the heart of this structural variability of wood. Both solute concentration and water-potential gradients extend longitudinally over branches and stem; cambial age and the processes leading to wood formation also vary along the axis of the tree. The intrinsic environment experienced by individual cambial cells will vary from one point to the next, even when the extrinsic environment of the whole tree is maintained constant. Irrigation, for instance, can greatly increase the latewood to earlywood ratio of temperate-zone conifers, evidently by forestalling the entry of the cambium into dormancy during the period of cambial growth in mid- to late-summer. Water availability also determines the nature of wood forming in hardwoods. Mature *Populus balsamea* leaves induce cambial cells to differentiate into fibres but not into vessel members, whereas young developing leaves induce both vessel members and fibres to differentiate. Differentiation of cambial derivatives into vessel members is well established to be under auxin regulation (Savidge 2003). The latter suggests that the development of vessels is closely linked to leaf area development and maturation. Increased vessel frequency and formation of smaller vessels may result from drought stress or mechanical stress (tension wood formation).

4.1.2.6 References

Anfodillo T, Sigalotti GB, Tomasi M, Semenzato P, Valentini R (1993). Applications of a thermal imaging technique in the study of the ascent of sap in woody species, *Plant Cell Env*. **16**, 997-1001.

Ceulemans R, Jach ME, Van de Velde R, Lin JX, and Stevens M (2002). *Global Change Biology* **8**, 153-162.

Cruiziat P, Cochard H, Améglio T (2002). Hydraulic architecture of trees: main concepts and results. *Ann. For. Sci.* **59**, 723-752.

Lev-Yadun S (2000). Cellular patterns dicotyledonous woods: their regulation, In: *Cell and molecular biology of wood formation* (Eds. RA Savidge, JR Barnett and R Napier), BIOS Scientific Publishers Ltd., Oxford, 315-324.

Savidge RA (2003) Tree growth and wood quality. In: *Wood quality and its biological basis*, (eds. JR Barnett and G Jeronimidis), Blackwell Publishing, CRC Press, 1-29.

4.1.3 *Draft paper*: Effects of Free-Air Carbondioxide Enrichment (FACE) on intra-ring microdensity variations and micromechanical properties of juvenile poplar trees (*Populus nigra* L.)

De Boever[a], L., Vansteenkiste[a], D., Van Acker[a], J., Ceulemans[b], R., Scarascia-Mugnozza[c], G. and CALFAPIETRA[c], C.

[a] Ghent University Belgium.(corresponding E-mail: Dries.Vansteenkiste@UGent.be); [b] University of Antwerpen, Belgium.; [c] Università degli Studi della Tuscia, Viterbo, Italy.

4.1.3.1 Abstract

Within the framework of the EU-funded research projects POPFACE and MEFYQUE, defect-free material was extracted from the second annual ring (*year 2001 ??*) of 22 three-year-old *Populus nigra* trees (clone 'Jean Pourtet'), 10 of which had been subjected to air with enhanced CO_2-concentrations ($[CO_2]$). Using a specially adapted microtome, 150 µm thin tangential sections (TL) were cut out sequentially along the radial direction in each annual ring. Each strip was subjected to gravimetrical analysis and micromechanical testing to

measure microdensity, modulus of elasticity (MOE) and modulus of rupture (MOR). Results are highly dependent on intra-ring position and showed considerable variation between trees. Wood density and mechanical properties generally decreased from the beginning towards the end of the growth ring. Effects of [CO_2] enhancement appeared to be most pronounced at the beginning and towards the end of the annual ring. Principal components analysis (PCA) revealed that microdensity, MOE and MOR increase significantly with respectively 5%, 8% and 6% under the influence of enhanced [CO_2]. It is assumed that intra-ring micro-density variations can be explained by changes in vessel porosity and fiber length, which are also affected by enhanced [CO_2]. The potential of the described methodology to establish early assessment criteria for evaluating wood quality at tree maturity are briefly discussed.

4.1.3.2 Materials and methods

Site description and plantation layout

The FACE study is located in central Italy, near Viterbo (Tuscania; 42°22• N, 11°48• E, altitude 150 m) on 9 ha of former agricultural land. Following detailed soil analyses, six 30 × 30-m experimental plots (120 m apart) were selected, and a FACE design was established in three of the plots. The remaining three plots were left under natural conditions and designated control plots. In late-spring 1999, the 9-ha plantation was established with poplar cuttings at a planting density of 10,000 trees ha^{-1} (1 × 1 m spacing) within the six experimental plots, and 5,000 trees ha^{-1} (2 × 1 m spacing) in the non-experimental surrounding plantation. The experimental plots were planted with three *Populus* genotypes (clones), *i.e. P.* × *euramericana* 'I-214', *P. nigra* 'Jean Pourtet' and a local selection of *P. alba* L. ('2AS-11'), whereas the non-experimental part of the plantation was planted with *P.* × *euramericana* 'I-214'. Each 314 m^2 plot contained 350 plants, and was divided into six triangular sectors, with two sectors per genotype. The plantation was designed and managed as a short-rotation forest with typical high plant densities (Mitchell *et al.* 1999). For plantation details see Scarascia-Mugnozza *et al.* (2000). Carbon dioxide enrichment is provided through a polyethylene octagonal ring (22 m diameter) mounted on 12-m telescopic poles. Pure CO_2 is injected through laser-drilled holes in the ring (target CO_2 concentration of 550 µmol mol–1). The CO_2 concentration was 544 ± 48 $\mu mol.mol^{-1}$ during the first year of treatment and 532 ± 83 $\mu mol.mol^{-1}$ during the second year. Daytime irrigation and CO_2 enrichment was provided from bud burst to leaf fall. For a detailed description of the FACE setup is referred to Gielen *et al*. 2001 and Miglietta *et al.* 2001.

Tree sampling, subsampling and experimental methods

In total, 22 plants of the clone *P. nigra 'Jean Pourtet'* were sampled, 12 plants from the three ambient plots (2, 3 and 6) and 10 plants from the plots with elevated [CO_2] (1, 4 and 5). These are referred to as respectively Ambient-1 to Ambient-12, and Elevated-1 to Elevated-10. From clear internode samples taken at ± 1 m height in these 22 plants, specimens including ring number 2 (year 2000) were isolated from the stem so that the dimensions were about 6 cm longitudinally and 8 mm tangentially (Figure 4.9).

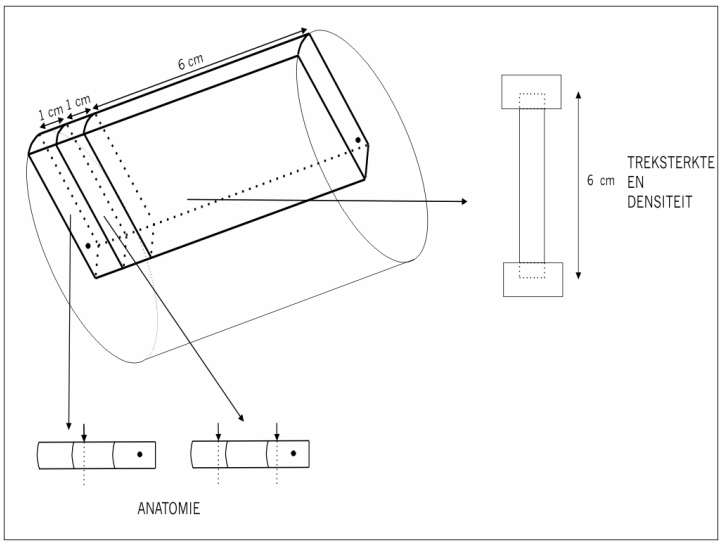

Figure 4.9: Sampling scheme applied to each poplar stem: radial sectioning of 150 µm thin tangential (TL) strips from the ring formed in the year 2000.

These tree-ring samples were saturated with de-ionised water and, using a specially adapted microtome, an intra-ring subsampling was carried out at 150 µm radial intervals. This yielded sets of successive strips of equal thickness covering the entire ring-width. After drying and conditioning to an equilibrium moisture content of 12 %, the strips were weighed individually and a 2D-image was scanned of their tangential face at 1200 dpi (pixels of 21.2 µm). Subsequently, mechanical tensile testing up to rupture was performed on each strip with a universal test-bench (Zwick) equipped with a low tensile stress-strain probe (Figure 4.10.).

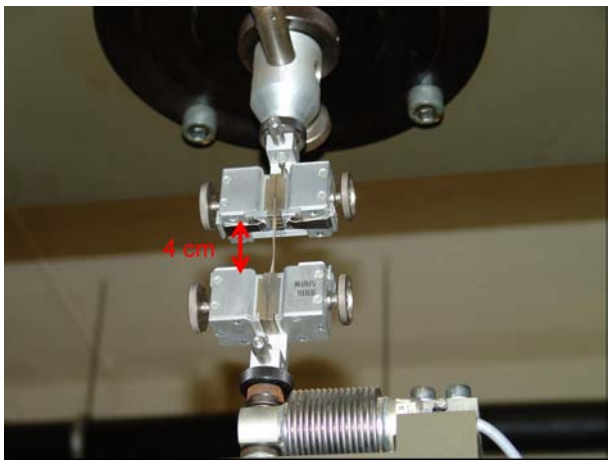

Figure 4.10: Close-up of a thin strip clamped for tensile testing (Zwick).

Typical dimensions of each strip and of five strip segments, such as tangential surface area, length and mid-strip width were estimated in the scanned images using automated digital image analysis (customised scripts written under Visilog 5.4). Strip thickness was estimated with a micro-meter gauge up to 0.001 mm. This information combined with the weight measurements allowed estimating the volumetric weight of each strip.

4.1.3.3 Results and Discussion

The first results indicate a clear relationship between the evolution of the physical and mechanical properties (Figure 4.12). The curves describing intra-ring density, MOE and MOR clearly follow similar or correlated trends

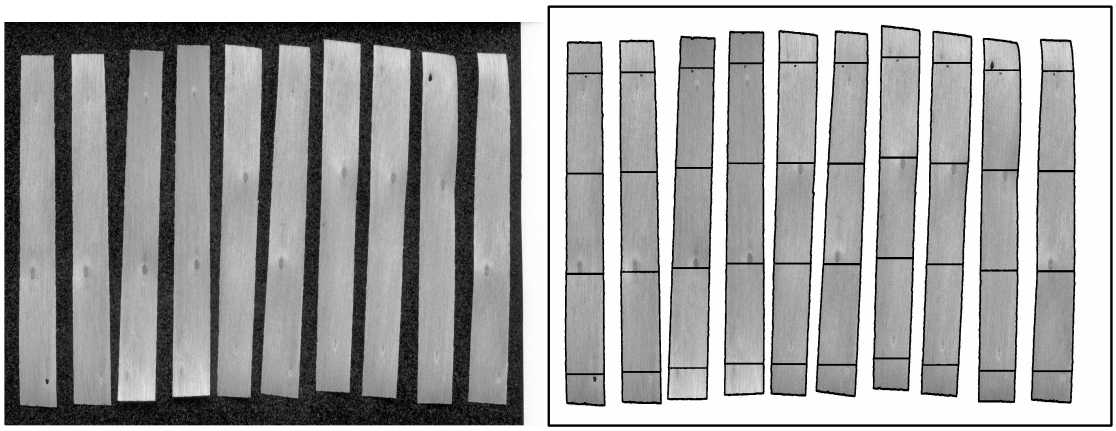

Figure 4.11: Left: scanned image of the tangential face of ten thin strips prior to testing - Right: output after image analysis showing different sections considered for dimensional characterisation of each strip. Note the presence of a small sleeping bud in all ten strips.

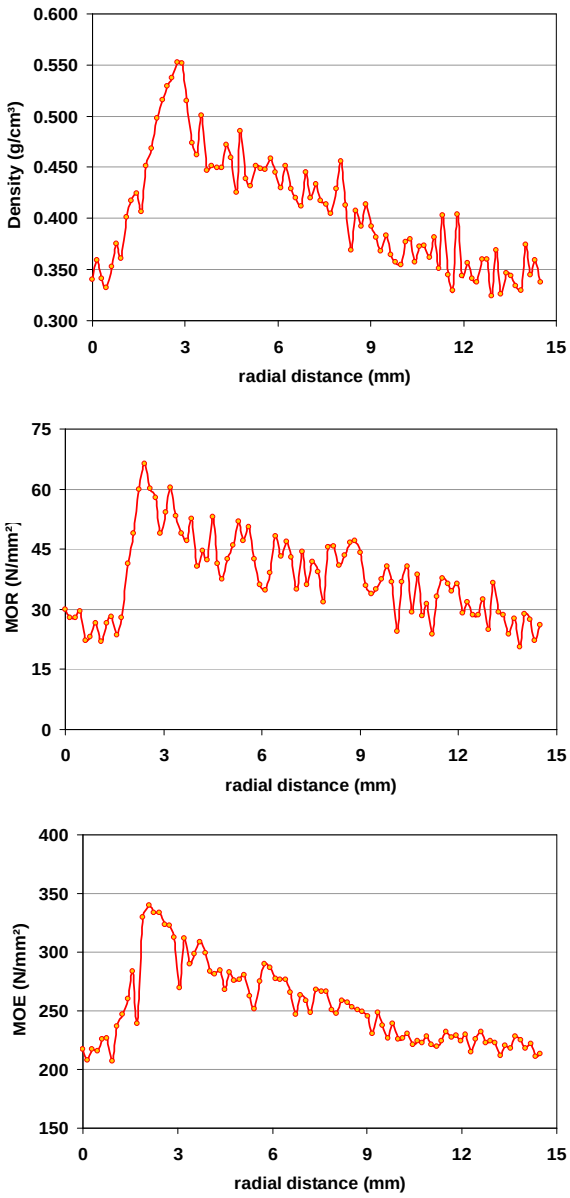

Figure 4.12: The evolutions of density (top graph), MOR (middle) and MOE (bottom) in the ring formed in 2000 of tree 'Elevated-7' show similar trends.

Although it is difficult to link wood anatomical properties directly to wood quality, an understanding of micro-allocation patterns is crucial for the understanding and prediction of wood formation and the resultant wood quality. The CO_2 and the temperature effect on wood formation and micro-allocation patterns are not necessarily synchronised. If due to CO_2 enhancement more assimilates are transferred from leaves to stem, a 'better' supply of cambial cells and their derivates should lead to higher production of cells and higher carbon allocation to cell wall. On the other hand, an increase in temperature can lead to faster rates of cell division, cell growth and cell maturation and consequently shorten the time in which the assimilates can be used by the cells (Morison and Lawlor 1999).

Wood formation can be divided in three processes: cell division, cell enlargement and cell maturation. At higher temperature the duration of organ growth (expansion) is shorter. Therefore, at higher temperature faster rates of cell division, cell enlargement and cell maturation can be expected for cambial cells and their derivates (Bannan 1962; Fritts 1976; Horacek *et al.* 1999). On a single cell basis, faster rates of cell production may cause an opposite trend to the effect of a 'better' substrate supply of the cambium by elevated CO_2. If at higher temperature levels the cells undergo higher rates of cell enlargement and cell maturation, then the duration in which the assimilates can be used is shortened. This explains why the cell walls tended to become thinner at higher temperature. On the other hand, faster growth rates of juvenile trees may lead to a faster aging of the cambial initials. The cell length and tangential diameter of tracheids is mainly determined by the size of the cambial initials that increase with time during the first 20-30 years. It was previously pointed out that differences in growth rate can lead, with time, to different development stages between different CO_2 treatments (Bruhn *et al.* 2000). In experiments in which the elevated/ambient ratio of tree ring width was high, a significant response of wood anatomical properties to CO_2 could be measured.

4.1.3.4 References

Morison JIL, Lawlor, DW (1999). Interactions between increasing CO_2-concentration and temperature on plant growth, *Plant, Cell and Environment* **22** (6), 659-682.

Thibaut B, Gril J (2003) Growth stresses. In: *Wood quality and its biological basis*, (eds. JR Barnett and G Jeronimidis), Blackwell Publishing, CRC Press, 137-156.

Savidge RA (2003) Tree growth and wood quality. In: *Wood quality and its biological basis*, (eds. JR Barnett and G Jeronimidis), Blackwell Publishing, CRC Press, 1-29.

Zink-Sharp A (2003) The mechanical properties of wood. In*: Wood quality and its biological basis,* (eds. JR Barnett and G Jeronimidis), Blackwell Publishing, CRC Press, 187-210.

4.2 Mature trees under normal conditions

In addition, experimental work has been performed on coniferous trees from mature forest stands (*Pinus sylvestris* L.), for which the main goal was to integrate quantitative information on tracheid anatomy into process-based models simulating tree growth and wood quality features. This resulted in paper, Vansteenkiste, D. *et al*. (in prep, c): The together with knowledge gathered by other partners has provided quantitative data that are useful to process-based modellers and resulted in a further paper in preparation, Deckmyn, et al. (in prep) (see also chapter 6):

- Extrapolation of cross-sectional anatomical features of tracheids in Scots Pine (*Pinus sylvestris* L.) using intra-annual porosity and microdensity profiles.
- Modelling wood tissue development as influenced by climate and tree dominance: a case study using the Mefyque model for a temperate pine forest.

4.2.2 Draft paper: Extrapolation of cross-sectional anatomical features of tracheids in Scots Pine (*Pinus sylvestris* L.) using intra-annual porosity and microdensity profiles

Vansteenkiste[a], D., Ziche[b], D., Deckmyn[c], G., De Boever[a], L., Overdieck[b], D., Ceulemans[c], R. and Van Acker[a], J.

[a] Ghent University, Belgium. (corresponding E-mail: Dries.Vansteenkiste@UGent.be); [b] Technical University of Berlin, Berlin, Germany.; [c] University of Antwerpen, Belgium.

4.2.2.5 Introduction

Scots pine (*Pinus sylvestris* L.) is the most widely distributed pine species in Eurasia and one of the important timber species. As a coniferous species, Scots pine has a uniform structure with tracheids forming the bulk of the wood. Tracheids are elongated cells arranged in radial files that account for both long-distance conduction of water and mechanical support. Wood produced by temperate trees in spring and summer is referred to as earlywood and that produced late in the growing season is termed latewood. This results in the formation of distinct annual growth-rings. Earlywood tracheids are thin-walled and large-lumened, while those of the latewood are thick-walled and small-lumened. The density of oven-dried cell wall material for all woody plants is about 1500 kg/m³. Wood with thicker-walled cells has a higher density than wood with thinner-walled cells of comparable size. Density is also determined by the diameter of the cells and the presence of extractives. The first few growth rings at any one level in the tree are usually wider than those produced further out in most trees. At low levels in the tree, this means that ring width decreases with ring number outwards from the pith. In most cases, the narrower the growth ring, the higher the proportion of latewood cells. However, variations in the proportion of early- to latewood are also a result of intra-specific differences and climatic variations (Butterfield 2003). Anatomical and chemical characteristics are the ultimate factors that determine the overall properties of wood as a material and distinguish the different types of wood within a living tree (Pereira et al. 2003). At the stem base the supply of the cambium with carbohydrates as a function of tree height is minimal so that the greatest sensitivity to environmental conditions can be expected at this height.

The objective of this research was to obtain detailed data on cell structure and microdensity variations by establishing a link between anatomical measurements at the individual cell level and radial cell porosity and microdensitometrical profiles at the annual ring level. Cell dimensions reflect the cambial activity throughout the vegetation period. For ascertaining environmental triggers of growth responses there is a need for measuring intra-annual profiles of the cell dimensions. This work was carried out within the framework of the European project MEFYQUE.

4.2.2.6 Materials and methods

Site description, tree selection and sampling

The field site is an even-aged, 70-year-old Scots pine (*Pinus sylvestris* L.) stand, representing a portion of a 150 ha mixed coniferous/deciduous forest called “De Inslag” in Brasschaat (51°18'33" N, 4°31'14" E), in the Belgian Campine region, Northern Belgium. The stand includes a Level II observation plot of the UN/ECE ICP Forest Health Monitoring Network. In 1997, stand density was 377 trees.ha^{-1}, basal area 28.5 m^2.ha^{-1}, mean DBH 29.7 cm and mean height 21.4 m. Overall, this pine forest has an open canopy, with a mean canopy gap fraction of 35 %. The soil has been described as a moderately wet sandy soil with a distinct humus and/or iron B-horizon. Needle analysis has shown the stand to be low in magnesium and phosphorus. However, needle nitrogen (N) concentrations were optimal as the site is located in an area with high NO_x and ammonia deposition. The soil is moist and often saturated, with a high hydraulic conductivity in the upper soil layers (sand). However, due to the presence of a clay layer the site has poor drainage. Groundwater is normally at 1.2 to 1.5 m. Topography is flat (slope less than 0.3 %), situated at an elevation of 16 m a.s.l.. Mean long-term annual temperature at the site is 9.8 °C, with 3 °C and 18 °C as mean temperatures of the coldest and warmest months, respectively. Mean annual precipitation is 767 mm; rainfall is fairly even distributed throughout the year but with slightly higher precipitation often occurring during July or August (Sampson *et al.* 2001).

In Autumn 2001, stem-discs were sawn at three different height-levels in three suppressed, three codominant and three dominant Scots Pine trees. Small cubes including at least the 15 outermost growth-rings were cut out along the N-radius from each stem-disc and subjected to sectioning with a sliding microtome. Prior to permanent embedding with Euparal on glass slides, the transverse sections of 20-30 µm thickness were lignin-stained with safranin (red). Two to five *replica* sections were made for each sequence of 15 rings. In addition, matching with these crosscuts, thin specimens of 3 mm longitudinally (L), 30 mm tangentially (T) and 30 mm radially (R) have been cut out for X-ray microdensitometrical analysis.

Anatomical profiles

A transmitted light microscope was used for the estimation of tracheid features, at a magnification of 400 x. The microscope was equipped with a digital camera connected to an image capturing board controlled by QWin 2.8 software (Leica Microsystems). This combination of microscope and digital imaging system resulted in 8-bit grey level images of 254 µm x 195 µm, with a resolution of 0.34 µm per pixel. Frame averaging (n=5) and contrast-stretching with a logarithmic look-up table (LUT) were performed in order to reduce noise and to improve contrast between cell walls and lumens. Subsequent image frames were taken in radial line every 200 µm within the outermost 10 growth-rings (1992-2001). Using an optimized automated segmentation method, cell walls were separated from lumens. The success of the segmentation was controlled manually by visual assessment. In the binary images of cell walls, the individual tracheid cells were then outlined by calculating a skeleton line representing an artificial middle lamella (ML). This way, a one-pixel-wide ML was set at half the distance between two lumen borders (Fig.). Subsequently, the widths and areas of cell wall and lumen could be calculated on a single cell basis. The ratio of double cell wall width to lumen width (Mork's index, to distinguish between latewood and earlywood tracheids) was derived from these variables and, in addition, the ratio of cell wall to total cell area as well as the roundness (perimeter² / 4*pi*area*1.067). Only complete cells were included in the analysis. The relative position within the tree ring as well as the distance to the 1991-1992 tree ring border were also determined for each frame.

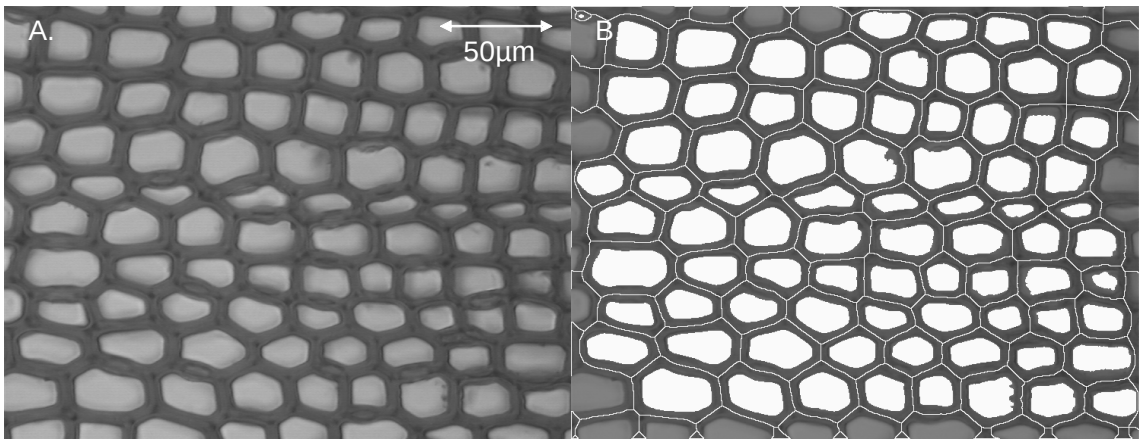

Figure 4.13: A) Input grey-level image; B) Result image overlayed with a white skeleton line outlining the middle lamella and a white mask covering lumens; Image size is 254 x 195 µm.

Cell porosity profiles

The same rings (1992-2001) have been analysed with transmitted light microscopy at lower magnification (10 x) and image analysis, in order to calculate radial cell porosity profiles. The image acquisition setup, a microscope equipped with a digital camera connected to a framegrabber on PC, allowed to digitise 8-bit grey level images (512 x 512 pixels) with a resolution of 3.7 µm. All images were digitised by averaging five frames, to reduce noise due to light-source fluctuations in the microscope and electronic instability in the camera CCD sensor. After manual selection of a rectangular area of interest (AOI of 500 µm wide T) and

delimitation of growth ring borders, a non-linear contrast stretch was performed to improve accuracy in the following segmentation step. This allowed automatic thresholding and correct separation of cell walls from lumens (Fig. 4.14).

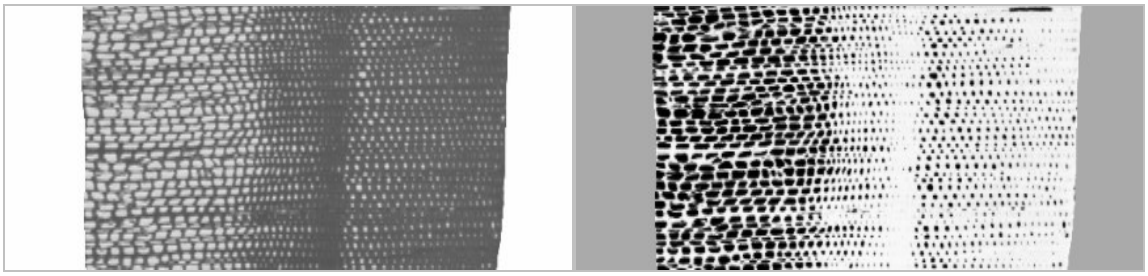

Figure 4.14: Digitized input image (left) and segmented image (right) of an annual ring in cross-section, showing earlywood cells (left) and latewood cells (right). In the segmented image, the black pixels correspond to tracheid lumens, white pixels are tracheid cell walls and grey areas are image background. Pixel size is 3.7 µm horizontally and 4.8 µm vertically.

Again, the success of the segmentation was controlled manually by visual assessment. Subsequently, greylevels of pixels located at the same radial position relative to the initial growth ring border were averaged. These data were exported to tab-delimited output files. Image acquisition, processing and analysis were carried out using self-written interactive image processing scripts (TimWin software). This procedure was applied three times to each ring by selecting three different AOI, free of resin canals.

Due to small intra-ring variations of ring width, the length as well as the shape of the three profiles describing the development of cell porosity in an annual ring may differ (Fig. left). To improve correspondence between profile triplets and to allow correct averaging, wiggle matching was performed (Matlab user script) (Figure 4.15, right).

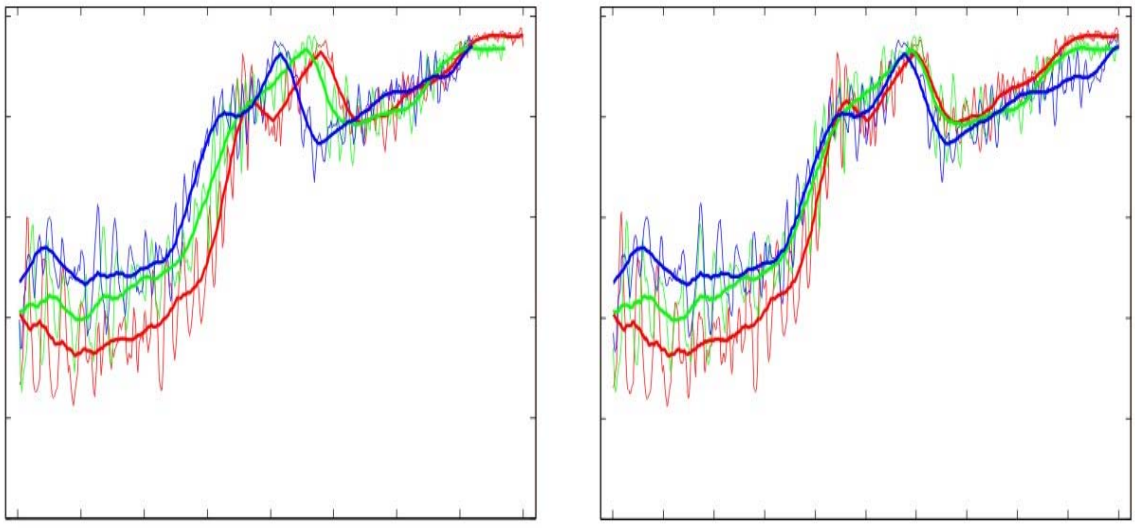

Figure 4.15: Set of radial porosity profiles derived from image analysis of cross-sections of an annual growth-ring before (left) and after (right) wiggle-matching, plotting mean intensity (maximum range 0 to 255) as a function of absolute pixel distance (left) and relative radial distance (right). Radial stepsize is approximately 3.7 µm.

Microdensity profiles

Covering the same 10 years, matching 3 mm-thick wood strips have been used to perform microdensitometrical analysis. X-ray imaging has been carried out at INRA Nancy, France. The radiographic photographs were digitised at 1200 dpi (Fig., right) and subjected to automated image analysis scripts (Visilog 5.4) of which the output are radial microdensity profiles with a stepsize of 21.2 µm. Each profile integrates the microdensity values of all pixels present in a tangential stretch of at least 2.5 cm wide (Figure 4.16.).

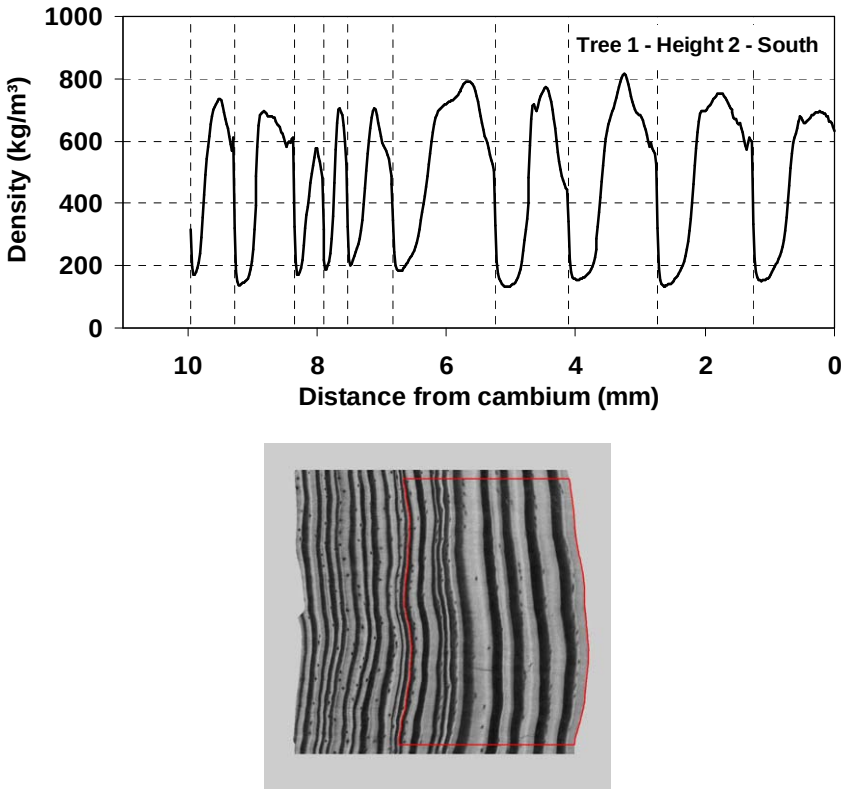

Figure 4.16: Radial microdensity profile with a stepsize of 21.2 µm calculated from image analysis of the X-ray image shown on the right. Ten outermost annual rings were analysed (period 1992-2001).

Cross-matching data from anatomical, porosity and microdensity profiles

In this study, anatomical and porosity profiles have been analysed in 171 rings, producing two datasets of respectively 81 (9 trees x 3 heights x 3 rings) and 90 rings (9 trees x 1 height x 10 rings). In addition, radial microdensity profiles have been assessed in 270 rings (9 trees x 3 heights x 10 rings), for the upper heights (2, 3 and 4). These different types of data will be cross-correlated to link cell porosity profiles to microdensity profiles and to allow interpolation of the rough anatomical profiles, for which only one datapoint is available every 200 µm.

4.2.2.7 Results and Discussion

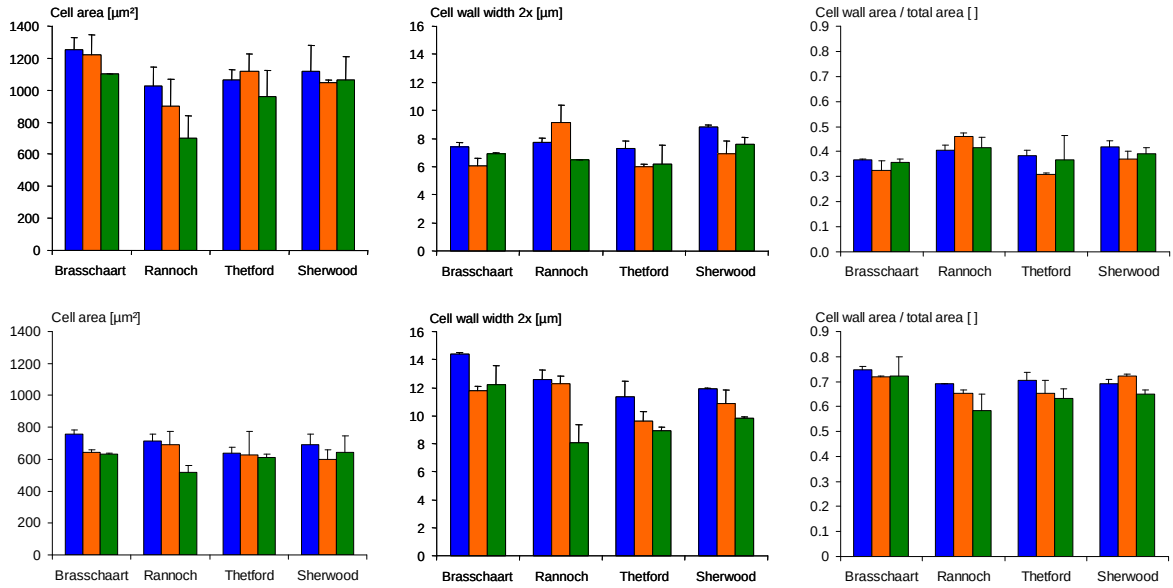

Figure 4.17: Effects of tree dominance class and site on cell area (a & d), cell wall width (b & e) and ratio of cell wall area to total cell area (c & f) of earlywood cells (a – c) and latewood cells (d – f); with blue = dominant, orange = subdominant and green = suppressed trees.

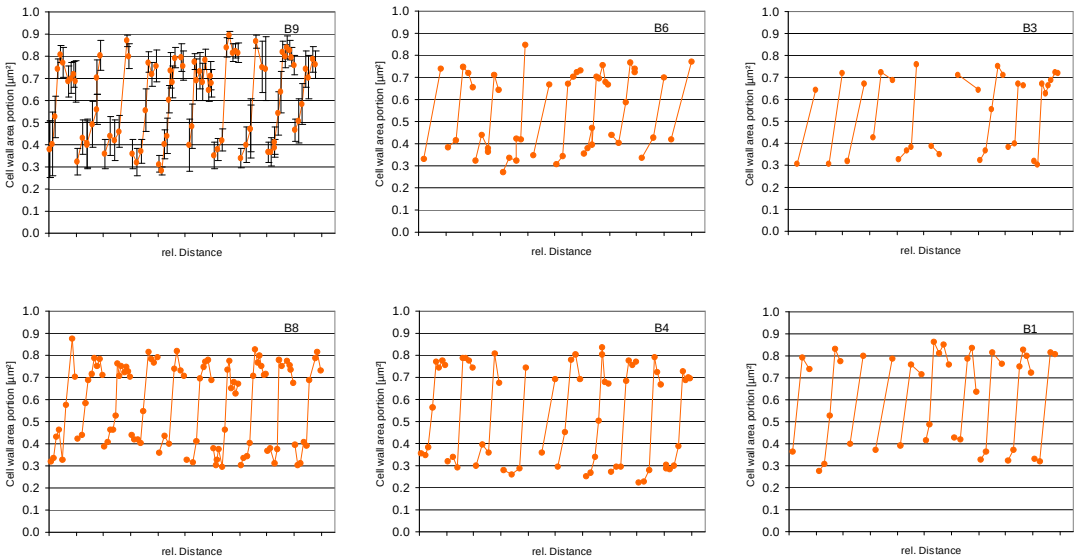

Figure 4.18: Intra-anual profiles of cell wall area proportion in the years 1992-2001 of six Scots pine trees. In the upper left graph (sample 1801) the standard deviation was included.

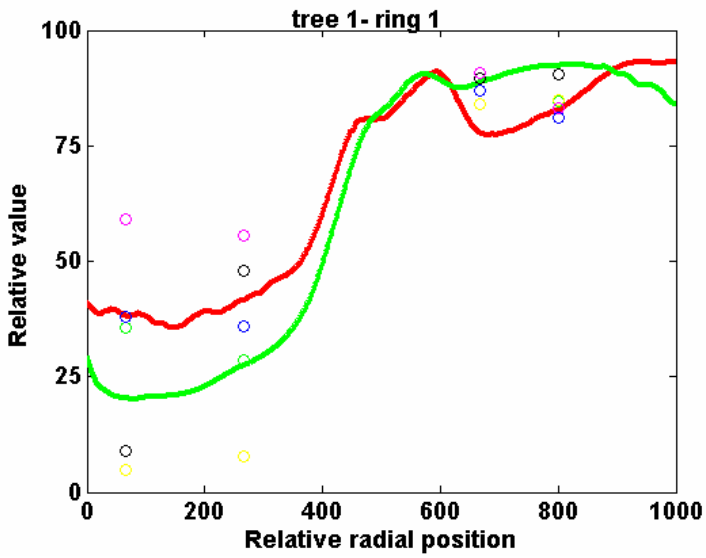

Figure 4.19: Red curve: porosity profile - Green curve: corresponding microdensity profile - Data points at four different relative positions: anatomical features of tracheid cells, such as cell wall thickness, lumen width and cell wall area.

With regard to the drop in the porosity profile around position 700 - which is actually an increase - this could be due to the presence of resin canals. The drop is not apparent in the microdensity profile at the same position.

It should be possible to evaluate the influence of tree dominance on cross-sectional tracheid anatomy, considering differences between earlywood, latewood and transition wood tracheids.

4.2.2.8 Discussion

Ratio of cell wall area to total cell area is one of the main components of wood density. The pattern of earlywood cell formation is often regarded to be influenced mainly by temperature whilst latewood formation is mainly considered as a product of assimilate supply. Uggla *et al.* (2001) reported constant carbohydrate levels in the cambial zone during earlywood / latewood transition and could support the theory that the duration and not the rate of wall material deposition causes variation in cell wall thickness (Whitmore and Zahner 1966; Skene 1969; Wodzicki 1971; Horacek *et al.* 1999). The radial cell width is affected by soil water supply during cell enlargement (Antonova et al., 1995; Horacek et al., 1999).

The detailed anatomical and microdensity profiles will be used to validate output generated by the Mefyque model for Scots Pine in Brasschaat.

4.2.2.9 References

Bues CT (1985). Der Einfluss von Bestockungsgrad und Durchforstung auf die Rohdichte von südafrikanischer *Pinus radiata*. *Holz Roh Werkst*. **43,** 69-73.

Butterfield BG (2003) Wood anatomy in relation to wood quality. In*: Wood quality and its biological basis,* (eds. JR Barnett and G Jeronimidis), Blackwell Publishing, CRC Press, 30-52.

Grosser D, Schulz H, Utschig H (1985). Mögliche anatomische Veränderungen in erkrankten Nadelbäumen, *Holz Roh Werkst*. **43**, 315-323.

Horá•ek P (2003). Wood structure: a tool for evaluating in growing conditions of Norway spruce, *Ekológia (Bratislava)* **22** suppl. 3, 147-162.

Horá•ek P, Šlezingerová J, Gandelová L (1996). Ecophysiology of xylogenesis - Interpretation of cambial activity and xylem development, IUFRO S2.01.10 Conference, August 6-10, Krasoyarsk, Russia, 144-148.

Horá•ek P, Šlezingerová J, Gandelová L (1999). Effect of environment on the xylogenesis of Norway spruce, In: *Tree ring analysis: biological, methodological and environmental asp*ects (Eds. R Wimmer, RE Vetter), CABI International, University Press, Cambridge, 33-53.

Koubaa A, Zhang SYT, Makni S (2002). Defining the transition from earlywood to latewood in black spruce based on intra-ring wood density profiles from X-ray densitometry, *Ann. For. Sci*. **59**, 511-518.

Lebourgeois F (2000). Climatic signals in earlywood, latewood and total ring width of Corsican pine from western France, *Ann. For. Sci*. **57,** 155-164.

Pereira H, Graça J, Rodrigues JC (2003) Wood chemistry in relation to wood quality. In: *Wood quality and its biological basis*, (eds. JR Barnett and G Jeronimidis), Blackwell Publishing, CRC Press, 53-86.

Rigling A, Waldner PO, Forster T, Bräker OU, Pouttu A (2001). Ecological interpretation of tree-ring width and intraannual density fluctuations in *Pinus sylvestris* on dry sites in the central Alps and Siberia, *Can J. For. Res*. **31,** 18-31.

Sampson DA, Janssens IA and Ceulemans R (2001). Simulated soil CO2 efflux and net ecosystem exchange in a 70-year-old Belgian Scots pine stand using the process model SECRETS. *Ann. For. Sci*. **58** (2001), 31–46.

4.2.3 Draft paper: Modelling wood tissue development as influenced by climate and tree dominance: a case study using the Mefyque model for a temperate pine forest

Deckmyn[a], G., Randle[b], T., Ziche[c], D., Vansteenkiste[d], D., Ceulemans[a], R. and Evans[b], S.
[a] University of Antwerpen, Belgium.(corresponding E-mail: Gaby.Deckmyn@ua.ac.be); [b] Technical University of Berlin, Germany.; [c] Ghent University, Belgium.; [d] Forestry Commission Research Agency, Farnham, UK.

4.2.3.5 Abstract

A plot scale forest model has been developed that dynamically simulates wood tissue development from physiological principles. The forest is described as consisting of dominant, sub-dominant and suppressed trees. In addition to total growth and yield, the model simulates the daily evolution in tracheid biomass and radius, parenchyma and branch development. From these data early and latewood biomass, wood tissue composition and density are calculated. Together with knots, derived from simulated branching, model outputs provide good approximations of wood quality. The model is validated using data from a temperate pine (*Pinus sylvestris* L.) forest where wood anatomical data (cell wall area, lumen area, density and ring widths) have been collected. Results indicate that dominance effects on wood development, present in the observational data, are adequately simulated in the model. Validated simulation experiments indicate that the Mefyque model is a useful tool for predicting environmental and management effects (as influencing tree competition) on wood quality.

5 The MEFYQUE modelling approach

Main Contributors:

Thies Eggers, Jeannette Meyer, Marcus Lindner, Gaby Deckmyn, Tim Randle, Keith Maun

5.1 Introduction

The overall objective of the MEFYQUE project was to study the relationships between site conditions and growth, yield and timber quality for current and future scenarios of atmospheric change. This objective was targeted by developing a prototype modelling system operating at an appropriate forestry management scale (the forest stand) to forecast timber growth, yield, and quality suitable for application in the EU. The system will also predict and quantify reversible and irreversible energy fluxes to and from the forest, including those due to fossil fuel consumption. Such a forecasting system must account for the reshaping of European forestry through policies aimed at the optimisation of sustainable management, the provision of renewable resources and the protection of the global and local environment, in particular the role of forestry in the carbon cycle. The project developed a tool for use both by researchers, the timber industry and national/governmental policy decision-makers.

The principal deliverable of the project was an integrated modelling system to assist forest managers, the timber industry and policy makers in decision making whether management of forests should be preliminary for production, conservation or amenity outputs, within the context of multi-purpose forest management.

This chapter documents the components of the integrated modelling system:

- A coupled empirical-process model of timber growth, yield, quality and carbon sequestration including non-harvestable fractions, operating at the stand scale (Sections 5.2, 5.3)
- A sawmilling model of log grading, cross cutting, and batten strength grading to predict the volumetric and product quality outputs from standing trees (section 5.4);
- A large-scale forest resource model to produce projections of the possible future development of forest resources on a European, national or regional scale (section 5.5);
- A carbon allocation model to follow carbon in harvested timber through the forest industries, the various usage categories of wood-based products and its final re-release to the atmosphere through landfill decay or combustion (section 5.6).

The report describes the models and how they interact with each other (Figure 5.2).

The growth model, cross-cut, saw-milling and summaraising programs have been linked through a simple interface in order to run the models sequentially (Figure 5.1).

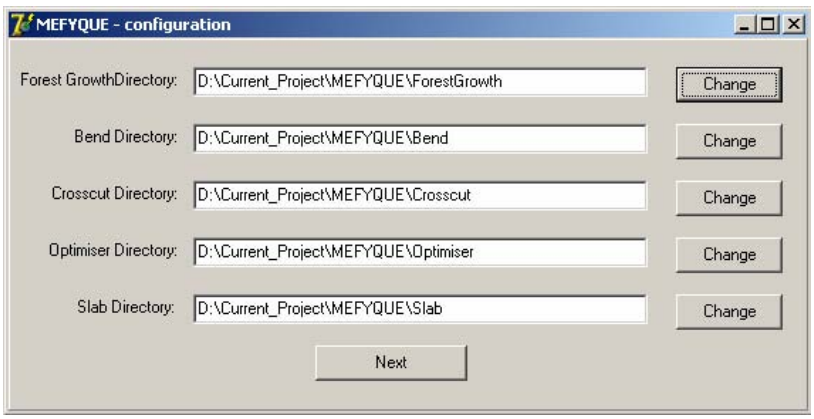

Figure 5.1: Linkage between Mefyque models

Many of the models (and modifications) resulted from discussions with other members of the consortium and external colleagues.

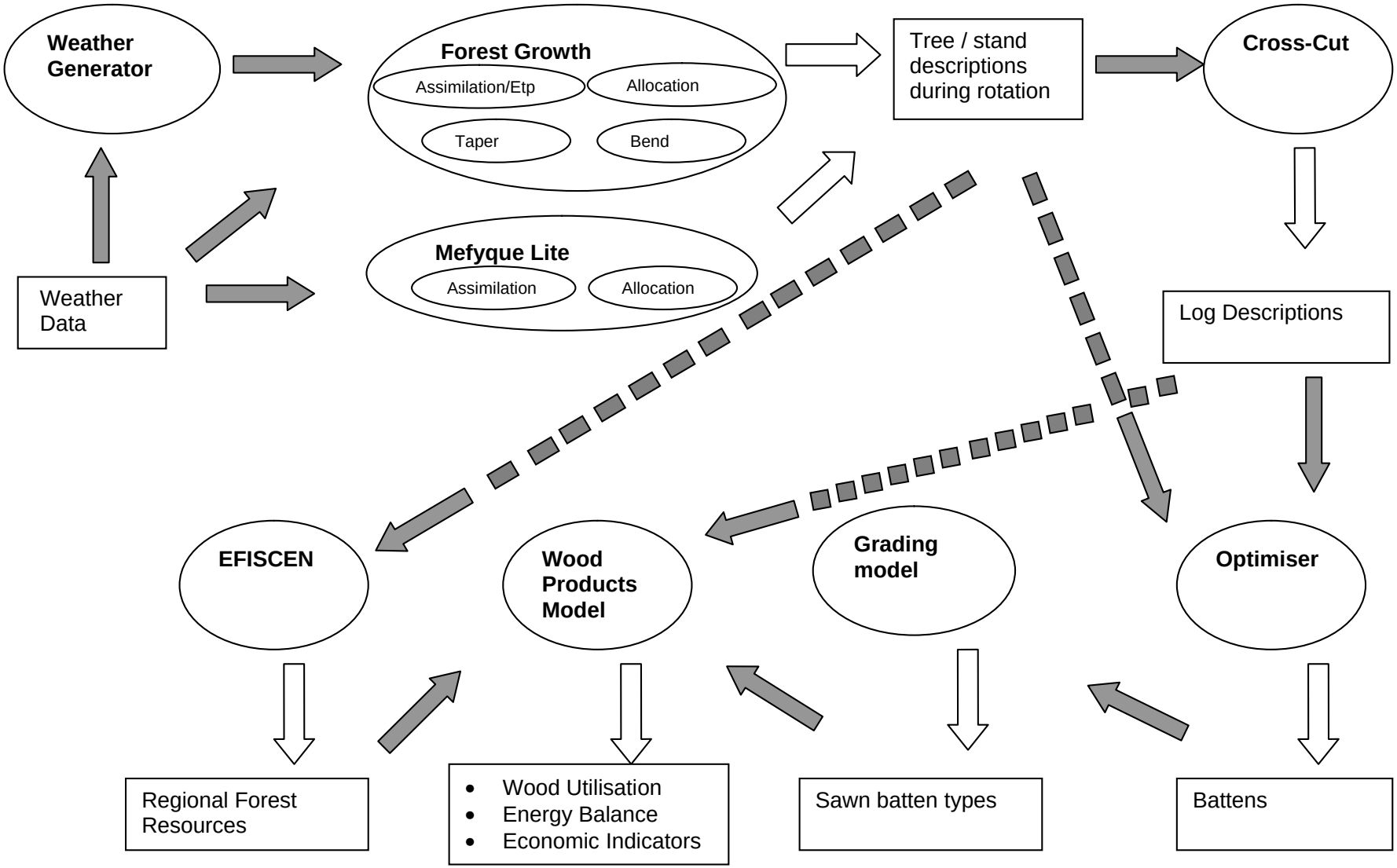

Figure 5.2: Modelling sequence pathway for the whole woodchain model. Boxes show output information. Dark arrows represent data input, light arrows output.

5.2 The MEFYQUE stand model - Lite version

Gaby Deckmyn, Tim Randle and Sam Evans

This model was developed primarily by UA for the Mefyque project, deriving new allocation rules in order to describe the constituent part of each growth ring more fully.

The model is less detailed than the Forest growth model, but was essential to develop and test the allocation rules, prior to inclusion within the more complex model. The description of the model is detailed as it follows a novel approach to allocation and wood quality

This description is to give insight into the fundamental principles of the model and to facilitate reading of the source code of the model. Existing models for processes (s.a. photosynthesis according to Farquhar *et al.* (1980) are not included in detail, the functions described within this manual are the new developments from the MEFYQUE project. Therefore, most emphasis is on the functions that will influence the wood quality of a stand: carbon allocation, lean, stem geometry and branching.

5.2.1 Concept

The MEFYQUE stand model simulates the growth, C, N and H_2O flows through a single stand (including the soil) of even or uneven-aged trees of the same species (either deciduous or coniferous). The main objective of the stand model is to yield a realistic simulation of the development of wood quantity and quality as influenced by climate, stand, and species characteristics.

Although the simulation is not spatially explicit (not every tree has a defined place in the forest), there is interaction between the trees, as competition is a major factor in explaining wood formation. The MEFYQUE model is a functional model and has only minimal requirements of empirical relationships. This functional character allows the model to be used for a wide range of environmental conditions and species.

Currently the model uses a simple DOS interface, demanding input files from the user, and yields results in tables. The input is provided through simple text files. In the description below, the names of the variables are the names used in the Fortran90 source code.

5.2.2 Forest description

A forest consists of trees of different categories. If we use three categories, these can be seen as the dominant, co-dominant and suppressed trees. Each category of trees is simulated separately, and then the total forest is calculated as a result. For the light version of the model, the maximum number of categories is three (Figure 5.3).

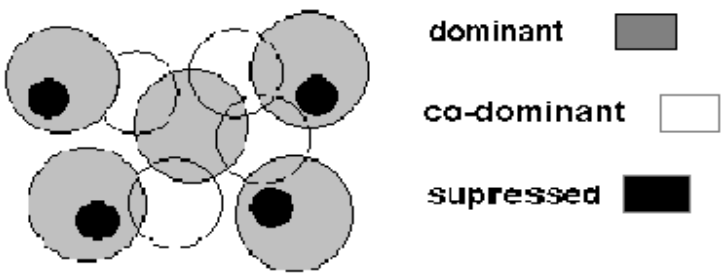

Figure 5.3: Example of tree categories in a simulated forest stand

A tree is defined by the biomass of its components (leaves, fine-and coarse roots, stem and branches), the composition of the stem (in fibres, vessels/pipes, parenchyma and storage carbon), and the size of the trees:

A tree crown is ellipsoid (see Figure 5.4); radius and top axis define the ellipse), and can be truncated at the bottom if layers have died (or if so defined from the start), so the liveStartCrown is then different of the startcrown (where the ellipse as a whole starts). The canopy is divided into layers (with layer height and number to be defined by the user up to a max of 60 layers in the light version).

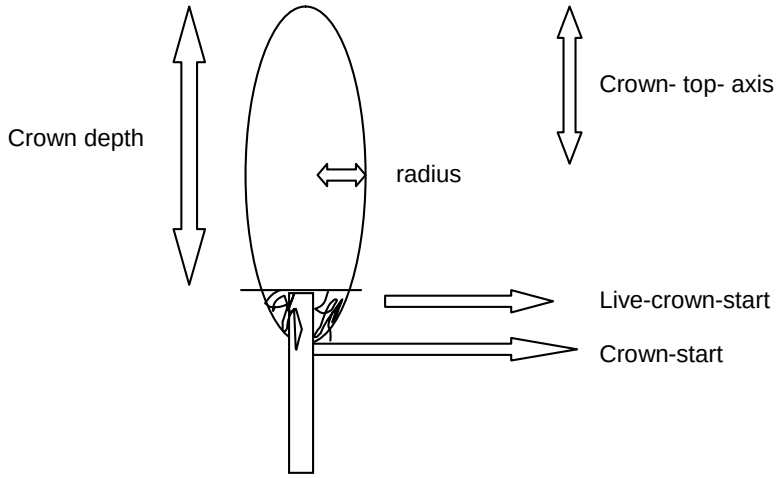

Figure 5.4: Tree crown shape and measures for the modelling

The crown is also divided into yearly sections: every year, the crown volume increases and the new volume becomes that year's section of the crown (Figure 5.5).

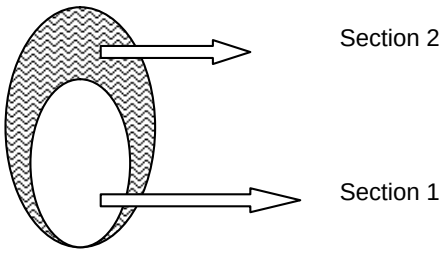

Figure 5.5: Yearly sections in the modelled crown

5.2.3 Overall structure and existing modules

The model is written in Fortran90 code, and exists of several modules. This allows professional users to change, replace or improve specific modules without altering the overall functioning of the model.

The main module calls the sub-modules that perform all calculations. These are:

- light, photosynthesis and transpiration,
- budburst,
- carbon allocation,
- mortality,
- wood quality,
- canopy summing,
- and soil-water and CN-ratio.

5.2.4 The main module

The main module includes the input interface. The program demands the name for the data-input files as follows (example full input files are found in Appendix J):

- Stand data: composition of the forest in tree-types, description of the different tree classes (size and biomass) at the start of the simulations, length of the runs (numYears)
- Species data: parameters for one specific species
- Climate data: climate (irradiance, rainfall, wind and T, monthly or daily values)
- Soil data: initial C and N pools, soil structure

The model then steps through the code for a given number of years (numYears) on a daily time-step, tree by tree (numTrees given), calling the other modules (or the subroutines within these modules) to grow a tree in the following sequence:

- Before the available carbon is allocated to the different tissues (stem parenchyma, fibres or vessels, branches, leaves, coarse or fine roots), in **branchingCalc** the requirements for branches (depending on crown geometry) are calculated.
- **AllocateCarbon** then allocates the available carbon and returns the changes in biomass of the different tissues
- The next step is the leaf fall at autumn (**broadleafLeafFall**) or because of needle age (**coniferNeedleFall**)
- Then **heartwoodFormation** is calculated from the predefined heartwood age.
- In **canopySum** all changes in biomass and size are added up to the tissue biomass and size.
- The diameter of the branches is then calculated in **branchDiamCalc**.
- The **lean** of the trees is calculated once yearly, in summer (when trees have leaves)
- Stem geometry and density are calculated on the first day of the following year (in **stemCalc**).
- **BREcalc** uses the output from stemCalc to produce an output file of a format similar to scanning output of real logs: the radius at 15° around the stem, of every 10 cm interval of the stem up to a defined diameter. As well as the position, start and end radius of knots in the wood.

After the calculations at the tree level, the stand level simulations are done:

- **SoilWater** calculates the flow of water through the soil
- **SoilCN** simulates the C and N fluxes through the soil

Finally, **main** writes the output to different out.dat files. Data are overwritten at each run, and there are no column labels. The output is very detailed, yielding daily values for all C and N pools in the system, as well as all fluxes at the tree and the stand level.

5.2.5 Light module

The final output of the lightmodule is absorbed radiation per tree layer (in •mol m^{-2} s^{-1}). For the sunlit and shaded leaf area separately, and the sunlit and shaded leaf area of every tree layer and section (yearly growth sections, not the vertical sections used only locally within the light module). Direct and diffuse radiation are both simulated.

Before the light is calculated, the layers and vertical sections are defined (Figure 5.6), and the radius (**radiusLayerCalc**) and the layer in which the crown is situated (startLayer, midLayer and endLayer) are calculated (**layerSituation**) For the calculation of the light in the canopy, vertical sections are defined (different from the yearly sections). The area and leaf area in each layer section is calculated (**verticalSectionCalc**).

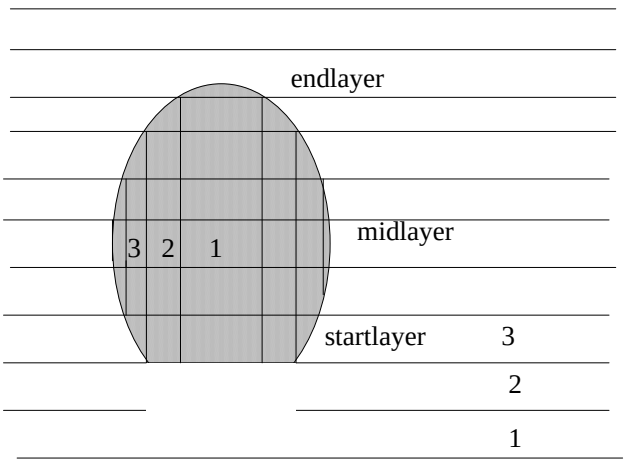

Figure 5.6: Horizontal layers and vertical sections as defined in the light module

Then, the extinction coefficients for direct and diffuse light are calculated (from sun angle and leaf angle, kcalc).

Finally, the actual light profile is calculated in lightmodel

1. The light coming in at the top of each vertical section is calculated first in three steps, always using

$$I = I_0 e^{-k\,LAI}$$

   a) The LAI in each layer section of the crown is calculated
   b) Light through the whole canopy (direct and diffuse) is calculated from canopy LAI, so there is an exponential reduction in incoming radiation due to the whole canopy
   c) Light above a section equals canopy light if there is no leaf crown above, else is calculated from the light in the section above

2. Sunlit leaf area in every layer section is calculated from incoming to outgoing radiation. Shaded leaf area is total-sunlit
3. Absorbed *I* (per unit leaf area) by sunlit leaves is all absorbed direct radiation (obviously) and part of the diffuse using the general formula:

$$I_{absorbed} = \int I_0 e^{-k\,LAI}(1 - refl).k$$

   For the shaded leaves only (the remaining part of) diffuse radiation is absorbed.

4 To get values per layer, the values of the sections (weighted with the leaf area in each section) are summed up.
5 Then recalculated to the yearly sections as defined in the rest of the model. In this case total absorbed radiation by sunlit and shaded fraction as well as sunlit leaf area are calculated.
6 In the final step of the light model some calculations necessary for the allocation module are done: **dWidthDheight** defines the crown shape and is modified by the incoming radiation (trees are narrower under low light). **AvailLight** states whether there is enough light in the canopy to allow adding more leaves (instead of growing upwards).

5.2.6 Photosynthesis and transpiration

In this module the photosynthesis per tree category (in kg C per half-hour) is calculated for sunlit and shaded leaves of each layer of each tree category, using Farquhars model (Farquhar *et al.* 1980). This needs as input the stomatal conductance. For this, the stomatal

model of Dewar (2002) is used, which is based on the control of ABA-synthesis through soil water and leaf water potential. Therefore, stomatal conductance becomes a function of the air humidity and the soil water.

From the stomatal conductance, internal C concentration C_i and photosynthesis are calculated in an iterative way. Photosynthesis is either light or N limited. N is simulated as exponentially declining (user defined how steep) through the canopy. The total N of the tree is a function of daily N gain (through uptake, influenced by mycorrhizae) and N loss through litter.

Finally, transpiration is calculated from the stomatal conductance using the Penman-Monteith equation (Monteith, 1981).

5.2.7 Budburst

Budburst calculates the day of budburst from soil temperature, and the end of height growth from soil water potential, as well as the start of leaf fall in autumn (constant as yet; will become function of light, T and/or actual photosynthesis).

5.2.8 Allocation

In the allocation module two main subroutines are found, as well as several small local ones. AllocateCarbon calculates the division between the different tissues of the carbon. BranchingCalc calculates the C requirements for new branch development and for the extension of existing branches, as well as the falling and overgrowing of dead branches.

5.2.8.1 Allocation of Carbon

The allocation of available carbon depends on the growing phase of the tree. There are three phases for pines, five for deciduous trees. Before allocating available carbon, however, a few calculations are made:

The basic assumption in the allocation is the pipe theory that says that there must be a balance between the leaf area (which results in transpiration) and the pipes/vessels through which the water flows to the leaves. In our concept, instead of relating leaf area simply to sapwood area, we relate directly to the actual number and size of the pipes (or vessels). The theory behind this is as follows:

$$TransMax * leafArea = water\ supply to leaves$$

$$watersupply = pipeflow * number\ of\ pipes$$

$$pipeflow = \Pi * (pressureGradient - \rho gh) * r^4 * pipeEfficiency/(8\eta * height)$$

which is the Posieuille flow, modified by efficiency with: *TransMax* = max transpiration per unit leaf area; *Pipeflow* = Volume Of Water Passing Through A Vessel; • = 0.001, viscosity of water; *pressureGradient* = from leaves to soil at full water availability; *pipeEfficiency* = reduces from ideal capillary, lower for pines; • = density of water; *g* = acceleration due to gravity; and *r* = *piperadius*.

$$r = r0(0.75 + \tanh(dPipe X/(StemWeight + dPipe X)))$$

The size of the pipes/vessels depends on the growth rate and is calculated from the previous day's pipegrowthrate and stem weight. The scaling factor *X* relates to the species-specific

responsiveness of piperadius *R*, which relates to the amount of carbon available for regrowth in spring.
The ratio of the leaf weight to pipeWeight is calculated in leafPipeRatioCalc before the rest of the allocation (allocateCarbon) as:

$$leafPipeRatio = pipeflow/(height * stPipeWHeightRatio * TransMax * SLA)$$

with: *stPipeWHeightRatio* = ratio of pipe Weight to height (kgC/m); and 1/*stPipeWHeightRatio x height* = number of pipes per kgC.

If available carbon is negative (respiration is higher than photosynthesis) this is subtracted from the stored carbon. If stored carbon becomes zero, the tree dies.

As some embolition always occurs, there is alway a minimal requirement of new pipes (and all other associate tissues) which is calculated before running through the phase (not in Phase 5). The requirement of replacement pipes is calculated in embolitionCalc, (called in the main module before allocation). If there is not enough C available to replace the pipes, the associated leaves will fall.

5.2.8.1.1 Phase 1: Leaf development from C-stock

From the pool of stored carbon, 1/25th can be used daily for 20 days following budburst. If the canopy is filled before that (avail-Light, calculated in the lightmodule becomes false), the tree will go into Phase 2 and no longer use stored carbon. Over winter, a number of pipes (defined by the parameter winterEmbolition) has lost functionality. Therefore, for part of the new leaves, new pipes need to be built.

Pipe theory gives requirement of vessels/pipes (so some increase in stem width) for these leaves, and a minimal requirement of fibres and parenchyma to support the vessels.

Fine root development is equal to leaves or under drought or N-deficiency more fine roots are grown.

5.2.8.1.2 Phase 2: Height or leaf growth

After the stored carbon is used or if the crown is filled, Phase 2 commences. If there is light in the canopy, leaves are added (with their associated pipes, fibres and parenchyma, and roots)

Height growth occurs as soon as there is not enough light within the canopy.

The first day of height growth, a new ring of branches is always formed. After that, there are two possibilities:

1. Extension: if the distance between the top of the tree and the second whorl of branches is lower than the maximal allowed distance (interWhorlMax), only stem length increases, and branch length of the existing branches. All carbon of that day will be used to expand the canopy with the same ratio of leaves to wood as in the existing crown. So leaves and branches develop simultaneously.
2. NewWhorl: if the distance between the last whorl and the second of the tree reaches interwhorlMax, a new whorl is formed at a distance interwhorlmin from the previous and the whole crown expands to reach this new height. The new crown will use all carbon available, but cannot normally fill itself. It might even be unrealistically thin. But this will fill out in the following days as avail-Light will then be true.

As pipe and leaf growth decrease, the produced wood will automatically be late wood during this phase.

5.2.8.1.3 Phase 3: Storage

The start of phase three is determined in the budburst module and depends (at the moment) on soil water potential. If no drought occurs, a fixed day (species specific) is used.

During Phase 3 height growth is no longer possible. Therefore, all available C will be used to replace pipes, possibly grow some leaves (though it is unlikely that there will be sufficient light within the canopy). Most carbon is allocated to storage, and stem width will only increase because of pipe replacement and if all available storage space is filled.

5.2.8.1.4 Phase 4: Leaf fall

For deciduous trees, leaves will fall from the start of Phase 4 onwards, layer by layer, (from the budburst module, depending on T and day length), which is simulated in the mortality module.

As far as allocation is concerned, there is no difference in growth compared to Phase 3 except there is no possibility to grow leaves, even though there might be light available. For the coniferous trees, needles fall throughout the year, depending on their age. The maximum needle age is a user-defined species parameter.

5.2.8.1.5 Phase 5: Dormancy

Deciduous trees reach Phase 5 when there is no leaf area left. Since there will be no available carbon there is no allocation. But available carbon will be negative (because of respiration) and this will be subtracted from the stored carbon.

5.2.8.2 Allocation of Carbon to Branches

The C allocation between the branches (both existing and new whorls) is calculated from the length required to reach the outside of the crown, and a species-specific parameter for the efficiency of the branches to reach the outside (depends on straightness and divisions).

The death of branches from light shortage is calculated in the mortality module. But once they are dead, the falling and overgrowing of the branches is calculated in branchingCalc. From the minimal number of years after death that a branch can drop (branchFall) and be overgrown (branchOvergrown) a random function calculates whether or not a branch falls or is overgrown at a chance of 50%.

5.2.9 Wood Quality

In this module 4 subroutines are found.

5.2.9.1 Calculation of Stem Lean

LeanCalc is called once a year (midsummer) and calculates the added lean to each tree segment from the wind, canopy LAI, width, density and crown of the tree. This module needs further calibration and validation.

The following theory has been included in the current version:

$$F_t = F_w + F_c$$

The force (F_t) on a tree is through the crown weight (F_c) and through the wind (F_w):
Where F_c is the bending by crown weight with $Fc=(h-z)\cos\bullet m$; with m as crown mass and • as the lean angle of the section above z.

But we hypothesise that this momentum is absorbed by the formation of compression wood.

F_w is the mean bending momentum by wind at any height (z) in the stem with $F_w=(d-z)\bullet A$ where • is the total force drag force over unit surface area: • =-• u_*^2 (Nm^{-2}) with • as the density of air (1.2226 kg m^{-3}).

First we need to know the wind profile in the forest.

Calculate u_* from the wind at the top of the canopy if this is known:

$$u_* = u_h k / \ln((z-d)/z_0)$$

But you need to know d (roughness length) and z_0 (zero-plane displacement) for that. This can be calculated from tree height, spacing, canopy depth and crown width according to Raupach (1994), thus:

$$z_0 = height * +(1-(1-\exp(\sqrt{7.5 * canopyArea}))/\sqrt{7.5 * canopyArea})$$

$$d = height * (1 - \frac{zeroPlaneDisplacement}{height}) + \exp(-0.41 * \sqrt{0.003 + 0.3 * \frac{canopyArea}{2}} - 0.193$$

We now know the total drag force per unit surface area of the whole forest. This drag force needs to be divided between the trees of different categories.
The drag force works only on any tree area above $d+z_0$. So for every tree we calculate the weighted area, which is the area of leaves, and stem above $d+z_0$ divided by the total canopy area of stem and leaves above $d+z_0$. The weighted area gives the portion of the total drag force working on an individual tree. We calculate F (the force on a specific tree) from the total drag force and the weighted area

$$Lean = \beta E \sigma_w \frac{1}{2} b$$

where • $_w$=4F/ • ab ^{2} with a and b as radius in short and long direction of the stem, d as the wood density and E as the modulus of elasticity, which has been measured for different tree species and • as a new parameter, called the lean factor, which is hopefully constant at least within species. It sort of averages the growth response of the tree (compression wood etc).

5.2.9.2 Calculation of Stem Radius (stemCalc)

Calculated once a year, on the first day of the year for the previous' year's data.

In this routine the biomass (in kgC) that has been allocated to the stem tissues (pipes, fibres and parenchyma). As density of the pipes changes with pipe radius, the average early wood and late wood density are used (calculated in canopySumming module).

First the volume of the ring (over the total height of the stem) is calculated. Then for each stem segment, a proportional part of volume is allocated. In the last step the ring radius in every segment is calculated from the exiting radius and height of the segment and the added volume (Figure 5.7).

If there is stem Lean, then the stem will be oval instead of round and the a and b (short) radius of the stem are different.

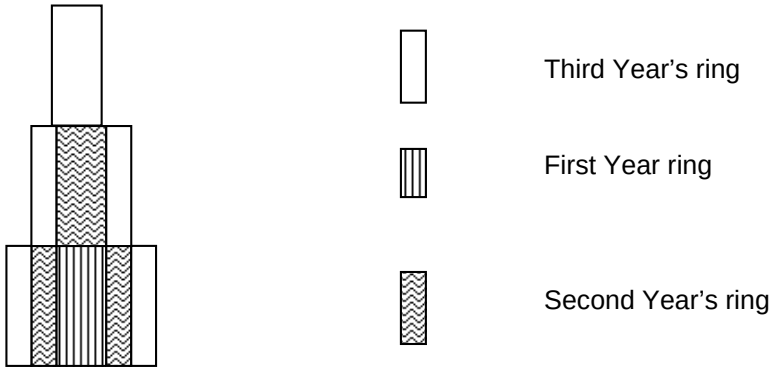

Figure 5.7: Stem growth in the MEFYQUE model**.**

Finally the average total density of the stem is calculated.

5.2.9.3 Calculation of Branch Diameter (branchDiamCalc)

Similar to stemCalc the diameter of the branches is calculated from the current diameter and the added C per unit length

5.2.9.4 Wood Quality Calculations (BREcalc)

The calculations in stemCalc, lean and branchDiamCalc define the outside of the stem, including the knots caused by branches.

A model has been developed at Building Research Establishment Ltd. (BRE), Garston UK, which can calculate the optimal sawing into batons of a scanned log (see 5.4.2). To use this model for our virtual logs, the output has to been in the same format as for a log going through the scanner in a sawmill. This means that the virtual tree is chopped into a single log, and the radiuses, branch positioning and branch diameter are given per 10 cm and over 36 angles around the log axis (from the middle of the bottom to the middle of the top of the log). The calculations in this module deal with changing the axis to which the radius relates from the centre of each segment (as in the model) to 1 axis for a whole log, which can be at an angle to the axis of a log-segment if the tree is bent. The flow through the routine is as follows:

1. Find top section
2. We lose a part of the bottom log = stump, calculate the true (vertical) height and shift (away from vertical axis through middle of the stem at the soil surface). Called startHeight and StartShift in the code.
3. *startShift=startHeight**sin*(startAngle)/*cos*(startAngle)*
4. Calculate the *startHeight* and shift of every tree section from the lean
5. Now we can calculate the length of the log from the height and shift
6. *logLength*=•*(a+b)* with
   a. *a=(sectionStartHeight(endSection+1)-startHeight)*^{2}
   b. b=*i.(sectionStartShift,(endSection+1)-startShift)*^{2}
7. Then we can calculate the angle of the log-axes
8. *logAngle*=arccos***((sectionStartHeight*(endSection+1)-startHeight) /logLength)***
9. The log is divided in 10 sections called sections. Calculate the number of sections in the log.
10. Calculate the realHeight of the logaxis in each of the sections to be described.

11. Calculate the projected a-radius in each section from the section angle compared to the logangle.
12. Calculate the displacement = horizontal shift between the centre of a section and the logaxis.
13. Calculate for each angle the radius towards the logAxis from the projected radius towards the sectionAxis
14. Solve this using the equations for a line (*y=m*x+midpointshift*)
15. crossing an ellipse ($b^2*x^2 + a^2*y^2 – a^2*b^2=0$)
16. Do the calculations for the half ellipse, because of symmetry for first quadrant:
    a. *X=X-midpointShift(section)* and *Y*=sin*(angle)* X*
    b. and for the second quadrant: *X=X+midpointShift(section)* and *Y*=sin*(angle)*X*
17. *BREsctionRadius(sction,angleNo)*= • ($X^2 + Y^2$)
18. Search the branches for those falling within a section
19. Then define the angle within a log the branches are spaced (random, but evenly spaced)
20. Now find whether some of these have been overgrown

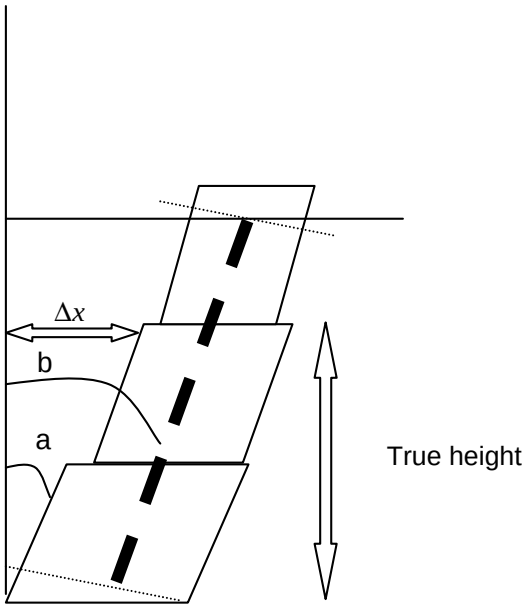

(a)

(**- - -** : axis used for the BRE calc ɪm a midpoint of the bottom of the log to a the midpoint of the top of the log.)

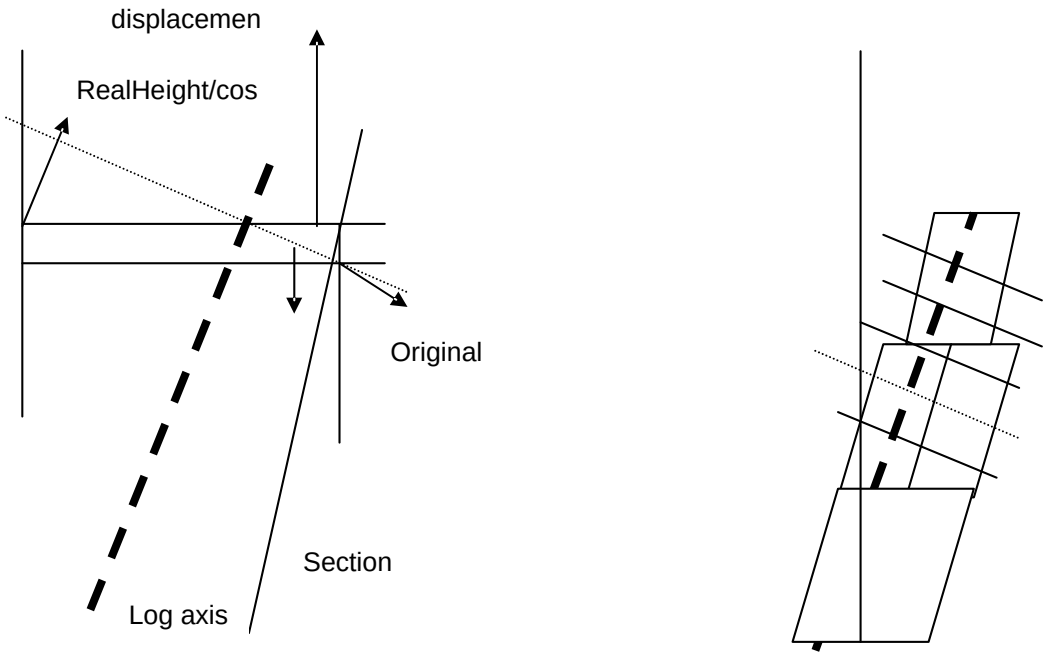

(b)

Figure 5.8: Calculation schemes. Subfigures (a) Simple stem profile, (b) show the comparison of the original axis (different axis through the centre of each section) to the new log axis (from the top to the bottom of the log)

5.2.10 Mortality

The mortality module holds 5 subroutines.

5.2.10.1 Death of a layer (layerDeath)

Kills a layer and associated leaves and branches and pipes when light is too low.

A layer dies when average absorbed *I* over five days is below half of lightCompensationpoint. The subroutine calculates the number of layers for which this is true (numlayerskilled). If the last leaf layer of a tree gets killed, the tree dies.

In the routine, the branches and pipes associated with this layer are also found and killed this is stored in the variable array ring.

Part (species specific, input in relocatecarbon) of the carbon however., is relocated to storage carbon. The remaining carbon goes into dLeafLitter.

5.2.10.2 Senescence (LeafFall)

5.2.10.2.1 broadleafLeafFall

Finds which layers (canopy level) are to die in autumn (only for broadleaves). This is decided on the forest level, so when the model runs the first live tree in autumn. The number of layers left to kill is divided over the remaining days of autumn (numDaysLeafFall) yielding the number of layers to kill of that day (numlayersToKill). Then kill all leaves of all trees for the specified layer(s), but not the associated pipes. Part (species specific, input in relocatecarbon) of the carbon however., is relocated to storage carbon. The remaining carbon goes into dLeafLitter.

5.2.10.2.2 ConiferNeedleFall

For conifers needles die at specific age (maxNeedleAge), throughout the year, associated pipes die too.

5.2.10.3 Embolition (embolitionCalc)

Random embolition of pipes, calculates biomass of pipes to be replaced. Calculates the C of pipes to die (from the daily chance of embolition: embolitionChance).

This amount of C is output as pipeReplacement (used in the allocation module) while pipeActivity (in vararray ring) is reduced by the corresponding amount.

5.2.10.4 Formation of Heartwood (HeartWoodFormation)

On the first day of each year, the ring that has reached heartWoodAge becomes heartWood (stored in the ring array).

5.2.10.5 Turnover of Fine Roots (FineRootLitter)

FRturnoverRate gives the yearly turnover. The daily FRlitter (dFRlitter) is calculated from that.

Leaves will fall layer by layer for the whole forest, from the bottom upwards. Therefore, trees with leaves lower down in the canopy will lose their leaves sooner.

5.2.11 Canopy Level Calculations (Canopy summing)

The last module at the tree level does not deal with any processes, but to facilitate the substitution of modules, we opted for an output from the modules in daily changes of the different C pools. In the canopy summing these changes are added to/subtracted from the existing pools.

Many data are stored in arrays. The most important arrays and their content are listed below, for the first array (tree) the array structure is clearly explained, all other arrays are similar.

Within the model there are more arrays, but mostly they are much smaller and have the name of the parameter or variable they hold.

Tree(numTrees, 8) holds 8 values for each tree category (there are numTrees categories of trees):

1 height of tree [m]
2 leaf area of tree [m^2]
3 Stem biomass [kg C]
4 branch biomass [kg C]
5 coarse root biomass [kg C]
6 fine root biomass [kg C]
7 leaf biomass [kg C]
8 branch length [m]

Crown(numTrees, 6) holds 6 values describing the size of the stem and crown:

1 Crownstart
2 LiveCrownStart
3 CrownRadius
4 CrownDepth
5 CrownTopAxis
6 CrownVolume

Ring(numTrees, numYears, 9) holds 9 numbers for each treeing (the number of rings equals the number of simulated years) of each tree:

1 Early wood pipe biomass [kg C]
2 Early wood fibre biomass
3 Early wood parenchyma biomass
4 Late wood pipe biomass
5 Late wood fibre biomass
6 Late wood paranchyma biomass
7 PipeActivity (biomass of pipes)
8 Heartwood (1/0: 1 = heartwood)
9 Height of that year's (ring) section

Branches(numTrees, numYears, 3*numYears, 12) holds 12 data for each whorl of each section (a section is the yearly growth) of each tree:

1 Biomass of 1 branch [kg C]
2 Length
3 Radius at the stem
4 Biomass of the pipes
5 Biomass of fibres
6 Biomass of parenchyma
7 If whorl alive or dead (1/0 0 = dead)
8 Number of branches in whorl
9 Number of fallen branches
10 Number of 'overgrown' branches
11 Year of appearance (= section)
12 Height

BREoutput(numTrees,15,25,72,4) gives 4 values for each angle (72 angles) of a slice (10 cm so there are 25/log) of a log (2.5m) of a tree:

1 Radius of stem [m]

2 Start radius of branch (if any)

3 Branch Diameter

4 End radius (if overgrown)

9 Height of that year's (ring) section **stemSectionGeometry**(numTrees, numYears,4). Gives 4 values for each stemSection (yearly growth in 1 year) of each tree.

1 Volume [m^3]

2 radius, a, (longest)

3 radius, b, (shortest)

4 Lean)

ringSectionRadius (numTrees, numYears, numYears, 2) holds 2 values:
(radius a, long and b short) of each ring in each section.
example: after three years there are three sections and the third ring has a radius in each of these sections, the first ring only has one radius. The radius is always the width of the specified ring at that height (not radius to the centre of the tree)

ringGraph(numTrees,numYears,numYears,7) for output graphs, per tree per ring per height sector holds 7 values:

1 Height of the sector

2 Earlywood volume of pipes

3 Earlywood volume of fibres

4 Earlywood volume of parenchyma

5 Late wood volume of pipes

6 Late owwd volume of fibres

7 Ilatewood volume of paranchyma

5.2.12 Calculations of Soil Water (SoilWater)

In this routine, the soil water and soilwater potential are calculated from the input (rainSoil not intercepted by the trees) and output (transpiration from the trees and leaching). In the 'light' version of the model, there is only 1 soil horizon defined.

5.2.13 Nutrients (SoilCN)

The concept of the model is in some ways similar to Thornley's soil model (Thornley, 1998): we distinguish soil (from roots) and surface (from leaves and branches) litter divided in metabolisable, cellulose and lignin according to their composition. Lignin is further degraded into different compounds that enter the soil organic matter (SOM). Depending on clay content, the SOM is more or less in the protected pSOM pool. Part of the unprotected (uSOM) and pSOM pool will enter the pool of very difficult to degrade SOM: the stabilised SOM.

In contrast to Thornley's model, the degradation of the litter and SOM is not simply correlated to T and humidity but to the specific activities of the soil biota. We distinguish and simulate three soil organism pools: fungi, mycorrhizae and bacteria (whereas Thornley has only 1). The main differences between these 3 are:

- Mycorrhizae get carbon (energy) from their host plants, they have some capacity to degrade cellulose as well. They can transport N from N-rich sources to N-poor material, so N-poor material can be degraded.

- Fungi can degrade cellulose and lignin well. They use the SOM mainly as N-source, and degrade lignin only to reach N-sources, so will degrade them less if there is an easier source of N (ammonium, nitrate, metabolisable substrate). They too can transport N.
- Bacteria are better able to cope with low pH. They are responsible for nitrification and for N-fixation. But since they cannot transport N, they will not degrade N-poor substances unless free ammonium and nitrate are available.

Transport of these substances is not specifically modelled, but where the bacteria only degrade substances with enough N, and exude excess N as ammonium or nitrate, the fungi and mycorrhizae degrade all energy-rich sources, then hunt for N elsewhere. This is modelled by simulating a stepwise procedure for the different organisms.

The E requirements of the biota consist of maintenance respiration and construction respiration. The soil model is still under development (part of the Euroface and Casiroz European projects) and will be further improved and parameterised in the course of these projects.

5.3 The MEFYQUE stand model - Forest Growth, with the ETp Engine

Sam Evans , Tim Randle, Paul Henshall, Gaby Deckmyn, Catia Arcangeli, and Sebastien Lafont

5.3.1 The ForestGrowth model

The ForestGrowth model represents an extension of the ForestETp 1-D model, where carbon units simulated by this model (net of respiration) are allocated to tree compartments such as foliage, branches, stem and roots, to dynamically simulate trees and stand growth. The rules and algorithms of allocation are described in section 5.2, giving rise to annual descriptions of tree rings, wood density etc. The ForestETp 1-D model below describes the central assimilation engine for the forest growth-wood quality-mefyque model. The growth model then builds upon the allocation mechanism described within the mefyque-light model, giving a more detailed stand growth model.

The model is complex and needs many parameters to define both the site and species characteristics, together with initial state variable conditions and management options. A front-end (Figure 5.9)) allows these inputs to be simply managed.

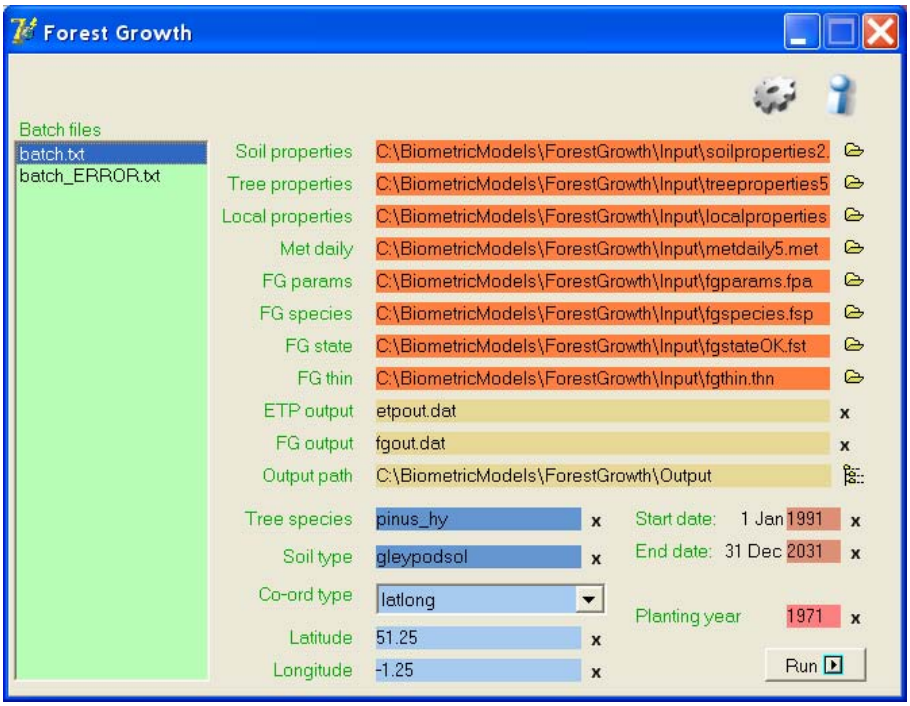

Figure 5.9: Front-end to the forest growth model

5.3.1.1 The ForestETp model

ForestETp (Evans *et al.* 2005) is a fully coupled, point scale and daily time step soil-vegetation-atmosphere transfer (SVAT) model, which predicts vertical and lateral water movement through the soil-plant-atmosphere continuum and gross primary productivity (GPP). The model simulates relevant terrestrial hydrology processes (rainfall interception, vertical and lateral soil water movement, runoff, soil and canopy evaporation, and photosynthesis-coupled transpiration) for a forest stand of known structure, growing in locally determined soil and climate. Particular attention has been given to the parameterisation, kept as simple as possible and reliant on widely available relevant data. As an alternative to observational meteorological daily data, the model is coupled with a weather generator that generates daily time series from monthly summary data. The model structure is illustrated in Figure 5.10 and detailed in the following sections.

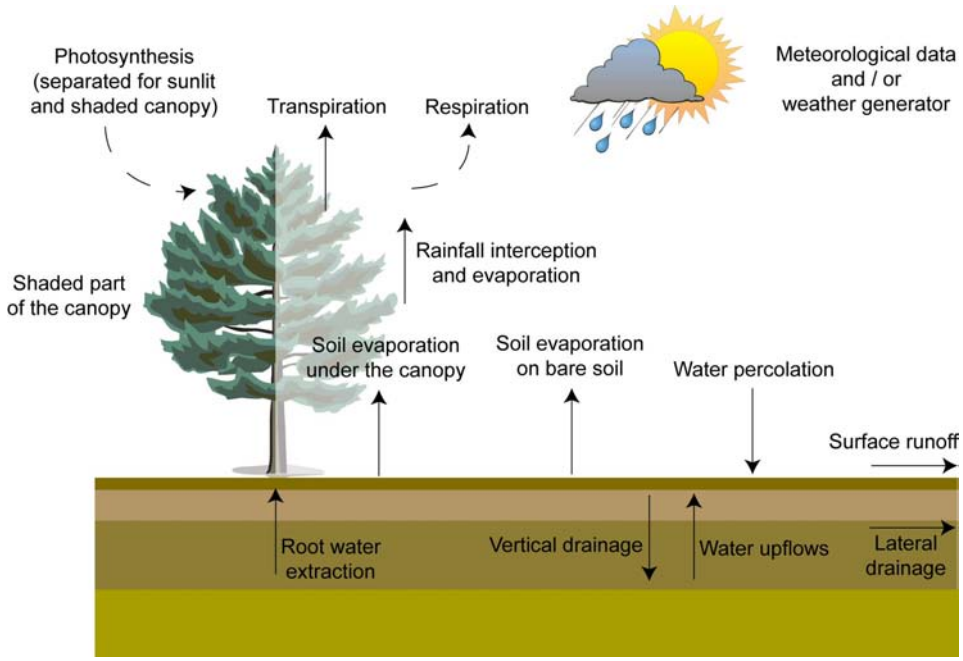

Figure 5.10: Schematic representation of water (solid lines) and carbon cycle (broken lines) processes simulated by ForestETp.

5.3.1.2 The climate module.

ForestETp can accept either daily meteorological data or monthly mean climatic values. If daily values of air temperature, air pressure, wind speed, global solar radiation, air humidity and rainfall are available, the model uses these data as inputs. If total net radiation is not available, it is estimated using the weather generator, otherwise, the measured value is used. Solar radiation is also split into direct and diffuse radiation as explained later in this section. Where only monthly input values are available, the model uses a stochastic-deterministic site-scale weather generator to downscale the monthly time step input data to the daily scales and generates the other meteorological fields. For illustrative purposes, the model structure is shown at Figure 5.11.

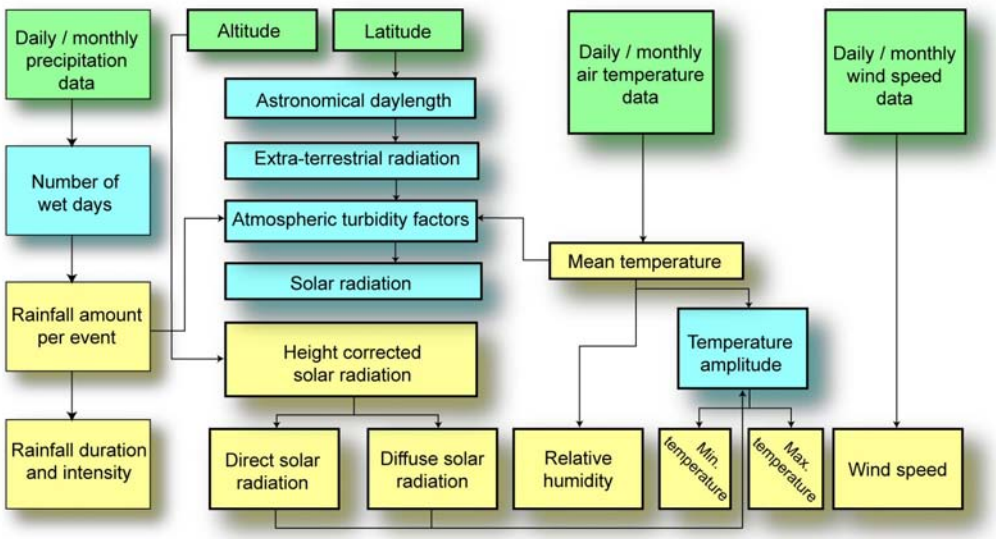

Figure 5.11: FR_weathergenerator Schematic representation of the weather generator structure.

5.3.1.3 The canopy radiative transfer module.

This module considers the heterogeneity of radiation in the canopy, as the necessary precursor to approximating the non-linear response of photosynthesis to irradiance. The model employs a radiative transfer scheme that approximates the transmittance, reflectance and absorption of long wave, near infra-red and direct and diffuse photosynthetically active radiation (PAR) by canopy layers, where canopy interaction are determined by the area and distribution of foliage. After Norman (1980) and De Pury and Farquhar (1997) the module separates penetration of direct and diffuse radiation (net of albedo) though a canopy in which two classes of leaves (sunlit and shaded) are distributed in a multi-layer canopy model. This approach allows the explicit description of within-canopy profiles (on a per layer basis) of both environmental (e.g. wind profile, vapour pressure deficit) and physiological variables (e.g. leaf temperature) in response to radiation attenuation. It does so through a canopy with uniform leaf distribution (spherical in the first instance; Russell *et al.* (1989) as prescribed by Beer's law (Monsei and Saeki, 1953) for each leaf class. The model does not allow for foliage clumping. By dynamically calculating the leaf areas of sunlit and shaded leaves, and their mean irradiance, mean layer assimilation, transpiration and conductance rates are obtained, adjusted for the photosynthetic capacity of each leaf class. Through integration, data are upscaled to approximate total canopy photosynthesis and gas exchange. In each layer, sunlit leaves are assumed to receive both direct and diffuse radiation from the macroclimate model; shaded leaves receive diffuse light only, assuming no radiative energy transmittance through leaves. The within-canopy profiles of leaf nitrogen follows the predicted distribution of absorbed irradiance through each canopy layer, separately for sunlit and shaded leaves and assuming a uniform leaf angle distribution (spherical). Seasonal variation of nitrogen content in foliage can also be represented with suitable input. Given the separate descriptions of sun and shade leaves and within-canopy variation of photosynthesis, the module allows non-uniform vertical profiles of photosynthetic capacity to be developed.

5.3.1.4 The gas exchange and carbon productivity module

Within each canopy layer, and to account for the changing light environment, the gas exchange and carbon productivity module operates at the leaf level. The well tested theoretical representation of C_3 photosynthesis developed by Farquhar *et al.*(1980) and Von Caemmerer and Farquhar (1981), widely used and tested across a range of species, that describes the regulation of ribulose 1,5-biphosphate carboxylase and electron transport in the leaf, has been combined with additions from Long (1991), McMurtrie and Wang (1993) and Friend (1995), with further adaptation. In turn the modified C_3 photosynthesis model is tightly coupled with the C_3 version of the Ball and Berry stomatal conductance model that provides a robust phenomenological description of stomatal behaviour. This coupling is required in order to predict leaf response to varying environmental conditions including, atmospheric CO_2 concentrations. After Farquhar *et al.*(1980), leaf nitrogen content (linearly) influences two of the rate-limiting photosynthetic processes, namely the potential maximum velocity of fully activated Rubisco that is inhibitor free (Vcmax) and the maximum potential rate of electron transport (Jmax). After Friend (1995), the module explicitly describes the role of nitrogen as a major influence on photosynthesis through influencing the Rubisco concentration in soluble leaf proteins involved in electron transport. Leaf nitrogen content also (linearly) influences mitochondrial (dark) respiration. After Ball *et al.*(1987), internal leaf CO_2 pressure (C_i) is determined within the leaf as a function of the interactions between CO_2 assimilation and stomatal conductance to CO_2, regulated by the leaf boundary layer and mesophyll cell surface resistances to CO_2 transfer. The same processes are assumed to apply for water vapour. As assimilation (demand) and conductance (supply) are inter-dependent, the values of C_i and assimilation are resolved by iteration, and accounting for both leaf water potential and canopy temperature. Foliage respiration is accounted for within the assimilation model. The balance of whole plant respiration during the leafy and non-leafy periods is approximated using a Q10 function, based on actual whole system respiration using eddy-covariance measurements of CO_2 fluxes data measured at each site.

5.3.1.5 The canopy rainfall interception

The tree canopy partitions gross rainfall into three downward water fluxes (free throughfall precipitation, canopy drip and stemflow) and an upward gaseous flux, intercepted water vapour resulting from evaporation. Along with meteorological conditions that determine the conditions for evaporation and canopy properties (determined by stand structure and growth as well as by management practices), the precipitation process (amount, intensity and its varying distribution in time and space) regulates rainfall interception. The canopy water environment module describes rainfall interception and wet canopy evaporation according to the revised analytical model of Gash *et al.* (1980, 1995). In this model each rainfall event is decomposed into three phases, a wetting up phase before canopy saturation occurs, a phase of canopy saturation and a drying phase after rainfall has ceased. Each phase contributes differently to the interception loss process, which is determined by the canopy structure and meteorological conditions. The canopy structure is characterised by four parameters, namely the canopy and trunk water storage capacities, the canopy cover fraction and the trunk diversion coefficient. The meteorological conditions are described through the ratio of mean evaporation rate from the wet canopy over mean rainfall rate. There are four main assumptions implicit in the model:

I. there should be enough time between storms to allow the canopy to completely dry,
II. there is no evaporation from the trunks during the storm,
III. no water drips from the canopy before saturation,
IV. the ratio of average evaporation rate over average rainfall rate is equal for all storms.

An example comparing observational data (open circles) for throughfall (rainfall minus Interception) with simulated module outputs (solid diamonds) is shown at Figure 5.12.

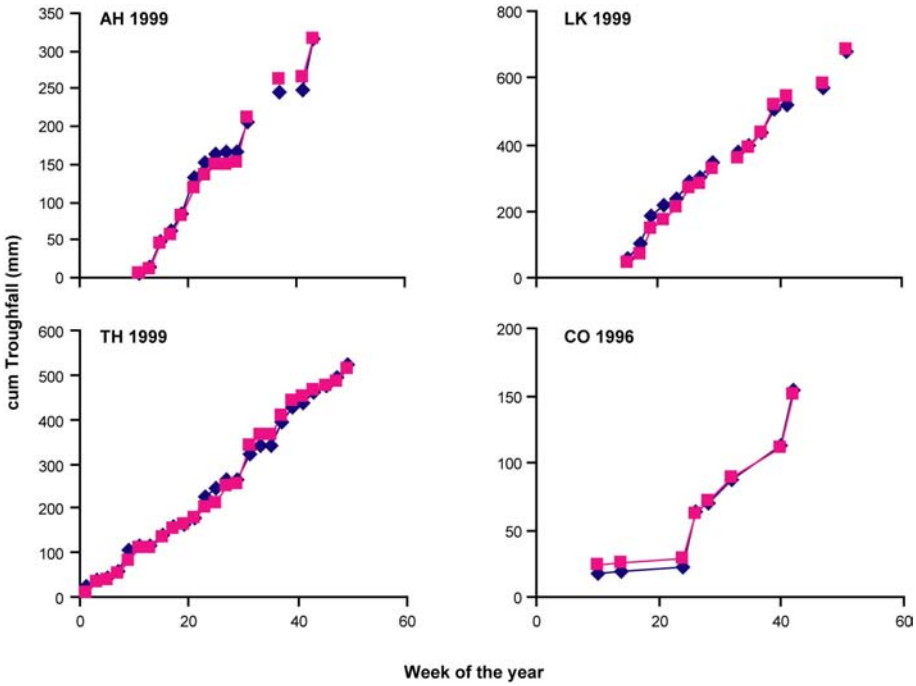

Figure 5.12: Throughfall for two oak [Alice Holt (AH) and Lakes (LK)] and two conifer sites [Thetford (TH) and Coalburn (CO)] for the year 1999.

5.3.1.6 The evapo-transpiration module.

After Richie (1972), selected outputs from all modules are used to parameterise the Penman-Monteith equation (Thompson *et al.* 1980; Burman and Pochop, 1994). In turn this equation is disaggregated to approximate daily leaf and canopy level evapo-transpiration, (bare and shaded) soil evaporation and wet canopy evaporation, separately for wet and dry days as determined by the climate module. The soil hydrology module. This module outlines a daily-

time step, multi-horizon capacity model of soil-water balance which requires climate data, together with soil survey and laboratory-measured physical data as input. The module simulates the generation of surface runoff, lateral and vertical drainage and the formation of transient perched water tables. It has been designed for application over a wide range of soil lower boundary conditions that commonly occur in most temperate high latitude countries such as the UK, that range from free-draining to impermeable. At each time step, after having computed the rainfall interception, wet canopy evaporation, tree transpiration, bare and shaded soil evaporation, light interception and photosynthesis, the water balance is updated for each soil layer as detailed is Evans *et al.*(1998).

5.3.2 Summary

A summary of the general features of ForestETp is provided in
Table 5.1. A comparison of process components from a range of stand and ecosystem models operating at various temporal and spatial scales, highlights significant commonality of approaches between the models; differences tend to refer to the scale of resolution in process description. The comparison indicates that ForestETp is comprehensive in the range of relevant processes simulated by the model. The principal innovations are the addition of a weather generator model, to downscale widely available gridded observational meteorological data and the use of generic parameters from available databases.

Table 5.1:**Table General features of the ForestETp model.**

Process	Strategy	Key references
Weather generator	*Stochastic-deterministic, site scale model downscaling widely available monthly time step input data to the daily scales*	*Richardson (1981) ;Ross (1983) ; Hutchinson (1991) ; Evans (1997)*
Radiative transfer	*Direct and diffuse radiation are accounted for though a canopy in which 2 classes of leaves (sunlight and shaded) within a multi-layered canopy.*	*Norman (1980), De Pury et al. (1997)*
Photosynthesis	*Biochemical model where photosynthetic rate is limited either by RuBP regeneration or by Rubisco kinetics*	*Farquhar et al. (1980), von Caemmerer and Farquhar (1981)*
Stomatal conductance	*Ball and Berry stomatal conductance model*	*Ball et al. (1987)*
Rainfall interception	*Tree canopy partitions gross rainfall into three downward water fluxes (free throughfall precipitation, canopy drip and stemflow) and an upward gaseous flux, resulting from evaporation of the intercepted rainfall*	*Rutter et al. (1975), Gash (1995), Valente et. al (1997)*
Evapotranspiration	*Evapotranspiration is computed using the Penman-Monteith equation separately for the tree transpiration, bare soil evaporation, shaded soil evaporation and rainfall intercepted water*	*Thompson et al. (1981) Burman and Pochop (1994), Ritchie (1972)*
Hydrology	*Multi-horizon capacity model of soil-water balance simulating the formation of transient perched water tables and the generation of surface runoff and lateral drainage*	*Evans et al. (1998)*

5.3.3 The integrated site model.

Testing of the integrated model (excluding the weather generator) has been conducted against published data on whole-ecosystem exchanges of CO_2 and water vapour collected in UK and European forest stands using the eddy-covariance technique (CARBOEUROPE project). Simulation experiments were conducted for each site at the daily time step using observational meteorological data as input. Model output were evaluated by comparison with experimentally-derived approximations of Gross Primary Production (GPP) and evaporation data provided by Falge *et al.* (2001a,b). Figure 5.13, presents the comparison between observational data and model output at the daily timestep for a coniferous site in Finland (Hyytiälä), the model is well able to reproduce the whole-ecosystem exchanges of CO_2 and water vapour. The over-estimation by the model of evapo-transpiration can in part be explained by deviations in the

observational record, as outlined below. Some temporal divergence between the simulated observed data is also evident, resulting from the use of fixed ecophysiological parameters used in the model, while some variability is known from field data. Across sites, the model showed good agreement for GPP (R^2 ranging from 0.51 to 0.79 with an average R^2 of 0.69), with no significant bias detected. The whole ecosystem evapotranspiration present a slightly lower correlation (R^2 range 0.35-0.62, average 0.47). As shown at Figure 5.14, annual timestep simulations were significantly better during dry days (without precipitation) than during rainy days. This difference between wet and dry estimates would suggest errors with the instrumental data, rather than with model outputs. A small bias has been detected with the model presenting higher values than a slight overestimation of the evaporation, possibly resulting from the use of a daily rainfall interception model and on the quality of eddy-covariance measurement during rainfall event.

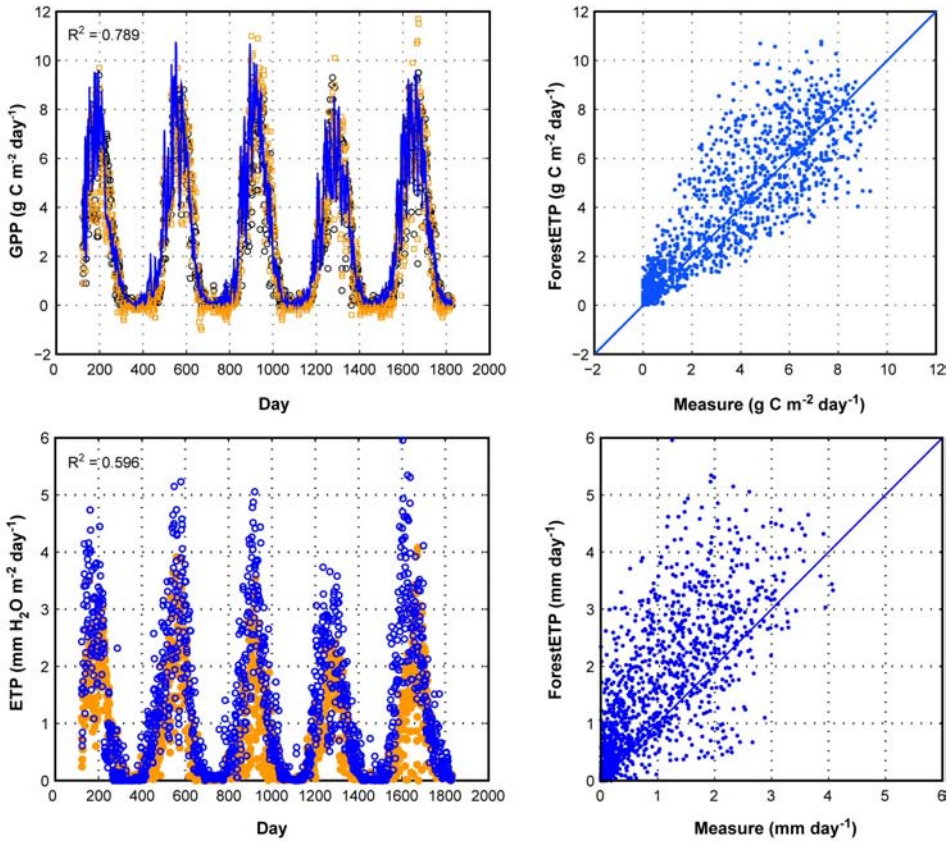

Figure 5.13: Comparison of modelled (dashed circles or squares) GPP and ETp with measurement (solid lines or circles) over 5 years. Note that observational values of GPP are approximated from measurement using two techniques, hence the illustration against two observational values.

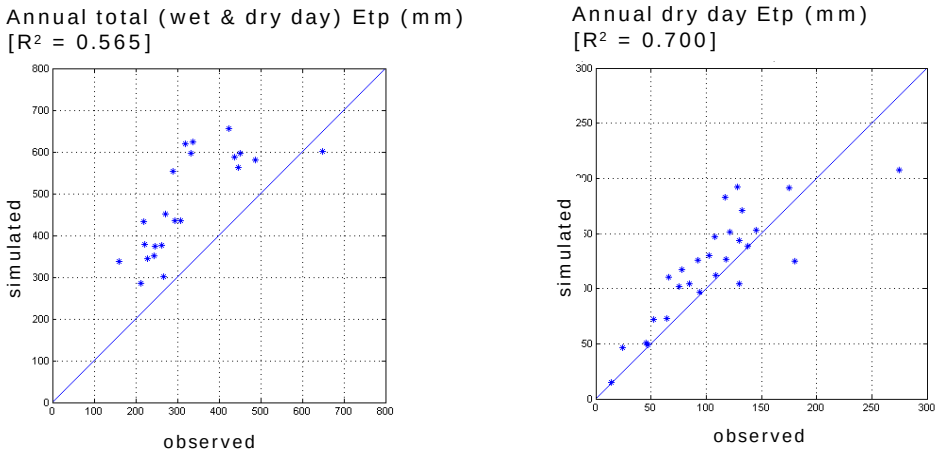

Figure 5.14: Comparison between modelled and measured system evaporation at the annual timestep: (a) for total (wet and dry day) evaporation: (b) dry day evaporation only.

Given the good approximations of GPP (R^2 ranging from 0.51 to 0.79 with an average R^2 of 0.69) and whole system evaporation (R^2 range 0.35-0.62, average 0.47) obtained at the site scale, national-scale approximations have been developed, as shown by Figure 5.15. These simulations use spatial data sets, such as the National Soils Database for England and Wales (National Soils Research Institute, Cranfield University) and gridded climatologies such as that developed by the Climate Research Unit, University of East Anglia, as input. Given the mechanistic approach of the model it is possible to dis-aggregate the signals into constituent components, as shown for example at Figure 5.15 and Figure 5.16.

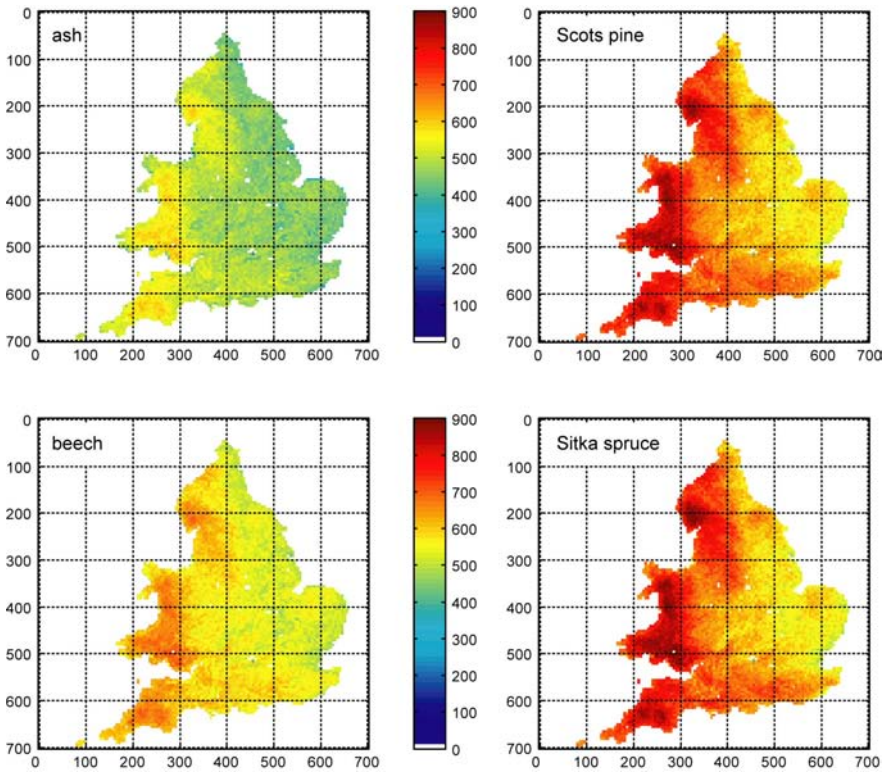

Figure 5.15: Simulated annual forest system evaporation (mm m^{-2} $year^{-1}$) assuming total land coverage by ash, Scots pine, beech and Sitka spruce.

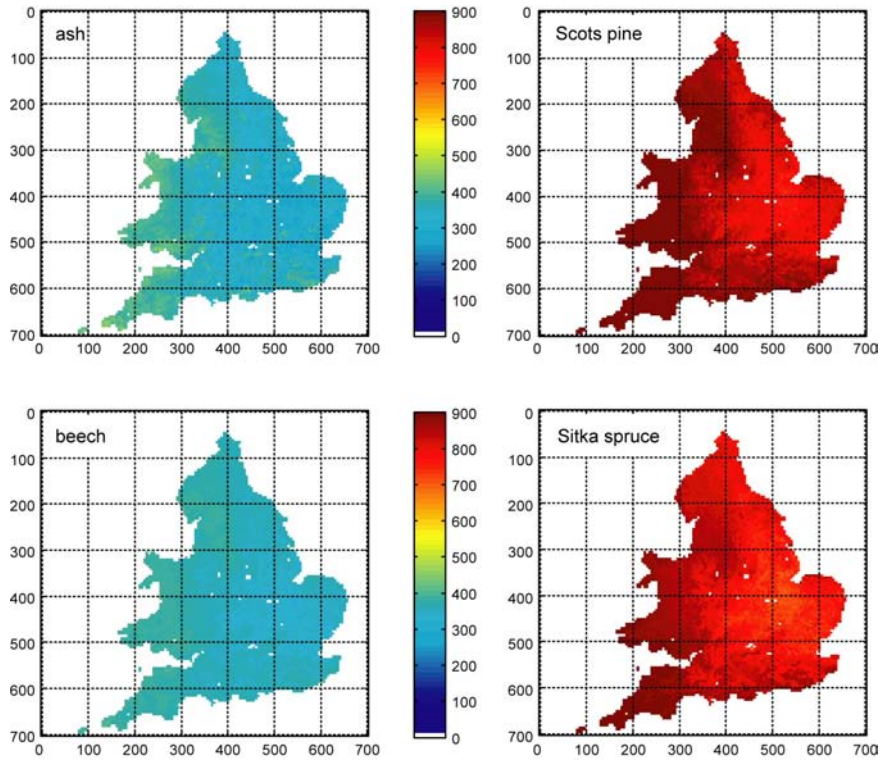

Figure 5.16: Simulated annual gross primary productivity (kg C year^{-1}) assuming total coverage by ash, Scots pine, beech and Sitka spruce.

5.3.4 ForestGrowthOutputs.

The model produces the typical mensurational variables; height, diameter etc, which can be interfaced with an existing graphical representation system (e.g. McGauhghey, 1997). An Example is shown at Figure 5.17. The output illustrates how the model can be used to generate stands of different structure and age and, with appropriate model parameterisation, the growth dynamics of stands composed by different species. In addition to the mensurational data, detailed outputs are available, describing each tree-ring at intervals up the stem. The ring data includes earlywood, latewood, density, branch sizes etc, allowing a qualitative analysis to be made.

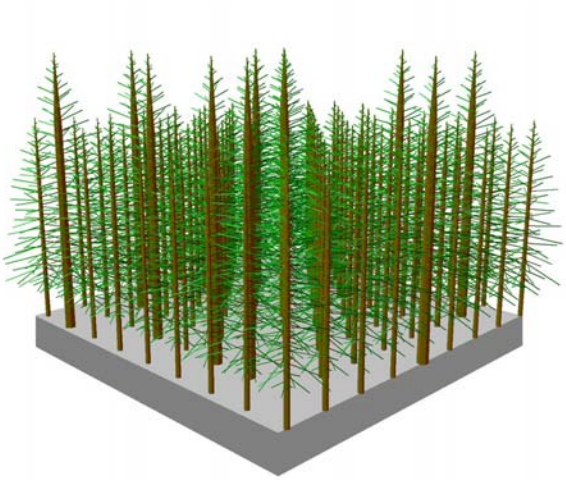

Figure 5.17: Outputs of the ForestGrowth model, interfaced with the Stand Visualisation System developed by the USDA (McGaughey). The visualisation tool is unable to project model simulations of root biomass.

5.3.5 Taper

Since the bole of the tree is represented by descriptions of discs at 10-cm intervals, the stem itself is not smooth. At various intervals, from one disc to the next, there may be the loss of more or more growth rings. In terms of profile, this means that 'shoulders' (or steps) would occur. A smoothing algorithm was written to taper growth rings from one 'shoulder'/step to the next.

5.3.6 Bend

In order to impose a 'bend' on otherwise straight bole the following principles were adopted- the main basis is a single fractal type approach:

- The stem continues to grow in the same direction for a year
- The central axis (currently pith) is to be able to bend each year.
- At the end of a year (node), the default is that the current direction will be maintained, though this is then potentially changed by a random factor, and the inclination of the tree to grow vertically seeking light.
- As the bend is imposed after the whole stem has grown, a node point is defined if the number of rings in a 'disc' has reduced.
- The change of the stem length due to bend is assumed to be negligible
- The application currently works in 2 dimensions, i.e. the bend will occur in one plane.
- The points defining the circumference of each ring are transformed to polar co-ordinates referring to a hypothetical vertical datum, which replaces the pith as the point of reference.

5.4 Log Conversion model (BREConversion)

Keith Maun, Tim Chase, Tim Randle

Developed as part of the MEFYQUE project (Forecasting the dynamic response of timber quality to management and environmental change: An integrated approach) under contract number QLK5-CT-2001-00345 contract, governed by the European Commission as part of it's Quality Of Life And Management Of Living Resources programme.

5.4.1 Introduction

The objective of the log conversion modelling system developed by BRE, BREConversion, is to be able to predict the volumetric and product quality outputs from standing trees. It is formed from a network of three models and four sub models that simulates the conversion of a standing tree into a number of product categories. They are:

1. Graded construction battens (C16 or higher),
2. C16 reject battens,
3. Falling boards,
4. Saw dust, and
5. Waste of cuts that are chips.

These categories were chosen as they are the most common found in European softwood sawmills (mainly producing construction material).

The model was developed to read data computed from the Growth and Allocation (designed to predict the current and future growth of trees due to the continuous changes in climate conditions) model developed by the Forestry Commission and Antwerp University. (see sections 5.2, 5.3) The output product (category) volumes are then fed into the EFISCEN (forest resources and wood products model (see section 5.6). The Growth and Allocation model grows virtual forest stands using a number of complex modelling systems to simulate the growth and photosynthesis of trees. Once the virtual forest stand has grown it is then

subjected to a tree form shape (generated from data collected by the Forestry Commission and BRE) that applies a shape to each individual tree. The model then re-distributes the revised polar co-ordinates already generated for the tree;

The model consist of the following outputs:

- The tree height,
- The stem diameter every 100mm along its length,
- The average density of individual growth ring,
- Branch sizes and positions,
- The polar co-ordinates of the stem linked to a common datum, representing the shape and size of the stem.
- The foliage volume.

The wood prodcuts module of the EFISCEN model has been designed to read the output volumes generated by the BREConversion model to calculate the carbon allocation along the forestry wood chain. It calculates the carbon required for, the trees growth, log harvesting, transport and conversion of the logs. The model then computes the re-allocation of carbon back into the environment, depending on the final product (category) i.e. construction materials, generally, will be in service 20 – 40 or so years longer than chips to make paper.

The BREConversion model consists of three integrated models; containing two sub models:

1. BRECrossCut
2. BREOptimiser
    a. BRELogOptimiser
    b. BRECantOptimiser
3. Grading.

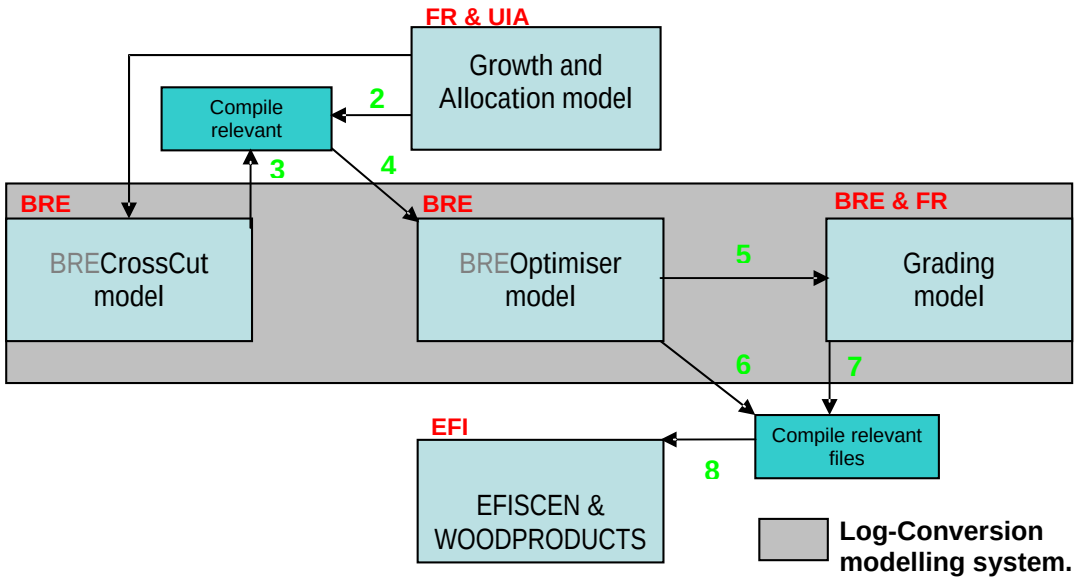

Figure 5.18: Schematic pathway of the log conversion modules 1 -8

Explanations for output parameters (1-8) shown in Figure 5.18:

1 Tree Height,
Stem diameter every 100mm along its length,
Branch sizes and positions,
Polar co-ordinates of the stem linked to a common datum, representing the shape and size of the stem.
The foliage volume.

2 Average density of individual growth rings.

3 Parameters as 1 but for the different logs generated by the BRECrossCut model.

4 Combined parameters from **1** + **2** but for the different logs generated by the BRECrossCut model.

5 Number of battens and their sizes, including batten density, knot position and size and battens distance from pith.

6 Side board volumes,
Saw dust volumes, and
Wood chip volumes produced from the BREOptimiser model

7 Volume of C24, C16 grade battens, and
Volume of C16 grade rejects

8 Compile volumes:
Volume of C24 grade battens,
Volume of C16 grade battens,
Volume of C16 grade rejects,
Side board volumes,
Saw dust volumes, and
Wood chip volumes.

5.4.2 BRECrossCut model

The BRECrossCut model processes the virtual tree's polar co-ordinates and branch position/size, grown from the Growth and Allocation[1] model, and cross-cuts the stem in an optimum fashion (simulating the "Classification and Presentation of Softwood Sawlogs" (Forestry Commission, 1993) grading system developed and used by the forestry commission and the UK sawmilling industry) to produce a number of logs, depending on the initial stem size and shape. The model considers log sweep (maximum deviation from the logs central axis Figure 5.19) and the number of branch's and branch sizes. The model can be manipulated to cross-cut logs to any length although the more common structural lengths, 4.8m, 3.6m and 2.4mm and fencing length, 1.8m are currently used. The model then picks up the average ring density data from the Growth and Allocation model and feeds the output files into the BREOptimiser model.

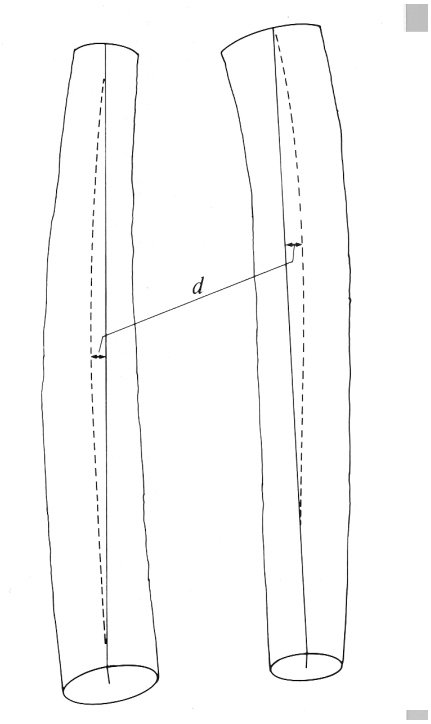

Figure 5.19: Schematic demonstation of log sweep (d)

This model has been designed to read the files produced in the Growth and Allocation (see sections 5.2, 5.3) model or by a sawmill log scanner (containing tree stem and branch size and position polar co-ordinates) to optimally cross-cut the virtual tree stems into construction grade logs, i.e. 4.8, 3.6, 2.4 or 1.8m long logs.

The model, written in C++ programming language, was developed to read .txt, .wsd and 3dl files generated from the Growth and Allocation model or by a sawmill log scanner (note: these files must be in a readable format). It is able to accurately calculate the diameter and cross-sectional area of the stem every 20mm long the stems length, depending on the accuracy of the readable file. It calculates the common area (the maximum area that can clear the whole length of the stem) and generates the logs volume.

These parameters (diameter and cross-sectional area of the stem every 20mm long the stem, the common area and log volume) can either be displayed on the visually interface (Figure 5.20) or produce “background” files to be used later on in the modelling process. The visual interface can be used to demonstrate the calculated variables and cross-cutting routine. However, if fast processing of results is necessary, when computing results for entire virtual forests, the model will produce “background” files for an individual log. These files will then be passed on to the next model, BREOptimiser, to enable another log to be processed. The process will continue until the complete forest was been calculated.

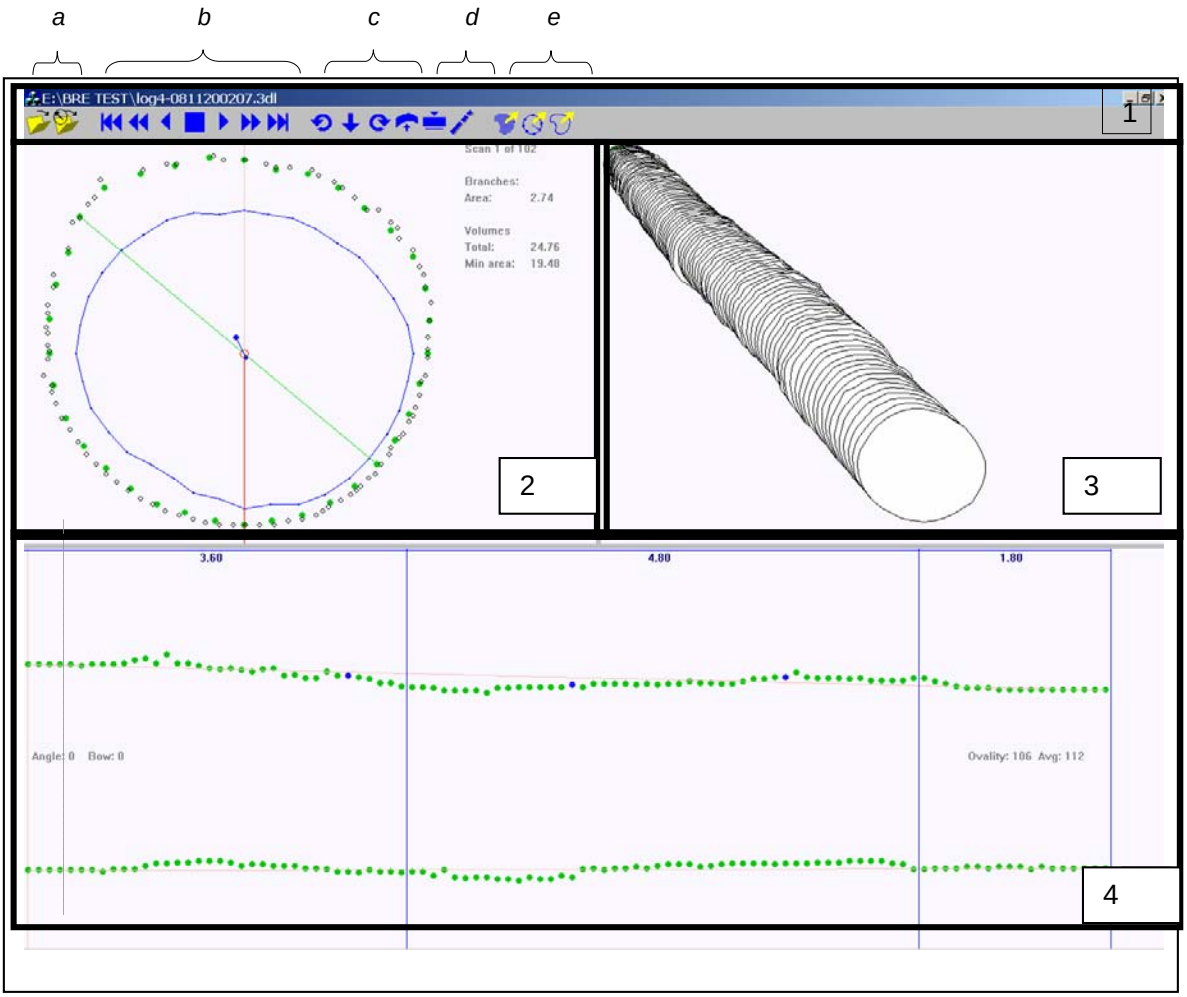

Figure 5.20: Graphical interface of the Cross-cut model

Figure 5.20 shows that there are four main components to the interface:

Tool bar (displayed at the top of the viewing window),

1. Cross-sectional view of a particular section of the stem/log (displayed on top right-hand side window),
2. Entire 3-D view of the stem/log (displayed on the top left-hand side window),
3. Entire 2-D view of the stem/log showing sweep values for different sawing angles (displayed on the bottom window).The model was able to rotate the log through 360° for 10° increments

Tool bar

a. The fist two buttons are used to open the relevant files. The first is used to open files obtained from sawmill scanners, .wsd and .3dl. The second button is used to open .txt files generated by the Growth and Allocation model. The later being the relevant files for the BREOptimiser modelling system.

b. The second set of buttons are used to scan through the log/stem. The red line, *a*, seen on the 4^{th} panel (Figure 5.20, far left of the bottom panel), scans along the log as you click the play button in the direction required. You can stop the scan at any point, using the stop button, proceed to the end or beginning scan using the skip buttons or increment along the length scan by scan at your own pace.

The information related to each scan is displayed on the right of the top left hand panel for that cross-section. The details displayed are:

Scan number: n of N
Branches:
Area/Size:
Volumes
Total:
Common volume:

The volumes calculated represent the log/stem properties and therefore do not change as the scan commences. It is only the branch area/size that changes, this value, descried later, is an important parameter used to determine the cross-cut log lengths.

c. The first three buttons in this section are used to rotate the log through 10degrees in either, a clockwise or an anti-clockwise direction. By doing you are able to see, on the left hand side of the bottom panel, the current viewing angle and also the related sweep along this angle. This information can be used to obtain an optimum cutting angle.

The fourth button on this display automatically rotates the log to show the maximum sweep angle and value, in mm (Figure 5.20, shown on the far right of the 4^{th} panel).

d. The first button in this section is used to straighten the log and the second button is the cross-cut button.

The cross-cut button is the main button used to cross-cut the tree stem into optimal log lengths (determined by the green and red log grading system developed and used by the forestry commission and the UK sawmilling industry) using inputted data from the user interface. The information required is:

Max deviation from straight (cm):
Max number of branches:
Max branch diameter (cm):

Once these parameters have been inputted into the model it begins the cross-cutting processes.

It uses an iterative process to produce green saw logs according to the inputted parameters, above. The cross-cutting process starts from the butt end of the log and

then works up the tree stem. First it will try to generate a log of 4.8m long. If this is not possible due to the set criteria it will try to obtain a log of 3.6m long, if not, a log of 2.4m long, if not, a log of 1.8m long. Finally, if a log of 1.8m can not be obtained the program will cross-cut the first 1m length and use this point as the start of the next search. This 1m log is then later added to the chip volumes of that stem. If, however, at any point a log, of any of the above lengths, can be obtained using the set criteria then the process will then start again, trying to produce a 4.8m long log, from the top of the previous log. This process is shown in Figure 5.21.

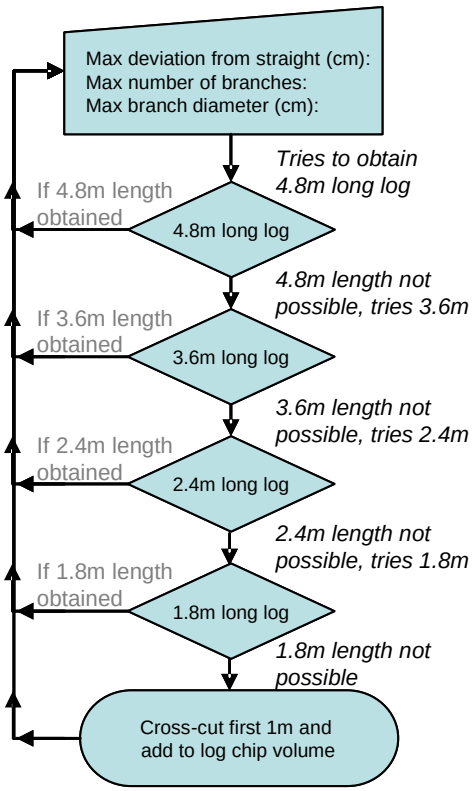

Figure 5.21: Flow chart of cross-cutting process in the model:

Figure 5.21 shows three logs could be obtained from the scanned stem. The following information was input to generate these lengths:

Max deviation from straight (cm): 10
Max number of branches: 24
Max branch diameter (cm): 6

This criterion generated three logs, 3.6m, 4.8m and 1.8m long.

In this case a relatively straight log was chosen as 10cm max deviation from straight is not a significantly bent stem. For example, if this max deviation from straight is increased to 15cm and the other parameters remain the same then the model produces two logs of 4.8m that will significantly increase the price of the end products.

e. Once the cross-cutting process has been completed the buttons in this section can be used to create the output files. The first button will export the logs in rectangular co-ordinates, used to allow compatibility with other models. The second button will export the logs in polar co-ordinate form, used in the BREOptimiser model and the third button is used to obtain information on the logs common area.

The output co-ordinate files contains information on the log shape and knot size and positions. Another file containing the volume of waste material is also generated.

The log files, using thier related polar co-ordinate information, is then used to compile all the data needed for the BREOptimiser model. This includes the logs shape and diameter every 100mm long it's length and branch position and size from the BRECrossCut model and ring densities from the Growth and Allocation model.

When the BREConversion model is run, i.e. all parts are fully integrated, the model will automatically process the above information, generating files for each log instantaneously, and then automatically moves on to the next tree stem from the virtual forest. This will continue until the forest has been completed.

5.4.3 BREOptimiser

The BREOptimiser model is made up of two sub models that combine their outputs to produce information on the volume of optimum products and their quality obtainable from the individual logs. The sub models used to achieve these volumetric and quality outputs are:

1. BRELogOptimiser, this model predicts the optimum conversion pattern used on the individual logs. In order to achieve the optimum conversion pattern the model has to predict the orientation of the log as it is brought to the saw. The outputs produced from this model are:

    a) The cant volume, including width and height,
    b) Falling board volumes,
    c) Wood chip volumes and
    d) Saw dust volumes

2. BRECantOptimiser, this model uses the data obtained from the BRELogOptimiser model and that generated from the Growth and Allocation model to maximise the quality and volume of construction battens sawn from the cant produced in the BRELogOptimiser model. It uses the knot size and position data to accurately saw the cant in an optimum fashion to reduce the amount and size of knots formed on the edges of the sawn battens. This increase the volume of C16 passes produced and reduces the volume of C16 rejects, as edge knots are one of the primary reasons for a batten to be downgraded. The model also tries to produce larger section from the outer part of the cant. This procedure is necessary, because higher value (larger section) sawn products will be less likely to be rejected due to twist, if they are cut further away from the pith.

Once the BREOptimiser (i.e. both the BRELogOptimiser and the BRECantOptimiser model) has been run the output files generate the following information:

1. Batten volumes, including sizes and stress-grading information (batten density, knot size and position, percentage of juvenile wood and distance form the pith),
2. Side board volumes,
3. Wood chip volumes,
4. Saw dust volumes.

Figure 1.4 below demonstrates how the BREOptimiser works. However, in reality logs are not as spherical and as straight as this. Therefore, more side-boards may result in order to generate the largest cant that can be produced from the logs common area.

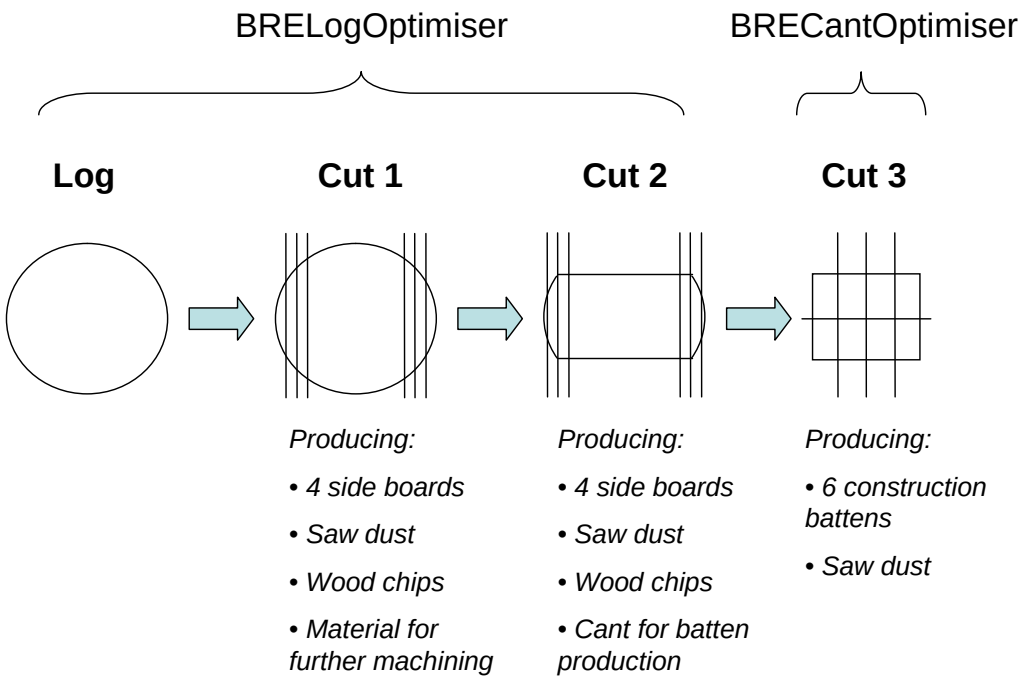

Figure 5.22: Schematic of a simplified sawing process used to utilise a logs volume**.**

The BREOptimiser model builds upon an existing model developed at BRE to predict the volumetric outputs from sawn timber. The program was original written in Basic programming langue but now runs using Java Script. This enables the use of more complex variables and a faster output.

The model uses the logs generated in the BRECrossCut model to produce an optimum product output, both in terms of volume and quality. In order to carry out this process the model uses important information on the logs' sweep, shape and knot sizes and positions to determine the optimum cutting angle and pattern for the log.

At present, the only information that a sawmill obtains as the logs emerge from the 3D scanner is its sweep and shape. This means that the sawmills are unable to predict where the knots will fall on the end product (the battens). Thus, not being able to completely maximise the batten quality. Although, sawmills are becoming very advanced and the use of x-ray machines are begging to be used. The BREOptimiser model demonstrates what effect knowing the knot size and positions has on the final quality of the battens sawn from the logs.

The model consists of two sub models:

1. BRELogOptimiser, and
2. BRECantOptimiser.

The BRELogOptimiser and the BRECantOptimiser model simulates the cutting procedure used by the sawmilling industry, Figure 5.22.

a) First the logs are debarked (adding to the chip volume), b) falling boards are sawn from two of the sides, c) the log is then rotated to remove falling boards from the other two faces producing the a square or rectangular cant, d) the cant is then sawn into construction battens.

The BRELogOptimiser models the procedures a) through to c), generating volumes of the different products at this point:

1) The cant volume, including width and height,
2) Side board volumes,
3) Wood chip volumes, and
4) Saw dust volumes.

However, the product volumes are not ready to be sent to the EFISCEN model until the saw dust volumes are calculated from the BRECantOptimiser model and the C16 reject volumes are calculated, as chips, from the Grading model.

The BRECantOptimiser then uses the cant computed in the BRELogOptimiser to generate structural battens of different cross-sectional sizes. The model is able to rotate the log in order to reduce the percentage of batten down grade due to knot formation. i.e. tries to avoid sawing the cant in a manner where the knots will fall on the edges of the battens. Figure 5.23 shows that this sawing position would cause the largest batten to contain detrimental knot formation.

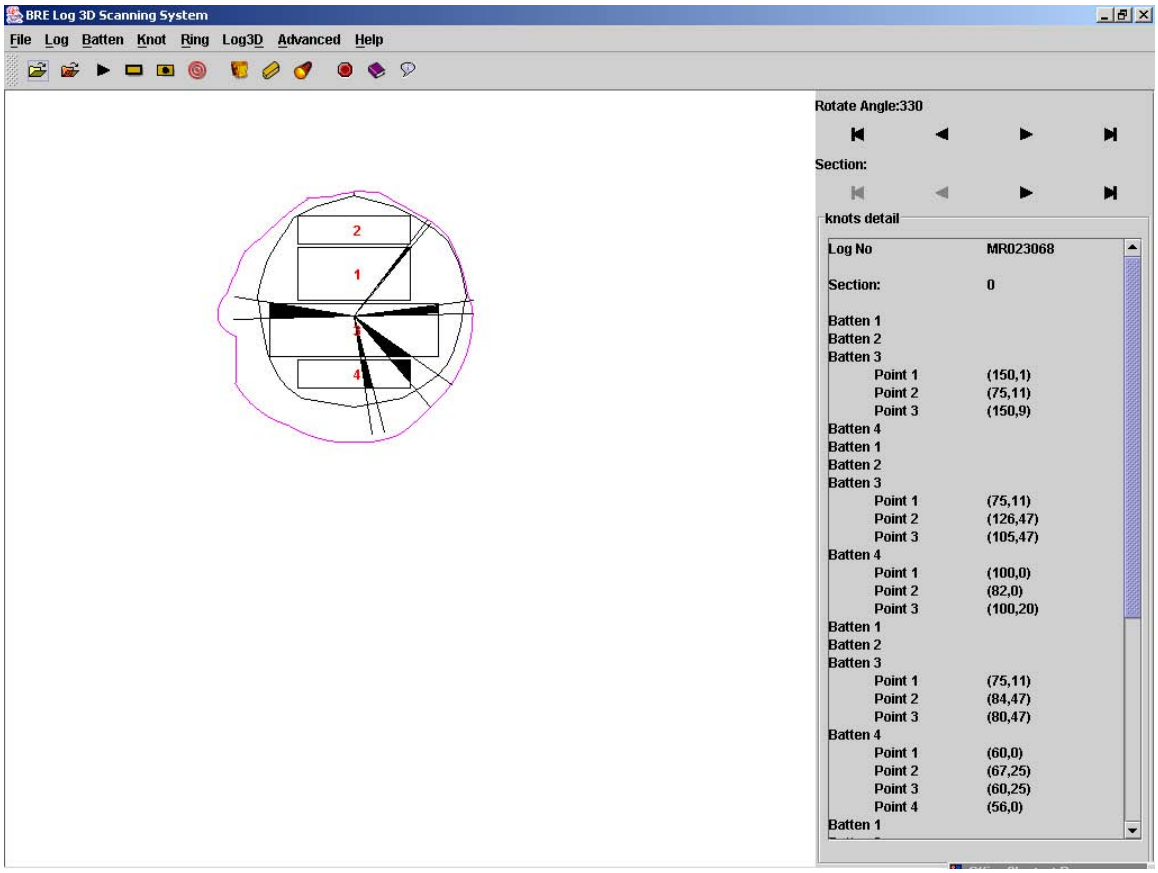

Figure 5.23: The visual interface of the BREOptimiser model**.**

Figure 5.23 shows the information produced on the BRECantOptimiser regarding batten production. On the right hand side of the screen, the grey area, it is possible to see the different size battens produced and the position of the knots as they are positioned within the batten. The program, when fully integrated into the BRE modelling sequence will automatically chose the best cutting pattern in terms of maximum batten size minimal knot splay.

Once the cutting procedure has been confirmed the battens are sent to the Grading model to determine whether they meet the C24, C16 pass or fail criteria.

5.4.4 Grading Model

It builds upon existing data and modelling previously carried out at BRE to predict whether a batten can be classed as a C16 (as described in BS EN338:1995 , BS EN384:1995, BS EN519:1995, British Standards, 1995 c, b, a) construction batten or a C16 reject. This

particular grade has been chosen as it is the most common construction material grade obtained from the UK sawmilling industry and is, therefore, a primary concern. It is also the lowest grade that enables it to be used for a construction component.

The model has been simplified by FR in conjunction with BRE. It takes the battens produced by the optimiser program and assigns them a strength characteristic based on the size of the batten and the wood density of the tree from which it was cut. The more complex model uses other characteristics such as knots, juvenile wood, compression wood etc. However since some of these characteristics are not as yet produced by the growth model, a simpler grading regime was used. The grades currently set are for C24, C16 and pulp/offcuts.

The outputs from the optimiser model are in effect a simple table of batten size and quantity for each log (with known density). The battens are allocated to be C24, C16 or offcuts/pulp according to their density and size. (A larger size will tend to show less twist and distortion after drying than a smaller batten). The results from each log are then aggregated to produce a summary file with the number of battens of each size and grade. This data is then suitable for input to the wood products model.

The information and files produced in the above procedures are then compiled into a readable format for the EFISCEN model to use. The output file contain volumes of the following products

1. Construction grade batten (C24 or higher)
2. Construction grade (C16)
3. C16 reject,
4. Falling boards,
5. Saw dust, and Chips. (waste)

5.5 The European Forest Information Scenario model (EFISCEN 3.0)

J. Meyer, S. Zudin, T. Eggers, A. Pussinen, M.J. Schelhaas, E. Verkaik, E. Heikkinen, J. Liski, T. Karjalainen, R. Päivinen and G.-J. Nabuurs

5.5.1 Summary

The European Forest Information Scenario Model (EFISCEN) is a large-scale scenario model, which uses forest inventory data as input (Pussinen *et al.*, 2001; Sallnäs, 1990). EFISCEN can be used to produce projections of the possible future development of forest resources on a European, national or regional scale (Naburrs *et al.* 2001, 2003, 2000; Karjalainen *et al.* 2002).

In EFISCEN, the state of the forest is described as an area distribution over age and volume classes in matrices. Growth is described as area changes to higher volume classes and ageing of forest is incorporated as a function of time up to the point of regeneration. The user defines the level of fellings for both thinnings and regeneration fellings and the model cuts it according to predefined management regimes, i.e. age limits for thinnings and felling probabilities for regeneration cuts. The management regimes are based on a country-level compilation of management guidelines (e.g. Yrjölä, 2002). In EFISCEN, wood demand is the main determinant of resource utilisation. If wood demand is high, management is intensive and rotation lengths are close to the lower limit defined in the management regimes. If wood demand is low, rotation lengths are longer, as less fellings are needed to fulfil the demand. The basic input data are derived from the national forest inventories. They include forest area, growing stock and increment by age-class and forest type. The quality and resolution of the input data determine how many regions, tree species, owner and site classes can be distinguished in a particular country. European wide data are gathered in the EFISCEN European Forest Resource Database (EEFR) at the European Forest Institute Schelhaas *et al.* 1999). The current version of EFISCEN can be used to study the carbon balance of the whole forest sector (Karjalainen *et al.* 2003). Stem wood volumes are converted to carbon of

stem, branches, leaves, roots and fine roots using dry wood density, carbon content and an age-dependent biomass distribution. Litter production is estimated using age-dependent turnover rates of each compartment, and litter is used as input to a dynamic soil carbon module (Liski *et al.* 2004).

Figure 5.24 presents the general structure of the EFISCEN model.

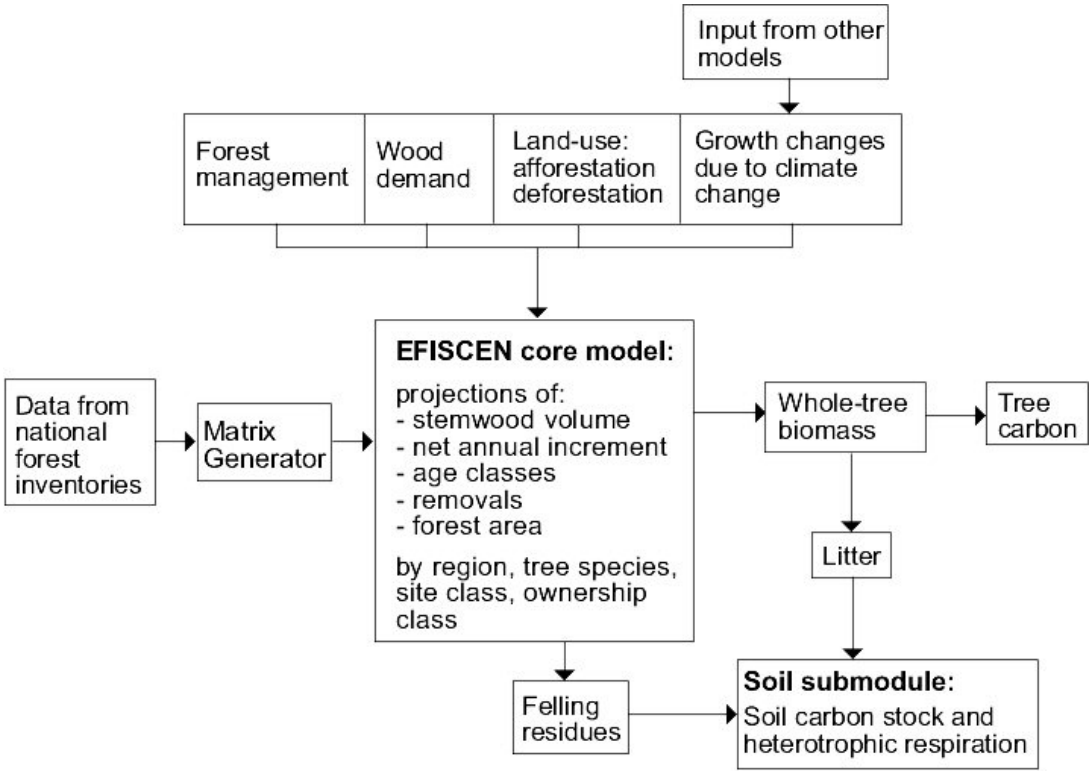

Figure 5.24: Structure of the EFISCEN model

5.5.2 Detailed model description

5.5.2.1 Needed input data

For each country, different forest types can be distinguished by region, owner class, site class and tree species depending on the level of detail of the input data. The following data should be available for each forest type and age class:

- area (ha)
- average standing volume over bark (m^3 ha^{-1})
- net current annual increment over bark (m^3 ha^{-1})

Furthermore, information is needed about the management regime, such as thinning regime and final cutting ages. If the carbon budget of the forest area is to be calculated, then biomass distribution parameters, dry-wood density, carbon content, weather data and turnover rates are needed as well. It is possible to account for forest cover changes due to afforestation and deforestation, and to incorporate the impact of environmental changes on tree growth.

5.5.2.2 Matrix set-up

EFISCEN is a matrix model, where the state of the forests is depicted as an area distribution over age and volume classes. For each forest type that is distinguished, a separate matrix is set up, which consists of 6 to 15 age classes and 10 volume classes (see Figure 5.25). The amount and width of the age classes is dependent on the input data. The width of the volume

$$f(x) = N(\mu_i, s_i^2) * f_{corr}$$

classes is set by a parameter, V1, which is the upper limit of the first volume class and can be set separately for all forest types. The area per forest type is divided over the cells using the input data. The area within an age class is distributed over the volume classes in such a way that the mean volume as given in the inventory data is matched.

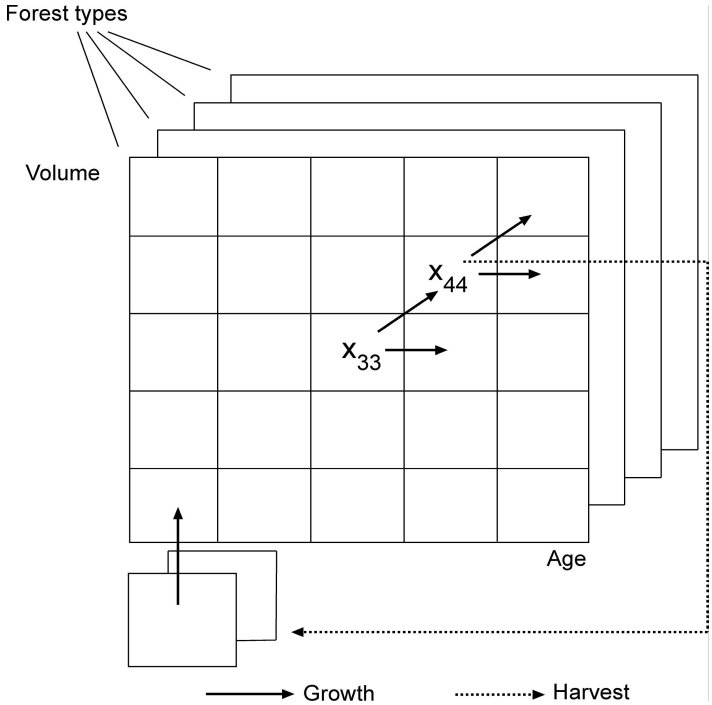

Figure 5.25: The area matrix approach (after Nilsson *et al.* 2002).

To keep the required initialisation data to a minimum, only the total area and the mean area are needed for each age class of a forest type. The volume distribution by age class is generated by an empirically based function, using a modified normal distribution of the following form:
with $\bullet_1$ denoting the mean volume in age class *i* from the inventory data and s^2 the assumed variance in age class *i*, while f_{corr} is defined as:

$$f_{corr}(x) = 1+\alpha_1[-\frac{1}{6}(3x+x^3)+\frac{10}{720}\alpha_1(x^6-15x^4+45x^2-15)]+\alpha_2\frac{1}{24}(x^4-6x^2+3)$$

where $\bullet_1$ and $\bullet_2$ are parameters to adjust the shape of the distribution. By default, their values are $\bullet_1$=1 and $\bullet_2$=2, but the values can be changed to adjust for irregular distributions. If *fcorr* is negative, it is set to zero.

The variance s_i^2 of age class *i* is calculated as

$$s_i^2 = kT_i \qquad \textbf{E: 5.1}$$

where T_i is the mid point of age class *i*. Parameter *k* is calculated according to:

$$k = \frac{(1 - cr^2)(\overline{V} * cv)^2}{\overline{T}}$$

where $\overline{V}$ is the average volume for the forest type, $\overline{T}$ is its average age, *cv* is the coefficient of variation in volume per hectare, and *cr* is the correlation between volume per hectare and age. The parameter *cv* is usually set to 0.65 for all forest types, whereas *cr* ranges from 0.45 to 0.7, depending on tree species, site classes and stocking of the forests. The higher the correlation between volume and age, the smaller is the variance.

Using equation E:5.1 the total area per age class is distributed over the volume classes. The lower and upper limits of the volume classes can differ between matrices.

The minimum limit for the largest volume class is calculated using the largest volume per hectare for that forest type, plus three times the largest standard deviation. The range between 0 and the minimum limit of the largest volume class is then divided into a sequence of volume classes, using the V1 parameter, which defines the width of the first volume class.

The distribution of area over the volume classes is calculated using the mean deviation and the standard deviation of volume in each age class and a modified normal distribution. The natural logarithm of age is used as a transformation of age in the calculations involving the correlation between age and volume.

5.5.2.3 Increment

In EFISCEN, growth dynamics are simulated by shifting proportions of the area in the matrix from one cell to another. Each five-year time step, the area in each cell will move up one age class. Part of the area will also move up one volume class. When area reaches the highest volume class it will remain there until it is harvested, i.e. it cannot grow anymore. Growth dynamics are incorporated as five year net annual increment as a percentage of the growing stock. The real volume increment percent per age class is calculated from the input data on the volume increment and the growing stock (cubic meters per hectare). The growth functions of the model are of the following type:

$$I_{vf} = a_0 + \frac{a_1}{T} + \frac{a_2}{T^2}$$

Where;

I_{vf}	five-year volume increment as a percentage of the growing stock
T	age of the stand in years
a_0, a_1, a_2	coefficients

The coefficients for the growth functions are usually derived from the relation between inventory data on age and real volume increment percent, or alternatively from yield tables. The mean volume in an age-volume cell will deviate from the mean volume series as provided in the input data. Accordingly, the volume increment percent also deviates from the value given by the function, which means that some correction must be made. The correction is made according to:

$$I_{va} = I_{vf} * (\frac{V_m}{V_a})^{beta} \qquad when\, V_a \leq V_m$$

$$I_{va} = \frac{I_{vf} * V_m}{V_a} \qquad when\, V_a > V_m$$

where

I_{va}	five-year percent volume increment for actual standing volume
I_{vf}	five-year percent volume increment given by the function
V_a	actual standing volume (m^3 ha^{-1})
V_m	standing volume (m^3 ha^{-1}) from the mean volume series
beta (•)	parameter

The relationship between the relative standing volume and the relative volume increment is described by the parameter ß(see Nilsson *et al.* 1992). From studies of this relationship in yield tables and other data, the value of the parameter ranges from 0.25 to 0.45, depending on species, site classification, and the type of data used to construct the yield tables. If the actual standing volume is higher than the standing volume in the mean volume series, the absolute increment does not increase any more, i.e. the stand is regarded as fully stocked and higher standing volume does not increase net annual increment (m^3 ha^{-1}).

In the matrix, increment is expressed as transition fractions between cells.

5.5.2.4 Management activities

In EFISCEN, the user specifies a certain harvest level and the model checks if it is possible to harvest that amount and simulates the development of the forest under that harvest level. Management is controlled at two levels in the model. First, for each forest type a basic management of thinning and final felling is incorporated. This is the theoretical management regime, which is applied according to handbooks or expert knowledge for forest management in the region or country to be studied. This theoretical regime must be seen as constraint of what might be felled. Second, total required volumes of removals from thinning and final felling are specified for the region or country as a whole for each time period. Removals are defined as cubic meters over bark. Furthermore, the proportion of the stemwood that is actually removed must be defined (ratio removals/fellings). Based on the theoretical management regimes, the model searches and might find, depending on the state of the forest, the required volumes. Further the success of a reforestation after clear felling can be incorporated per tree species, as well as a possible tree species change after a clear felling, and forest area change due to afforestation or deforestation.

5.5.2.5 Thinning

For each forest type, age limits for thinnings can be defined. The actual thinning is a fraction of the increment, i.e. the maximum thinning volume is the total increment in all cells subjected to thinnings. When an area in a cell is thinned it does not move one volume class higher, but actually stays in the same volume class. Thinned volume is the volume class change that did not happened due to thinning. In the next period the thinned area grows normally according to the rules. However, because the growing stock of the thinned area is lower than the growing stock of the forest that was not thinned, the increment of the thinned area is somewhat lower than the increment of the unthinned area. Besides the normal increment rate, part of the thinned area will grow one volume class extra during the second period, the so called growth boost. As soon as the forest has got the extra volume class, it will no longer be counted as thinned area, and it can be thinned again. The areas which have not got growth boost yet, cannot be subjected to thinning. However, two time steps after the thinning, the forest will loose its thinning status and is again available for thinnings or regeneration fellings.

The growth boost is defined as the fraction of thinned area, which grows back to the original volume per time step. According to growth and yield tables (Koivisto, 1959), 0.4 was assessed as a growth boost parameter for pine forest in Myrtillus site type in Finland (the volume of thinned and remaining standing stock in the model is then approximately the same as in managed and unmanaged stands). Furthermore, the proportion of the forest area, which has lower standing volume due to recent thinnings at the beginning of the simulation must be estimated. If the annually thinned area (A_{thi}) is known in the past, the thinned area in the beginning of simulation, *A is:*

$$A = 5 * A_{thi} * (1 + \frac{Re_{thi}}{1 + Re_{thi}})$$

where Re_{thi} is the growth boost parameter.

5.5.2.6 Final felling

The final felling regime is expressed as the proportion of each cell that can be felled, depending on the stand age. A felled area is moved outside the matrix to a bare-forest-land class. The final felling regimes can be obtained by handbooks, yield tables or other sources, such as statistical yearbooks. Depending on total demanded harvesting volume a number of final fellings are executed.

5.5.2.7 Regeneration

Regeneration is regarded as the movement of area from the bare-forest-land class to the first volume and age class. The amount of area that is regenerated is regulated by a parameter that expresses the intensity and success of regeneration, the young forest coefficient. This parameter is the percentage of area in the bare-forest-land class that will move to the first volume and age class during five years. This area will then attain the average volume and age of that class. It is possible to change tree species after clear-cutting. The tree species (change) to be regenerated on clear felled areas can be defined by forest type.

5.5.2.8 Forest area change

It is also possible to take afforestation and deforestation into account. The user can add or remove area per tree species in each time step of the simulations. The area will then be added to the bare-forest-land class of each forest type of that tree species, or the area is removed from the bare-forest-land class.

5.5.2.9 Change of increment due to changed environment

The model can simulate the development of the forest for decades. For various reasons, e.g. climate change, increment rates may change during long simulation periods. The model can take into account such changes in increment rate. The basis of the increment calculation is always the increment as calculated by the incorporated growth functions, which are based on the inventory data. These growth functions are used to calculate the increment in the matrix, and from that the transition probabilities in the matrix are derived.

If changes in the growth function will be simulated, the transition possibilities in the matrix are to be adapted. The new increment rates are defined relative to the basic ones (the ones from the inventory data), and can be defined by regions, tree species as well as site and owner class. Increment change rates can be derived, for example, from mechanistic forest models.

5.5.2.10 Biomass and litter production

Based on the calculated stem volumes, the model calculates the biomass of branches, coarse roots, fine roots and foliage. For this calculation the model requires biomass distribution tables by age classes. These tables can be based on the results of more detailed models, e.g. mechanistic models, or on values taken from the literature. The biomass distribution is defined by regions and tree species. For calculating carbon stocks and fluxes of the tree biomass, dry wood density and carbon content are also needed.

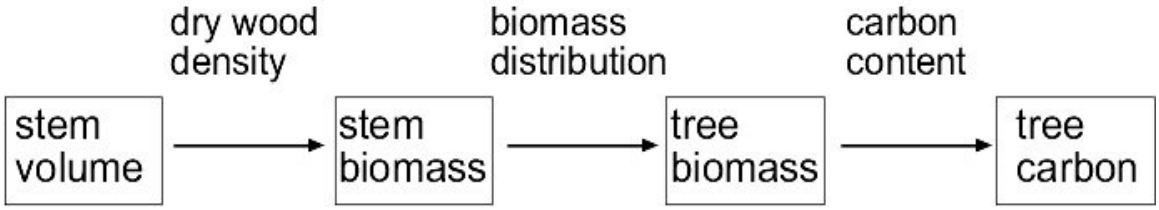

Figure 5.26: Calculation of biomass and carbon

Each year a proportion of the stems, branches, roots and leaves of the trees die, resulting in litter production. To calculate litter production, a proportion of annual litterfall of the standing biomass is needed. Also, when a thinning or final felling is carried out, all tree biomass left in the forest (harvest residues) is added to the litter pool and thus litter production depends on the harvest level in the region.

5.5.2.11 Soil

The EFISCEN model contains a dynamic soil carbon sub-module (Yasso) that calculates the amount of carbon in soil. The carbon input into the soil module is from the litter production of trees (calculated in the tree module). The sub-module consists of two woody litter compartments, each describing physical fractionation of litter (one for stem litter, one for branch and coarse root litter) and five compartments describing microbiological decomposition in soil (one for the soluble compounds of litter (extractives), one for holocellulose, one for lignin-like compounds and the other two for humus compounds) (see Figure 5.27). Non-woody litter (foliage and fine roots) is divided into the decomposition compartments of extractives, celluloses and lignin-like compounds according to its chemical composition. Each of the litter compartments has a specific fractionation rate (a_i) and each of the soil compartments a specific decomposition rate (k_i). These rates determine fractions that are removed from the contents of the compartments each year. Carbon removed from the litter compartments is divided into the soluble, holocellulose and lignin-like soil compartments according to the chemical composition of the litter (c_i). A part of carbon removed from the soil compartments (p_i) is transferred to the subsequent compartment and the rest out of the system; from the second humus compartment, carbon is only transferred out of the system.

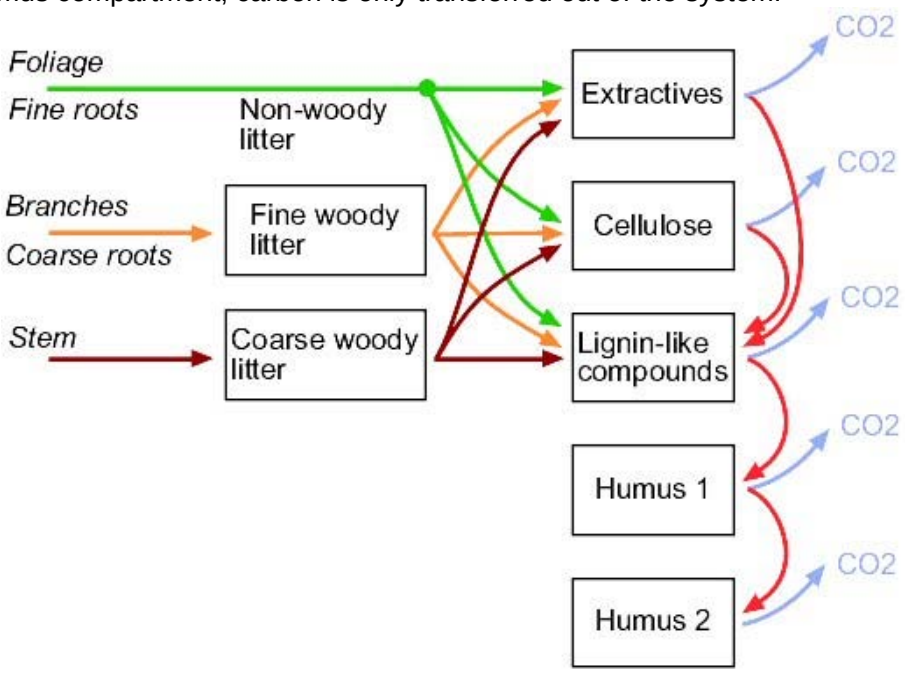

Figure 5.27: Flow chart of the soil carbon sub-module (Yasso) in EFISCEN. The boxes represent carbon compartments and the arrows represent fluxes.

The fractionation rates (a_i) and the decomposition rates (k_i) depend on annual mean temperature (T) and the difference between precipitation and potential evapotranspiration from May to September (P-E)

$$a_i(T, P-E) = 1 + (0.0937 * (T-4)) + 0.00229((P-E) - (-50)) * a_0 \quad \textbf{E: 5.2}$$

$$k_i(T, P-E) = 1 + s * (0.0937 * (T-4)) + 0.00229((P-E) - (-50)) * k_0 \quad \textbf{E: 5.3}$$

These dependencies were established by reanalysing data on the decomposition of Scots pine needles across Europe (Berg *et al.* 1993). The reference rates, a_0 and k_0, were determined for conditions where T = 4°C and $(P\text{-}E)$ = -50 mm by adjusting model-calculated mass loss rates to litter bag experiments (Berg *et al.* 1982, 1984) and model-calculated steady state amounts and accumulation rates of soil carbon to measured values (Liski and Westman, 1995; Liski *et al.* 1998). According to (Liski *et al.* 1999; Giardina and Ryan, 2000), the decomposition of humus is less sensitive to temperature than the decomposition of the more labile compounds. Therefore a temperature sensitivity parameter (s_j) decreases the temperature dependence of humus decomposition in the model. This parameter was set to 0.6 for the first humus compartment and to 0.36 for the second one; it was set to 1 for all other compartments.

The soil sub-module operates on an annual time step. It is initialised by setting the compartments to steady state with the input of the first studied year 1990. At the start of the simulations an initial soil carbon content should be known. The model calculates this initial content from the first year litter input. It assumes that this level of input occurred for years in the past, and calculates the steady state from first simulation period input. The model was developed for Finnish conditions (mean annual temperature +4°C), and therefore weather data of the country to be simulated should be added to the weather file before starting a simulation.

Table 5.2: Parameters of the soil carbon sub-module for the reference conditions (annual mean temperature 4°C, the difference between precipitation and potential evaporation 50 mm between May-September). The fractionation and decomposition rates were dependent on climate according to equations E: 5.2 and E: 5.3. The other parameters were similar for all conditions.

Parameter	Value
Exposure rates of woody litter to microbial decomposition (year $^{-1}$)	
Fine woody litter	0.54
Coarse woody litter	0.054
Litter Composition	
Extractives in non-woody litter, conifer	0.27
Celluloses in non-woody litter, conifer	0.51
Extractives in fine woody litter, conifer	0.03
Celluloses in fine woody litter, conifer	0.65
Extractives in coarse woody litter, conifer	0.03
Celluloses in coarse woody litter, conifer	0.69
Extractives in non-woody litter, hardwood	0.38
Celluloses in non-woody litter, hardwood	0.36
Extractives in fine woody litter, hardwood	0.03
Celluloses in fine woody litter,, hardwood	0.65
Extractives in coarse woody litter, hardwood	0.03
Celluloses in coarse woody litter, hardwood	0.75
Decomposition rates (per year)	
Extractives for conifers	0.48
Extractives for deciduous trees	0.82
Celluloses	0.3
Lignin-like compounds	0.22
Faster Humus	0.012
Slower Humus	0.0012
Formation of more complex compunds in decomposition (proportion of decomposed mass)	
Extractives to lignin-like compounds	0.2
Celluloses to lignin-like compunds	0.2
Lignin-like compunds to faster humus	0.2
Lignin-like compounds to slower humus	0.2

5.6 EFISCEN Wood products model

T. Eggers, S. Zudin

5.6.1 Summary

The current EFISCEN wood products model is a re-programmed version based on the concepts developed by Karjalainen *et al.* (1994) and the further development by Eggers (2002). From this basis, the model had been inter alia adapted by Briceño-Elizondo and Lexer (2004) and is also in use by other research groups.

The idea of the model is to follow the flow of carbon in harvested timber through different forest industries processes and the entire life-span until its final usage for either energy generation (product combustion), product recycling or re-usage, or its disposal on a landfill site. The model is constructed in such a way, that the carbon sequestered in timber is released back to the atmosphere after a user-defined period, which depends on the product

allocation to usage categories and the connected life-spans of the products in use. During this life-span the carbon is cascaded through several levels of either processing or usage. The model is still in an unvalidated status (due to the lack of available inventories of harvested wood product stocks and fluxes), but uses the input from previous studies that estimated parts of the complex wood product sector (Pingoud *et al.* 1996, 2000).

5.6.2 Model description

5.6.2.1 Model structuring and initial carbon stocks

The model components (raw material as input, products, and usage categories) can be defined freely by the user with some logical constraints. The amount of carbon in timber/products allocated either to processes, products, or usage must never exceed the actual amount available and must be fully distributed. Product losses can be included in the parametrisation, but must be clearly defined.

The initial carbon stocks in both raw material as well as wood-based product stocks can be either defined by the user or calculated by the model using statistical data from the past (e.g. FAOSTAT forestry statistics) on timber input and product allocations as done by Eggers (2002). The impact assessment of changing timber allocation could also be studied with non-initialised stocks (either empty or predefined), but in this case the product fluxes will take a certain time to reach an equilibrium.

The amount of input assortments, semi-products, usages, and end-uses can be defined by the user in the input files to the model. As the base-setup it is suggested to use only the level of precision, in which parameters for product processing and later product allocation are known or can be estimated with the help of statistics or producer information. For the MEFYQUE project the model was constructed to project the flow of softwood (both Scots pine and Norway spruce) for southern Finland. From this initial situation the model structure included the following:

Raw material: The amount of raw material (harvested timber) was modelled with the EFISCEN model for three different quality assortments. In this case the very simple, but justifiable, structure of saw logs, pulp logs, and residues was used. The allocation from the total harvest (from the EFISCEN model) was done by using statistics on assortment proportions (TAPIO, 1994; Peltola, 2004).

Products: The harvested timber is allocated to seven product groups depending on the species and quality assortment: two saw milling grades (C24, and C16), wood chips, chemical pulp (incl. semi-chemical pulp), mechanical pulp (incl. semi-mechanical pulp), other harvested wood products (e.g. particle board), and biofuel.

Usage categories: In the next modelling step the products mentioned above are then distributed to seven usage categories: building materials, other building materials, structural support materials, furnishing, packing materials, long life paper products, and short life paper products. These categories and the life-span connected with each are described in Table 5.3.

Table 5.3: Description of the usage categories in the harvested wood products model and their life-span.

Usage category and its life-span	Description
Building materials (50 years)	Products made of sawn timber, plywood/veneer or particle board used for construction work in buildings, civil engineering and otherlong-life constructuion work; (eg wooden houses or bridges)
Other building materials (16 years)	Products made from sawn timber, plywood/veneer or particle board used for maintaining in houses or civil engineering. Includes commodities such as fences, window frames, panels, floors and doors.
Strcutural support materials (1 year)	Products made from sawn timber, plywood/veneer or particle board used for form works, scaffolds and other wood-based products neded on building sites..
Furnishing (16 years)	Products made from sawn timber, plywood/veneer or particle board used for furnishing houses, offices and other private land and public buildings
Packing materials (1 year)	Products made from sawn timber, plywood/veneer or particle board or paper and paperboard products used for packing and other commodities (eg shipping boxes, wrapping and boxing)
Long-life paper products (4 years)	Products made from pulp used for longer periods such as books, maps and posters
Short life paper products (1 year)	Products made of pulp used for short periods such as newsprint and sanitary papers

End use categories: When a product has reached its end of use it has three options to be utilised. Either it is recycled back into usage and distributed again to one of the usage categories, or it is burnt to generate energy, or disposed to a landfill and left there for slow decay.

In the following sections the relevant parts from the input file (defprod.txt) will be shown to illustrate the different allocation steps in the model. The parametrisation is taken from model runs for Norway spruce (*Picea abies*) in southern Finland.

This first part shows the definition of raw materials, products, and usage categories.

```
#RAW MATERIALS
#How many
3
#ID Name initial
1 saw_logs 0 1
2 pulp_logs 0 1
3 residues 0 1
#PRODUCTS
#How many
7
#ID Name initial_stock Life_Span
11 C24 0 1
12 C16 0 1
13 chips 0 1
14 chem_pulp 0 1
15 mech_pulp 0 1
```

16 other_HWP 0 1
17 biofuels 0 1
#How many
7
#ID Name initial_stock Life_Span
101 Building_materials 0 50
102 Other_building_materials 0 16
103 Structural_support_materials 0 1
104 Furnishing 0 16
105 Packing_materials 0 1
106 Long-life_paperproducts 0 4
107 Short-life_paperproducts 0 1

5.6.2.2 Raw material allocation

In the current model version the allocation of harvested timber is done slightly different than in Eggers (2002). The logical step of allocating the assortments (saw logs, pulp logs, and residues) first to a processing line (e.g. saw milling, pulping, etc.) and then to the product (e.g. sawn timber, chemical pulp, mechanical pulp, etc.) was not included, but the assortments were directly distributed in shares to the products by integrating these two steps in one.

Beside the allocation of timber into the different products it is also possible to define other variables that can be taken into account. Currently only the variables 'share' and ' production' are used. The economic variables (benefit, cost) and environmental variables (emission, energy, losses, and release) are currently not in use.

#RAW MATERIALS Section
#Saw_logs
1
#how many flows
7
#destination Share Benefit Cost Emission Energy Losses Production Release
11 0.12557 0.0 0.0 0.0 0.0 0.0 1.0 0.0
12 0.25114 0.0 0.0 0.0 0.0 0.0 1.0 0.0
13 0.42048 0.0 0.0 0.0 0.0 0.0 1.0 0.0
14 0.00016 0.0 0.0 0.0 0.0 0.0 1.0 0.0
15 0.00414 0.0 0.0 0.0 0.0 0.0 1.0 0.0
16 0.04958 0.0 0.0 0.0 0.0 0.0 1.0 0.0
17 0.14892 0.0 0.0 0.0 0.0 0.0 1.0 0.0
#Pulp_logs
2
#how many flows
7
#destination Share Benefit Cost Emission Energy Losses Production Release
11 0.00000 0.0 0.0 0.0 0.0 0.0 1.0 0.0
12 0.03150 0.0 0.0 0.0 0.0 0.0 1.0 0.0
13 0.03150 0.0 0.0 0.0 0.0 0.0 1.0 0.0
14 0.08749 0.0 0.0 0.0 0.0 0.0 1.0 0.0
15 0.68211 0.0 0.0 0.0 0.0 0.0 1.0 0.0
16 0.00141 0.0 0.0 0.0 0.0 0.0 1.0 0.0
17 0.16598 0.0 0.0 0.0 0.0 0.0 1.0 0.0
#Residues
3
#how many flows
1
#destination Share Benefit Cost Emission Energy Losses Production Release
17 1.0 0.0 0.0 0.0 0.0 0.0 1.0 0.0

5.6.2.3 Product allocation

In the products section the materials are allocated to their usage. Again only the variables for the actual share within the allocation and the production are defined at this stage of the modelling approach. The other variables are included, but not defined.

Many of the share-variables are based on expert assessment and give only a general impression how the timber might be distributed to the defined usage categories. To decrease the uncertainties connected with this rather coarse parametrisation it would be necessary to study the product flows in detail with the help from the commodity producers.

```
#PRODUCTS Section
#C24
11
#how many flows
3
#destination Share Benefit Cost Emission Energy Losses Production Release
101 0.50 0.0 0.0 0.0 0.0 0.0 1.0 0.0
102 0.30 0.0 0.0 0.0 0.0 0.0 1.0 0.0
104 0.20 0.0 0.0 0.0 0.0 0.0 1.0 0.0
#C16
12
#how many flows
4
#destination Share Benefit Cost Emission Energy Losses Production Release
101 0.50 0.0 0.0 0.0 0.0 0.0 1.0 0.0
102 0.15 0.0 0.0 0.0 0.0 0.0 1.0 0.0
103 0.20 0.0 0.0 0.0 0.0 0.0 1.0 0.0
105 0.15 0.0 0.0 0.0 0.0 0.0 1.0 0.0
#Chips
13
#how many flows
3
#destination Share Benefit Cost Emission Energy Losses Production Release
15 0.70 0.0 0.0 0.0 0.0 0.0 1.0 0.0
16 0.10 0.0 0.0 0.0 0.0 0.0 1.0 0.0
17 0.20 0.0 0.0 0.0 0.0 0.0 1.0 0.0
#Chemical pulp
14
#how many flows
3
#destination Share Benefit Cost Emission Energy Losses Production Release
105 0.20 0.0 0.0 0.0 0.0 0.0 1.0 0.0
106 0.40 0.0 0.0 0.0 0.0 0.0 1.0 0.0
107 0.40 0.0 0.0 0.0 0.0 0.0 1.0 0.0
#Mechanical pulp
15
#how many flows
3
#destination Share Benefit Cost Emission Energy Losses Production Release
105 0.20 0.0 0.0 0.0 0.0 0.0 1.0 0.0
106 0.40 0.0 0.0 0.0 0.0 0.0 1.0 0.0
107 0.40 0.0 0.0 0.0 0.0 0.0 1.0 0.0
#other_HWP
16
#how many flows
4
#destination Share Benefit Cost Emission Energy Losses Production Release
102 0.25 0.0 0.0 0.0 0.0 0.0 1.0 0.0
103 0.25 0.0 0.0 0.0 0.0 0.0 1.0 0.0
104 0.25 0.0 0.0 0.0 0.0 0.0 1.0 0.0
105 0.25 0.0 0.0 0.0 0.0 0.0 1.0 0.0
#biofuel
17
```

#how many flows
1
#destination Share Benefit Cost Emission Energy Losses Production Release
1000 1.00 0.0 0.0 0.0 0.0 0.0 1.0 0.0

5.6.2.4 Product life-span

The life-span of wood products is calculated using a simple exponential decay function in the product module. The user provides the half-time values (in this case either 1, 4, 16, or 50 years) for the product categories and then the model calculates the corresponding value of the exponential multiplier coefficient as follows. If *Y(t)* is a share of the initial amount of a product at time *t*, the model uses the exponential function for $Y(t)=exp^{-at}$. From the equation $Y_{t0}=0.5$ (which means that at time t_0 only 50% of the initial stock are still present - so called half-life) the parameter *a* can be calculated as $a=(ln^2) / (t_0)$.

The applied life-spans for the product categories are derived from previous studies in this field. They must be seen as rather uncertain and difficult to verify. The following Table 5.4 gives an overview on life-span categories used in previous studies in this field.

Table 5.4: Half-life-periods-of Half-life periods of wood products in different studies (from Eggers (2002).

	Half life period (years)				
Study	short	Medium-short	Medium	Medium-long	long
Row & Phelps (1990)	1	6	12	30	50,60,67
Karjalainen *et al.*(1994)		4	13	30	65
Pingoud *et al.*(2004)			16		50
Eggers (2002)	1	4	16		50

5.6.2.5 Product recycling / re-usage

Also the parameters for the recycling and end-use of products are based on expert assessments. For each usage category it is assumed that a major proportion is taken out of use and either burnt or disposed to a landfill. Only a small part is recycled or reused and thus brought back to the product pool, which is in use.

Again only the variables for the actual share within the allocation and the production are defined at this stage of the modelling approach. The other variables are included, but not defined.

#END USE RECYCLING and LANDFILL
#Buildings materials
101
#how many flows
5
#destination Share Benefit Cost Emission Energy Losses Production Release
101 0.10 0.0 0.0 0.0 0.0 0.0 1.0 0.0
102 0.10 0.0 0.0 0.0 0.0 0.0 1.0 0.0
103 0.10 0.0 0.0 0.0 0.0 0.0 1.0 0.0
1000 0.35 0.0 0.0 0.0 0.0 0.0 1.0 0.0
1001 0.35 0.0 0.0 0.0 0.0 0.0 1.0 0.0
#Other Buildings materials
102
#how many flows
5
#destination Share Benefit Cost Emission Energy Losses Production Release
102 0.05 0.0 0.0 0.0 0.0 0.0 1.0 0.0
103 0.10 0.0 0.0 0.0 0.0 0.0 1.0 0.0
105 0.10 0.0 0.0 0.0 0.0 0.0 1.0 0.0
1000 0.50 0.0 0.0 0.0 0.0 0.0 1.0 0.0
1001 0.25 0.0 0.0 0.0 0.0 0.0 1.0 0.0
#Struct. support

103

#how many flows

3
#destination Share Benefit Cost Emission Energy Losses Production Release
103 0.15 0.0 0.0 0.0 0.0 0.0 1.0 0.0
1000 0.40 0.0 0.0 0.0 0.0 0.0 1.0 0.0
1001 0.45 0.0 0.0 0.0 0.0 0.0 1.0 0.0
#Furnishing
104
#how many flows
3
#destination Share Benefit Cost Emission Energy Losses Production Release
104 0.15 0.0 0.0 0.0 0.0 0.0 1.0 0.0
1000 0.40 0.0 0.0 0.0 0.0 0.0 1.0 0.0
1001 0.45 0.0 0.0 0.0 0.0 0.0 1.0 0.0
#Packing
105
#how many flows
3
#destination Share Benefit Cost Emission Energy Losses Production Release
105 0.15 0.0 0.0 0.0 0.0 0.0 1.0 0.0
1000 0.40 0.0 0.0 0.0 0.0 0.0 1.0 0.0
1001 0.45 0.0 0.0 0.0 0.0 0.0 1.0 0.0
#Long-life paper
106
#how many flows
4
#destination Share Benefit Cost Emission Energy Losses Production Release
106 0.18 0.0 0.0 0.0 0.0 0.0 1.0 0.0
107 0.18 0.0 0.0 0.0 0.0 0.0 1.0 0.0
1000 0.32 0.0 0.0 0.0 0.0 0.0 1.0 0.0
1001 0.32 0.0 0.0 0.0 0.0 0.0 1.0 0.0
#Short-life paper
107
#how many flows
3
#destination Share Benefit Cost Emission Energy Losses Production Release
107 0.36 0.0 0.0 0.0 0.0 0.0 1.0 0.0
1000 0.32 0.0 0.0 0.0 0.0 0.0 1.0 0.0
1001 0.32 0.0 0.0 0.0 0.0 0.0 1.0 0.0

5.6.2.6 Model output

The model generates two output files per model run. One of the files includes the yearly stocks of carbon in raw materials, products, usage categories, landfills, and carbon emitted to the atmosphere. The other file includes all defined flows of carbon from one stock to another. The output is in comma-separated-value (CSV) format and can be easily imported to database applications for further analysis.

5.7 References

Ball, J.T., Woodrow, I.E. and Berry, J.A. (1987). *A model predicting stomatal conductance and its contribution to the control of photosynthesis under different environmental conditions*. In: *Progress in Photosynthesis Research*, eds J. Biggins and M. Nijhoff, Dordrecht, Vol. 4, 221-224.

British Standards Institute (1995a). Structural timber – Determination of characteristic values of mechanical properties and density. *Technical Report EN:384:1995.* British Standards Institute, London.

British Standards Institute (1995b). Structural timber – Grading – Requirements for machine strength graded timber and grading machines. *Technical Report EN:519:1995.* British Standards Institute, London.

British Standards Institute (1995c). Structural timber – Strength classes. *Technical Report EN:338:1995.* British Standards Institute, London.

Brisitsh Standards Institute (1996). Specification for visual strength grading of softwood. *Technical Report EN:4978:1996.* British Standards Institute, London.

Berg, B. Bottner, M., Box, E., Breymeyer, A., Calvo De Anta, R., Couteaux, M., and 11 others (1993). Litter mass loss rates in pine forests of Europe and Eastern United States: Some replationships with climate and litter quality. *Biogeochemistry* **20:** 127-159.

Berg, B., Ekbohom, G. and McClaugherty, C. (1984). Lignin and holocellulose relations during long-term decomposition of some forest litters. Long-term decomposition in a Scots pine forest. IV. *Canadian Journal of Botany* **62:** 2540-2550.

Berg, B., Hannus, K., Popoff, T. and Theander, O. (1982). Changes in organic chemical components of needle litter during decomposition. Long-term decomposition in a Scots pine forest. I. *Canadian Journal of Botany* **62:** 1310-1319.

Briceño-Elizondo, E. and Lexer, M. (2004). Estimating carbon sequestration in the wood products pool: Model adaptation and application for Austrian conditions. *Austrian Journal of Forest Science* **121:** 99-119.

Burman, R. and Pochop, L. O. (1994). *Evaporation, Evapotranspiration and Climatic Data*. Elsevier Science B. V., Amsterdam

De Pury, D.G.G., Farquhar, G.D. (1997). Simple scaling of photosynthesis from leaves to canopies without the errors of big-leaf models. *Plant, Cell and Environment* **20:** 537-557.

Deckmyn, G., Evans, S. P. and Randle, T.J. (submitted). Refined pipe theory for mechanistic modelling of wood development. *Tree physiology*, submitted.

Dewar, R. (2002). The Ball-Berry and Thardeiu-Davies stomatal models: synthesis and extension within a spatially aggregated picture of guard cell function*. Plant, Cell and Environment* **25:** 1383-1398.

Eggers, T. (2002). The impacts of Manufacturing and Utilisation of Wood Products on the European Carbon Budget. *EFI Internal Report 9*. European Forestry Institute, Joensuu, Finland.

Evans S.P. (1997). The potential use of weather generators in palaeoclimatic and palaeoecological research: the SWELTER (Synthetic Weather Estimator for Land use and Terrestrial Ecosystem Research) model. *Italian Journal of Quaternary Sciences*, *(Il Quaternario),* **9:** 643-648.

Evans, S.P., Mayr, T.J., Hollis, M. and Brown, C.D. (1998). SWBCM: a soil water balance capacity model for environmental applications in the UK. *Ecological Modelling* **121:** 17-49.

Evans, S., Randle, T., Henshall, P., Arcangeli, C., Pellenq, J., Lafont, S. and Vials, C. (in press). Recent Advances in the mechanistic modelling of forest stand and catchments. In: *Forest Research Annual Report and Accounts 2003-2004.* 98-111, The Stationery Office, Edinburgh, UK.

Falge, E., Baldocchi, D., Olson, R., Anthoni, P., Aubinet, M, Bernhofer, C. and 28 others. (2001a). Gap filling strategies *for long term energy flux data sets, a short communication. Agricultural* and Forest Meteorology **107:** 71-77.

Falge, E., Baldocchi, D., Olson, R., Anthoni, P., Aubinet, M, Bernhofer, C. and 28 others. (2001b). Gap filling strategies *for defensible annual sums of net ecosystem exhange. Agricultural* and Forest Meteorology **107:** 43-69.

Farquhar, G.D., von Caemmerer, S. and Berry, J.A. (1980). A biochemical model of photosynthetic CO_2 assimilation in leaves of C_3 plants. *Planta* **149**: 78-90.

Forestry Commission (1993). *Classification and Presentation of Softwood Sawlogs*, field book 9, HMSO, London, UK

Friend, A. (1995). PGEN: an integrated model of leaf photosynthesis, transpiration and conductance. *Ecological Modelling* **77:** 233-255.

Gash, J.H.C., Lloyd, C.R. and Lachaud, G. (1995). Estimating sparse forest rainfall interception with an analytical model. *Journal of Hydrology* **170:** 79-86.

Gash, J., Wright, I., and Lloyd, C. (1980). Comparative estimates of interception loss from three coniferous forests in Great Briatain. *Journal of Hydrology* **48:** 89-105.

Giardina, C. and Ryan, M. (2000). Evidence that decomposition rates of organic carbon in mineral soil do not vary with temperature. *Nature* **404:** 858-861.

Helle, G. and Schleger, G.H. (2004). Beyond CO_2-fixation by Rubisco – an interpretation of $^{13}C/^{12}C$ variations in tree rings from novel intra-seasonal studies on broad-leaf trees. *Plant, Cell and Environment* **27**: 367-380.

Hutchinson, M.F. (1991). Climatic analysis in data sparse regions. In: *Climatic risk in crop production: Models and measurement for the semiarid tropics and arid subtropics* eds R.C. Muchow and J.A. Bellamy. CAB International, Wallingford, UK, 55-73.

Karjalainen, T., Kellomäki, S., and Pussinen, A. (1994). Role of wood based products in absorbing atmospheric carbon. *Silva Fennica* **28:** 67-80.

Karjalainen, Pussinen, A., Liski, J., Nabuurs, G-J., Erhard, M., Eggers, T.,Lapvetelainen, T. and Kaipainen, T. (2003). Scenario analysis of the impacts of forest management and climate change on the European forest sector cabon budget. *Forest Policy and Economics* **5:** 141-155.

Karjalainen, Pussinen, A., Liski, J., Nabuurs, G-J., Erhard, M., Eggers, T., Sonntag, M. and Mohren, G. (2002). An approach towards an estimate of the impact of forest management and climate change on the European forest sector carbon budget: Germany as a cse study. *Forest Ecology and Management* **162:** 87-103.

Koivisto, P. (1959). Kasvu- ja tuottotaulukoita (Growth and Yield tables). Technical Report *Communicationes Instituti Forestalis Fenniae* , **51.8:** 49pp.

Liski, J., Ilvesniemi, H.A. and Starr, M. (1998). Model analysis of the effects of soil age, fires and harvesting on the carbon storage of boreal forest soils. *European Journal of Soil Science* **49:** 407-416.

Liski, J., Ilvesniemi, H.A., Mäkäkä, A. and Westman, C. (1999). CO2 emissions from soil in response to climatic warming are overestimated – the decomposition of old soil organic matter is tolerant of temperature. *Ambio* **28:** 171-174.

Liski, J. Palosuo, T., Peltoniemi, M. and Sievanen, R. (in press). Carbon and decomposition model Yasso for forest soils. *Ecological mode*lling (in Press)

Liski, J., Pussinen, A., Pingoud, K., Mäkipää, R. and Karjalainen, T. (2001). Which rotation length is favourable for carbon sequestration*. Canadian Journal of Forest Research* **31:** 2004-2013.

Liski, J. and Westman, C. (1995). Density of organic carbon in soils at coniferous forest sites in southern Finland. *Biogeochemistry* **29:** 183-197.

Long, S. (1991), Modification of the response of photosynthetic productivity to rising temperature bu CO2 concentrations: Has its importance been underestimated*? Plant, Cell and Environment* **14:** 729-739.

McGaughey, R. (1997). Visualising forest stand dynamics using the stand visualisation system. In: *Proceedings of the 1997 ACSM/ASPRS Annual convention and exposition, April 7-10 1997*. Volume 4. American society for photogrammetry and remote sensing, Seattle, WA.

McMurtie, R. and Wang, Y. (1993). Mathematical models of the photosynthetic response of tree stands to rising CO2 concentrations and temperatures. *Plant, Cell and Environment* **16:** 1-13.

Monsei, M. and Saeki, T. (1953). Über den Lichtfaktor in den Pflanzengesellenschaften und seine Bedeutung für dir Stoffproduktion. *Japanese Journal of Botany* **14:** 22-52.

Monteith, J. (1981) Evaporation and surface temperature*. Quarterly Journal of the Royal Meteorological Society 107:* 1-27.

Nabuurs, G.J., Päivinen, R., Pussinen, A. and Schelhaas, M.J. Development of European forests until 2050 – a projection of forests and forest management in thirt countries. *EFI Research Report 15*, European Forestry Institute, Joensuu, Finland.

Nabuurs, G.J., Päivinen, R., and Schanz, H. (2001). Sustainable management regimes for Europe's forests - a projection with EFISCEN until 2050. *Forest Policy and Economics* **3:** 155-173.

Nabuurs, G.J., Schelhaas, M.J. and Pussinen, A. (2000). Validation of the European forest information scenario model (EFISCEN) and a projection of Finnish forests. *Silva Fennica* **34:** 167-179.

Norman, J.M. (1980). *Interfacing leaf and canopy light interception models*. In: *Predicting photosynthate production and use for ecosystem models*, Vol. II. CRC Press, West Palm Beach, FL, 49-67.

Päivinen, R, Nabuurs, G.J, Lioubimow, A. and Kuusela, K. (1999). The state, utilisation ans possible future development of Leningrad region forests. *EFI working paper 18*, European Forestry Institute, Joensuu, Finland, 59 pp.

Peltola, A. (Ed) (2004). *Metsätilastollinen vuosikirja 2004*. Metsantukimuslaitos Helsinki, Finland.

Pingoud, K., Peräla, A-L. and Pusinen, A. (2000). Inventorying and modeliing of carbon dynamics in wood products. In: *Bioenergy for mitigation of CO2 emissions: To power, transportation and industrial sectors*. Eds. K Robertson and B. Schlamadinger). Joanneum Research Gatlinburg, TN.

Pingoud, K. Savolainen, I., and Seppälä, H. (1996). Greenhouse impact of the Finnish forest sector including forest products and waste management. *Ambio* **25:** 318-326.

Pussinen, A., Schellaas, M., Verkaik, E., Heikkinen, E., Liski, J. Karjalainen, T., Päivinen, R and Nabuurs, G.J. (2001). Manual for the European forest information scenario model (EFISCEN 2.0). *EFI internal report 5*, European forestry institute, Joensuu, Finland.

Raupach, M. (1994). Simplified expression for vegetation roughness length and zero-plane displacement as function of canopy height and area index. *Boundary-layer meteorology* **71:** 211-216.

Richardson, C.W. (1981). Stochastic simulation of daily precipitation, temperature and solar radiation. *Water Resources Research* **17:** 182-190.

Ritchie, J.T. (1972). A model for predicting evaporation from a row crop with incomplete cover. *Water Resources Research* **8:** 1204-1213.

Ross, S. M. (1983). *Stochastic Processes*, John Wiley and Sons, New York.

Row, C. and Phelps, R. (1990). Tracing the flow of carbon through U.S. forest product sector. *Presentation*, IUFRO 19th World congress, Montreal, Canada.

Russell, G. Jarvis, P. and Monteith, J. (1989). Absorption of radiation by canopies and stand growth. In: *Plant canopies: their growth, form and function*. Eds. G. Russell, B. Marshall and P. Jarvis. Cambridge University Press, Cambridge

Rutter, A., Morton, A. and Robins, P. (1975). A predictive model of rainfall interception in forests. II. Generalisation of the model comparison with observations in some coniferous and hardwood stands. *Journal of Applied Ecology* **12:** 367-380.

Sallnäs, O. (1990). A matrix growth model of the Swedish forest. *Studia Forestalia Suecica 183*. SUAS, Uppsala.

Schelhass, M., Varis, S., Schuck, A. and Nabuurs, G.J. (1999). EFISCEN's European forest resource database.

TAPIO (1994). Tapion taskukirja. *Metsakeskus Tapio 22*, Helsinki.

Thompson, N., Barrie, I.A. and Ayles, M. (1981). The Meteorological Office rainfall and evaporation calculation system MORECS. *Hydrological Memorandum No 45*, Hydromet. Services. UK.

Thornley, J. (1998). *Grassland dynamics. An ecosystem simulation model*. CAB international, Wallingford, UK.

Tyree, M.T., Salleo S., Nardini A., Lo Gullo M.A. and Mosca, R. (1999). Refilling of embolized vessels in young stems of laurel. Do we need a new paradigm? *Plant Physiology* **120**: 11-21.

Valente, F., David, J.S. and Gash, J.H.C. (1997). Modelling interception loss for two sparse eucalypt and pine forests in central Portugal using reformulated Rutter and Gash analytical models. *Journal of Hydrology* **190:** 141-162.

Von Caemmerer, S., and Farquhar, G.D. (1981). Some relationships between the biochemistry of photosynthesis and the gas exchange of leaves. *Planta* **153:** 376-387.

Yrjölä, T. (2002). Forest management guidelines and practices in Finland, Sweden and Norway. *EFI internal report 11*, European Forestry Insitute, Joensuu, Finland.

6 Modelling of wood quality, tree growth and the woodchain at stand scale for representative sites across Europe

Main Contributors:
Gaby Deckmyn, Tim Randle, Paul Henshall. Sam Evans, Keith Maun

6.1 Parameterisation

6.1.1 Parameterisation of the plot scale model

For the parameterisation and the validation of the models, experimental data from within the project were mainly used.
The parameters required for the model fall into 4 categories: stand data, species data, climate data and soil data.

- **Stand data** are the forest inventory data of the stand, as well as data on management. The stand data were collected from the primary, secondary and tertiary sites in the field (see chapter 2).

- **Species data** contain all species-specific values that describe how a species grows and interacts with the environment. Most of these data were pertained from the wood anatomical and biochemical studies. For some of the parameters on photosynthesis, transpiration and respiration, where no measurements were performed within this project, data from literature were used. In most cases, data from the same sites were available as these sites have been used in many previous studies and are well documented. These data are supposed to be independent of the stand or environment in which the tree will grow. For example, a tree species has a specific crown shape, determined by parameters in the species-parameters list. However, the actual crown shape will be determined by the stand density, the thinning management etc. defined in the stand data. As an example the *Pinus sylvestris* and *Populus alba* files are included.

- **Climate data** at the sites, the individual research groups were responsible. For the Brasschaat site, measurements had only been performed since 1996. Therefore, a 10-year climate set was purchased from the Belgian Meteorological Society (KMI). Part of this file is added here as an example. The plot scale model can run using hourly, daily or monthly data, whichever are available. Obviously for the micro-allocation such as the density profile throughout a year-ring, working with monthly averages does not yield realistic results. For an overall simulation of total yield over longer time periods however, monthly data are adequate and reduce the simulation time considerably. Moreover, while monthly averages are generally easy to find for sites in Europe, daily or hourly values are often unavailable or expensive.

  To overcome some of the difficulties relating to the lack of suitable meteorological data, A synthetic weather generator, validated for the UK (Evans *et al*., 2002) has been further developed and can be used with monthly summary data.

- **Soil data** input is a rather long list of not-so-easily obtained values. Within the MEFYQUE project, there was less emphasis on the functioning of the soil, as forest yield quantity and quality were the focus, not the forest ecosystem as such. However, since the soil needed to be simulated to get realistic results for the forest growth, some data concerning soil composition were required. The soil module of the stand model was developed within different European Projects (CASIROZ (EVK2-2002-00165) and EUROFACE (EVRI-CT-2002-40027)). Most of the input values have no or very minor influence on the growth of the trees (such as the exact content of the C-pools in the soil, and their stabilisation to clay minerals), and therefore values from literature were used. Only for these sites where soil analysis had been performed within the course of past research, more exact values were used for the MEFYQUE simulations (for example the data for the Brasschaat site where soil functioning has been intensively studies over the past years). For all the sites, the site-specific sand and clay content, soil depth and humus layer depth were recorded and used as input.

As an examples the input files describing the Brasschaat *Pinus sylvestris* site (secondary site) and the Viterbo *populus Alba* site (tertiary site) are in the appendix.

6.1.2 Parameterisation of the sawing optimisation

Outputs from the growth model become inputs for the sawing optimisation programs. Development of the modelling sequence has concentrated on the pathway for coniferous species. The sawing optimisation consists of three programs (see chapter 5, modelling methods)

- Cross-Cut *(Calculates where the cuts along the bole are made, creating logs of a specified length.)*
  Stem diameter every *10* cm along its length (in Polar co-ordinates of the stem linked to a common datum, representing the shape and size of the stem).
  A more complex version of the model (not applied in this work) also uses branch sizes and positions to determine knot area, there therefore potential weak spots to be avoided in the cutting of the logs.

  A maximum deviation from straightness is input to the model, this enables badly distorted sections to be excluded from logs to be processed at a mill. The cross-cut model tries to produce 4.8m lengths, but shorter ones are produced if the shape and size of the stem warrant it.

  Cross-cut identifies the sections where a 'cut' is made, allowing the detailed stem description (tree rings and densities) to be divided into 'log' files. Sections of unsuitable timber are stored in 'loss' files

- Optimiser (Calculates the best cut of timber battens from a log)
  This model requires, the description of each growth ring at intervals along each log (logs cut-points described as output from Cross-Cut. The uncut volume is also calculated (eg slab offcuts). The lengths of timber produced are the same as the log–length. The battens are then cut to specified lengths, with unused lengths calculated. For simplicity, Standard lengths of 1.8, 2.4, 3.0, 4.8 m were chosen, though these can be set to any number and size.

- Strength-Grade (determines the strength quality of each cut batten)
  This model requires the dimensions of the battens output from the optimiser model, together with the wood density of each growth-ring (and therefore each piece of timber) from the forest growth model. The primary feature in determining grade is wood density. Each batten is 'tested' against these criteria, with an associated pass-fail percentage. If a batten failed the top criteria it would be tested against the next etc. The quality classes used were C24, C16, other.

  Again the model has been simplified for application within this work; A more sophisticated model requires additional information about the timber structure (spiral grain, juvenile wood, compression wood etc.), which at this time are not provided by the growth model.

6.2 Validation

The MEFYQUE stand model is a very complex model, that yields an enormous quantity of output (see chapter 5) concerning a wide range of physiological and anatomical data at various time scales. The development of the allocation module was based on the results of the anatomical studies, and a continuous improvement of the correlation between measured and simulated data has finally resulted in the current version of the model. Therefore, rather than saying these data were used to validate our model, they were used to develop the initial mechanistic rules concerning the formation of wood, on which the model was based (see chapter 5). The most important measured features in this context were the early-and latewood width through the last 10 years, the pipe radius in early- and latewood, the density profile and the cell-wall width.

6.2.1 Validation of the plot scale model for Brasschaat, *Pinus sylvestris*

So far, the most complete validation of the model has been for *Pinus sylvestris* at Brasschaat. On this site, the total productivity, macro-allocation and wood quality development over the last 10 years (1991-2001) was validated with measured values leading to a first paper (presented at the wood chain conference, September 2004). Furthermore, the detailed, daily evolution of the wood, using daily climatic data of the last 3 year rings (1999-2001) has been validated using the measured density profiles (see chapters 3 and 4). This has yielded new insight into the daily development of wood tissues, together with the influence of drought, photosynthesis and transpiration thereon. These findings will be presented (Deckmyn *et al*. (in prep), section 6.4.2). Finally, gas-exchange (respiration, gross and net-photosynthesis and transpiration as well as the total carbon balance of the ecosystem will be integrated into an additional paper.

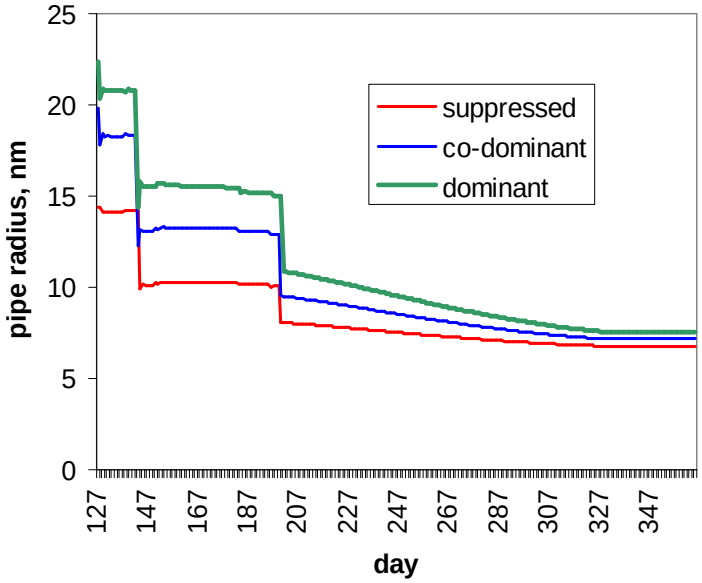

Figure 6.1: Simulated yearly evolution of pipe radius in suppressed, dominant and co-dominant Scots pine (*Pinus sylvestris).*

The model is able to simulate the normal pattern of pipe radius evolution: wide pipes are formed in early spring. Due to changes in allocation and photosynthesis, the pipe radius diminishes through the year. Latewood formation (radius <10 nm) commences around day 205 for suppressed and co-dominant trees, and little later for the dominant trees. This agrees well with the experimental data. The average pipe radius in early and latewood (18nm and 7.8nm) agree well with the measured values in this species (see Chapter 3). As was measured, dominant trees develop wood with wider pipe radius and therefore lower wood density.

The stand model includes the simulation of soil Carbon, and the effects of soil micro-organisms on the global C-cycle. This feature is important as it allows the simulation of global change effects on the total C-cycle in a realistic way, where soil processes depend on the activities, and growth and energy requirements of the competing soil-micro-organisms. This soil model was developed in the CASIROZ (EVK2-2002-00165) and EUROFACE (EVRI-CT-2002-40027) projects but integrated in the MEFYQUE stand model.

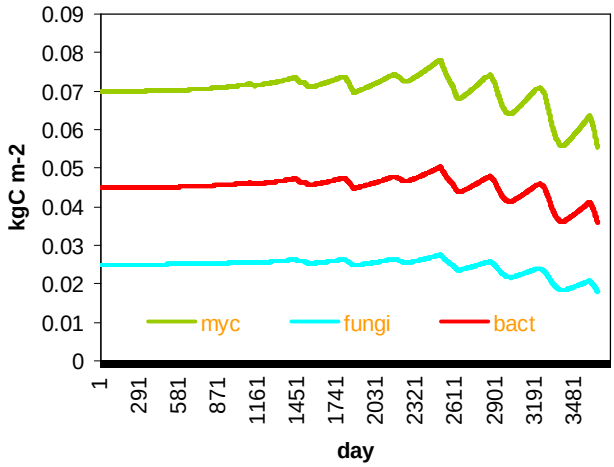

Figure 6.2: Simulated evolution of the C in soil micro-organisms (mycorrhisae, bacteria and fungi) over 10 years at the Scots pine site in Brasschaat

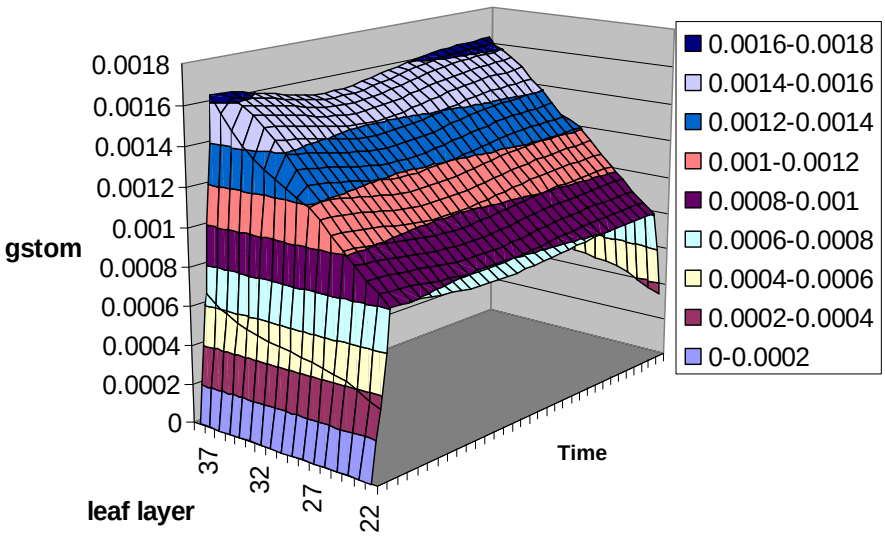

Figure 6.3: Simulated daily evolution in stomatal conductance of Scots pine trees in Brasschaat in full summer

6.2.2 Validation concerning effects of enhanced CO_2 on poplar, Viterbo tertiary site

Concerning the effects of global environmental change on the growth, yield and yield quality of trees, the simulations on the Italian poplar site of Viterbo are the furthest advanced. For these simulation data from within the MEFYQUE project (on the wood anatomical properties) as well as from past and ongoing projects at Viterbo (POPFACE, EUROFACE) have been integrated into the validation exercise, Liberloo *et al.* (in prep), section 6.4.3.

The stand model was run for *Populus alba* under normal and enhanced CO_2 for 3 years.
The results are used for validation against the experimental data. The data clearly show the model is able to simulate processes at different time scales realistically.

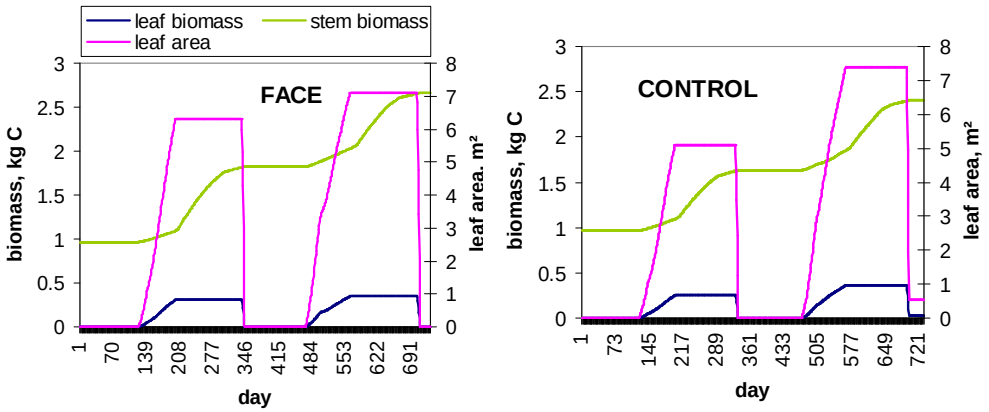

The simulated values are realistic as this species develops an LAI or leaf area (each tree has a space of 1 m²) of 7 in 2 years and biomass increases by 70% in the first years. Under FACE conditions biomass accumulation and leaf area are higher.

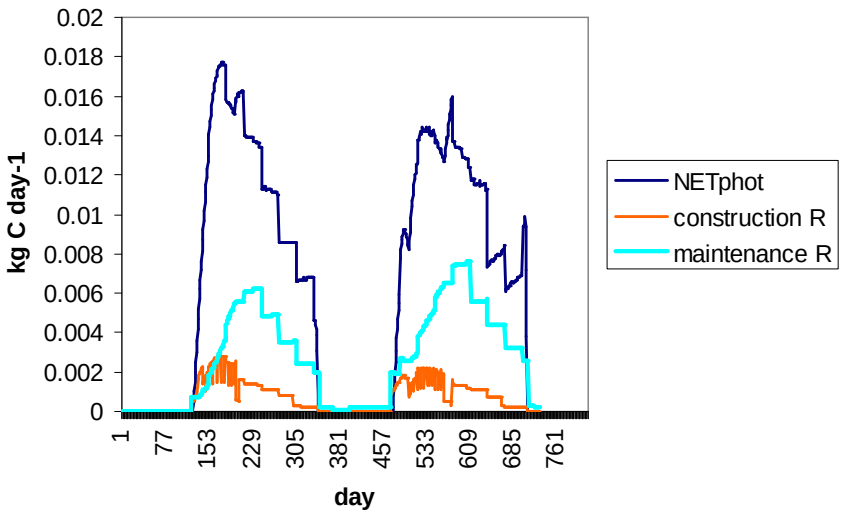

Figure 6.5. Simulated daily C fluxes (photosynthesis, construction and maintenance respiration) of *Populus alba* in 3 years

The fluctuations in simulated C fixation are a result of the changes in climate. As monthly values were used for the radiation and temperature this is reflected in the evolution of the C-budget. The model can be run y-using daily values if these are available. In summer, higher irradiation increases photosynthesis, but higher temperatures increase respiration. The total C budget of the plant equals the measured values at the Viterbo field sites.

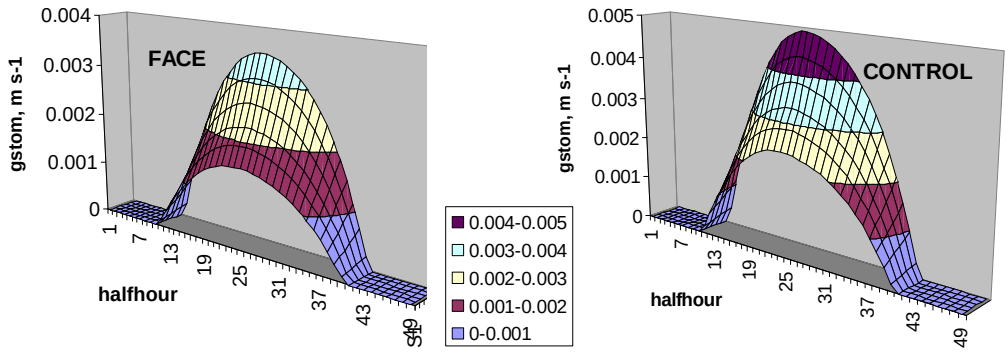

Figure 6.6: Simulated half-hourly stomatal conductance of sunlit leaves in different leaf layers of *Populus alba* in 3 years under CONTROL and FACE conditions.

This graph shows how detailed the output from the model can be. Such output is interesting because it allows the study of partial processes that are important to the total C budget. The stomatal conductance is especially important in relation to global change effects because as stomata close under enhanced CO_2, transpiration is reduced while photosynthesis remains at the same level. The model clearly is able to simulate this response to CO_2 realistically. As the trees were irrigated, there is no water stress and therefore no midday depression caused by stomatal closure in response to low soil water potential.

6.2.3 The Wood-chain Model – an example from the UK

In order to follow the sequence of models, a site was selected, and simulated, and followed through the various models. The model can simulate any number of trees, though experience has shown that because of the complexity of the model runs become prohibitively slow, and parameterisation of the different tree types difficult. To this extent we limit ourselves to the growth of three types of tree, with a number of individuals in each 'class'.

Physiological parameters remain constant through the different classes; Field measurements are variable at best, with little evidence in literature defining such complex parameterisation though different classes of trees.

The stand growth was simulated to an age of 60 years, using repeated meteorological data in order to generate sufficient data. An alternative would to have used summary data and the weather generator. For this simulation, ambient CO_2 concentration was held to 370ppm, which is easily changeable for the application of climate change scenarios.

6.2.3.1 Site

The site simulated, is a *Pinus sylvestris* site (51.25N, 1.25W). The site has soil with Gley-Podsol characteristics; the forest-growth model was parameterised for this species and site. The classes were only defined by a difference in initial conditions, which are summarised in Table 6.1:

Table 6.1: Summary of initial conditions for the Simulation of a Scots pine Stand, UK.

	Class 1	Class 2	Class 3
Age	20	20	20
Mean DBH (cm)	3.0	3.0	3.0
Mean Height (m)	6.2	6.0	6.5
Number in Class	1000	1000	1000
LAI	2.65	2.57	2.65
Crown Radius (m)	0.9	1.05	1.1
Crown Depth (m)	4.7	4.5	5.0
Soil	Gley-Podsol	Gley-Podsol	Gley-Podsol

6.2.3.2 Management

The growth model allows management to be specified as High, Low or Neutral. The trees are assigned to diameter classes (allows for more than 3 types), and thinnings are taken from the diameter classes to either match a fixed number of trees, or a basal area to be removed. The user is able to specify the proportion of thinning from each diameter class.

In this case, we followed a neutral thin, occurring every 5 years, governed by number of trees (Table 6.2), such that

Table 6.2: Management regime for the forest growth simulation.

Forest age	Standing crop	Trees thinned
0	3000	-
20	2700	300
25	2580	120
30	1690	890
35	1210	480
40	950	260
45	780	170
50	660	120
55	570	90
60	0	570

6.2.3.3 Forest growth Interface and example

As demonstrated in Fig 5.9, the sequence of models can be run from a single graphical interface window. The interface provides for quick visualisation of key outputs, with all the ability to save all outputs in a spreadsheet.

Figure 6.1 demonstrates example growth of a stand of *Pinus sylvestris.* Detailed descriptions of ring growth are kept for all trees (whether thinning or main-crop), in order to progress the simulation along the wood-chain.

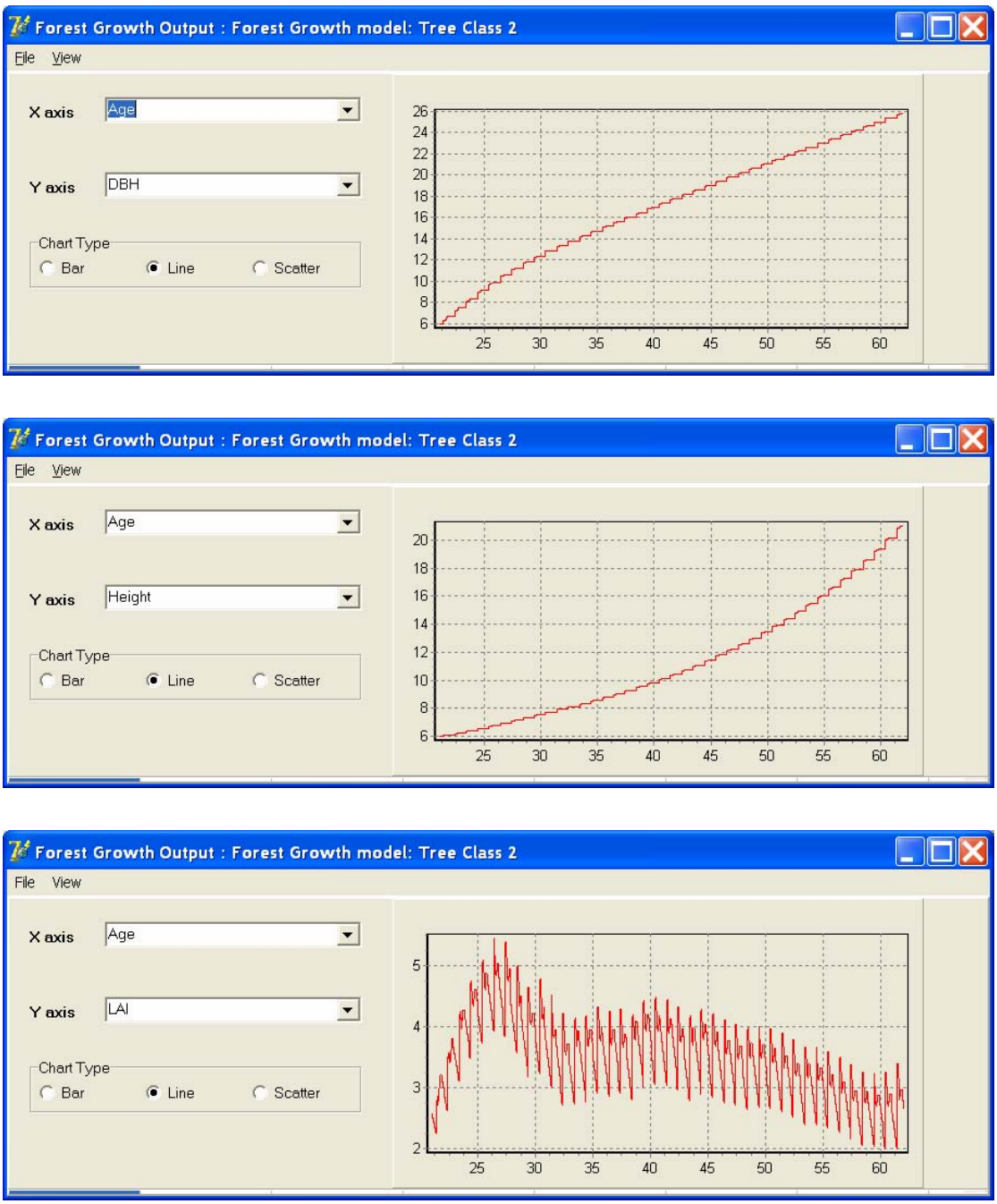

Figure 6.1: Example outputs from the forest growth model, and its graphical interface. (top – Diameter, (cm) middle; Height (m), and bottom (leaf area index).

6.3 Wood-Chain Outputs

The outputs from the growth model are progressed through the sequence of models, so each tree is assessed and cut into appropriate log-lengths. These log-lengths are the cut into utilisable battens. In turn the battens are graded. The final output is a table of number of battens by size and grade, together with losses from (I) the cutting of logs, (ii) the sawing of battens from logs, and (iii) any losses in converting the log (or batten) length into defined lengths – though in practice the logs will normally be cut to industry standard lengths.

Table 6.3: Summary output from the wood-chain sequence of models. The table contains the number of battens of each size and class produced by the woodchain modelling sequence.

Quality/size	Batten-Length			
C24	**1.8 m**	**2.4 m**	**3.0 m**	**4.8 m**
100x25 mm	429	3	21	509
100x47 mm	1759	3	43	773
150x47 mm	333	0	0	104
200x47 mm	0	0	0	0
C16				
100x25 mm	873	50	40	178
100x47 mm	1799	70	199	230
150x47 mm	1184	47	220	286
200x47 mm	525	0	151	105
Other				
100x25 mm	196	6	14	38
100x47 mm	454	19	53	57
150x47 mm	306	11	44	70
200x47 mm	141	0	39	30

The values include thinnings, which were taken at intervals during the growth of the stand. The total yield from sawn battens approximates to 236 m^3. Losses due to sawing the battens are approximately 275 m^3, which equates to a 46% conversion efficiency of sawn softwood. This matches well the average UK value, which is approximately 50% (Forestry Commission, 2004). The simulation above gave a loss of 4.1 m^3 due to off-cuts in battens, given that lengths were constrained to the 4 above. Losses from standing timber to Saw-log timber (ie, parts of the stem discarded for being too bent) amounted to 193 m^3

6.4 Abstracts of papers in preparation

As the models and their validation occur late in the project, papers concerning their use are still in draft form. Examples of such papers are given below.

6.4.1 Modelling wood tissue development as influenced by climate and tree dominance: a case study using the Mefyque model for a temperate pine forest.

G. Deckmyn, D. Ziche, D. Vansteenkiste, J. Curiel-Yuste,T. Randle, S. Evans

A plot scale forest model has been developed that dynamically simulates wood tissue development from physiological principles. The forest is described as consisting of dominant, sub-dominant and suppressed trees. In addition to total growth and yield, the model simulates the daily evolution in tracheid biomass and radius, parenchyma and branch development. From these data early and latewood biomass, wood tissue composition and density are calculated. Together with knots, derived from simulated branching, model outputs provide good approximations of wood quality. The model is validated using data from a temperate pine (*Pinus sylvestris* L.) forest where wood anatomical data (cell wall area, lumen area, density and ring widths) have been collected. Results indicate that dominance effects on wood development, present in the observational data, are adequately simulated in the model. Validated simulation experiments indicate that the Mefyque model is a useful tool for predicting environmental and management effects (as influencing tree competition) on wood quality.

6.4.2 Understanding density-profiles: results from the validation of a mechanistic wood formation model (MEFYQUE).

G. Deckmyn, D. Vansteenkiste, D.Ziche, R. Ceulemans

Understanding the daily variations in wood formation is of great importance to elucidate the anatomy of wood rings, and from this the variations in wood quality as influenced by stand, climate and species. Although understanding of wood development has increased over the past years, many issues remain unclear, such as the causes for daily variations in pipe radius, for the transition from early to latewood and the timing of carbon storage. Recent improvements in wood anatomical studies allow the measurement of density profiles through year rings.

To improve our understanding of the mechanisms underlying wood tissue development, and to test existing hypotheses concerning the developmental mechanisms, a mechanistic stand model has been developed (MEFYQUE) that includes detailed daily development of woody tissues. In this study the results from the model for 3 year-rings (1999 to 2001) of suppressed and dominant Scots pine (*Pinus sylvestris*) for a plantation in Belgium, were compared to X-ray studies on wood discs.

The results show an overall reasonable correlation between measured and simulated wood density. The differences between the dominant and the suppressed tree are modelled realistically. Concerning the daily variations in wood density however, more insight is required into the mechanistic interactions between wood development, C-availability, air and soil humidity and temperature.

6.4.3 Understanding the effects of enhanced CO_2 on poplar growth and ecosystem functioning: results from the plot scale model MEFYQUE validated with field data

M. Liberloo, G. Deckmyn, C. Calfapietri, B. Gielen, R. Ceulemans

Enhanced CO_2 is known to increase the productivity of many tree species. On the other hand, fast growing trees often produce lower quality wood. A new forest stand simulation model MEFYQUE (modelling forest yield and quality) was developed that includes simulation of wood tissue development in three pools (parenchyma, fibres and vessels), as well as vessel diameter and derived density variation along the stem cross-section. The model is fully mechanistic and includes the effects of T, CO_2 , fertilisation and drought on the wood formation. The model was validated with data from 2 growth years of a high-density plantation of three *Populus* genotypes under free-air CO_2 enrichment (FACE). The data used for the validation includes wood anatomical studies on cross-sections of harvested trees.

The results indicate that the model is able to simulate the total productivity, annual ring width, and ring composition adequately. Use of the model at a regional scale will be possible, giving an indication of possible effects of CO_2 on wood quality on a greater scale.

6.5 Conclusions

The model runs clearly indicate that the developed MEFYQUE plot scale model is able to simulate the total growth and yield as well as the micro-allocation and yield quality of forests under a range of environmental and management conditions adequately. The developed plot scale model therefore fully meets the requirements of the project deliverables (where a prototype model was expected as output). Concerning the simulation of wood quality, insight into the mechanisms of wood formation has increased considerably during the development of the model. Where the correlation between simulated and measured wood anatomy is not yet perfect, use of the model aids us in

asking pertinent questions about the timing of wood formation that should yield an even better insight in future.

The simulated results following the woodchain already clearly indicate the great importance of management and climate on the development of wood quality, and thereby confirm the experimental results. Furthermore, the results clearly show that climate, soil and management interact, so the overall effect is not simply the sum of the individual effects. Therefore, to understand and predict the effects of global change on forests, we need to take account of the management of the forests. The developed models will allow the future development of management scenario's better adapted to the changing environment and to the requirements of the forest industry.

Furthermore the MEFYQUE plot scale model is already being used within several other European projects and will be further improved, extended, and validated in the coming years. The current inclusion of an improved soil module as well as the inclusion of an ozone module will increase the applicability of the model to a wide range of research areas.

6.6 References

Deckmyn, G., Vansteenkiste, D., Ziche, D. and Ceulemans, R. (in prep). Understanding density-profiles: results from the validation of a mechanistic wood formation model (MEFYQUE).

Evans, S.P., Randle, T., Henshall, P. and Taylor, P. (2002). A coupled soil-forest-atmosphere dynamic model for predicting evapo-transpiration (ETp) demands at the plot and landscape scales in the UK. *Report to Scotland and Northern Ireland Forum For Environmental Research (SNIFFER)*

Forestry Commission (2004), British Timber statistics 2003: Statistics on British timber harvested and used by primary wood processing industries in the Great Britain. Economics and Statistics, Forestry Commission, Edinburgh, UK

Liberloo, M, Deckmyn, G., Calfapietri, C., Gielen,B. and Ceulemans, R. (in prep). Understanding the effects of enhanced CO_2 on poplar growth and ecosystem functioning: results from the plot scale model MEFYQUE validated with field data.

7 The MEFYQUE upscaling and integration approach using the large scale forest scenario model EFISCEN and a harvested wood products model

Main Contributors:
Marcus Lindner, Thies Eggers, Sergey Zudin and Jeannette Meyer

7.1 Intoduction

Within the national forestry sector carbon fluxes, the changes in carbon stocks of wood products are rather small and when the total carbon fluxes of a country are taken into account they seem to be negligible. Globally, Winjum et al. (1998) estimated a global carbon sink in wood products of approximately 0.1 Gt C, whereas the annual carbon emission from fossil fuel combustion account for 6.3 Gt C and e.g. from tropical deforestation for 1.6 Gt C. But still the accounting in wood products may have impacts on national and international forestry policies and therefore also climate change (Niles and Schwarze 2001).

Beside knowing the general magnitude of carbon fluxes for wood products (Hashimoto et al. 2002)(Nabuurs and Sikkema 2001), which can be estimated using different methods such as flow consumption approaches (Skog and Nicholson 2000), dynamic modelling (Karjalainen 1994) (Heath et al. 1996), or backwards calculations (Burschel et al. 1993; Gjesdal et al. 1996), it is also important to study the direct implications of climate change on the behaviour of forest growth, timber qualities and resulting consequences for the forest industries. Several studies aimed already at the possibilities to model timber quality (Houllier et al. 1995; Kellomäki et al. 1999) or direct linkage of growth modelling to generate virtual 3D sawlogs, which could be further processed with saw milling models (Mäkelä and Mäkinen 2003).

The overall objective of the MEFYQUE project was to increase understanding of the relationships between site conditions and growth, yield and timber quality for current and future scenarios of atmospheric change. The principle deliverable of the project was an integrated modelling system that could capture these effects and link them in a scenario modelling framework to support decision making in the forest sector. In this chapter we present the upscaling and integration component of MEFYQUE. We study potential impacts of climate change on growth and timber quality and how these affect the carbon balance in wood products. Finally we discuss possible implications for the forest industry.

7.2 Methods and materials

It was originally planned to apply the MEFYQUE modelling framework in this study (Figure 7.1). A process-based tree growth model linked with a sawmilling and stress-grading model would produce input for the large-scale forest resource model EFISCEN. Due to technical problems in the model integration the upscaling with the EFISCEN model could not be realised during the project life time. To demonstrate the conceptual integration approach, alternative scenarios were developed to reflect the expected input variations on tree growth, timber quality and timber allocation. A scenario study was conducted using data from the forestry-wood chains in Southern Finland based on the two main tree species Scots pine (*Pinus sylvestris* L.) and Norway spruce (*Picea abies* (L.) KARST.). The anticipated data flow from the forest growth model as well as the saw milling components (see Figure 7.1) were replaced by empirical and/or synthetic scenario data.

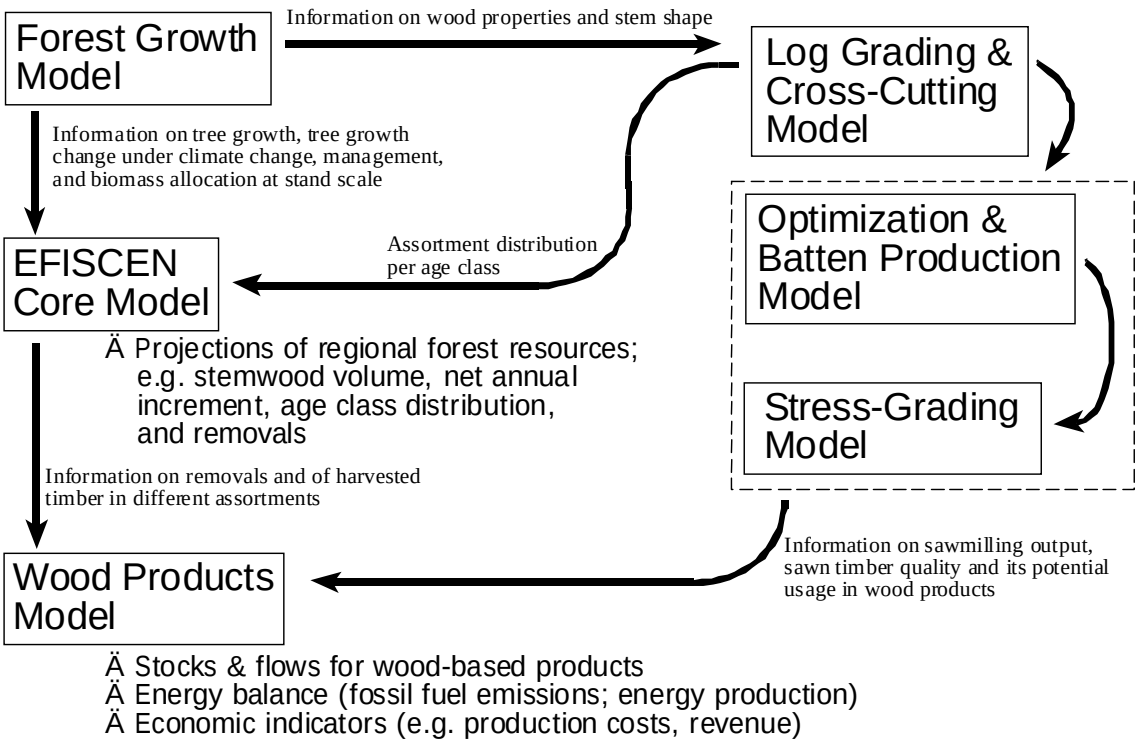

Figure 7.1: Initial modelling framework for the upscaling approach. Boxes represent stand-alone models or modelling components. The integrated stand-scale model consists of the forest growth model and the three sawmilling models (log grading & cross cutting, optimisation & batten production, and stress grading). The upscaling model has two components: the forest resource model EFISCEN and a wood products model coupled with it. The arrows indicate data flow from one modelling component to the other.

7.2.1 Applied models

7.2.1.1 Forest resource model

This study applied the European Information Scenario Model (EFISCEN). Based on a matrix model originating from Sweden (Sallnäs 1990), EFISCEN was further developed and applied for forest resource projections in Europe, including carbon dynamics in the forest soils (Karjalainen et al. 2003; Liski et al. 2001). Links to mechanistic growth models were established to incorporate climate change impacts into the forest resource projections. EFISCEN can be used to produce projections of the possible future development of forest resources on a European, national or regional scale (Karjalainen et al. 2002; Nabuurs et al. 2003; Nabuurs et al. 2001; Nabuurs et al. 2000; Päivinen et al. 1999)

The basic input data are derived from national forest inventories. They include forest area, growing stock and increment by age-class and forest type. The quality and resolution of the input data determine how many regions, tree species, owner and site classes can be distinguished in a particular country. European wide data are gathered in the EFISCEN European Forest Resource Database (EEFR) at the European Forest Institute (Schelhaas et al. 1999). A more detailed description of the EFISCEN model version used in this study can be found in Eggers et al. (2005).

For Southern Finland (Figure 7.2) the inventory data is from the National Forest Inventory conducted from 1986 to 1992 and gives the following initial state for the coniferous forests

Table 7.1: EEFR database information on Scots pine and Norway spruce in Southern Finland.

Region	Species	Area [ha x 1000]	Growing stock [m^3 x 1000]	Increment [m^3 ha^{-1} a^{-1}]
Southern Finland	Scots pine	5,573.0	550,753.8	3.9
Southern Finland	Norway spruce	3,500.6	591,834.0	6.0

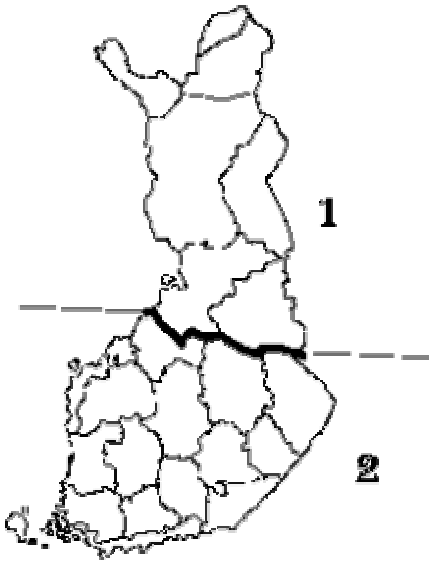

Figure 7.2: Regions of Finland for EFISCEN. Region 1 is Northern Finland and region 2 is Southern Finland, which was modelled in this study. The southern Finnish region includes inventory data from the following forestry centres: Ahvenanmaa, Rannikko, Lounais-Suomi, Häme-Uusimaa, Kaakkois-Suomi, Pirkanmaa, Etelä-Savo, Etelä-Pohjanmaa, Keski-Suomi, Pohjois-Savo, and Pohjois-Karjala

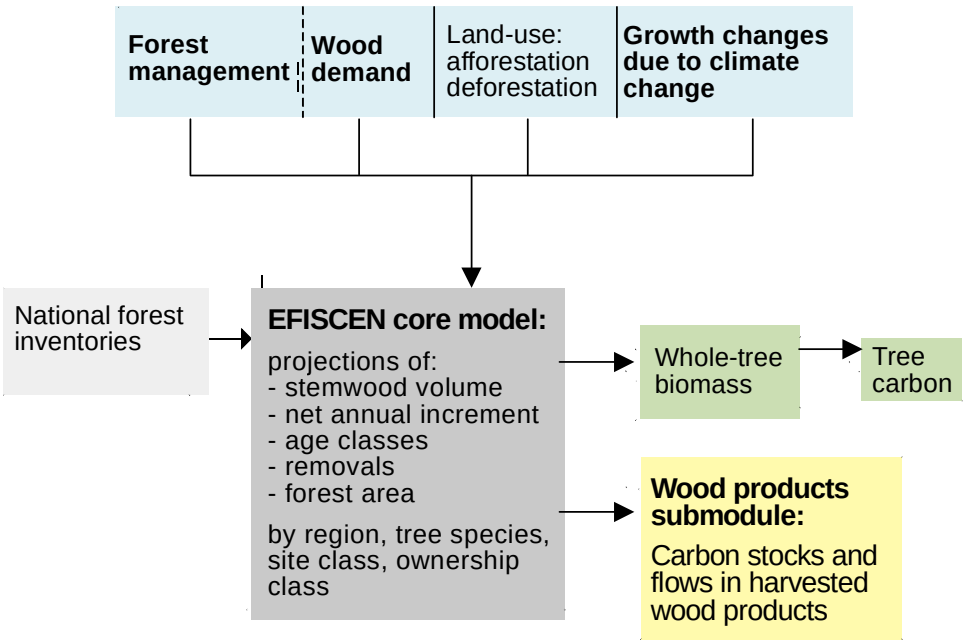

Figure 7.3: Outline of the EFISCEN model

7.2.1.2 Harvested wood products model

The harvested wood product model is a reprogrammed version of the model developed by Karjalainen (1994) and Eggers (2002). It was constructed as a cascade model to follow the flow of carbon in harvested timber from the forest through the forest industries, different usages and its way back to the atmosphere either by combustion or efflux from landfills. It operates on a yearly basis.

The allocation of timber to assortments and product groups was derived from statistics of the Finnish forest industries (Peltola 2004; TAPIO 1994). For life-span of wood products, recycling and allocation to usage categories, parameters from Karjalainen (1994) were adjusted using expert assessments.

In the applied version the carbon is followed in a multi-level system. The initial amount of carbon in harvested timber is divided into three categories: sawlogs, pulplogs, and residues. These raw materials are then further allocated into processing lines resulting in the following commodities: high quality sawn timber (C24 and similar), lower grade sawn timber (C16 and similar), wood chips, chemical pulp, mechanical pulp, other harvested wood products such as particle boards etc., and biofuels. In the next step these commodities are allocated to the usage categories (see Table 7.2), each with a certain life-span until the products are taken out of use and either disposed to a landfill, burnt to produce energy or recycled (reallocation to usage categories of Table 7.2). The life-span of wood products was calculated using an exponential decay function in the product module. A user can provide the lifespan (in this case either 1, 4, 16, or 50 years) and then the model calculates a corresponding exponential multiplier coefficient. If $Y(t)$ is a share of the initial amount of a product at time t, we use the exponential function for $Y(t)$, $Y(t)=exp(-at)$. From the equation $Y(t_0)=0.5$ (it means that at time t_0 we have half of initial stock - so named half-life) we got $a=ln2/t_0$.

A more detailed description of the mechanisms applied in the current version of the harvested wood product model can be found in Eggers *et al*. (2005).

Table 7.2:.Usage categories in the harvested wood products model.

Category	Description
Building materials (life-span of 50 years)	Products made of sawn timber, plywood / veneer, or particle board used for construction work in buildings, civil engineering and other long-life construction work; e.g. wooden houses or bridges.
Other building material (life-span of 16 years)	Products made of sawn timber, plywood / veneer, or particle board used for maintaining in houses or civil engineering. Includes also such commodities as fences, window frames, panels, wooden floors and doors.
Structural support materials (life-span of 1 year)	Products made of sawn timber, plywood / veneer, or particle board used for form works, scaffolds, and other wood-based products needed on building sites.
Furnishing (life-span of 16 years)	Products made of sawn timber, plywood / veneer, or particle board used for furnishing houses and offices or other private and public buildings.
Packing materials (life-span of 1 year)	Products made of sawn timber, plywood / veneer, particleboard, or paper- and paperboard-products used for packing other commodities; e.g. shipping boxes, wrapping, and boxing.
Long-life paper products (life-span of 4 years)	Products made of pulp used for longer periods such as books, maps, or posters.
Short-life paper products (life-span of 1 year)	Products made of pulp used for short periods such as newsprint and sanitary papers.

Table 7.3: Emissions from silvicultural treatments and site amelioration for carbon dioxide (CO_2), di-nitrogen oxide (N_2O), carbon monoxide (CO), methane (CH_4), nitro oxides (NO_x), non-methane volatile organic compounds (NMVOC) from (Karjalainen and Asikainen 1996).

	CO_2	N_2O	CO	CH_4	NO_x	NMVOC
Scarification [kg ha^{-1}]	81.3380	0.0020	0.6800	0.0059	0.9800	0.1400
Tending of seedling stands [kg ha^{-1}]	16.0360	0.0004	0.1280	0.0023	0.3190	0.0480
Ditch cleaning [kg km^{-1}]	40.3100	0.0010	0.3370	0.0029	0.4860	0.0690

Table 7.4: Emission from timber cutting and haulage [kg m^{-3}] from (Karjalainen and Asikainen 1996) for thinnings and final cuttings.

	CO_2	N_2O	CO	CH_4	NO_x	NMVOC
Thinning						
Manual cutting	0.5320	0.0000	0.0042	0.0001	0.0106	0.0016
Mechanized cutting	3.8960	0.0001	0.0326	0.0003	0.0469	0.0067
Haulage tractor	4.6590	0.0001	0.0389	0.0003	0.0561	0.0080
Haulage forwarder	1.9180	0.0000	0.0160	0.0001	0.0231	0.0033
Final cutting						
Manual cutting	0.3330	0.0000	0.0027	0.0000	0.0066	0.0010
Mechanized cutting	1.8570	0.0000	0.0155	0.0001	0.0224	0.0032
Haulage tractor	3.1060	0.0001	0.0260	0.0002	0.0374	0.0053
Haulage forwarder	1.4230	0.0000	0.0119	0.0001	0.0171	0.0024
Haulage other	2.6620	0.0001	0.0222	0.0002	0.0321	0.0046

The timber cutting and haulage operations were distributed to the different options with the follows:

- Thinning: Manual cutting 40%, mechanized cutting 60%; haulage by tractor 40%, haulage by forwarder 60%
- Final cutting: Manual cutting 10%, mechanized cutting 90%; haulage by tractor 15%, haulage by forwarder 75%, haulage by other means 10%.

Emissions from fossil fuel usage in the forest industries were taken from (Liski et al. 2001). They refer to studies in energy consumption and raw material use of the forest industries in Finland in 1995 (Carlson and Heikkinen 1998; Lehtilä 1995).

Table 7.5: Emissions of fossil carbon in production lines [Mg fossil carbon / Mg carbon in raw material] according to (Lindner et al. 2000).

Production line	Fossil carbon emissions
Sawmill	0.032
Plywood mill	0.069
Mechanical pulp and paper mill	0.490
Chemical pulp and paper mill	0.130

7.2.2 Scenario runs

To study the various impact factors on tree growth and changing timber properties a range of scenarios has been set up. The simulation period was 1990 to 2050. In total five climate scenarios were investigated:

- Current climate,
- HadCM2 a1fi,
- HadCM2 a2,
- HadCM2 b1, and
- PCM a2,

For each of the climate scenarios, wood demand projections consistent with the underlying economic assumptions of the climate scenarios were used.

To study the potential impacts of changing timber properties, five scenarios in changing log assortment (LAT= log assortment tables):

- LATBase,
- LAT+10,
- LAT-05,
- LAT-10,
- LAT-20 and

one to five efficiency scenarios for the sawmilling industries:

- SLBase,
- SL+10,
- SL+05,
- SL-05, and
- SL-10

were set up and run for both tree species (Scots pine and Norway spruce).
The base line climate scenario (i.e. current climate) was applied to all available combinations (LAT and SL) whereas the climate change scenarios (i.e. HadCM2 a1fi, a2, b1 and PCM a2) were only analysed with the different LAT scenarios under the SLBase standard parameters.

7.2.2.1 Descriptions of climate change scenarios

1. Current climate

   The forest growth in the current climate scenario is based on the original forest inventory data. So the net annual increment per species and site class is according to the measurements in the forests at the time of the forest inventory.

2. Climate change (HadCM3 and PCM)

   It is expected that forest growth will change with a changing climate. Already now an increasing growth trend is visible throughout Europe. With the help of a plant physiological growth model the potential impact of climate change on tree growth in Finland was estimated.

   Scenarios of monthly temperature, precipitation and cloudiness changes for the years 2001-2050 were taken from the climate data sets provided by the ATEAM project (Mitchell et al. 2004). These data are comprised of results from two different global circulation models (HadCM3 and PCM) under three different emission scenarios from the Special Report on Emissions Scenarios of the Intergovernmental Panel on Climate Change (IPCC SRES scenarios; (Nakicenovic and Swart 2000)). In this study we used the HadCM3 model with three emission scenarios (a1fi, a2, b1), which are described in
   . In addition, the PCM climate model was applied with the a2 emission scenario in order to study the effect of different climate models on the projected climate change.

The influence of the different climate scenarios on forest growth in EFISCEN was simulated using output of the process-based Lund-Potsdam-Jena global vegetation model (LPJ). Change in NPP projected by LPJ was used to scale inventory-based forest growth in EFISCEN. The LPJ model (Sitch et al. 2003; Smith et al. 2001) is one of a family of models derived from the BIOME terrestrial biosphere model (Prentice et al. 1992). It simulates distribution, growth and dynamics of 10 plant functional types (PFTs) with different photosynthetic, phenological, and physiognomic attributes, and PFT-specific parameters that govern plant competition for light and water (Sitch et al. 2003).

Table 7.6: Overview of the three emission scenarios applied in this study (Image Team 2001; Nakicenovic and Swart 2000).

Emission scenario	Keywords	Main assumptions
a1fi	Global economic	Fossil-fuel intensive; very rapid economic growth; fast increase in productivity and GDP; high consumption, very little environmental concern
a2	Regional economic	Focus on regional identity; emphasis on self-reliance in terms of resources; high energy and carbon intensity; high population growth; little environmental concern
b1	Global environmental	High economic growth; large preference for clean fuels; fast increase in productivity; high level of environmental consciousness; emphasis on global solutions to environmental and social sustainability

7.2.2.2 Wood demand scenarios

The current (2000) wood demand was scaled with demand projections from Image 2.2 (Image Team 2001) for each of the three emission scenarios. Figure 7.4 presents the development of the wood demand in EFISCEN for Finland. In the a1 scenario, wood demand increases strongly. Wood demand also increases in the a2 scenario, but to a smaller extent and more steadily than in a1. In b1, wood demand decreases.

Table 7.7: Deviation [%] of actual removals from the demand given in the EFISCEN model for Finland (whole country; incl. all tree species).

Scenario	1991-1995	1996-2000	2001-2005	2006-2010	2011-2015	2016-2020	2021-2025	2026-2030	2031-2035	2036-2040	2041-2045	2046-2050
Current climate	98.6	98.2	97.9	97.7	97.5	97.3	97.1	96.8	96.5	96.6	97.1	97.6
Had-a1	98.6	98.2	97.9	97.5	97.1	96.7	96.1	95.4	94.6	94.5	95.2	95.9
Had-a2	98.6	98.2	97.9	97.7	97.5	97.4	97.3	97.3	97.2	97.5	98.1	98.6
Had-b1	98.6	98.2	97.9	97.6	97.2	96.9	96.5	96.0	95.4	95.3	95.9	96.6
PCM-a2	98.6	98.2	97.9	97.6	97.2	96.8	96.5	95.9	95.3	95.2	95.8	96.5

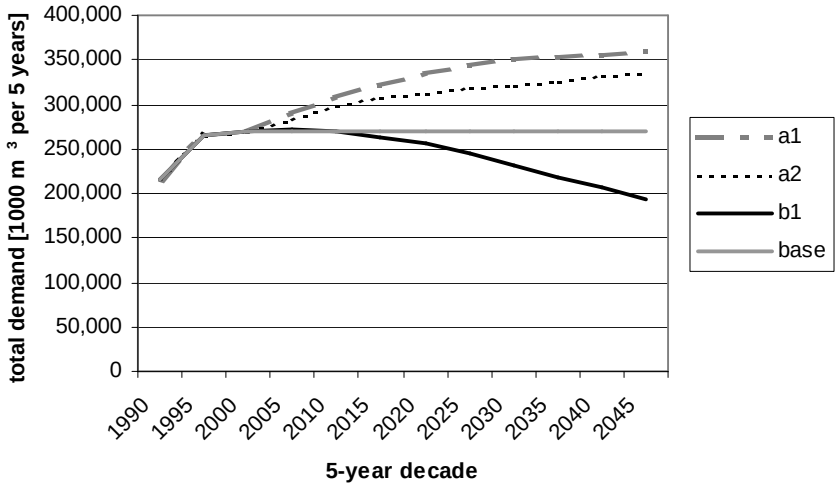

Figure 7.4: Total timber demand [1000 m^3 per 5 years] for whole Finland for the three different SRES scenarios and the base scenario (i.e. stable current demand). Each 5-year represents the period following the next year from the time mentioned (i.e. 1990 = 1991 to 1995).

7.2.2.3 Changes in timber quality

To represent potential changes in timber quality, five log assortment scenarios were developed. The base scenario was derived from the statistical information on the proportion of sawlogs and pulplogs in the total felling amount. This information was available for the Finnish conditions (TAPIO 1994). For the three main tree species in Finland – Scots pine, Norway spruce, birch – tables show the assortment proportions over stand height and mean diameter at breast height (DBH). With the help of growth and yield tables (Koivisto 1959) age-depended relationships have been estimated. For Scots pine the growth and yield tables for a fertile Myrtillus site type (MT) and Norway spruce for a fertile Oxalis-Myrtillus site type (OMT) were applied; both for managed stands.

Functions were fitted to this data to provide a continuous series instead of the 5-yearly time steps that resulted from the growth and yield table data. It was not possible to fit a curve to the amount of pulplogs coming from fellings, due to its unusual form. Thus only the data of sawlogs and the amount of residues, which was calculated as the remaining percentage to 100 when the sawlog and pulplog proportions were summed up, was fitted with the help of the curve wizard in SigmaPlot 9.01 (Systat 2004). It seemed obvious from the data that only after a certain stand age the assortment of sawlogs will be available as for this a minimum DBH and height should be reached. Thus it was assumed that for Norway spruce no sawlogs are assorted before stand age 50 and for Scots pine not before stand age 45.

For the sawlog percentages a 3-parametric sigmoidal equation was fitted to the statistical data. The equation is shown below.

$$f = \frac{a}{1 + e^{-\left(\frac{x - x0}{b}\right)}}$$

Table 7.8: Parameters used for Scots pine and Norway spruce to estimate the share of sawlogs in fellings over stand age.

Parameters	Scots pine (age > 45)	Norway spruce (age > 50)
a	89.1252	87.5150
b	10.2619	8.7369
x_0	42.9526	49.8722

The residues were fitted to a 3-parametric single equation as shown below without any age-limitation.

$$f = y0 + ae^{-bx}$$

Table 7.9: Parameters used for Scots pine and Norway spruce to estimate the share of residues in fellings over stand age.

Parameters	Scots pine (age > 45)	Norway spruce (age > 50)
A	0.4067	0.5675
B	99.9166	98.9929
y_0	0.0734	0.0585

The original data from the statistics as well as the fitted and calculated data are shown in Figure 7.5 and Figure 7.6.

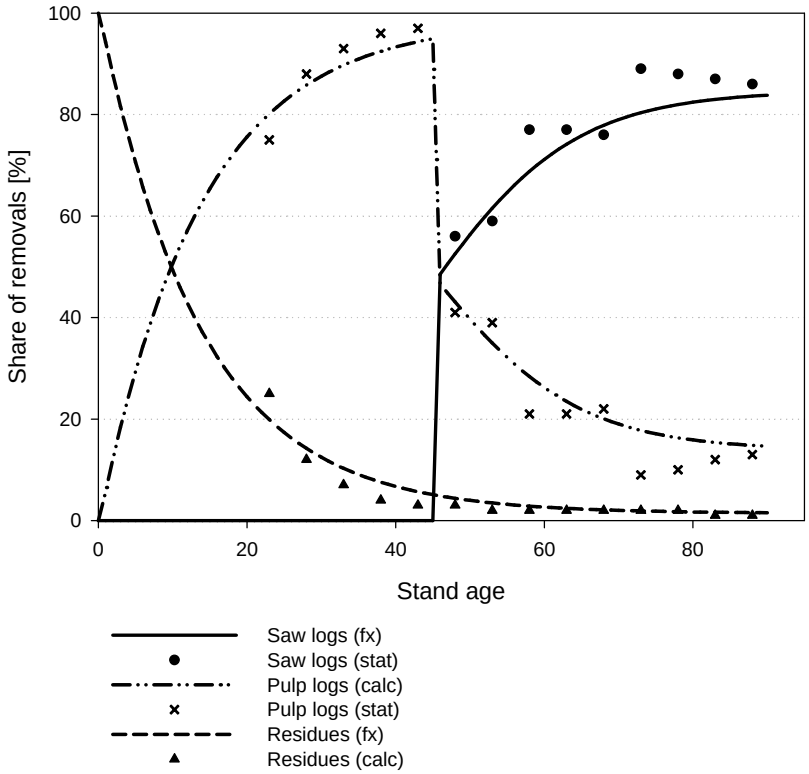

Figure 7.5: Percentages (LATBase scenario) of assortments (sawlogs, pulplogs and residues) in removals for Scots pine on a MT site class. The curves are fitted to the point data derived from statistics. Explanations to the abbreviations: 'fx' indicates a fitted function, 'stat' means statistical data and 'calc' means that the values are calculated. See text for detailed descriptions.

From these two base settings four more scenarios were developed. Altered tree growth under a changing climate might result also in changing log qualities. This could theoretically be a change towards better quality attributes for the sawmilling industries (straight trunks with less branches and high diameters) or towards lower quality trunks (with a lean and possibly also more branches). The latter would be used mainly in the pulp industries or for particle boards and only a smaller proportion would be suitable to produce high quality sawn timber. So the expected proportion of sawlogs in the total felling amount was increased or decreased by +10%, -5%, -10%, and –20% for both Scots pine and Norway spruce, respectively. More than 10% increase in log outputs were not possible to model, because the base scenario already uses a rather height proportion of sawlogs from the total amount of fellings.

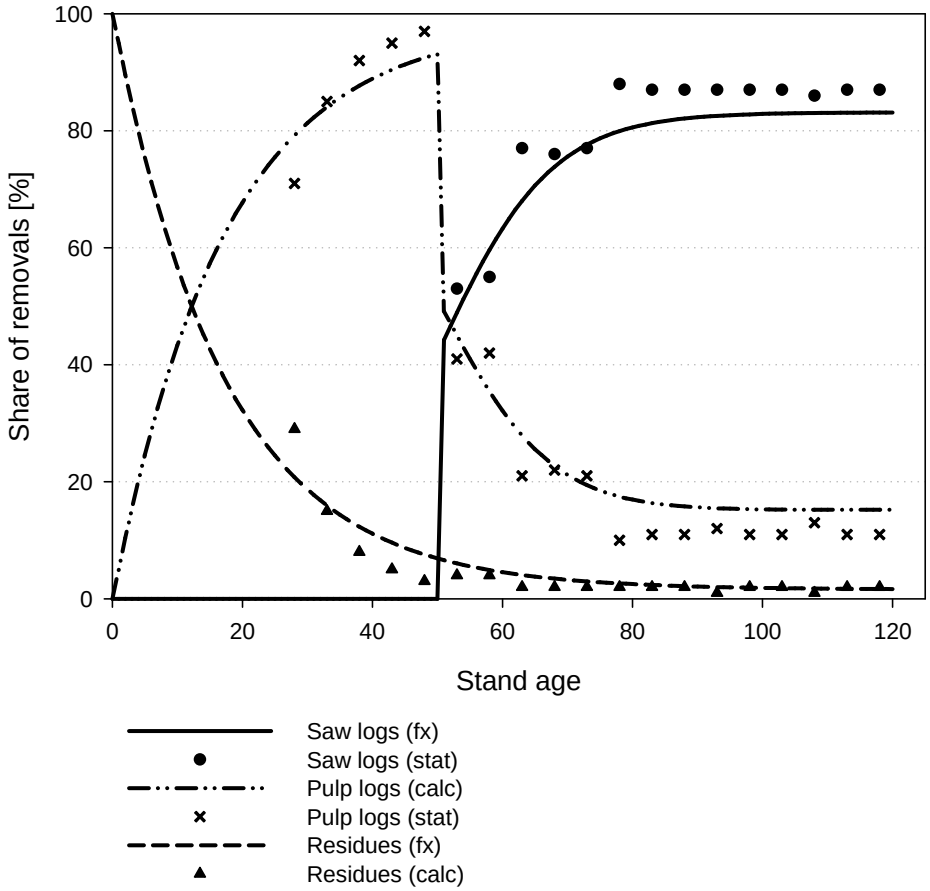

Figure 7.6: Percentages (LATBase scenario) of assortments (sawlogs, pulplogs and residues) in removals for Norway spruce on a OMT site class. The curves are fitted to the point data derived from statistics. Explanations to the abbreviations: 'fx' indicates a fitted function, 'stat' means statistical data and 'calc' means that the values are calculated. See text for detailed descriptions

Table 7.10: Summary table for LAT scenarios for timber quality assorting.

Scenario acronym	Description
LATBase	Base scenario for timber assorting; uses the shares of sawlogs and pulplogs from the available statistics (TAPIO 1994)
LAT+10%	Increased sawlog proportion of +10% compared to the base scenario resulting in a decreased pulplog proportion by 10%.
LAT-05%	Decreased sawlog proportion of –5%; resulting in an increased pulplog proportion by 5%.
LAT-10%	Decreased sawlog proportion of –10%; resulting in an increased pulplog proportion by 10%.
LAT-20%	Decreased sawlog proportion of –20%; resulting in an increased pulplog proportion by 20%.

7.2.2.4 Changes in sawmilling efficiency

Another factor influencing the stocks and fluxes of carbon in wood-based products is the efficiency in sawmills; i.e. how much timber ends up in the sawn timber, how much can be used as a secondary product (e.g. chips for pulping) and how much is burnt. The expected

changes in tree growth and timber properties might not only have an effect on the assorting (LAT scenarios) but also on the sawmilling products. Thus another group of scenarios (SL …) was set up to analyse the potential impact of this. Starting from the base industry parameters (Eggers 2002; Karjalainen 1994) a range of ± 5% and ± 10% in processing efficiency was set up for each of the five LAT scenarios in the current climate scenario. Table 7.11 shows the efficiency parameters for the sawmilling industries. The parameters for the other industry lines (plywood, particle board, mechanical pulp, and chemical pulp) were not altered.

Table 7.11: Summary of the use of sawlogs in the production processes to produce sawn timber for the sawmilling scenarios (SLBase parameters from Karjalainen (1994)).

Scenario	Product	Processable product (chips)	Non-processable residue (bark & sawdust)
SLBase	0.435	0.435	0.130
SL+10	0.535	0.335	0.130
SL+05	0.485	0.385	0.130
SL-05	0.385	0.485	0.130
SL-10	0.335	0.535	0.130

Figure 7.7 shows the total number of scenarios that were run for this study. For simplicity and to avoid repetition, not all of these scenarios will be analysed and presented in the results. The combined effects of climate change scenarios with SL or LAT-scenarios are not shown. The presentation focuses on the assessment of scenarios with one changing factor against the baseline of the other two factors. Both, changes in log assortments and saw milling efficiency occur in the harvested wood products model and have no impact on the amount of removals from EFISCEN. Therefore, the relative change to the baseline of the SL and LAT scenarios can be easily combined with other climate scenarios. Similarly, the combined impact of varying both SL and LAT scenarios can be directly derived from the presented tables.

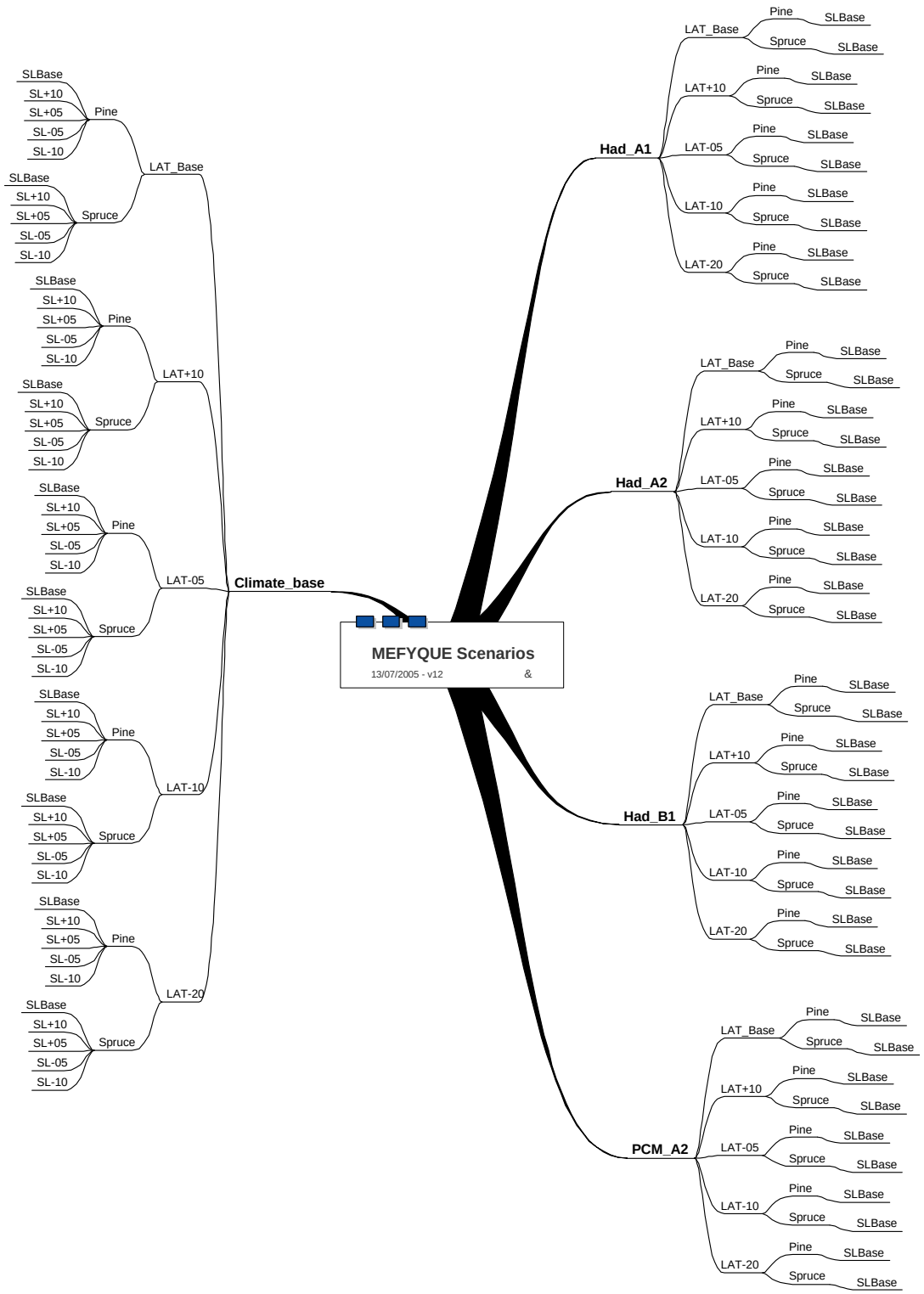

Figure 7.7: Outline of the scenarios used in this study.

7.3 Results and scenario analysis

7.3.1 Fossil fuel emissions from forest management, timber harvest and processing

7.3.1.1 Emissions from silvicultural and site amelioration work for southern Finland

Emissions from scarification to facilitate natural regeneration and seeding / planting, tending of seedling stands, and ditch cleaning have been estimated based on some statistics from 2004. The figures could not be calculated separately by species.

Table 7.12: Emissions [Mg a^{-1}] from silvicultural work and site amelioration in southern Finland; based on 2004 figures.

	CO_2	N_2O	CO	CH_4	NO_x	NMVOC
Scarification	2326.27	0.06	19.45	0.17	28.03	4.01
Tending of seedling stands	1515.40	0.04	12.10	0.22	30.15	4.54
Ditch cleaning	423.26	0.01	3.54	0.03	5.10	0.73

Converting emissions of CO_2, CO, and CH_4 to pure carbon emissions results in 0.64 Gg C a^{-1} from scarification, 0.42 Gg C a^{-1} from tending of seedling stands, and 0.12 Gg C a^{-1} from ditch cleaning activities. This is a total of 1.18 Gg fossil carbon emissions per year. This estimate does not include the emissions related to construction and maintenance of forest roads, and also some other small emissions from forest operations were neglected (cf. Berg and Karjalainen 2003 for relative magnitude of these emissions). Therefore we applied a slightly higher value of 1.5 Gg a^{-1} fossil carbon emissions to both the Scots pine and Norway spruce chains.

7.3.1.2 Fossil carbon emission from harvest and hauling operations

Fossil carbon emission from harvesting and hauling depend on the amount of removals from thinnings and final fellings. Therefore they vary between climate scenarios and they also reflect the different trends in removals of spruce and pine after 2040 (Table 7.13, Table 7.14).

Table 7.13:. Fossil carbon emission [Gg C a^{-1}] from harvest and hauling operations for Scots pine in southern Finland, based on removals projected with EFISCEN.

Scenario	2000	2010	2020	2030	2040	2050
Current climate	21.03	21.60	21.56	20.86	20.10	21.56
Had-a1	21.03	23.14	25.68	26.31	25.68	28.91
Had-a2	21.03	22.68	24.48	24.40	23.95	26.88
Had-b1	21.03	21.68	20.99	18.84	16.25	15.31
PCM-a2	21.03	22.68	24.48	24.39	23.93	26.90

7.3.1.3 Fossil carbon emission from forest industries

Even though the forest industries can produce a large proportion of their needed energy from non-processable residues such as sawdust and bark, they do also use fossil fuels as energy carrier. The related emissions are small in energy-self-sufficient production lines such as chemical pulping or plywood production. Other processes such as mechanical pulping are very energy consuming and as most of Norway spruce pulpwood is used in mechanical pulping the fossil carbon emissions are more than twice as large for Norway spruce than for Scots pine.

Table 7.14:. Fossil carbon emission [Gg C a^{-1}] from harvest and hauling operations for Norway spruce in southern Finland, based on removals projected with EFISCEN.

Scenario	2000	2010	2020	2030	2040	2050
Current climate	21.65	23.29	23.69	23.30	22.39	21.23
Had-a1	21.65	24.94	28.31	29.59	28.32	26.23
Had-a2	21.65	24.45	26.96	27.38	26.54	25.27
Had-b1	21.65	23.37	23.06	21.02	18.12	15.43

7.3.1.3.1 Impact of changing growth and harvesting levels

The emission lines follow the annual amount of removals. Compared to the current climate scenario, all but the B1 scenario show increasing emissions because more forest resources are utilised.

Table 7.15: Fossil carbon emission [Gg C a^{-1}] from forest industry processes for Scots pine in southern Finland, based on processed raw materials modelled with EFISCEN and the harvested wood product model, and converted according to Liski et al. (2001) (LATBase, SLBase).

Scenario	2000	2010	2020	2030	2040	2050
Current climate	237.75	248.83	251.62	246.62	242.01	253.15
Had-a1	237.75	266.55	299.64	311.73	310.95	338.91
Had-a2	237.75	261.28	285.67	289.02	289.47	315.35
Had-b1	237.75	249.75	245.10	222.90	195.86	180.64
PCM-a2	237.75	261.28	285.63	288.82	289.15	315.43

Table 7.16: Fossil carbon emission [Gg C a^{-1}] from forest industry processes for Norway spruce in southern Finland, based on processed raw materials modelled with EFISCEN and the harvested wood product model, and converted according to Liski et al. (Liski et al. 2001) (LATBase, SLBase).

Scenario	2000	2010	2020	2030	2040	2050
Current climate	536.31	565.78	566.42	553.54	537.93	521.54
Had-a1	536.31	605.96	676.31	703.11	682.19	649.87
Had-a2	536.31	593.98	644.27	650.57	638.60	623.89
Had-b1	536.31	567.78	551.41	499.49	435.20	378.55
PCM-a2	536.31	594.06	644.36	650.14	637.48	621.76

7.3.1.3.2 Impact of changing log assorting

In case of a changing log assortment due to climate change the fossil carbon emissions from the forest industries will also change. As most of the wood is allocated to the pulp industries, they form the most important factor here. Compared to the business-as-usual (LATBase) scenario, only the scenario with an increasing share of sawlogs in the total removals (LAT+10) will lead to a decrease of fossil carbon emissions. All other scenarios show an increasing trend of carbon emissions. Scots pine and Norway spruce show similar trends.

Table 7.17: Fossil carbon emission [Gg C a^{-1}] from forest industry processes for Scots pine in southern Finland under the LAT-scenario group (current climate; SLBase).

Scenario	2000	2010	2020	2030	2040	2050
LATBase	237.75	248.83	251.62	246.62	242.01	253.15
LAT+10	223.97	234.75	237.33	232.73	229.05	238.99
LAT-05	244.64	255.88	258.77	253.56	248.49	260.24
LAT-10	251.53	262.92	265.91	260.50	254.97	267.32
LAT-20	265.30	277.00	280.21	274.39	267.94	281.48

Table 7.18: Fossil carbon emission [Gg C a^{-1}] from forest industry processes for Norway spruce in southern Finland under the LAT-scenario group (current climate; SLBase).

Scenario	2000	2010	2020	2030	2040	2050
LATBase	536.31	565.78	566.42	553.54	537.93	521.54
LAT+10	528.81	557.65	558.13	545.65	530.66	515.04
LAT-05	540.82	570.66	571.40	558.29	542.29	525.44
LAT-10	543.81	573.90	574.71	561.44	545.19	528.04
LAT-20	551.31	582.03	583.00	569.33	552.46	534.54

7.3.1.3.3 Impact of changing sawmill efficiency

A similar trend as for the changing log assortments is seen in the sawmilling scenarios (SL …). With increasing efficiency of the sawmilling industry, more lumber ends up in the process product sawn timber, and the fossil carbon emissions decrease compared to the base line scenario. With decreasing efficiency, which might occur due to reduced log qualities (e.g. knottiness, lean), the fossil carbon emissions from the forest industries increase, because more raw material is used in the pulping industries. Scots pine and Norway spruce show similar trends.

Table 7.19: Fossil carbon emission [Gg C a^{-1}] from forest industry processes for Scots pine in southern Finland under the SL-scenario group (current climate; LATBase).

Scenario	2000	2010	2020	2030	2040	2050
SLBase	237.75	248.83	251.62	246.62	242.01	253.15
SL+10	221.57	232.33	234.99	230.43	226.77	236.60
SL+05	229.66	240.58	243.31	238.52	234.39	244.88
SL-05	245.84	257.09	259.94	254.71	249.64	261.43
SL-10	253.93	265.34	268.25	262.81	257.26	269.71

Table 7.20: Fossil carbon emission [Gg C a^{-1}] from forest industry processes for Norway spruce in southern Finland under the SL-scenario group (current climate; LATBase).

Scenario	2000	2010	2020	2030	2040	2050
SLBase	536.31	565.78	566.42	553.54	537.93	521.54
SL+10	467.04	490.47	489.27	479.55	469.22	459.50
SL+05	501.68	528.12	527.84	516.55	503.57	490.52
SL-05	570.95	603.43	604.99	590.54	572.28	552.55
SL-10	605.58	641.08	643.57	627.54	606.64	583.57

7.3.2 Changes in carbon pools and fluxes of harvested wood products

The absolute figures for both carbon fluxes and stocks indicate an increasing trend over time. The initial stocks and fluxes were set to zero as the precise numbers were not known. Therefore the results show only the impact of the changes in wood allocation to the forest industry lines in the modelled scenarios. The already existing stock of products and the associated fluxes in e.g. recycling, burning, and burning of wood-based products was neglected in our study.

The carbon fluxes were grouped from the single stock-to-stock fluxes into six broader categories. These categories comprise raw materials, recycling, products to landfill, products burning, process burning, and landfill emissions.

7.3.2.1 Impacts of climate change and socio-economic development

Annual removals of Scots pine timber have been increasing strongly since 1990. Under the investigated climate and demand scenarios, the removals will more or less stabilize in the

base scenario, but they continue to increase in all a- scenarios during 2000-2020 and from 2040 onwards. In the contrary, the b1-scenario projects declining removals after 2020
(
Figure **7.8**). According to the EFISCEN projections, the availability of Norway spruce will be limited towards the mid 21st century. The total fellings for southern Finland reached 94.6 % to 99.6 % of the requested volume: Figure 7.9 shows decreasing fellings (i.e. decreasing availability) for Norway spruce even though felling request (demand; see Figure 7.4) is kept constant for the base scenario or increasing in the a1 and a2 scenarios. The second phase of increasing removals for Scots pine coincides with the decreasing trend of Norway spruce after 2040. The shortage of spruce should be kept in mind when interpreting the following results.

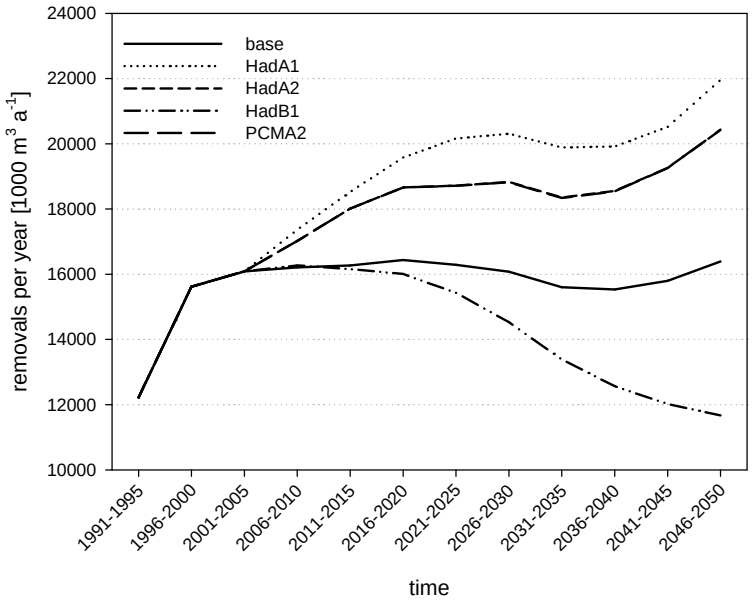

Figure 7.8: Annual removals [1000 m^3 a^{-1}] for Scots pine in southern Finland under the different climate scenarios. The removals for both a2 scenarios (Had & PCM) are more or less identical and show only a few percent difference, which cannot be seen in the figure

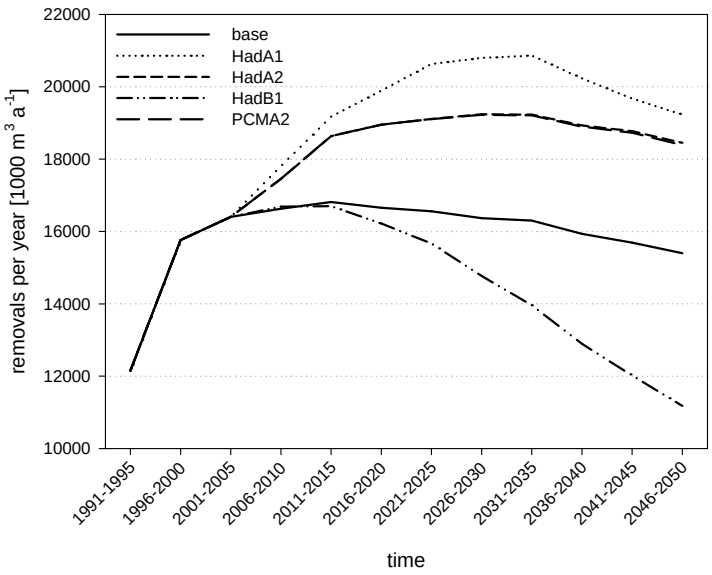

Figure 7.9: Annual removals [1000 m^3 a^{-1}] for Norway spruce in southern Finland under the different climate scenarios. The removals for both a2 scenarios (Had & PCM) are more or less identical and show only a few percent difference, which cannot be seen in the figure

7.3.2.1.1 Carbon fluxes

Different components of the carbon balance have been analysed:

1) raw materials: carbon flux from harvested wood into raw materials in the forest industry (e.g. sawn timber, pulp)
2) process burning: carbon release from burning wood residues (e.g. black liquor, sawdust)
3) recycling: carbon flux from old forest products into recycled products (e.g. paper recycling)
4) product burning: carbon release from burning disposed wood products (e.g. demolition wood)
5) landfill emission: carbon release from landfills
6) products to landfill: carbon flux from wood products at end-of-use to landfills

Flux 1) represents the carbon sink in the wood products, whereas fluxes 2), 4), and 5) are carbon sources from the forest-wood chain (although they might substitute fossil fuels; see Discussion). Fluxes 3) and 6) are carbon neutral regarding the carbon stored in wood products. The overall sink or source in wood products can thus be calculated as
Flux 1 – (Flux 2+4+5) – Emissions (Forest Industry + Forest Management Operations).

Compared to the base scenario, all 3 scenarios from the a-group show increasing carbon fluxes whereas the b-scenario shows a decreasing trend both for Scots pine and Norway spruce. Table 7.21 and Table 7.22 show the absolute figures for the base scenario as well as the changes in the other scenarios as percentages relative to the base scenario.

Table 7.21: Carbon fluxes [Gg C a^{-1}] for Scots pine in the base scenario and changes for the other climate scenarios compared to the base scenario [%].

	2000	2010				2020				2030				2040				2050			
	Base	Base	Had-a1	Had-a2	Had-b1	Base	Had-a1	Had-a2	Had-b1	Base	Had-a1	Had-a2	Had-b1	Base	Had-a1	Had-a2	Had-b1	Base	Had-a1	Had-a2	Had-b1
raw materials	2380.1	2452.0	7.1	5.0	0.4	2473.8	19.0	13.5	-2.6	2414.5	26.0	16.9	-9.7	2310.7	27.5	19.0	-19.1	2472.7	33.6	24.4	-28.9
process burning	1049.3	1104.8	7.1	5.0	0.4	1131.5	19.3	13.7	-2.6	1112.1	26.8	17.5	-9.6	1092.8	29.4	20.2	-19.2	1122.2	34.7	25.1	-28.7
Recycling	520.7	675.3	4.4	3.1	0.2	735.5	14.6	10.5	-1.6	757.9	22.0	14.4	-6.6	759.6	25.1	16.9	-14.2	790.6	28.9	20.7	-21.9
product burning	657.9	837.8	4.7	3.3	0.2	919.8	14.7	10.5	-1.7	955.2	21.7	14.3	-6.7	961.7	24.6	16.6	-14.0	1008.7	28.6	20.5	-21.7
landfill emission	15.5	51.9	0.5	0.3	0.0	91.9	4.6	3.4	-0.2	132.5	9.3	6.5	-1.3	171.6	13.1	8.9	-3.6	205.8	15.8	10.8	-6.4
products to landfill	672.4	835.9	4.9	3.4	0.2	906.3	15.1	10.9	-1.8	932.9	22.3	14.6	-7.0	933.7	25.0	17.0	-14.6	979.6	29.2	20.9	-22.5

Table 7.22: Carbon fluxes [Gg C a^{-1}] for Norway spruce in the base scenario (Base) and changes for the other climate scenarios compared to the base scenario [%].

	2000	2010				2020				2030				2040				2050			
	Base	Base	Had-a1	Had-a2	Had-b1	Base	Had-a1	Had-a2	Had-b1	Base	Had-a1	Had-a2	Had-b1	Base	Had-a1	Had-a2	Had-b1	Base	Had-a1	Had-a2	Had-b1
raw materials	2572.0	2724.2	7.1	5.0	0.4	2735.8	19.4	13.7	-2.7	2666.8	27.0	17.5	-9.8	2576.0	26.7	18.6	-19.1	2475.2	24.2	19.4	-27.4
process burning	730.7	764.3	7.1	5.0	0.4	763.2	19.5	13.8	-2.6	766.7	27.3	17.7	-9.8	760.2	27.6	19.2	-19.2	739.4	26.4	20.7	-27.7
Recycling	592.0	760.6	4.5	3.1	0.2	816.4	14.9	10.8	-1.6	840.7	23.0	15.1	-6.8	859.1	25.4	17.2	-14.5	873.3	25.1	18.8	-21.6
product burning	739.9	941.9	4.8	3.4	0.2	1024.2	15.1	10.8	-1.7	1062.7	22.7	14.9	-6.9	1085.4	24.7	16.8	-14.3	1095.9	24.2	18.2	-21.1
landfill emission	17.7	58.9	0.5	0.3	0.0	104.4	4.7	3.5	-0.2	150.1	9.6	6.6	-1.3	194.9	13.6	9.1	-3.7	233.7	15.8	10.9	-6.5
products to landfill	761.4	950.7	5.0	3.5	0.2	1022.3	15.5	11.1	-1.8	1052.6	23.2	15.1	-7.1	1070.1	25.0	17.1	-14.8	1078.0	24.4	18.4	-21.7

There are small differences between the two tree species due to their different usage in the forest industries. Towards the end of the simulation there is also a strong effect of the shortage of Norway spruce supply in the A scenarios, which is to large extend replaced by Scots pine. While in 2050 the climate change induced increase of carbon fluxes into the raw materials for Norway spruce is 24.2 % and 19.4 % compared to the current climate baseline under the a1 and a2 scenarios, respectively, the corresponding values for Scots pine are 33.6 % and 24.4 %.

The shares of the sink and source related flux categories (in the beginning and at the end of the simulations) are changing in all scenarios including the baseline. This is because the product and landfill pools were not initialised. Table 7.23 shows the relative size of the carbon fluxes compared to the carbon pool in the removals. From 2000 to 2050, the share of the end-of-use fluxes increases by 2.2 – 3.5 % (recycling), 2.9 – 3.2 % (product burning), 2.8 – 3.3 % (landfill emission), and 2.2 – 2.5 % (products to landfill).

Table 7.23: Relative share of the different flux categories [%] for Scots pine and Norway spruce compared to the carbon pool in removals of the base scenario in 2000 and 2050.

	Scots pine		Norway spruce	
	2000	2050	2000	2050
raw materials	44.9	37.6	47.5	38.1
process burning	19.8	17.1	13.5	11.4
recycling	9.8	12.0	10.9	13.4
product burning	12.4	15.3	13.7	16.9
landfill emission	0.3	3.1	0.3	3.6
products to landfill	12.7	14.9	14.1	16.6

Results for the PCM-a2 scenario are not shown as they are almost identical with the changes shown for the Had-a2 scenario (see explanation on removals in the two a2 scenarios).

7.3.2.1.2 Carbon stocks

Similar to the carbon fluxes also the carbon stocks follow the trend from the socio-economically driven demand scenarios for the EFISCEN model. All scenarios but the b1 scenario show increasing stocks in raw materials, semi-products and final products. In the b1 scenario all stocks are decreasing due to smaller removals compared to the base line scenario.

Table 7.24. Carbon stocks [Gg C] during the simulation period for Scots pines under current climate (LATBase, SLBase) and changes for the other climate scenarios compared to the base scenario [%].

	2000	2010				2020				2030				2040				2050			
	Base	Base	HadA1	HadA2	HadB1	Base	HadA1	HadA2	HadB1	Base	HadA1	HadA2	HadB1	Base	HadA1	HadA2	HadB1	Base	HadA1	HadA2	HadB1
saw logs	2197.0	2234.3	7.1	5.0	0.3	2249.8	19.0	13.4	-2.7	2188.2	25.7	16.7	-9.7	2049.4	26.7	18.5	-19.2	2236.6	33.4	24.2	-29.1
pulp logs	945.5	1023.7	7.2	5.0	0.4	1040.2	19.2	13.6	-2.5	1028.3	27.2	17.8	-9.5	1060.4	30.3	20.7	-18.9	1060.6	34.4	25.0	-28.2
residues	137.4	146.2	7.1	5.0	0.4	161.6	20.2	14.3	-2.7	160.4	28.8	18.6	-9.9	152.7	33.7	22.9	-19.8	144.7	40.2	28.6	-29.8
C24	307.8	313.0	7.1	5.0	0.3	315.2	19.0	13.4	-2.7	306.6	25.7	16.7	-9.7	287.1	26.7	18.5	-19.2	313.3	33.4	24.2	-29.1
C16	664.3	678.8	7.1	5.0	0.3	684.0	19.0	13.4	-2.7	666.1	25.8	16.8	-9.7	628.9	27.0	18.7	-19.2	681.3	33.5	24.2	-29.0
chips	997.3	1017.5	7.1	5.0	0.3	1025.0	19.0	13.4	-2.7	997.8	25.7	16.7	-9.7	939.5	26.9	18.6	-19.2	1020.4	33.4	24.2	-29.0
chem pulp	780.3	819.9	7.1	5.0	0.4	829.6	19.1	13.5	-2.6	813.9	26.5	17.3	-9.6	803.6	28.7	19.8	-19.1	836.0	33.9	24.6	-28.6
mech pulp	0.7	0.7	7.1	5.0	0.4	0.7	19.2	13.6	-2.5	0.7	26.9	17.5	-9.6	0.7	29.6	20.3	-19.0	0.7	34.2	24.8	-28.4
other HWP	128.3	130.8	7.1	5.0	0.3	131.7	19.0	13.4	-2.7	128.2	25.7	16.7	-9.7	120.6	26.9	18.6	-19.2	131.1	33.4	24.2	-29.0
biofuel	1398.4	1460.9	7.1	5.0	0.4	1490.3	19.2	13.6	-2.6	1461.3	26.6	17.3	-9.7	1421.6	28.8	19.8	-19.2	1479.3	34.4	24.9	-28.8
building materials	3230.4	7515.0	1.4	1.0	0.1	11332.5	6.7	4.9	-0.4	14667.0	12.0	8.2	-2.3	17361.6	15.7	10.5	-5.5	19804.8	18.9	13.1	-9.9
other building materials	1632.5	3419.7	1.6	1.1	0.1	4658.0	8.0	5.9	-0.6	5495.4	14.4	9.7	-3.0	5955.8	18.8	12.5	-7.4	6324.9	22.7	15.7	-13.5
structural support	205.2	226.2	6.3	4.4	0.3	240.6	16.9	12.0	-2.3	245.4	23.0	15.1	-8.1	241.5	24.6	16.9	-16.0	262.6	30.2	21.7	-24.6
furnishing	271.7	595.3	1.4	1.0	0.1	820.9	7.6	5.6	-0.5	973.5	14.1	9.5	-2.8	1056.4	18.6	12.4	-7.1	1117.4	22.5	15.6	-13.2
packing	345.0	367.9	6.8	4.7	0.3	377.9	18.3	13.0	-2.5	374.6	25.2	16.4	-9.1	365.9	27.2	18.7	-18.0	387.4	32.7	23.7	-27.4
long-life paper products	1321.4	2079.9	2.5	1.8	0.1	2272.1	12.6	9.3	-1.0	2299.5	21.8	14.3	-5.4	2271.3	26.7	17.6	-13.3	2304.8	30.4	21.7	-22.6
short-life paper products	531.3	610.8	5.7	4.0	0.3	628.5	17.3	12.4	-2.1	621.9	25.2	16.4	-8.3	613.7	28.2	19.1	-17.4	632.9	32.9	23.8	-26.9
atmosphere	11642.0	32258.1	1.0	0.7	0.1	54597.7	5.5	4.0	-0.3	77877.4	10.1	6.9	-1.6	101287.3	13.6	9.2	-4.0	125389.6	16.4	11.3	-7.2
landfill	2497.5	8246.4	0.5	0.4	0.0	14627.5	4.6	3.4	-0.2	21166.9	9.3	6.5	-1.3	27550.3	13.1	8.8	-3.6	33839.2	16.1	11.0	-6.8

Table 7.25: Carbon stocks [Gg C] during the simulation period for Norway spruce under current climate (LATBase, SLBase) and changes for the other climate scenarios compared to the base scenario [%].

	2000	2010				2020				2030				2040				2050			
	Base	Base	HadA1	HadA2	HadB1	Base	HadA1	HadA2	HadB1	Base	HadA1	HadA2	HadB1	Base	HadA1	HadA2	HadB1	Base	HadA1	HadA2	HadB1
saw logs	2329.3	2540.3	7.1	5.0	0.3	2608.3	19.4	13.8	-2.7	2497.1	26.7	17.3	-9.8	2307.8	25.5	18.0	-19.0	2067.1	20.8	17.4	-27.1
pulp logs	707.0	674.1	7.1	5.0	0.4	618.6	19.3	13.7	-2.6	649.3	28.2	18.3	-9.7	733.7	30.3	20.7	-19.3	858.4	32.4	24.3	-28.1
residues	116.2	110.6	7.1	5.0	0.4	104.6	19.7	14.0	-2.6	126.4	29.4	19.0	-9.9	145.7	32.3	21.9	-19.6	154.6	36.4	26.9	-28.8
C24	292.5	319.0	7.1	5.0	0.3	327.5	19.4	13.8	-2.7	313.6	26.7	17.3	-9.8	289.8	25.5	18.0	-19.0	259.6	20.8	17.4	-27.1
C16	607.2	659.2	7.1	5.0	0.3	674.5	19.4	13.8	-2.7	647.6	26.7	17.3	-9.8	602.7	25.7	18.1	-19.0	546.2	21.4	17.7	-27.1
chips	1001.7	1089.4	7.1	5.0	0.3	1116.2	19.4	13.8	-2.7	1070.5	26.7	17.3	-9.8	993.5	25.7	18.0	-19.0	896.2	21.2	17.6	-27.1
chem pulp	62.2	59.4	7.1	5.0	0.4	54.5	19.3	13.7	-2.6	57.2	28.2	18.3	-9.7	64.6	30.3	20.7	-19.3	75.4	32.4	24.2	-28.1
mech pulp	1193.1	1232.9	7.1	5.0	0.4	1214.1	19.4	13.7	-2.6	1202.6	27.2	17.7	-9.8	1205.5	27.6	19.2	-19.1	1221.5	26.6	20.8	-27.6
other HWP	216.7	235.8	7.1	5.0	0.3	241.8	19.4	13.8	-2.7	231.8	26.7	17.3	-9.8	214.8	25.6	18.0	-19.0	193.3	21.1	17.5	-27.1
biofuel	780.7	818.7	7.1	5.0	0.4	819.0	19.5	13.8	-2.6	820.2	27.3	17.7	-9.8	809.9	27.5	19.1	-19.2	784.2	26.1	20.6	-27.6
building materials	2915.5	7075.4	1.5	1.0	0.1	10949.2	7.0	5.2	-0.4	14308.9	12.6	8.6	-2.3	17008.8	16.2	10.9	-5.6	18994.7	17.7	12.4	-9.3
other building materials	1371.0	3017.9	1.7	1.2	0.1	4239.6	8.3	6.1	-0.6	5056.0	15.1	10.1	-3.0	5504.1	19.3	12.9	-7.4	5641.1	20.3	14.5	-12.6
structural support	216.1	249.7	6.4	4.5	0.3	268.0	17.6	12.5	-2.3	268.7	24.3	15.8	-8.4	260.2	24.0	16.7	-16.2	244.8	20.7	16.6	-23.0
furnishing	654.9	1464.9	1.6	1.1	0.1	2069.2	8.2	6.0	-0.5	2471.8	15.0	10.1	-3.0	2686.4	19.3	12.9	-7.3	2740.7	20.4	14.5	-12.6
packing	470.8	504.2	6.9	4.8	0.3	509.6	18.8	13.4	-2.5	504.4	26.4	17.1	-9.4	496.5	26.5	18.5	-18.4	487.3	24.8	19.6	-26.5
long-life paper products	2120.6	3283.6	2.4	1.7	0.1	3537.9	12.6	9.3	-1.0	3555.4	22.3	14.7	-5.5	3584.5	26.8	17.7	-13.5	3633.5	27.1	20.0	-22.2
short-life paper products	852.1	961.7	5.6	3.9	0.3	965.5	17.4	12.5	-2.1	961.9	26.0	16.8	-8.4	970.4	27.6	18.8	-17.5	988.8	27.0	20.8	-26.1
atmosphere	8560.6	25175.0	0.8	0.6	0.0	43766.9	5.2	3.8	-0.2	63370.8	9.9	6.8	-1.5	83746.1	13.4	9.1	-3.9	104505.8	15.6	10.8	-6.8
landfill	3447.5	11472.7	0.5	0.4	0.0	20330.8	4.7	3.5	-0.2	29224.4	9.6	6.6	-1.3	37950.4	13.6	9.1	-3.7	46374.0	16.0	11.1	-6.9

Results for the PCM-a2 scenario are not shown as they are almost identical with the changes shown for the Had-a2 scenario (see explanation on removals in the two a2 scenarios).

7.3.2.2 Impacts of changing log assorting (LAT scenarios)

The basis for the LAT scenarios was the potential effects of a changing climate on log quality.

7.3.2.2.1 Carbon fluxes

The carbon flows in the forest industries and wood products for Scots pine and Norway spruce show distinctly different patterns due to the allocation of timber to different process lines.
Whereas an increasing sawlog percentage (LAT+10 scenario) for Scots pine results in increased available raw materials by 3.8% it only shows a very slight increase by 0.2% for Norway spruce. The carbon flow in process burning (i.e. material directly allocated to generate energy) is decreasing by about 7% for Scots pine because of less amount of pulp wood compared to the base scenario and thus also less black liquor from the chemical pulping process which is usually used to generate energy. This trend is opposite for Norway spruce where the carbon flows to process burning are actually increasing by 1.3 to 1.6% during the simulation period. This increase is due to more side products from the sawmilling that can be burnt. More details can be found in Table 7.25 and Table 7.26. The carbon fluxes for the LAT scenarios are directly reflecting the changes in the log allocation and are therefore linearly related to each other.

Table 7.26. Changes in carbon fluxes [%] for the LAT scenarios compared with the base scenario (no climate change, SLBase) for Scots pine.

	2000					2010					2020					2030					2040					2050				
	LATBase	LAT+10	LAT-05	LAT-10	LAT-20	LATBase	LAT+10	LAT-05	LAT-10	LAT-20	LATBase	LAT+10	LAT-05	LAT-10	LAT-20	LATBase	LAT+10	LAT-05	LAT-10	LAT-20	LATBase	LAT+10	LAT-05	LAT-10	LAT-20	LATBase	LAT+10	LAT-05	LAT-10	LAT-20
raw materials	2380.1	3.8	-1.9	-3.8	-7.7	2452.0	3.8	-1.9	-3.8	-7.6	2473.8	3.8	-1.9	-3.8	-7.7	2414.5	3.8	-1.9	-3.8	-7.6	2310.7	3.7	-1.9	-3.7	-7.4	2472.7	3.8	-1.9	-3.8	-7.6
process burning	1049.3	-7.3	3.7	7.3	14.6	1104.8	-7.1	3.6	7.1	14.2	1131.5	-7.0	3.5	7.0	14.1	1112.1	-7.0	3.5	7.0	13.9	1092.8	-6.6	3.3	6.6	13.2	1122.2	-7.0	3.5	7.0	14.1
recycling	520.7	-1.0	0.5	1.0	1.9	675.3	-0.3	0.1	0.3	0.5	735.5	0.2	-0.1	-0.2	-0.3	757.9	0.5	-0.3	-0.5	-1.0	759.6	0.8	-0.4	-0.8	-1.7	790.6	0.9	-0.4	-0.9	-1.8
product burning	657.9	0.8	-0.4	-0.8	-1.6	837.8	1.4	-0.7	-1.4	-2.9	919.8	1.9	-1.0	-1.9	-3.8	955.2	2.3	-1.2	-2.3	-4.6	961.7	2.6	-1.3	-2.6	-5.2	1008.7	2.7	-1.3	-2.7	-5.3
landfill emission	15.5	0.0	0.0	0.0	0.0	51.9	0.7	-0.3	-0.7	-1.4	91.9	1.0	-0.5	-1.0	-2.0	132.5	1.2	-0.6	-1.2	-2.5	171.6	1.5	-0.7	-1.5	-2.9	205.8	1.6	-0.8	-1.6	-3.2
products to landfill	672.4	0.7	-0.4	-0.7	-1.5	835.9	1.2	-0.6	-1.2	-2.4	906.3	1.6	-0.8	-1.6	-3.1	932.9	1.9	-0.9	-1.9	-3.8	933.7	2.1	-1.1	-2.1	-4.3	979.6	2.2	-1.1	-2.2	-4.4

Table 7.27. Changes in carbon fluxes [%] for the LAT scenarios compared with the base scenario (no climate change, SLBase) for Norway spruce.

	2000					2010					2020					2030					2040					2050				
	LATBase	LAT+10	LAT-05	LAT-10	LAT-20	LATBase	LAT+10	LAT-05	LAT-10	LAT-20	LATBase	LAT+10	LAT-05	LAT-10	LAT-20	LATBase	LAT+10	LAT-05	LAT-10	LAT-20	LATBase	LAT+10	LAT-05	LAT-10	LAT-20	LATBase	LAT+10	LAT-05	LAT-10	LAT-20
raw materials	2572.0	0.2	-0.1	-0.2	-0.4	2724.2	0.2	-0.1	-0.2	-0.4	2735.8	0.2	-0.1	-0.2	-0.4	2666.8	0.2	-0.1	-0.2	-0.4	2576.0	0.2	-0.1	-0.2	-0.4	2475.2	0.2	-0.1	-0.2	-0.3
process burning	730.7	1.6	-0.8	-1.6	-3.1	764.3	1.6	-0.8	-1.6	-3.3	763.2	1.7	-0.8	-1.7	-3.3	766.7	1.6	-0.8	-1.6	-3.2	760.2	1.5	-0.7	-1.5	-2.9	739.4	1.3	-0.7	-1.3	-2.7
recycling	592.0	-7.4	3.7	7.4	14.8	760.6	-6.7	3.4	6.7	13.5	816.4	-6.2	3.1	6.2	12.5	840.7	-5.5	2.8	5.5	11.0	859.1	-4.7	2.3	4.7	9.4	873.3	-3.9	1.9	3.9	7.8
product burning	739.9	-4.5	2.2	4.5	9.0	941.9	-3.7	1.9	3.7	7.5	1024.1	-3.1	1.5	3.1	6.1	1062.7	-2.4	1.2	2.4	4.7	1085.4	-1.7	0.8	1.7	3.4	1095.9	-1.1	0.6	1.1	2.3
landfill emission	17.6	-5.4	2.7	5.4	10.7	58.9	-4.6	2.3	4.6	9.2	104.4	-4.2	2.1	4.2	8.4	150.1	-3.8	1.9	3.8	7.7	194.9	-3.5	1.7	3.5	7.0	233.7	-3.2	1.6	3.2	6.3
products to landfill	761.4	-4.5	2.2	4.5	9.0	950.7	-4.0	2.0	4.0	7.9	1022.2	-3.4	1.7	3.4	6.9	1052.6	-2.8	1.4	2.8	5.6	1070.0	-2.2	1.1	2.2	4.4	1078.0	-1.6	0.8	1.6	3.2

7.3.2.2.2 Carbon stocks

A relative increase of 10% in the share of sawlogs in the removals (e.g. from 60% to 70% at a certain stand age) results in a slightly higher net-increase of 12% in the carbon stocks. The figures shown in Table 7.28 and Table 7.29 show the relative change to the base scenario. More sawlogs have a clear impact on the sawmilling products such as C24 and C16 as well as chips and also sawdust. The higher amount of sawdust that is used for energy production is only visible for Norway spruce, because in the case of Scots pine the lower amount of pulp wood results in less black liquor for energy production and this decreases the amount of biofuels. For both species the increase in sawn timber usage categories is clearly visible.

7.3.2.3 Impacts of changing sawmill efficiency (SL scenarios)

7.3.2.3.1 Carbon fluxes

The possible improvement of production efficiency in the sawmilling industry was modelled by increasing the output of the two sawn timber assortments. This resulted in a decreasing amount of the sawmilling by-product wood chips; the amount of sawdust (for energy generation) stayed unaltered. The results show the same pattern for the two tree species; however, the effect on Norway spruce was a little smaller (Table 7.30 and Table 7.31).

With an increasing efficiency for sawmills the overall fluxes of carbon between the harvested-wood product pools can be decreased. Less side products will be burnt and the general amount of products taken from use is decreasing due to a larger amount of sawn timber usage in mostly long-life product categories. But over time these decreasing fluxes diminish when also the products with a longer life-span are replaced.

7.3.2.3.2 Carbon stocks

The changes in carbon stocks for wood products can be seen in the Table 7.32 and Table 7.33. The main impact on carbon stock from an increasing sawmilling efficiency is in the higher amounts of sawmilling products (C24, C16) and a lower proportion of the side product chips, which would be usually used in the pulping industries. Thus the amount of pulp and also paper products is lower compared to the base scenario.

Table 7.28: Changes in carbon stocks [%] during the simulation period for Scots pines in the LAT scenarios (no climate change, SLBase) compared to the LATBase scenario.

	2000					2010					2020					2030					2040					2050				
	LATBase	LAT+10	LAT-05	LAT-10	LAT-20	LATBase	LAT+10	LAT-05	LAT-10	LAT-20	LATBase	LAT+10	LAT-05	LAT-10	LAT-20	LATBase	LAT+10	LAT-05	LAT-10	LAT-20	LATBase	LAT+10	LAT-05	LAT-10	LAT-20	LATBase	LAT+10	LAT-05	LAT-10	LAT-20
saw logs	2197.0	11.6	-5.8	-11.6	-23.3	2234.3	11.7	-5.8	-11.7	-23.4	2249.8	11.8	-5.9	-11.8	-23.6	2188.2	11.8	-5.9	-11.8	-23.5	2049.4	11.7	-5.9	-11.7	-23.5	2236.6	11.7	-5.9	-11.7	-23.5
pulp logs	945.5	-27.0	13.5	27.0	54.0	1023.7	-25.5	12.8	25.5	51.0	1040.2	-25.5	12.7	25.5	50.9	1028.3	-25.0	12.5	25.0	50.1	1060.4	-22.7	11.3	22.7	45.3	1060.6	-24.8	12.4	24.8	49.5
residues	137.4	0.0	0.0	0.0	0.0	146.2	0.0	0.0	0.0	0.0	161.6	0.0	0.0	0.0	0.0	160.4	0.0	0.0	0.0	0.0	152.7	0.0	0.0	0.0	0.0	144.7	0.0	0.0	0.0	0.0
C24	307.8	11.6	-5.8	-11.6	-23.3	313.0	11.7	-5.8	-11.7	-23.4	315.2	11.8	-5.9	-11.8	-23.6	306.6	11.8	-5.9	-11.8	-23.5	287.1	11.7	-5.9	-11.7	-23.5	313.3	11.7	-5.9	-11.7	-23.5
C16	664.3	8.8	-4.4	-8.8	-17.6	678.8	8.8	-4.4	-8.8	-17.6	684.0	8.9	-4.4	-8.9	-17.7	666.1	8.8	-4.4	-8.8	-17.7	628.9	8.7	-4.4	-8.7	-17.5	681.3	8.8	-4.4	-8.8	-17.6
chips	997.3	9.7	-4.9	-9.7	-19.5	1017.5	9.8	-4.9	-9.8	-19.5	1025.0	9.8	-4.9	-9.8	-19.7	997.8	9.8	-4.9	-9.8	-19.6	939.5	9.7	-4.9	-9.7	-19.4	1020.4	9.8	-4.9	-9.8	-19.6
chem pulp	780.3	-8.2	4.1	8.2	16.5	819.9	-8.0	4.0	8.0	16.0	829.6	-8.0	4.0	8.0	16.1	813.9	-7.9	4.0	7.9	15.9	803.6	-7.5	3.8	7.5	15.0	836.0	-7.9	3.9	7.9	15.8
mech pulp	0.7	-18.2	9.1	18.2	36.4	0.7	-17.4	8.7	17.4	34.8	0.7	-17.4	8.7	17.4	34.9	0.7	-17.2	8.6	17.2	34.4	0.7	-15.9	7.9	15.9	31.7	0.7	-17.0	8.5	17.0	34.1
other HWP	128.3	10.1	-5.1	-10.1	-20.3	130.8	10.2	-5.1	-10.2	-20.3	131.7	10.2	-5.1	-10.2	-20.5	128.2	10.2	-5.1	-10.2	-20.5	120.6	10.2	-5.1	-10.2	-20.3	131.1	10.2	-5.1	-10.2	-20.4
biofuel	1398.4	-3.1	1.5	3.1	6.1	1460.9	-3.0	1.5	3.0	6.0	1490.3	-3.0	1.5	3.0	6.0	1461.3	-3.0	1.5	3.0	5.9	1421.6	-2.8	1.4	2.8	5.7	1479.3	-3.0	1.5	3.0	6.0
building materials	3230.4	9.7	-4.8	-9.7	-19.4	7515.0	9.7	-4.8	-9.7	-19.4	11332.5	9.7	-4.9	-9.7	-19.4	14667.0	9.7	-4.9	-9.7	-19.5	17361.6	9.7	-4.9	-9.7	-19.5	19804.8	9.7	-4.9	-9.7	-19.4
other building materials	1632.5	10.4	-5.2	-10.4	-20.8	3419.7	10.4	-5.2	-10.4	-20.8	4658.0	10.4	-5.2	-10.4	-20.9	5495.4	10.4	-5.2	-10.4	-20.9	5955.8	10.4	-5.2	-10.4	-20.9	6324.9	10.4	-5.2	-10.4	-20.8
structural support	205.2	9.1	-4.6	-9.1	-18.2	226.2	9.2	-4.6	-9.2	-18.4	240.6	9.3	-4.6	-9.3	-18.6	245.4	9.3	-4.7	-9.3	-18.6	241.5	9.3	-4.6	-9.3	-18.5	262.6	9.3	-4.7	-9.3	-18.6
furnishing	271.7	10.7	-5.3	-10.7	-21.4	595.3	10.6	-5.3	-10.6	-21.3	820.9	10.7	-5.3	-10.7	-21.4	973.5	10.7	-5.4	-10.7	-21.4	1056.4	10.7	-5.4	-10.7	-21.4	1117.4	10.7	-5.3	-10.7	-21.4
packing	345.0	-0.1	0.0	0.1	0.2	367.9	0.2	-0.1	-0.2	-0.4	377.9	0.4	-0.2	-0.4	-0.7	374.6	0.5	-0.3	-0.5	-1.0	365.9	0.6	-0.3	-0.6	-1.2	387.4	0.6	-0.3	-0.6	-1.2
long-life paperproducts	1321.4	-9.2	4.6	9.2	18.4	2079.9	-8.2	4.1	8.2	16.4	2272.1	-8.1	4.0	8.1	16.2	2299.5	-8.0	4.0	8.0	16.0	2271.3	-7.7	3.9	7.7	15.4	2304.8	-7.8	3.9	7.8	15.6
short-life paperproducts	531.3	-8.5	4.3	8.5	17.1	610.8	-8.1	4.0	8.1	16.1	628.5	-8.0	4.0	8.0	16.1	621.9	-8.0	4.0	8.0	15.9	613.7	-7.6	3.8	7.6	15.1	632.9	-7.9	3.9	7.9	15.8
atmosphere	11642.0	-3.5	1.7	3.5	6.9	32258.1	-2.8	1.4	2.8	5.6	54597.7	-2.5	1.3	2.5	5.1	77877.4	-2.3	1.2	2.3	4.6	101287.3	-2.1	1.1	2.1	4.3	125389.6	-2.0	1.0	2.0	4.0
landfill	2497.5	-2.3	1.2	2.3	4.6	8246.4	-1.7	0.8	1.7	3.3	14627.5	-1.2	0.6	1.2	2.5	21166.9	-0.9	0.4	0.9	1.8	27550.3	-0.6	0.3	0.6	1.2	33839.2	-0.3	0.2	0.3	0.7

Table 7.29: Changes in carbon stocks [%] during the simulation period for Norway spruce in the LAT scenarios (no climate change, SLBase) compared to the LATBase scenario.

	2000					2010					2020					2030					2040					2050				
	LATBase	LAT+10	LAT-05	LAT-10	LAT-20	LATBase	LAT+10	LAT-05	LAT-10	LAT-20	LATBase	LAT+10	LAT-05	LAT-10	LAT-20	LATBase	LAT+10	LAT-05	LAT-10	LAT-20	LATBase	LAT+10	LAT-05	LAT-10	LAT-20	LATBase	LAT+10	LAT-05	LAT-10	LAT-20
saw logs	2329.3	12.0	-6.0	-12.0	-23.9	2540.3	11.9	-5.9	-11.9	-23.8	2608.3	11.8	-5.9	-11.8	-23.6	2497.1	11.7	-5.9	-11.7	-23.5	2307.8	11.7	-5.8	-11.7	-23.4	2067.1	11.7	-5.8	-11.7	-23.3
pulp logs	707.0	-39.4	19.7	39.4	78.8	674.1	-44.8	22.4	44.8	89.5	618.6	-49.8	24.9	49.8	99.5	649.3	-45.1	22.6	45.1	90.2	733.7	-36.8	18.4	36.8	73.5	858.4	-28.1	14.1	28.1	56.2
residues	116.2	0.0	0.0	0.0	0.0	110.6	0.0	0.0	0.0	0.0	104.6	0.0	0.0	0.0	0.0	126.4	0.0	0.0	0.0	0.0	145.7	0.0	0.0	0.0	0.0	154.6	0.0	0.0	0.0	0.0
C24	292.5	12.0	-6.0	-12.0	-23.9	319.0	11.9	-5.9	-11.9	-23.8	327.5	11.8	-5.9	-11.8	-23.6	313.6	11.7	-5.9	-11.7	-23.5	289.8	11.7	-5.8	-11.7	-23.4	259.6	11.7	-5.8	-11.7	-23.3
C16	607.2	10.1	-5.0	-10.1	-20.1	659.2	10.1	-5.0	-10.1	-20.1	674.5	10.0	-5.0	-10.0	-20.0	647.6	9.9	-5.0	-9.9	-19.9	602.7	9.8	-4.9	-9.8	-19.7	546.2	9.7	-4.9	-9.7	-19.4
chips	1001.7	10.8	-5.4	-10.8	-21.6	1089.4	10.8	-5.4	-10.8	-21.5	1116.2	10.7	-5.4	-10.7	-21.5	1070.5	10.6	-5.3	-10.6	-21.3	993.5	10.6	-5.3	-10.6	-21.1	896.2	10.5	-5.2	-10.5	-20.9
chem pulp	62.2	-39.1	19.5	39.1	78.2	59.4	-44.4	22.2	44.4	88.7	54.5	-49.3	24.6	49.3	98.6	57.2	-44.7	22.4	44.7	89.5	64.6	-36.5	18.2	36.5	73.0	75.4	-27.9	14.0	27.9	55.9
mech pulp	1193.1	-9.5	4.7	9.5	18.9	1232.9	-9.9	5.0	9.9	19.9	1214.1	-10.3	5.1	10.3	20.6	1202.6	-9.9	4.9	9.9	19.8	1205.5	-9.1	4.5	9.1	18.2	1221.5	-8.0	4.0	8.0	16.0
other HWP	216.7	11.2	-5.6	-11.2	-22.4	235.8	11.1	-5.6	-11.1	-22.3	241.8	11.1	-5.5	-11.1	-22.2	231.8	11.0	-5.5	-11.0	-22.0	214.8	10.9	-5.5	-10.9	-21.9	193.3	10.9	-5.4	-10.9	-21.7
biofuel	780.7	2.2	-1.1	-2.2	-4.3	818.7	2.2	-1.1	-2.2	-4.5	819.0	2.3	-1.1	-2.3	-4.6	820.2	2.2	-1.1	-2.2	-4.3	809.9	2.0	-1.0	-2.0	-4.0	784.2	1.9	-0.9	-1.9	-3.7
building materials	2915.5	10.7	-5.3	-10.7	-21.4	7075.4	10.7	-5.3	-10.7	-21.4	10949.2	10.7	-5.3	-10.7	-21.3	14308.9	10.6	-5.3	-10.6	-21.3	17008.8	10.6	-5.3	-10.6	-21.2	18994.7	10.5	-5.3	-10.5	-21.1
other building materials	1371.0	11.0	-5.5	-11.0	-22.1	3017.9	11.0	-5.5	-11.0	-22.1	4239.6	11.0	-5.5	-11.0	-22.0	5056.0	10.9	-5.5	-10.9	-21.9	5504.1	10.9	-5.4	-10.9	-21.8	5641.1	10.8	-5.4	-10.8	-21.7
structural support	216.1	10.4	-5.2	-10.4	-20.9	249.7	10.4	-5.2	-10.4	-20.9	268.0	10.4	-5.2	-10.4	-20.8	268.7	10.4	-5.2	-10.4	-20.7	260.2	10.3	-5.1	-10.3	-20.6	244.8	10.2	-5.1	-10.2	-20.4
furnishing	654.9	11.6	-5.8	-11.6	-23.3	1464.9	11.6	-5.8	-11.6	-23.2	2069.2	11.5	-5.8	-11.5	-23.1	2471.8	11.5	-5.7	-11.5	-23.0	2686.4	11.4	-5.7	-11.4	-22.9	2740.7	11.4	-5.7	-11.4	-22.8
packing	470.8	-2.9	1.5	2.9	5.9	504.2	-2.8	1.4	2.8	5.5	509.6	-2.7	1.3	2.7	5.3	504.4	-2.4	1.2	2.4	4.9	496.5	-2.2	1.1	2.2	4.4	487.3	-1.9	1.0	1.9	3.8
long-life paperproducts	2120.6	-12.0	6.0	12.0	23.9	3283.6	-11.5	5.8	11.5	23.1	3537.9	-11.8	5.9	11.8	23.5	3555.4	-11.7	5.8	11.7	23.3	3584.5	-10.9	5.5	10.9	21.8	3633.5	-9.8	4.9	9.8	19.5
short-life paperproducts	852.1	-11.3	5.7	11.3	22.6	961.7	-11.5	5.8	11.5	23.1	965.5	-11.9	6.0	11.9	23.8	961.9	-11.5	5.7	11.5	23.0	970.4	-10.5	5.3	10.5	21.1	988.8	-9.3	4.6	9.3	18.6
atmosphere	8560.6	-1.3	0.6	1.3	2.5	25175.0	-1.3	0.6	1.3	2.6	43766.9	-1.2	0.6	1.2	2.5	63370.8	-1.1	0.6	1.1	2.3	83746.1	-1.0	0.5	1.0	2.1	104505.8	-0.9	0.5	0.9	1.9
landfill	3447.5	-5.8	2.9	5.8	11.5	11472.7	-5.0	2.5	5.0	10.0	20330.8	-4.6	2.3	4.6	9.2	29224.4	-4.2	2.1	4.2	8.5	37950.4	-3.9	1.9	3.9	7.7	46374.0	-3.5	1.7	3.5	7.0

Table 7.30: Changes in carbon fluxes [%] for the SL scenarios compared with the base scenario (no climate change, LATBase) for Scots pine.

	2000					2010					2020					2030					2040					2050				
	SLBase	SL+10	SL+05	SL-05	SL-10	SLBase	SL+10	SL+05	SL-05	SL-10	SLBase	SL+10	SL+05	SL-05	SL-10	SLBase	SL+10	SL+05	SL-05	SL-10	SLBase	SL+10	SL+05	SL-05	SL-10	SLBase	SL+10	SL+05	SL-05	SL-10
raw materials	2380.1	0.0	0.0	0.0	0.0	2452.0	0.0	0.0	0.0	0.0	2473.8	0.0	0.0	0.0	0.0	2414.5	0.0	0.0	0.0	0.0	2310.7	0.0	0.0	0.0	0.0	2472.7	0.0	0.0	0.0	0.0
process burning	1049.3	-3.2	-1.6	1.6	3.2	1104.8	-3.1	-1.5	1.5	3.1	1131.5	-3.0	-1.5	1.5	3.0	1112.1	-3.0	-1.5	1.5	3.0	1092.8	-2.9	-1.4	1.4	2.9	1122.2	-3.1	-1.5	1.5	3.1
recycling	520.7	-9.4	-4.7	4.7	9.4	675.3	-8.3	-4.2	4.2	8.3	735.5	-7.2	-3.6	3.6	7.2	757.9	-6.3	-3.1	3.1	6.3	759.6	-5.3	-2.6	2.6	5.3	790.6	-4.9	-2.5	2.5	4.9
product burning	657.9	-5.3	-2.7	2.7	5.3	837.8	-4.2	-2.1	2.1	4.2	919.8	-3.0	-1.5	1.5	3.0	955.2	-2.1	-1.0	1.0	2.1	961.7	-1.1	-0.6	0.6	1.1	1008.7	-0.8	-0.4	0.4	0.8
landfill emission	15.5	-4.1	-2.0	2.0	4.1	51.9	-5.0	-2.5	2.5	5.0	91.9	-4.8	-2.4	2.4	4.8	132.5	-4.4	-2.2	2.2	4.4	171.6	-4.0	-2.0	2.0	4.0	205.8	-3.6	-1.8	1.8	3.6
products to landfill	672.4	-5.6	-2.8	2.8	5.6	835.9	-4.9	-2.5	2.5	4.9	906.3	-4.0	-2.0	2.0	4.0	932.9	-3.1	-1.6	1.6	3.1	933.7	-2.3	-1.2	1.2	2.3	979.6	-1.9	-1.0	1.0	1.9

Table 7.31: Changes in carbon fluxes [%] for the SL scenarios compared with the base scenario (no climate change, LATBase) for Norway spruce.

	2000					2010					2020					2030					2040					2050				
	SLBase	SL+10	SL+05	SL-05	SL-10	SLBase	SL+10	SL+05	SL-05	SL-10	SLBase	SL+10	SL+05	SL-05	SL-10	SLBase	SL+10	SL+05	SL-05	SL-10	SLBase	SL+10	SL+05	SL-05	SL-10	SLBase	SL+10	SL+05	SL-05	SL-10
raw materials	2572.0	0.0	0.0	0.0	0.0	2724.2	0.0	0.0	0.0	0.0	2735.8	0.0	0.0	0.0	0.0	2666.8	0.0	0.0	0.0	0.0	2576.0	0.0	0.0	0.0	0.0	2475.2	0.0	0.0	0.0	0.0
process burning	730.7	-4.2	-2.1	2.1	4.2	764.3	-4.4	-2.2	2.2	4.4	763.2	-4.5	-2.3	2.3	4.5	766.7	-4.3	-2.2	2.2	4.3	760.2	-4.0	-2.0	2.0	4.0	739.4	-3.8	-1.9	1.9	3.8
recycling	592.0	-7.6	-3.8	3.8	7.6	760.6	-7.3	-3.7	3.7	7.3	816.4	-6.7	-3.3	3.3	6.7	840.7	-5.8	-2.9	2.9	5.8	859.1	-4.7	-2.4	2.4	4.7	873.3	-3.8	-1.9	1.9	3.8
product burning	739.9	-4.4	-2.2	2.2	4.4	941.9	-3.8	-1.9	1.9	3.8	1024.1	-3.0	-1.5	1.5	3.0	1062.7	-2.0	-1.0	1.0	2.0	1085.4	-1.1	-0.6	0.6	1.1	1095.9	-0.4	-0.2	0.2	0.4
landfill emission	17.6	-3.2	-1.6	1.6	3.2	58.9	-4.1	-2.0	2.0	4.1	104.4	-4.0	-2.0	2.0	4.0	150.1	-3.7	-1.9	1.9	3.7	194.9	-3.4	-1.7	1.7	3.4	233.7	-3.0	-1.5	1.5	3.0
products to landfill	761.4	-4.5	-2.3	2.3	4.5	950.7	-4.2	-2.1	2.1	4.2	1022.2	-3.5	-1.8	1.8	3.5	1052.6	-2.7	-1.4	1.4	2.7	1070.0	-1.9	-1.0	1.0	1.9	1078.0	-1.2	-0.6	0.6	1.2

Table 7.32: Changes in carbon stocks [%] during the simulation period for Scots pines in the SL+05 scenario (no climate change, LATBase) compared to the SLBase scenario.

	2000					2010					2020					2030					2040					2050				
	SLBase	SL-10	SL-05	SL+05	SL+10	SLBase	SL-10	SL-05	SL+05	SL+10	SLBase	SL-10	SL-05	SL+05	SL+10	SLBase	SL-10	SL-05	SL+05	SL+10	SLBase	SL-10	SL-05	SL+05	SL+10	SLBase	SL-10	SL-05	SL+05	SL+10
saw logs	2197.0	0.0	0.0	0.0	0.0	2234.3	0.0	0.0	0.0	0.0	2249.8	0.0	0.0	0.0	0.0	2188.2	0.0	0.0	0.0	0.0	2049.4	0.0	0.0	0.0	0.0	2236.6	0.0	0.0	0.0	0.0
pulp logs	945.5	0.0	0.0	0.0	0.0	1023.7	0.0	0.0	0.0	0.0	1040.2	0.0	0.0	0.0	0.0	1028.3	0.0	0.0	0.0	0.0	1060.4	0.0	0.0	0.0	0.0	1060.6	0.0	0.0	0.0	0.0
residues	137.4	0.0	0.0	0.0	0.0	146.2	0.0	0.0	0.0	0.0	161.6	0.0	0.0	0.0	0.0	160.4	0.0	0.0	0.0	0.0	152.7	0.0	0.0	0.0	0.0	144.7	0.0	0.0	0.0	0.0
C24	307.8	-23.0	-11.5	11.5	23.0	313.0	-23.0	-11.5	11.5	23.0	315.2	-23.0	-11.5	11.5	23.0	306.6	-23.0	-11.5	11.5	23.0	287.1	-23.0	-11.5	11.5	23.0	313.3	-23.0	-11.5	11.5	23.0
C16	664.3	-23.0	-11.5	11.5	23.0	678.8	-23.0	-11.5	11.5	23.0	684.0	-23.0	-11.5	11.5	23.0	666.1	-23.0	-11.5	11.5	23.0	628.9	-23.0	-11.5	11.5	23.0	681.3	-23.0	-11.5	11.5	23.0
chips	997.3	22.4	11.2	-11.2	-22.4	1017.5	22.4	11.2	-11.2	-22.4	1025.0	22.4	11.2	-11.2	-22.4	997.8	22.4	11.2	-11.2	-22.4	939.5	22.4	11.2	-11.2	-22.4	1020.4	22.4	11.2	-11.2	-22.4
chem pulp	780.3	11.5	5.7	-5.7	-11.5	819.9	11.1	5.6	-5.6	-11.1	829.6	11.1	5.5	-5.5	-11.1	813.9	11.0	5.5	-5.5	-11.0	803.6	10.5	5.2	-5.2	-10.5	836.0	10.9	5.5	-5.5	-10.9
mech pulp	0.7	0.0	0.0	0.0	0.0	0.7	0.0	0.0	0.0	0.0	0.7	0.0	0.0	0.0	0.0	0.7	0.0	0.0	0.0	0.0	0.7	0.0	0.0	0.0	0.0	0.7	0.0	0.0	0.0	0.0
other HWP	128.3	17.4	8.7	-8.7	-17.4	130.8	17.4	8.7	-8.7	-17.4	131.7	17.4	8.7	-8.7	-17.4	128.2	17.4	8.7	-8.7	-17.4	120.6	17.5	8.7	-8.7	-17.5	131.1	17.4	8.7	-8.7	-17.4
biofuel	1398.4	8.0	4.0	-4.0	-8.0	1460.9	7.8	3.9	-3.9	-7.8	1490.3	7.7	3.9	-3.9	-7.7	1461.3	7.7	3.8	-3.8	-7.7	1421.6	7.4	3.7	-3.7	-7.4	1479.3	7.7	3.9	-3.9	-7.7
building materials	3230.4	-23.0	-11.5	11.5	23.0	7515.0	-23.0	-11.5	11.5	23.0	11332.5	-23.0	-11.5	11.5	23.0	14667.0	-23.0	-11.5	11.5	23.0	17361.6	-23.0	-11.5	11.5	23.0	19804.8	-23.0	-11.5	11.5	23.0
other building materials	1632.5	-18.7	-9.4	9.4	18.7	3419.7	-18.4	-9.2	9.2	18.4	4658.0	-18.4	-9.2	9.2	18.4	5495.4	-18.4	-9.2	9.2	18.5	5955.8	-18.5	-9.2	9.2	18.5	6324.9	-18.5	-9.3	9.3	18.5
structural support	205.2	-15.4	-7.7	7.7	15.5	226.2	-15.8	-7.9	7.9	15.8	240.6	-16.0	-8.0	8.0	16.0	245.4	-16.3	-8.1	8.1	16.3	241.5	-16.5	-8.2	8.2	16.5	262.6	-16.5	-8.3	8.3	16.5
furnishing	271.7	3.0	1.5	-1.5	-3.0	595.3	3.9	2.0	-2.0	-3.9	820.9	4.1	2.1	-2.1	-4.1	973.5	4.2	2.1	-2.1	-4.2	1056.4	4.3	2.2	-2.2	-4.3	1117.4	4.3	2.2	-2.2	-4.3
packing	345.0	-0.2	-0.1	0.1	0.2	367.9	-0.7	-0.3	0.3	0.7	377.9	-1.0	-0.5	0.5	1.0	374.6	-1.2	-0.6	0.6	1.2	365.9	-1.4	-0.7	0.7	1.4	387.4	-1.4	-0.7	0.7	1.4
long-life paperproducts	1321.4	10.9	5.5	-5.5	-10.9	2079.9	11.1	5.6	-5.6	-11.1	2272.1	11.1	5.5	-5.5	-11.1	2299.5	11.1	5.5	-5.5	-11.1	2271.3	10.8	5.4	-5.4	-10.8	2304.8	10.7	5.3	-5.3	-10.7
short-life paperproducts	531.3	11.3	5.6	-5.6	-11.3	610.8	11.1	5.6	-5.6	-11.1	628.5	11.1	5.5	-5.5	-11.1	621.9	11.0	5.5	-5.5	-11.0	613.7	10.6	5.3	-5.3	-10.6	632.9	10.8	5.4	-5.4	-10.8
atmosphere	11642.0	5.6	2.8	-2.8	-5.6	32258.1	5.6	2.8	-2.8	-5.6	54597.7	5.3	2.6	-2.6	-5.3	77877.4	5.0	2.5	-2.5	-5.0	101287.3	4.7	2.3	-2.3	-4.7	125389.6	4.4	2.2	-2.2	-4.4
landfill	2497.5	-0.3	-0.1	0.1	0.3	8246.4	0.5	0.3	-0.3	-0.5	14627.5	0.3	0.1	-0.1	-0.3	21166.9	-0.2	-0.1	0.1	0.2	27550.3	-0.6	-0.3	0.3	0.6	33839.2	-1.0	-0.5	0.5	1.0

Table 7.33: Changes in carbon stocks [%] during the simulation period for Norway spruce in the SL+05 scenario (no climate change, LATBase) compared to the SLBase scenario.

	2000					2010					2020					2030					2040					2050				
	SLBase	SL-10	SL-05	SL+05	SL+10	SLBase	SL-10	SL-05	SL+05	SL+10	SLBase	SL-10	SL-05	SL+05	SL+10	SLBase	SL-10	SL-05	SL+05	SL+10	SLBase	SL-10	SL-05	SL+05	SL+10	SLBase	SL-10	SL-05	SL+05	SL+10
saw logs	2329.3	0.0	0.0	0.0	0.0	2540.3	0.0	0.0	0.0	0.0	2608.3	0.0	0.0	0.0	0.0	2497.1	0.0	0.0	0.0	0.0	2307.8	0.0	0.0	0.0	0.0	2067.1	0.0	0.0	0.0	0.0
pulp logs	707.0	0.0	0.0	0.0	0.0	674.1	0.0	0.0	0.0	0.0	618.6	0.0	0.0	0.0	0.0	649.3	0.0	0.0	0.0	0.0	733.7	0.0	0.0	0.0	0.0	858.4	0.0	0.0	0.0	0.0
residues	116.2	0.0	0.0	0.0	0.0	110.6	0.0	0.0	0.0	0.0	104.6	0.0	0.0	0.0	0.0	126.4	0.0	0.0	0.0	0.0	145.7	0.0	0.0	0.0	0.0	154.6	0.0	0.0	0.0	0.0
C24	292.5	-23.0	-11.5	11.5	23.0	319.0	-23.0	-11.5	11.5	23.0	327.5	-23.0	-11.5	11.5	23.0	313.6	-23.0	-11.5	11.5	23.0	289.8	-23.0	-11.5	11.5	23.0	259.6	-23.0	-11.5	11.5	23.0
C16	607.2	-23.0	-11.5	11.5	23.0	659.2	-23.0	-11.5	11.5	23.0	674.5	-23.0	-11.5	11.5	23.0	647.6	-23.0	-11.5	11.5	23.0	602.7	-23.0	-11.5	11.5	23.0	546.2	-23.0	-11.5	11.5	23.0
chips	1001.7	20.6	10.3	-10.3	-20.6	1089.4	20.6	10.3	-10.3	-20.6	1116.2	20.6	10.3	-10.3	-20.6	1070.5	20.6	10.3	-10.3	-20.6	993.5	20.7	10.3	-10.3	-20.7	896.2	20.7	10.3	-10.3	-20.7
chem pulp	62.2	0.0	0.0	0.0	0.0	59.4	0.0	0.0	0.0	0.0	54.5	0.0	0.0	0.0	0.0	57.2	0.0	0.0	0.0	0.0	64.6	0.0	0.0	0.0	0.0	75.4	0.0	0.0	0.0	0.0
mech pulp	1193.1	12.1	6.1	-6.1	-12.1	1232.9	12.8	6.4	-6.4	-12.8	1214.1	13.3	6.6	-6.6	-13.3	1202.6	12.9	6.4	-6.4	-12.9	1205.5	11.9	6.0	-6.0	-11.9	1221.5	10.6	5.3	-5.3	-10.6
other HWP	216.7	9.5	4.8	-4.8	-9.5	235.8	9.5	4.8	-4.8	-9.5	241.8	9.5	4.8	-4.8	-9.5	231.8	9.5	4.8	-4.8	-9.5	214.8	9.6	4.8	-4.8	-9.6	193.3	9.6	4.8	-4.8	-9.6
biofuel	780.7	5.3	2.6	-2.6	-5.3	818.7	5.5	2.7	-2.7	-5.5	819.0	5.6	2.8	-2.8	-5.6	820.2	5.4	2.7	-2.7	-5.4	809.9	5.1	2.5	-2.5	-5.1	784.2	4.7	2.4	-2.4	-4.7
building materials	2915.5	-23.0	-11.5	11.5	23.0	7075.4	-23.0	-11.5	11.5	23.0	10949.2	-23.0	-11.5	11.5	23.0	14308.9	-23.0	-11.5	11.5	23.0	17008.8	-23.0	-11.5	11.5	23.0	18994.7	-23.0	-11.5	11.5	23.0
other building materials	1371.0	-16.0	-8.0	8.0	16.0	3017.9	-15.8	-7.9	7.9	15.8	4239.6	-15.8	-7.9	7.9	15.8	5056.0	-15.8	-7.9	7.9	15.8	5504.1	-15.9	-8.0	8.0	15.9	5641.1	-16.0	-8.0	8.0	16.0
structural support	216.1	-13.2	-6.6	6.6	13.2	249.7	-13.5	-6.8	6.8	13.5	268.0	-13.8	-6.9	6.9	13.8	268.7	-14.1	-7.0	7.0	14.1	260.2	-14.3	-7.2	7.2	14.3	244.8	-14.6	-7.3	7.3	14.6
furnishing	654.9	-8.2	-4.1	4.1	8.2	1464.9	-7.7	-3.8	3.8	7.7	2069.2	-7.5	-3.8	3.8	7.5	2471.8	-7.4	-3.7	3.7	7.4	2686.4	-7.4	-3.7	3.7	7.4	2740.7	-7.3	-3.7	3.7	7.3
packing	470.8	3.1	1.5	-1.5	-3.1	504.2	2.9	1.4	-1.4	-2.9	509.6	2.8	1.4	-1.4	-2.8	504.4	2.5	1.3	-1.3	-2.5	496.5	2.2	1.1	-1.1	-2.2	487.3	1.9	0.9	-0.9	-1.9
long-life paperproducts	2120.6	10.7	5.4	-5.4	-10.7	3283.6	11.8	5.9	-5.9	-11.8	3537.9	12.4	6.2	-6.2	-12.4	3555.4	12.5	6.2	-6.2	-12.5	3584.5	11.9	5.9	-5.9	-11.9	3633.5	10.8	5.4	-5.4	-10.8
short-life paperproducts	852.1	11.3	5.6	-5.6	-11.3	961.7	12.1	6.0	-6.0	-12.1	965.5	12.6	6.3	-6.3	-12.6	961.9	12.3	6.2	-6.2	-12.3	970.4	11.5	5.7	-5.7	-11.5	988.8	10.2	5.1	-5.1	-10.2
atmosphere	8560.6	3.9	1.9	-1.9	-3.9	25175.0	4.3	2.2	-2.2	-4.3	43766.9	4.2	2.1	-2.1	-4.2	63370.8	4.0	2.0	-2.0	-4.0	83746.1	3.8	1.9	-1.9	-3.8	104505.8	3.5	1.7	-1.7	-3.5
landfill	3447.5	2.8	1.4	-1.4	-2.8	11472.7	3.6	1.8	-1.8	-3.6	20330.8	3.5	1.8	-1.8	-3.5	29224.4	3.3	1.6	-1.6	-3.3	37950.4	2.9	1.5	-1.5	-2.9	46374.0	2.5	1.3	-1.3	-2.5

7.3.3 Comparison of Scenario Effects

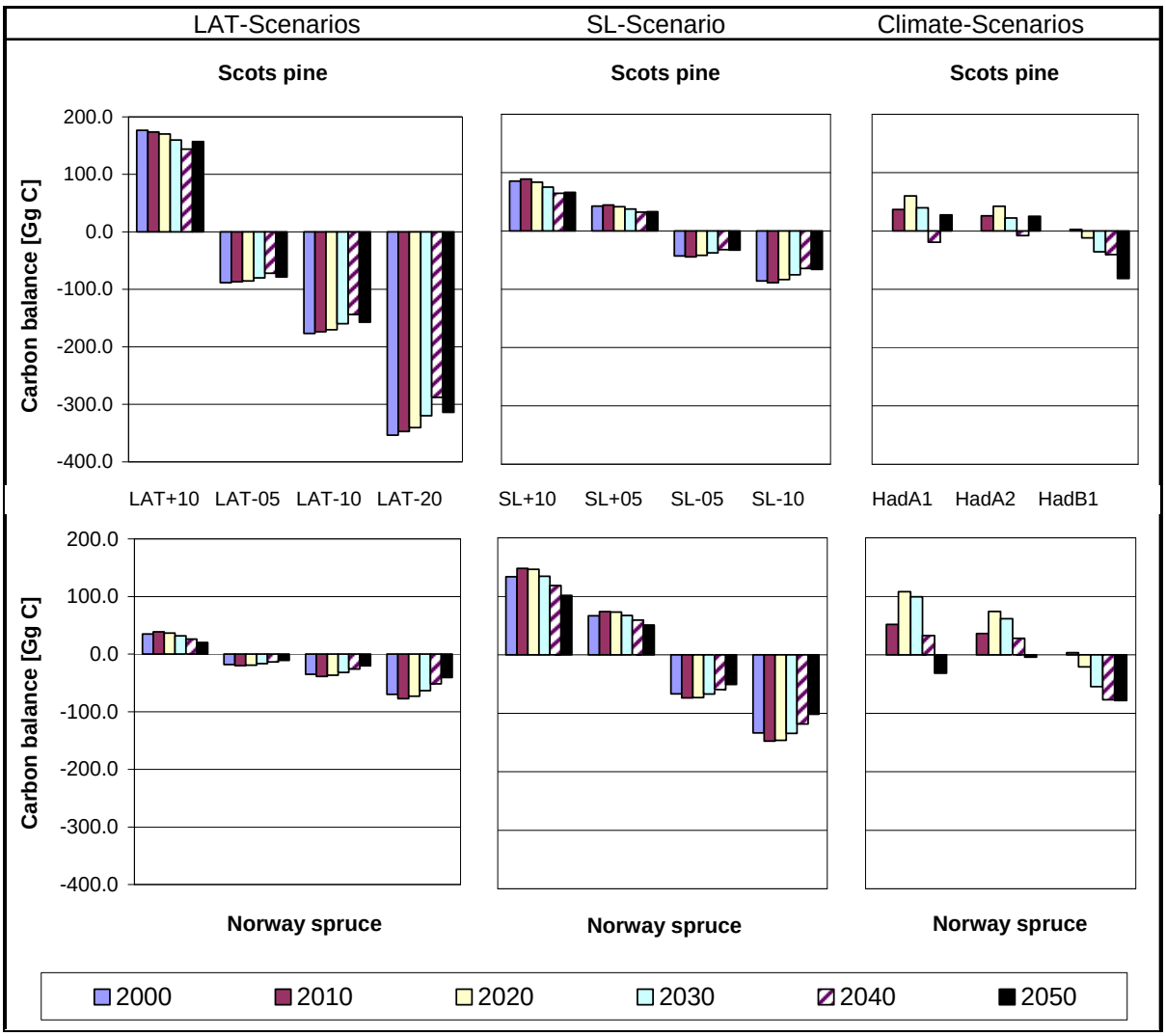

Figure 7.10: Influence of scenarios of changing log assortments (LAT*), saw milling efficiency (SL*) and climate (Had*) on the carbon balance of the wood products in Southern Finland from 2000 – 2050.

The effects of different scenarios have been compared using the carbon balance for the wood products (Figure 7.10). The emissions from forest management operations and forest industry (section 7.3.1) have been subtracted from the balance of sinks and sources in/from wood products (section 7.3.2). The species respond quite differently to the three scenario factors: the largest change in the carbon balance of the forest-wood chain occurred when log assortments were changed for Scots pine. The carbon balance of the Norway spruce forest-wood chain showed smaller response to changes in the log assortment, but was more sensitive to changes in saw milling efficiency and climate change scenarios. Thus, the relative importance of the three factors was:

- Ø for Scots pine LAT > SL > Climate
- Ø for Norway spruce SL > Climate > LAT

7.4 Discussion

The scenario study showed that climate change induced changes in forest growth and timber quality affect the stocks and fluxes of carbon in wood products. Increased fellings due to higher increment and demand for wood products under the a1 and a2 climate scenarios increase the carbon sink in the wood product pools. Even larger changes in the wood product carbon balance result from changes in the process efficiency in saw mills, and for Scots pine, from changes in the allocation of wood between logs and pulp wood. Changes in timber quality impact the carbon balance through shifting shares of quality solid timber products with longer life time. The large sensitivity of Scots pine to the log assortments is due to the fact that the chemical pulping process produces a lot of black liquor which is burned as bio-energy and thereby returns carbon quickly into the atmosphere.

We investigated a broad range of scenarios. But which scenarios are more likely than others? If climate change results in higher growth rates in Nordic countries and most other parts of Europe (Schröter et al., Science paper in preparation), it would be conceivable that timber quality would tend to decline. Normally, slow growth rates are beneficial for timber quality, and the projected increases in climate variability and extremes could result in more irregular tree ring widths, which are problematic for high quality uses of the wood. If we thus assume that log assortments would shift towards more pulp and paper, would it be possible to balance the effect on the carbon balance by more efficient saw milling technology? In the case of Norway spruce this might be possible, as a 5% increase in saw milling efficiency would approximately balance the impact of a 20% shift in log assortments towards pulp & paper and particle boards. According to the a1 and a2 climate scenarios, increased harvest volumes would enable the forest industry to maintain the production of sawn timber at comparable level, even with 20% decreasing share of saw timber assortments. Only in the case of combined negative effects of lower log assortments and less saw mill efficiency because of declining timber quality under climate change there would be no possibility to mitigate the negative impacts of climate change on the saw mill industry. It would be important to reassess the scenario impacts with the fully coupled simulation models, because only more detailed forest growth models, as originally planned in the MEFYQUE approach, could project how strongly timber quality would really be affected by the changing climatic conditions.

For the forest industry sector as a whole, the increased growth rates under climatic change would overall result in favourable production conditions in Southern Finland. The impact of climate change on growth rates was projected to be positive for the carbon balance in Southern Finland for both species. However, the sensitivity of spruce was larger than for pine. Towards the end of the simulation period, demand for spruce wood could not be met under most climate scenarios and therefore the carbon sink in Norway spruce wood products diminished. It should be noted that the shift from spruce to pine wood in most scenarios for 2040 and especially 2050 did affect the overall carbon balances of the wood products because of the contrasting allocation to product lines between both species.

In our carbon balance calculation for the wood products we did not consider possible substitution effects of fossil fuels replacement with bio-energy produced from wood residues like black liquor or saw dust (cf. (Marland and Schlamadinger 1995; Schlamadinger and Marland 1996). Taking into account energy substitution would significantly improve the carbon balance of the Scots pine forest wood chain and the negative impact of log assortment changes would be reversed. It is recommended to include the substitution effect in a further scenario analysis, because the net impact on the GHG balance is important and the bio-energy option allows generating multiple mitigation potentials while the sink in the wood products will ultimately saturate (Schlamadinger and Marland 1996).

7.5 References

Berg, S. and Karjalainen, T. (2003). Comparison of greenhouse gas emissions from forest operations in Finland and Sweden. *Forestry*. **76:** 271-284.

Burschel, P., Kürsten, E. and Larson, B. (1993). Die Rolle von Wald und Forstwirtschaft im Kohlenstoffhaushalt - Eine Betrachtung für die Bundesrepublik Deutschland*. Forstliche Forschungsberichte München*. **126:** 135.

Carlson, E. and Heikkinen, P. (1998). Energy consumption by the Finnish pulp and paper industry and comparison of electricity prices in certain European countries. [In Finnish]. *Report*, Finnish Pulp and Paper Research Institute, Helsinki.

Eggers, T. 2002. The Impacts of Manufacturing and Utilisation of Wood Products on the European Carbon Budget. European Forest Institute, Joensuu, Finland, Internal Report. 9, p. 90.

Eggers, T., Meyer, J. and Lindner, M. (in press). Modelling impacts of climate change in timber quality on a regional level - The MEFYQUE upscaling approach. *EFI report*, European Forest Institute, Joensuu.

Gjesdal, S., Flugsrud, K., Mykkelbost, T. and Rypdal, K. (1996). A balance of use of wood products in Norway - Part I. Norwegian Pollution Control Authority, Olso, *SFT Report*. *96:04*, 54 pp.

Hashimoto, S., Nose, M., Obara, T. and Moriguchi, Y. (2002). Wood products: potential carbon sequestration and impact on net carbon emissions of industrialized countries. *Environmental Science & Policy*. **214:** 1-11.

Heath, L., Birdsey, R., Row, C. and Plantinga, A. (1996). Cabon pools and fluxes in U.S. forest products. In: *Forest ecosystems, forest management and the global carbon cycle* (Eds. M. Apps and D. Price.) Springer, Berlin, pp. 271-278.

Houllier, F., Leban, J.M and Colin, F. (1995). Linking Growth Modeling to Timber Quality Assessment for Norway Spruce. *Forest Ecology and Management*. **74:** 91-102.

Image Team 2001 (2001). The IMAGE 2.2 implementation of the SRES scenarios: A comprehensive analysis of emissions, climate change and impacts in the 21st century. *Main disc.* National Institute for Public Health and the Environment, Bilthoven, the Netherlands.

Karjalainen, T. and Asikainen, A. (1996). Greenhouse gas emissions from the use of primary energy in forest operations and long-distance transportations of timber in Finland. *Forestry*. **69:** 215-228.

Karjalainen, T., Kellomäki, S. and Pussinen, A (1994). Role of wood-based products in absorbing atmospheric carbon. *Silva Fennica*. **28:** 67-80.

Karjalainen, T., Pussinen, A., Liski, J, Nabuurs, G.J., Eggers, T., Lapveteläinen, T. and Kaipainen, T. (2003). Scenario analysis of the impacts of forest management and climate change on the European forest sector carbon budget. *Forest Policy and Economics*. **5:** 141-155.

Karjalainen, T., Pussinen, A., Liski, J., Nabuurs, G.J., Erhard, M., Eggers, T., Sonntag, M. and Mohren, F. (2002). An approach towards an estimate of the impact of forest management and climate change on the European forest sector carbon budget: Germany as a case study. *Forest Ecology and Management*. **162:** 87-103.

Kellomäki, S., Ikonen, V., Peltola, H. and Kolström, T. (1999). Modelling the structural growth of Scots pine with implications for wood quality. *Ecological Modelling*. **122:** 117-134.

Koivisto, P. (1959). Kasvu- ja tuottotaulukoita (Growth and yield tables). Finnish Forest Research Institute, Helsinki, Finland.

Lehtilä, A. 1995. New energy technologies and emission reduction potential for Finland. *Report*, Technical Research Centre of Finland (VTT), Espoo.

Lindner, M., Lasch, P. and Erhard, M. (2000). Alternative forest management strategies under climatic change - prospects for gap model applications in risk analyses. *Silva Fennica*. **34:**101-111.

Liski, J., Pussinen, A., Pingoud, K. Mäkipää, R. and Karjalainen, T. (2001). Which rotation length is favourable to carbon sequestration? *Canadian Journal of Forest Research*. **31:** 2004-2013.

Mäkelä, A. and Mäkinen, H. (2003). Generating 3D sawlogs with a process-based growth model. *Forest Ecology and Management.* **184:** 337-354.

Marland, G. and Schlamadinger, B. (1995). Biomass fuels and forest-management strategies: How do we calculate the greenhouse-gas emissions benefits? *Energy.* **20:**1131-1140.

Mitchell, T., Carter, T., Jones, P., Hulme, M. and New, M. (2004). A comprehensive set of high-resolution grids of monthly climate for Europe and the globe: the observed record (1901-2000) and 16 scenarios (2001-2100). In: Tyndall Centre Working Paper. Tyndall Centre for Climate Change Research. 30 pp.

Nabuurs, G.J., Päivinen, R., Pussinen, A. and Schelhaas, M.J. (2003). Development of European forests until 2050 - a projection of forests and forest management in thirty countries. In: *European Forest Institute Research Report*. Brill, Leiden, Boston, Köln. 255 pp.

Nabuurs, G.J., Pussinen, A., Liski, J. and Karjalainen, T. (2001). Upscaling based on forest inventory data and EFISCEN. In: *Long-term effects of climate change on carbon budgets of forests in Europe* (Eds. K. Kramer and G.M.J. Mohren). *Alterra*, *Green World Research*, Wageningen.

Nabuurs, G.J., Schelhaas, M.J. and Pussinen, A. (2000). Validation of the European Forest Information Scenario Model (EFISCEN) and a projection of Finnish forests. *Silva Fennica*. **34:** 167-179.

Nabuurs, G.J. and R. Sikkema 2001. International trade in wood products: Its role in the land use change and forestry carbon cycle. Climatic Change. 49:377-395.

Nakicenovic, N. and Swart, R. (2000). Special Report on Emissions Scenarios. Cambridge University Press, Cambridge, United Kingdom.

Niles, J.O. and Schwarze, R. (2001). The value of careful carbon accounting in wood products. *Climatic Change*. **49:** 371-376.

Päivinen, R., Nabuurs, G.J. Lioubimow, A. and Kuusela, K. (1999). The state, utilisation and possible future development of Leningrad region forests, Joensuu, Finland, *EFI Working Paper. 18*, European Forestry Institute, Joensuu, Finland. 59 pp.

Peltola, A. (2004). Metsätilastollinen vuosikirja 2004. Metsäntutkimuslaitos, Helsinki, 416 pp.

Prentice, I.C., Cramer, W., Harrison, S.P., Leemans, R., Monserud, R.A. and Solomon, A.M. (1992). A global biome model based on plant physiology and dominance, soil properties and climate. *Journal of Biogeography*. **19:** 117-134.

Sallnäs, O. 1990. A matrix model of the Swedish forest. *Studia Forestalia Sue*cica. 183:23.

Schelhaas, M.J., Varis, S., Schuck, A. and Nabuurs, G.J. (1999). EFISCEN's European Forest Resource Database. *Report*, European Forest Institute, Joensuu, Finland.

Schlamadinger, B. and Marland, G. (1996). The role of forest and bioenergy strategies in the global carbon cycle. *Biomass and Bioenergy*. **10:** 275-300.

Sitch, S., Smith, B., Prentice, I.C., Arneth, A., Bondeau, A., Cramer, W. and 6 other authors. (2003). Evaluation of ecosystem dynamics, plant geography and terrestrial carbon cycling in the LPJ dynamic global vegetation model. *Global Change Biology*. **9:** 161-185.

Skog, K.E. and Nicholson, G.A. (2000). Carbon Sequestration in Wood and Paper Products. *USDA Forest Service Gen. Tech. Rep*. *RMRS-GTR*-**59:** 79-88.

Smith, B., Prentice, I.C. and Sykes, M.T. (2001). Representation of vegetation dynamics in the modelling of terrestrial ecosystems: comparing two contrasting approaches within European climate space. *Global Ecology and Biogeography Letters*. **10:** 621-637.

Systat 2004. SigmaPlot 2004 for Windows 9.01 (TrialVersion). Systat Software, Inc.

TAPIO 1994. Tapion taskukirja. Metsäkeskus Tapio, Helsinki. 640 pp.

Winjum, J.K., Brown, S. and Schlamadinger, B. (1998). Forest harvests and wood products: Sources and sinks of atmospheric carbon dioxide. *Forest Science*. **44:** 272-284.

8. The Mefyque Database

Main Contributor::
Tracy Houston

See also accompanying CD for Database

8.1 Data Collection

Data collection was done according to the sampling protocols (Appendix E). Data was forwarded to the Database Manager who performed quality checks and contacted the originator of the data about outliers/implausible values. Where possible, these were corrected. Data points that were clearly impossible but for which correction could not be made were removed. Only data that were specifically collected for the MEFYQUE project are included within the database; flux and meteorological data, and data from the tertiary sites are already stored within other structures and do not need to be duplicated here.

8.1.1 Data Types

The database contains 3 main types of data:

- Site parameters
  This includes location, plot size, species, ground vegetation, elevation, precipitation and soil type.
- Standing crop data
  These are basic mensurational parameters (height, diameter, upper/lower crown, crown width, tree lean) of the selected plot, plus more detailed measurements for the trees at each site that were felled. This includes taper and branch length/weights.
- Destructive data
  Logs were sawn into battens and these were subjected to a variety of stress tests including spring, twist, bow, MOE and MOR. Moisture content was logged. Green/dry weights were recorded for various tissue types. Discs were sent to Berlin for C/N analysis. Tree rings and wood anatomy were also measured.

Table 8.1: Measurement types stored in the database

Measurement type	FR01	FR02	FR03	FR04	FR05	FR06	FR07	FR08	FR10	IT01	IT02	IT03	IT04	UIA01	TUB01	TUB02
C/N data (bark)	ü		ü	ü	ü		ü	ü	ü					ü		ü
C/N data (branches)	ü	ü	ü	ü	ü	ü		ü	ü							ü
C/N data (cones)																ü
C/N data (heartwood)	ü	ü	ü	ü	ü	ü	ü	ü	ü					ü		ü
C/N data (leaves)	ü				ü											
C/N data (needles)		ü	ü	ü		ü	ü	ü	ü							ü
C/N data (roots)	ü	ü	ü	ü		ü		ü	ü			ü		ü		ü
C/N data (sapwood)	ü	ü	ü	ü	ü	ü	ü	ü	ü					ü		ü
C/N data (transient zone)	ü				ü			ü	ü							
Green/dry weights (Branch)	ü	ü	ü	ü	ü	ü	ü	ü	ü							
Green/dry weights (Disk)	ü	ü			ü	ü	ü	ü	ü							
Green/dry weights (Leaves)	ü				ü											
Green/dry weights (Needles)		ü	ü	ü		ü	ü	ü	ü							
Green/dry weights (Root)	ü	ü			ü		ü	ü	ü							
Log data - bark thickness	ü	ü	ü	ü	ü	ü	ü	ü	ü	ü	ü	ü				
Log data - mid diameter	ü	ü	ü	ü	ü	ü	ü	ü	ü	ü	ü	ü	ü			
Log data - quality score	ü	ü	ü	ü	ü	ü	ü	ü	ü	ü	ü	ü	ü	ü		
Stress test - Bow		ü	ü			ü	ü	ü	ü			ü				
Stress test - MOE		ü	ü			ü	ü	ü	ü			ü				
Stress test - Moisture content		ü	ü			ü	ü	ü	ü			ü				
Stress test - MOR		ü	ü			ü	ü	ü	ü			ü				
Stress test - reaction load		ü	ü			ü	ü	ü	ü			ü				
Stress test - Spring		ü	ü			ü	ü	ü	ü			ü				
Stress test - Twist		ü	ü			ü	ü	ü	ü			ü				
Tree bow												ü	ü			
Tree branch lengths	ü	ü	ü	ü	ü	ü	ü	ü	ü							
Tree branch weights	ü		ü	ü	ü		ü		ü							
Tree crown width										ü	ü				ü	ü
Tree DBH	ü	ü	ü	ü	ü	ü	ü	ü	ü	ü	ü	ü	ü	ü	ü	ü
Tree diameters (sections)	ü	ü	ü	ü	ü	ü	ü	ü	ü	ü	ü	ü	ü	ü		
Tree dominance						ü	ü	ü		ü	ü	ü	ü	ü	ü	ü
Tree ht to 1st dead branch										ü	ü	ü	ü			
Tree lower crown	ü	ü	ü	ü	ü		ü		ü	ü	ü	ü	ü	ü		
Tree ring data	ü	ü	ü	ü	ü	ü	ü	ü	ü	ü	ü	ü				
Tree stem form	ü	ü			ü	ü		ü	ü	ü	ü	ü	ü		ü	ü
Tree stem lean (measured)	ü	ü	ü	ü	ü	ü	ü	ü	ü	ü	ü	ü	ü	ü		
Tree stem lean (scores)	ü	ü			ü	ü	ü	ü	ü						ü	ü
Tree timber height	ü	ü	ü	ü	ü	ü	ü	ü	ü	ü	ü	ü	ü	ü		
Tree total height	ü	ü	ü	ü	ü	ü	ü	ü	ü	ü	ü	ü	ü	ü	ü	ü
Tree upper crown	ü	ü	ü	ü	ü	ü	ü	ü	ü	ü	ü	ü	ü	ü		
Wood anatomy parameters				ü										ü		

Table 8.2: Number of trees measured for each variable/parameter at the project primary sites.

	FR01	FR02	FR03	FR04	FR05	FR06	FR07	FR08.1	FR08.2	FR10	IT01	IT02	IT03	IT04	TUB01	TUB02	UIA01
Stem form	71	7	205	244	29	128	104	99	29	128	72	70	75	85	102	175	79
Dominance class	55	227	208	274	23	145	114	95	27	122	72	70	79	85	102	179	9
Dbh	72	242	213	283	29	154	117	103	31	150	72	70	78	85	102	176	79
Total height	17	18	19	19	16	39	19	18	14	39	27	43	44	51	62	41	79
Timber height	18	27	19	35	14	39	31	20	14	40	19	38	38	19	62	0	9
Height of 1st dead branch	4	8	7	9	3	9	9	8	4	9	8	11	32	16	0	0	0
Height of lower crown	6	18	19	19	15	10	19	18	14	19	19	38	39	19	62	41	4
Height of upper crown	1	18	19	19	12	19	19	18	14	19	19	38	39	19	62	41	4
Crown width	0	10	10	10	10	10	10	10	10	10	10	30	0	0	62	40	0
Crown area	0	0	0	0	0	0	0	0	0	0	0	0	30	10	0	0	0
Tree lean measurement	54	187	195	213	23	117	102	91	23	119	61	61	71	76	0	0	70
Tree lean score	6	8	0	0	6	9	3	6	4	9	0	0	0	0	102	175	0

8.1.2 Database structure

The database was designed in and created using Microsoft™ Access™. This was selected because of its simple, visual user interface and the fact that the program is readily available in most scientific and government organisations.

The database design is broadly based around three levels of measurement: site, tree and sub-tree levels. At the site level, the SITE INFORMATION table contains information about the location, species and type of site (primary/secondary). Linked to this and at the same level of resolution is specific information about tertiary sites (experiment design etc), and vegetation details.

The next level contains the TREE table, and stores information about individual trees selected for detailed measurement within each site. The table contains all those parameters relevant to a whole tree (e.g. DBH, height, stem quality).

Codes (as opposed to measurements) used within the database are suffixed by _C. They are explained by meta-data tables (identified by the prefix REF_).

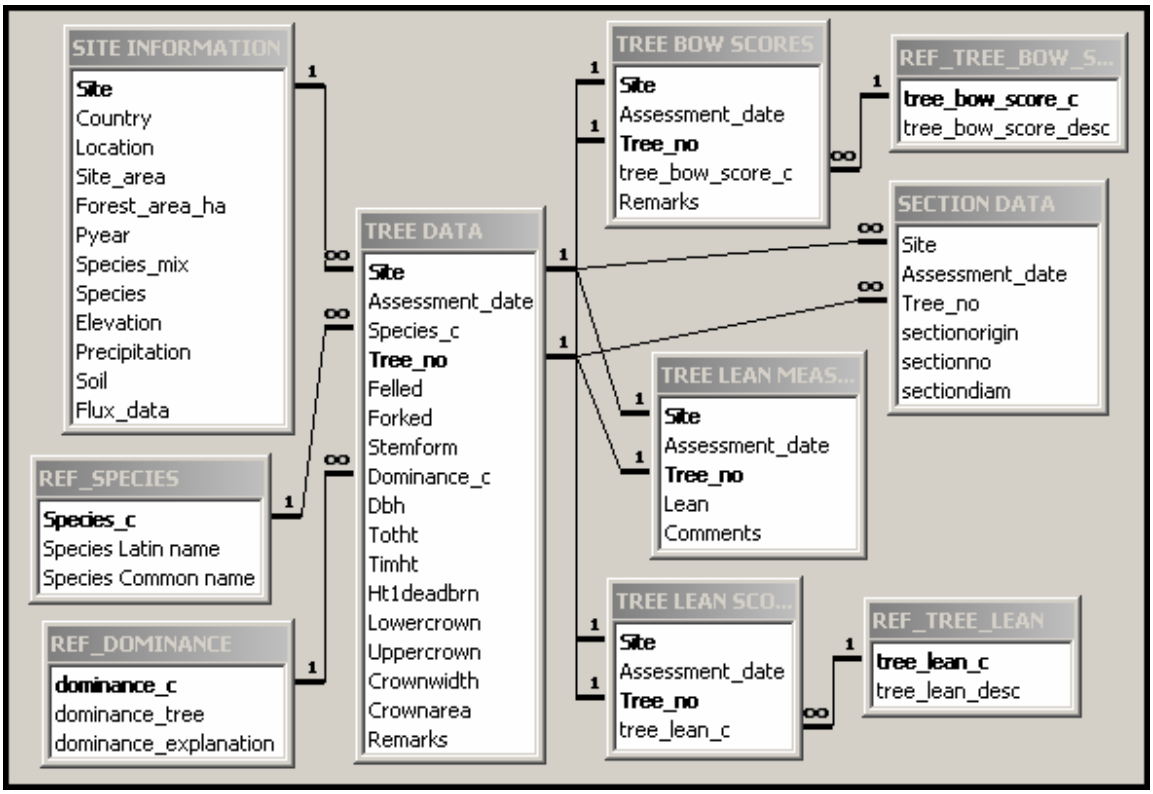

Figure 8.1: SITE and TREE data and relationships

The sub-tree components are stored in separate tables because of the different parameters and identifiers that are required for each part. However, sub-tree parameters data are stored according to the tree from which they are derived, so a composite picture of all parts of any individual tree can easily be built.

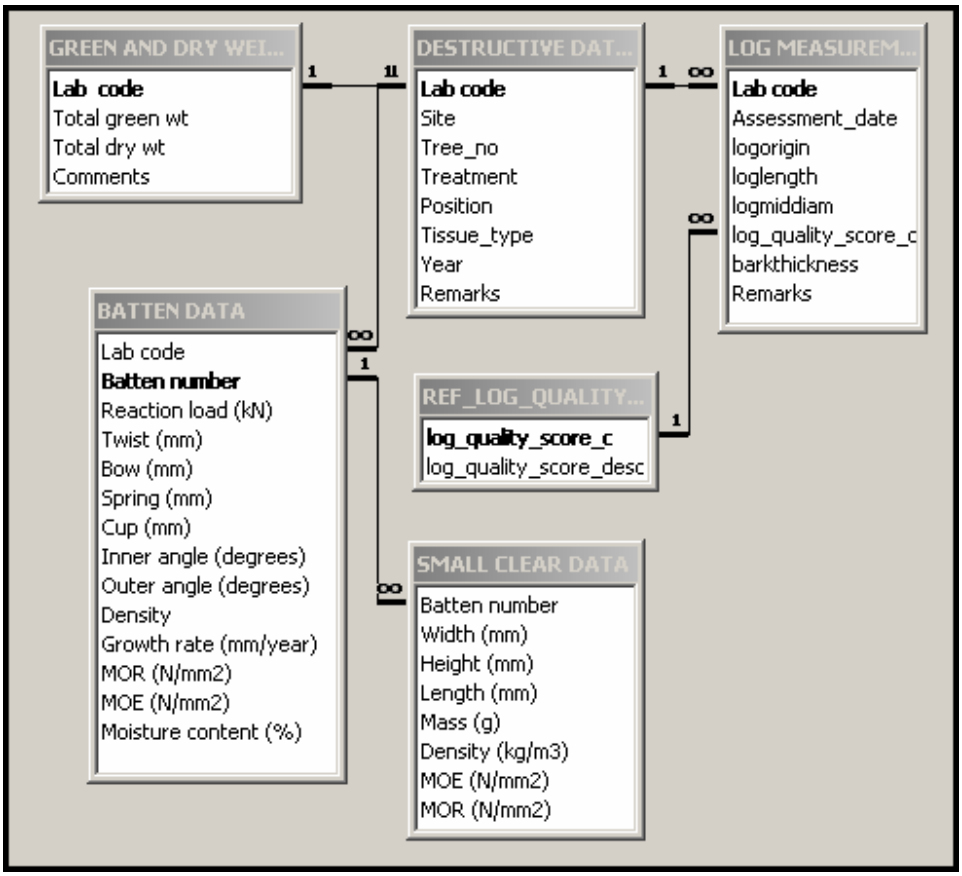

Figure 8.2: Green/dry weights and log measurements

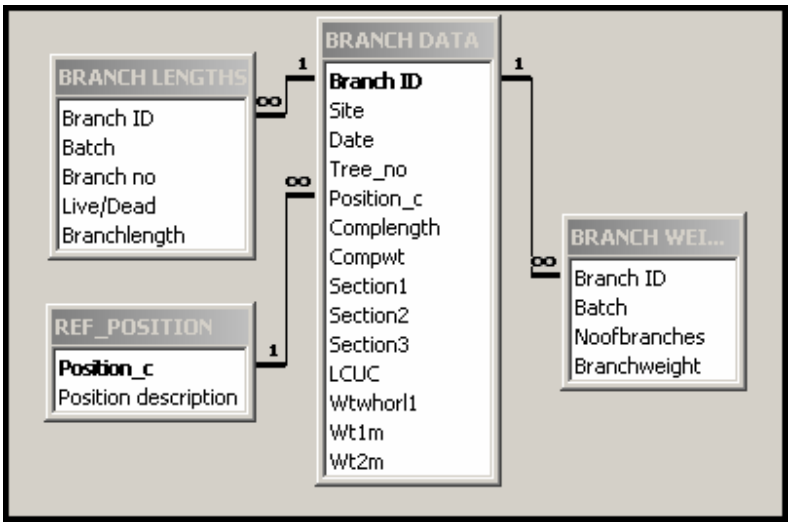

Figure 8.3: Branch weights and lengths

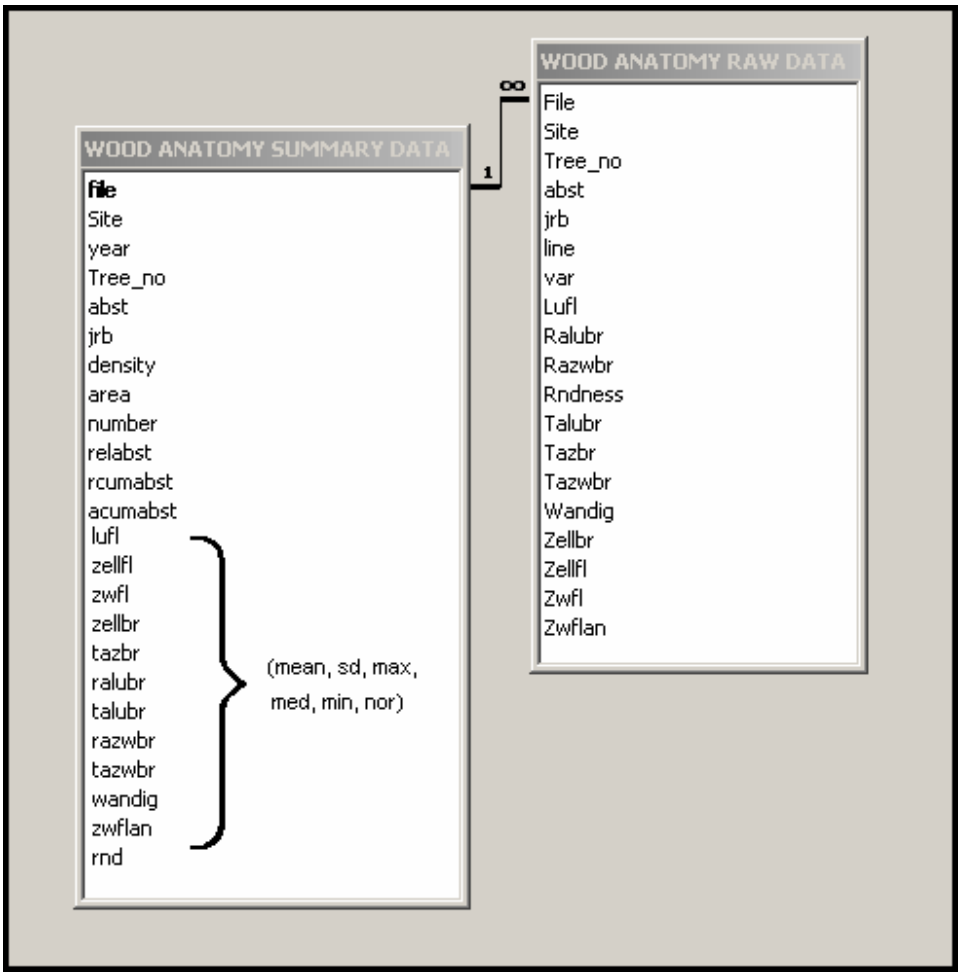

Figure 8.4: Wood anatomy data

8.2 Tree Data Tables

8.2.1 Site Information

Column Name	Description	Data Type	Length	PK
Site		Text	8	PK*
Country		Text	8	
Location		Text	25	
Site area		Number		
Forest area ha	Forest are in hectares	Number		
Pyear	Planting year (if known)	Number		
Species mix	Indication of whether the plot is one (pure) species or a mixture	Text	8	
Species	Main species	Text	10	
Elevation	(metres)	Number		
Precipitation	(mm)	Number		
Soil	General description of dominant soil type	Text	30	
Flux data	Indication of whether flux data collected here.	Text	5	

** PK denotes Primary Key*

8.2.2 Tree Data

Contains all basic mensurational data on a complete tree. Includes general data measured on all trees in the plot as well as the more detailed measurements on those that were felled.

Column Name	Description	Data Type	Length	PK
Site		Text	8	PK
Assessment date		Date/Time		
Species c		Text	5	
Tree_no		Text	5	PK
Felled	Whether the tree was one of the 9 felled in each plot	Text	1	
Forked	Whether the tree is forked (Y/ N) where known	Text	1	
Stemform	Stem form score	Text	2	
Dominance c	Dominance class	Number		
Dbh	Diameter at Breast Height	Number		
Totht	Total Height	Number		
Timht	Timber height (ht at which diameter is 7cm)	Number		
Ht1deadbrn	Height to first dead branch	Number		
Lower crown	Height to 1st live branch	Number		
Upper crown	Height to 1st live whorl	Number		
Crown width	Width of crown	Number		
Crown area	Area of crown	Number		
Remarks		Text	50	

8.2.3 Tree Bow Scores

These assessments were only taken on some of the Italian sites and give an indication of the straightness of the stem (differs slightly from the Stem Form score contained within the TREE table)

Column Name	Description	Data Type	Length	PK
Site		Text	8	PK
Assessment date		Date/Time		
Tree_no		Number		PK
Tree_bow_score_c		Number		
Remarks		Text	25	

8.2.4 Tree Lean Measurements

For some sites it was possible to measure the degree of lean precisely (cm distance from base of tree to a vertical line taken from a point on the stem 4m above ground). Where the equipment was not available for measuring lean a score was assigned instead (table LEAN SCORES below).

Column Name	Description	Data Type	Length	PK
Site		Text	8	PK
Assessment date		Date/Time		
Tree_no		Text		PK
Lean		Number		
Comments		Text		

8.2.5 Tree Lean Scores

Column Name	Description	Data Type	Length	PK
Site		Text	8	PK
Assessment date		Date/Time		
Tree_no		Text	5	PK
Tree_lean_c		Number		

8.2.6 Section Data

Diameters were measured every metre up the tree to allow calculations of taper to be made.

Column Name	Description	Data Type	Length	PK
Site		Text	8	
Assessment date		Date/Time		
Tree_no		Text		
Section origin	Stem: the section comes from the main stem of the tree. Fork: the section comes from one of the branches of the tree.	Text		
Section no	For Italian sites, also represents height of section above ground.	Number		
Section diam		Number		

8.3 Tree Branch data

8.3.1 Branch Data

Branch data were collected according to the sampling protocols (Appendix E).

Column Name	Description	Data Type	Length	PK
Branch ID		Text	15	PK
Site		Text	8	
Date		Date/Time		
Tree_no		Number		
Position_c	Code for position: L(ower), M(iddle), U(pper)	Text	1	
Complength	Component length	Number		
Compwt	Total weight of component	Number		
Section1	1st section length	Number		
Section2	Mid section (1m)	Number		
Section3	Top section length	Number		
LCUC	Length of 1st live branch to live crown	Number		
Wtwhorl1	Weight whorl 1	Number		
Wt1m	Weight of 1st metre	Number		
Wt2m	Weight of 2nd metre	Number		

8.3.2 Branch Lengths

Column Name	Description	Data Type	Length	PK
Branch ID		Text	15	PK
Batch	Contain branches from 1 or more whorls	Number		
Branch no		Number		
Live/Dead	L=Live, D=Dead	Text	1	
Branch length		Number		

8.3.3 Branch Weights

Column Name	Description	Data Type	Length	PK
Branch ID		Text	15	PK
Batch	Contain branches from 1 or more whorls	Number		
No of Branches	Number of branches in that batch	Number		
Branch Weight	Total weight of branches	Number		

8.4 Log Quality and destructive data

8.4.1 Destructive data ID

This table gives identifying codes to the parts of felled trees used in the various destructive analyses (eg fresh/dry weights, strength tests etc).

Column Name	Description	Data Type	Length	PK
Lab code		Text	15	PK
Site		Text	8	
Tree_no		Text	5	
Treatment		Text	25	
Position		Text	25	
Tissue_type		Text	12	
Year		Text	12	
Remarks		Text	50	

8.4.2 Green and Dry Weights

Column Name	Description	Data Type	Length	PK
Lab code		Text	15	PK
Total green wt		Number		
Total dry wt		Number		
Comments		Text	50	

8.4.3 Small Clear Data

Column Name	Description	Data Type	Length	PK
Site		Text	50	
Code		Number		
Width (mm)		Number		
Height (mm)		Number		
Length (mm)		Number		
Mass (g)		Number		
Density (kg/m3)		Number		
MOE (N/mm2)		Number		
MOR (N/mm2)		Number		

8.4.4 Batten Data

Column Name	Description	Data Type	Length	PK
Lab code		Text	15	PK
Batten number		Number		PK
Reaction load (kN)	Force in KiloNewtons to deflect the batten by a fixed displacement; used to determine the grade of the batten	Number		
Twist (mm)	Amount the batten distorted (twisted) over a 2m length during unconstrained kiln drying	Number		
Bow (mm)	Amount the batten distorted (bowed) over a 2m length during unconstrained kiln drying	Number		
Spring (mm)	Amount the batten distorted (sprung) over a 2m length during unconstrained kiln drying	Number		
Cup (mm)		Number		
Inner angle (degrees)		Number		
Outer angle (degrees)		Number		
Density		Number		
Growth rate (mm/year)		Number		
MOR (N/mm2)	Specimen modulus of rupture	Number		
MOE (N/mm2)	Specimen modulus of rupture	Number		
Moisture content (%)	Moisture content of the batten after kiln drying	Number		

8.4.5 Log Measurements

Column Name	Description	Data Type	Length	PK
Lab code		Text	15	PK
Assessment date		Date/Time		
Log origin		Number		
Log length		Number		
Log mid diam		Number		
Log quality score c		Number		
Bark thickness		Number		
Remarks		Text	100	

8.5 Wood anatomy data

8.5.1 Wood Anatomy Raw Data

Wood anatomy parameters were measured in Berlin. A variety of statistics were calculated from the raw data and stored in table WOOD ANATOMY SUMMARY DATA.

Column Name	Description	Data Type	Length	PK
File		Text		
Site		Text		
Tree_no		Number		
Abst		Number		
Jrb	Tree ring width of the running year	Number		
Line		Number		
Var	Repetition number	Number		
Lufl	Lumen area	Number		
Ralubr	Radial lumen width	Number		
Razwbr	Double width of tangential cell wall	Number		
Rndness	Roundness = perimeter² / 4*pi*area*1.067	Number		
Talubr	Tangential lumen width	Number		
Tazbr	Tangential cell width	Number		
Tazwbr	Double width of radial cell wall	Number		
Wandig	Mork factor (radial lumen width divided by double width of tangential cell wall)	Number		
Zellbr	Radial cell width	Number		
Zellfl	Cell area	Number		
Zwfl	Cell wall area	Number		
Zwflan	Ratio of cell wall area to total cell area	Number		

8.5.2 Wood Anatomy Summary Data

Column Name	Description	Data Type	Length	PK
File	File	Text	12	PK
Site	Site	Text	8	
Year	Running year	Number		
Tree_no	Tree number	Number		
Abst	Distance from tree ring border	Number		
Jrb	Tree ring width of the running year	Number		
Density	Density (lumen pixel per total pixel within measuring frame)	Number		
Area	Area of measuring frame	Number		
Number	Number of measured cells	Number		
Relabst	Relative distance to tree ring border	Number		
Rcumabst	Relative distance to tree ring border + position in last ten tree rings	Number		
Acumabst	Distance to tree ring border 1991/1992	Number		
Mw_xxxx	Mean of variable	Number		
St_xxxx	Standard deviation of variable	Number		
Max_xxxx	Maximum of variable	Number		
Med_xxxx	Median of variable	Number		
Min_xxxx	Minimum of variable	Number		
Nor_xxxx	Testvariable for normality of variable	Number		

8.6 Other data tables

8.6.1 C/N Data

Disks were sent to Berlin for Carbon/Nitrogen analysis.

Column Name	Description	Data Type	Length	PK
Site		Text	15	PK
Tree_No		Text	5	
Sample No	Most tissue types were sampled twice; occasionally an extra pair of samples was taken to confirm values	Number		
Extra_info	The TUB tree that was sampled was catogorised in more detail than the other felled trees; extra descriptive info is in this field	Text	25	
Position	Combines both the position and the type of tissue sampled; eg. Stem (transient zone)	Text	25	
C		Number		
N		Number		
Comments		Text	25	

8.6.2 FR Fork Lengths

This table gives the total lengths of the forks from those FR trees that were forked.

Column Name	Description	Data Type	Length	PK
Site		Text	8	PK
Tree_no		Number		
Section origin	Identifier of the fork	Text	5	
Fork length		Number		

8.6.3 Root Weights

(2 Italian sites only)

Column Name	Description	Data Type	Length	PK
Site		Text	8	
DBH	DBH of the tree whose roots were sampled	Number		
Sample	Sample identifier	Text	10	
Horizon	Soil horizon from which roots were sampled	Text	4	
Alive/Dead	A=Alive; D=Dead	Text	1	
Size Class	Roots were divided into 3 size classes: <2mm, 2-5mm, >5mm	Text	5	
Initial weight	Fresh weight	Number		
Final weight	Dry weight	Number		

8.6.4 Vegetation Details

Column Name	Description	Data Type	Length	PK
Site		Text	8	PK
Tree Species		Text	50	
Other tree species		Text	50	
Understorey ground veg		Text	100	

8.6.5 Tree Rings

Discs were cut and sent to Ghent for tree ring analysis.

Column Name	Description	Data Type	Length	PK
Site		Text	8	PK
Tree		Text	5	PK
Height		Number		PK
Radius		Text	1	PK
Year		Number		PK
Early width		Number		
Late width		Number		
Total ring width		Number		

8.6.6 Tertiary Sites

Column Name	Description	Data Type	Length	PK
Location	Name of site	Text	25	
Country		Text		
Elev CO2 conc	Concentration of CO2 in the elevated chambers	Number		
Enrichment type		Text	25	
Reps	Number of replications	Number		
Plot size		Number		
Pyear	Planting year	Number		
Enrich yrs	Number of years in which trees grown in enriched conditions	Number		
Species		Text		
Expt start	Starting year of experiment	Number		
Harvest date	Date of harvest	Text		
Tree height	Average height of trees at harvest	Text		
Soil		Text		
Soil richness		Text		

8.7 Reference Tables

These describe the codes used elsewhere in the database. Any variable with the form XXX_C is a score or a code and has a corresponding reference table of the form REF_XXX.

8.7.1 REF_DOMINANCE

Column Name	Description	Data Type	Length	PK
Dominance_c	Code (1-5)	Number		PK
Dominance_tree	Tree dominance class (Dominant, Co-dominant, Sub-dominant, Suppressed, Dead)	Text	20	
Dominance_explanation	Full description of each dominance class	Text	220	

8.7.2 Ref_Log_Quality_Score

Column Name	Description	Data Type	Length	PK
Log_quality_score_c	Code (1-4)	Number		PK
Log_quality_score_desc	Definitions: 1=Straight log; 2=Maximum deviation does not exceed 1cm over 1 metre length; 3= Maximum deviation exceeds 1cm over 1 metre length; 4= Log bows in more than one direction.	Text	75	

8.7.3 Ref_Position

Column Name	Description	Data Type	Length	PK
Position_c	Code (B,L,M,U)	Text	1	PK
Position_description	Definitions: B=Bottom; L=Lower; M=Middle; U=Upper.	Text	8	

8.7.4 Ref_Species

Column Name	Description	Data Type	Length	PK
Species_c	Code	Text		PK
Species Latin name		Text	50	
Species common name		Text	50	

8.7.5 Ref_Tree_Bow_Score

Column Name	Description	Data Type	Length	PK
Tree_bow_score_c	Code (0,1,2,3)	Number		PK
Tree_bow_score_desc	Definitions: 0= Straight tree; 1= Simple lean (straight but leaning); 2=One bow; 3= S shape (2 or more bows)	Text	50	

8.7.6 Ref_Tree_Lean_Score

Column Name	Description	Data Type	Length	PK
Tree_lean_c	Code (1,2,3)	Number		PK
Tree_lean_desc	Definitions: 1= Deviation from vertical 0-10cm; 2= Deviation from vertical 11-20cm; 3= Deviation from vertical >20cm	Text	50	

9 Technical Transfer

Main Contributor:
Tim Randle

9.1 CONFERENCE

An international conference was held at 28-30 September 2004 at Heriot-Watt University, Edinburgh. *The Forestry Woodchain* Conference attracted over 120 international participants, primarily from Europe, but with also from further afield (eg Canada, New Zealand). Approximately 30 oral presentations were made, together with 50 poster presentations in addition.

The conference was primarily a result of presenting results from 3 EU projects, working on various aspects of the wood chain. (MEFYQUE, COMPRESSION WOOD (QLK5-2000-001) and, STRAIGHT (QLK5-2000-00276).

The conference was divided into 7 sessions to cover aspects of the woodchain, with invited speakers introducing each topic.

- Wood Properties
- Quality in standing Timber
- Laboratory and Industrial Processes
- Timber Drying and Distortion
- Climate change Impacts
- The Forestry Woodchain
- Grading and Forecasting

Abstracts accepted for the conference were edited printed and bound, and made available for delegates on the first day of the conference.

An Electronic (PDF) form of the publication is available and can be found on the accompanying CD.

9.1.1 Conference and Workshop Participation

In addition to the *Forestry Woodchain Conference*, members of the project consortium attended several conferences and workshops in relation to their work within the project, often making presentations, displaying posters and disseminating the results.

September 2001

Cuelemans, R. Symposium: Forest and the land-atmosphere interface. Edinburgh

March 2002

Cuelemans, R. CarboEurope Conference, Budapest

Curiel-Yuste, J. CarboEurope Conference, Budapest

Carrara, A., CarboEurope Conference, Budapest

Janssens, I., CarboEurope Conference, Budapest

May 2002

Maun K, Workshop for Sawmillers, Edinburgh, UK

June 2002

Deckmyn, G., Workshop on Reality, Models and Parameters and Estimation (IUFRO), Sesimbra, Portugal

March 2003

Curiel-Yuste, J., The continental carbon cycle (CarboEurope) Lisbon, Portugal

April 2003

Deckmyn, G., Carbon Balance in Forest Biomes (Society of Experimental Biology), Southampton, UK

Overdiek, D., Experimental Ecology Working group (Society Ecology), Stuttgart-Hohenheim, Germany

Ziche, D., Experimental Ecology Working group (Society Ecology), Stuttgart-Hohenheim, Germany

September 2003

Overdiek, D., Ecological Society meeting, Halle/Salle, Germany.

Ziche, D., Ecological Society meeting, Halle/Salle, Germany

March 2004

Scarascia-Mugnozza, G. Short- and long-term effects of elevated atmospheric CO2 on managed ecosystems, Ascona, Switzerland

Calfpietra, C., Short- and long-term effects of elevated atmospheric CO2 on managed ecosystems, Ascona, Switzerland

Moscatelli, C., Short- and long-term effects of elevated atmospheric CO2 on managed ecosystems, Ascona, Switzerland

De Angelis, P., Short- and long-term effects of elevated atmospheric CO2 on managed ecosystems, Ascona, Switzerland

April 2004

Deckmyn, G., International Conference on Forest Modelling (IUFRO), Vienna

Randle, T., International Conference on Forest Modelling (IUFRO), Vienna

August 2004

De Angelis, P., Forests Under Changing Climate, Enhanced UV And Air Pollution (IUFRO), Oulu, Finland

Calfpietra, C., Forests Under Changing Climate, Enhanced UV And Air Pollution (IUFRO), Oulu, Finland

Participation in several COST actions and meetings:

- E9: Life Cycle Assessment of Forestry and Forest Products
- E13: Wood adhesion and glued products
- E15: Advances in the drying of wood
- E21: Contribution of Forests and Forestry to Mitigate Greenhouse Effects
- E44: Wood Processing Strategy

9.2 Project Web-Site

The project web-site has been and continues to be hosted by EFI, and has periodically been updated

http://www.efi.fi/projects/mefyque/

9.3 Publications

A number of scientific papers are still in preparation as results from the project are further anaylsed.

9.3.1 Scientific papers

Submitted/in press

- Curiel Yuste, J., Janssens, I.A. and Ceulemans, R. Calibration and validation of an empirical approach to model soil CO_2 efflux in a deciduous forest. Accepted in *Biogeochemistry* (special issue: *Recent Advances in Soil Respiration*).
- Curiel Yuste, J., Konopka, B., Coenen, K., C. W. Xiao, Janssens, I.A. and Ceulemans, R. Contrasting differences in NPP and Carbon distribution between neighbouring stands of *Quercus robur* (L.) and *Pinus sylvestris* (L.). Accepted in *Tree Physiology*.
- Curiel Yuste, J., Nagy, M., Janssens, I.A., Carrara, A. and Ceulemans, R. Soil respiration in a mixed temperate forest and its contribution to total ecosystem respiration. Accepted in *Tree physiology*
- Deckmyn, G., Evans, S. P. and Randle, T.J. Refined pipe theory for mechanistic modelling of wood development. *Tree physiology*, submitted
- Evans, S., Randle, T., Henshall, P., Arcangeli, C., Pellenq, J., Lafont, S. and Vials, C. Recent Advances in the mechanistic modelling of forest stand and catchments. In: *Forest Research Annual Report and Accounts 2003-2004.* 98-111, The Stationery Office, Edinburgh, UK.
- Hibbard, K.H., Law, B.E, Reichstein, M., Sulzman, J., Aubinet, M., Baldocchi, D. and 28 other authors. An Analysis of Soil Respiration Across Northern Hemisphere Temperate Ecosystems. Accepted in *Biogeochemistry* (special issue: *Recent Advances in Soil Respiration*).
- OverDieck, D., Ziche, D., Böttcher-Jungclaus, K. Impact of elevated CO2 Concentration and temperature increase on growth and the vessel/parenchyma content in stem wood of juvenile European beech. Submitted, Tree Physiology

2004

- Carrara, A., Janssens, I.A. , Curiel Yuste, J. and Ceulemans, R. (2004). Seasonal changes in photosynthesis, respiration and NEE of a mixed temperate forest. *Agricultural and Forest Meteorology,* **126**(2004) 15-31
- Curiel Yuste, J., Janssens, I.A. Carrara A. and Ceulemans, R. (2004). The annual Q10 of soil respiration reflects plant phenological patterns as well as temperature sensitivity. *Global Change Biology* **10:** 161-169.
- Deckmyn, G., Laureysens, I. Garcia, J., Muys, B. and Ceulemans, R. (2004). Poplar growth and yield in short rotation coppice: model simulations using the process model SECRETS. *Biomass and Bioenergy* **26:** 221-227.
- Deckmyn, G., Muys, B. Garcia-Quiano, J. and Ceulemans, R. (2004). Carbon sequestration following afforestation of agricultural soils: comparing oak/beech forest to short rotation poplar coppice combining a process and a carbon accounting model. *Global Change Biology* **10:** 1482-1491.
- Overdieck, D. (2004): Effects of elevated CO_2 concentration on stomatal conductance and respiration of beech leaves in darkness. In: Forests at the Land-Atmosphere Interface, eds M. Mencuccini, J. Grace, J. Moncrieff, and K.G. McNaughton. CABI Publishing, Wallingford, UK, 29-35.
- Ziche, D. and Overdieck, D. (2004). CO_2 and temperature effects on growth, biomass production and stem wood anatomy of juvenile Scots pine (*Pinus sylvestris* L.). *Journal of Applied Botany*, **78:** 120-132.

2003

- Anselmi, N., Mazzaglia, A. , Nasini, M. Corvi, R.,Falessi, T. , Vannini, A., Scarascia-Mugnozza, G. De Angelis, P and Sabatti, M. (2003). Influenza dell'incremento della CO_2 atmosferica sugli attacchi di patogeni in piante forestali. In: *Società Italiana di Selvicoltura ed Ecologia Forestale,* eds P. De Angelis, A. Macuz, G. Bucci and G. Scarascia*, Atti SISEF* **3**: 363-367.
- Calfapietra, C., De Angelis, P., Kuzminsky, E. and Scarascia-Mugnozza, G. (2003). Impact of elevated CO_2 concentration on leaf development in *Populus nigra*, in A "Free Air CO_2 Enrichment" experiment. In: *Società Italiana di Selvicoltura ed Ecologia Forestale,* eds P. De Angelis, A. Macuz, G. Bucci and G. Scarascia *Atti SISEF* **3**: 357-362.
- Calfapietra, C., Gielen, B., Galema, A.N.J., Lukac, M., De Angelis, P., Moscatelli, M.C., Ceulemans, R. and Scarascia-Mugnozza, G. (2003). Free-air CO_2 enrichment (FACE) enhances biomass production in a short-rotation poplar plantation (POPFACE). *Tree Physiology* **23:** 805-814
- Carrara, A., Kowalski, A.S., Neirynck, J., Janssens, I.A., Curiel Yuste, J. and Ceulemans, R. (2003). Net ecosystem CO2 exchange of mixed forest in Belgium over 5 years. *Agricultural and Forest Meteoro*logy **119:** 209-227.
- Cotrufo, M.F., Anniciello, M. and De Angelis, P. (2003). Decomposizione della lettiera di foglie di pioppo in un 'mondo ad elevata CO_2': uno studio nell'ambito del progetto Europeo POPFACE. In: *Società Italiana di Selvicoltura ed Ecologia Forestale,* eds P. De Angelis, A. Macuz, G. Bucci and G. Scarascia, *Atti SISEF* **3**: 375-379.
- Curiel Yuste, J., Janssens, I.A., Carrara, A., Meiresonne, L. and Ceulemans, R. (2003). Interactive effects of temperature and precipitation on soil respiration in a temperate maritime pine forest. *Tree Physiology* **23:** 1263-1270.
- Deckmyn, G., Ceulemans, R., Rasse, D., Sampson, D.A., Garcia, J. and Muys, B. (2003). Modelling the carbon sequestration of a mixed, uneven-aged, managed forest using the process model SECRETS. In: *Modelling Forest Systems* (eds. A.Amaro, D.Reed and P.Soares) CAB international Wallingford, UK, 143-155.
- Del Galdo, I., Squeglia, A., Cotrufo, F., and De Angelis, P. (2003). C sequestration in afforested soils under elevated CO_2 concentration: preliminary results. In*: Proceedings of the first Italian IGBP Conference: " Mediterraneo e Italia nel Cambiamento Globale: un ponte fra scienza e società?* ", Paestum (SA*),* November 2002.
- Gielen, B., Liberloo, M., Bogaert, J., Calfapietra, C., De Angelis, P., Miglietta, F., Scarascia-Mugnozza, G. and Ceulemans, R. (2003). Three years of free-air CO2 enrichment (POPFACE) only slightly affect profiles of light and leaf characteristics in closed canopies of Populus. *Global Change Biology* **9:** 1022-1037.
- Hovenden, M.J. (2003). Photosynthesis of coppicing poplar clones in a free-air CO_2 enrichment (FACE) experiment in a short-rotation forest. *Functional Plant Biology* **30**(4) 391-400.
- Lukac, M., Calfapietra, C. and Godbold, D. (2003). Production, turnover and mycorrhizal colonization of root systems of three *Populus* species grown under elevated CO_2 (POPFACE). *Global Change Biology* **9:** 838-848.
- Moscatelli, M.C., De Angelis P., Vilardo V., Larbi H., Grego S. and Scarascia-Mugnozza G. (2003). Risposte microbiologiche ed ecofisiologiche del suolo in un pioppeto mutliclonale esposto ad un'elevata concentrazione di CO_2 atmosferica: risultati preliminari. In: *Società Italiana di Selvicoltura ed Ecologia Forestale,* eds P. De Angelis, A. Macuz, G. Bucci and G. Scarascia, *Atti SISEF* **3**: 369-374*.*
- Xiao, C.W., Curiel Yuste, J., Janssens, I.A., Roskams, P., Nachtergale, L., Carrara, A., Sanchez, B.Y. and Ceulemans, R. (2003). Above- and belowground biomass and net primary production in a 73-year-old Scots pine forest. *Tree Physiology* **23:** 505-516.

2002

- Carnol, M., Hogenboom, L., Ewa Jach, A., Remacle, J. and Ceulemans, R. (2002). Elevated atmospheric CO2 in open top chambers increases net nitrification and potential denitrification. *Global Change Biology* **8:** 590-598.
- Ceulemans, R., Jach, M.E., Van De Velde, R., Lin, J.X. and Stevens, M. (2002). Elevated atmospheric CO2 alters wood production, wood quality and wood strength of Scots pine (*Pinus sylvestris* L) after three years of enrichment. *Global Change Biology* **8:** 153-162.
- Hendrickx, W. (2002). Effecten van biotische and abiotische factoren op de bodemrespiratie in een eiken- en dennenbos. *Graduate dissertation*, University of Antwerp.
- Janssens, I.A., Sampson, D.A., Curiel Yuste, J., Carrara, A. and Ceulemans, R. (2002). The carbon cost of fine root turnover in a Scots pine forest. *Forest Ecology and Management* **168:** 231-240.
- Karjalainen, T., Pussinen, A., Liski, J., Nabuurs, G.J., Erhard, M., Eggers, T., Sonntag, M. and Mohren, F. (2002). An approach towards an estimate of the impact of forest management and climate change on the European forest sector carbon budget: Germany as a case study. *Forest Ecology and Management* **162**(1) 87-103.
- Lindner, M., Sohngen, B., Joyce, L.A., Price, D.T., Bernier, P.Y. and Karjalainen, T. (2002). Integrated Forestry Assessments for Climate Change Impacts. *Forest Ecology and Management* **162**(1)117-136.
- Nabuurs, G.J., Pussinen, A., Karjalainen, T., Erhard, M. and Kramer, K. (2002). Increment changes in European forests due to climate change. *Global Change Biology* **8:** 1-13.
- Overdieck, D. (2002). Effects of elevated CO_2 concentration on stomatal conductance and respiration of beech leaves at darkness. *Botanical Congress in Freiburg,* Germany, Sept. 22-27, 2002.
- Pussinen, A., Karjalainen, T., Mäkipää, R., Kellomäki, S. and Valsta, L. (2002). Forest carbon sequestration and harvests in Scots pine stand under different climate and nitrogen deposition scenarios. *Forest Ecology and Management* **158:** 103-115.

2001

- Calfapietra, C., Gielen, B., Sabatti, M., De Angelis, P. Scarascia-Mugnozza, G. and Ceulemans, R. (2001). Growth performance of Populus exposed to "Free Air Carbon dioxide Enrichment" during the first growing season in the POPFACE experiment. *Annals of Forest Science* **58:** 819-828.
- Gielen, B., Calfapietra, C., Sabatti, M. and Ceulemans, R. (2001). Leaf area dynamics in a closed poplar plantation under free-air carbon dioxide enrichment. *Tree Physiology* **21:** 1245-1255.
- Janssens, I.A., Kowalski, A.S. and Ceulemans, R. (2001). Forest floor CO2 fluxes estimated by eddy covariance and chamber-based model. *Agricultural and Forest Meteorology* **106:** 61-69.
- Janssens I.A., Lankreijer, H., Matteucci, G., Kowalski, A.S., Buchmann, N., Epron, D., and 29 pther authors. (2001). Productivity overshadows temperature in determining soil and ecosystem respiration across European forests. *Global Change Biology*, **7**(2001) 269-278.
- Liski, J., Pussinen, A., Pingoud, K., Mäkipää, R. and Karjalainen, T. (2001). Which rotation length is favourable for carbon sequestration. *Canadian Journal of Forest Research* **31:** 2004-2013.
- Pingoud, K., Perälä, A.L., and Pussinen, A. (2001). Carbon dynamics in wood products. Mitigation and Adaptation Strategies for *Global Change Biology* **6:** 91-111.

- Sampson, D.A., Janssens, I.A. and Ceulemans, R. (2001). Simulated soil CO2 efflux and net ecosystem exchange in a 70-year-old Belgian Scots pine stand using the process model SECRETS. *Annals of Forest Science* **58:** 31-46.

9.3.2 Technical reports, papers and articles

- Begona Yuste Sanchez (2002). Measurements of height, DBH and root biomass in a coniferous-decideous forest in the Belgian campine region *Internal report*.
- Karjalainen, T., Zimmer, B., Berg, S., Welling, J., Schwaiger, H., Finér, L. and Cortijo, P. (2001). *Energy, Carbon and Other Material Flows in the Life Cycle Assessment of Forestry and Forest Products. Achievements of the Working Group 1 of the COST Action E9.*, European Forest Institute Discussion Paper 10, 68 pp.
- Maun K., (2001) Best Utilisation. *News of BRE-CTTC's work on Timber*. BRE, Watford UK.
- Maun K., (2002) Best Utilisation. *News of BRE-CTTC's work on Timber.* BRE, Watford UK
- Mefyque. (2002). Forest and Timber Quality in Europe – modelling and forecasting yield and quality in Europe. Annual Report (QLK5-CT-2001-00345), period 1, July 2001 – June 2002. DG XII Brussels, 168 pp
- Mefyque. (2003). Forest and Timber Quality in Europe – modelling and forecasting yield and quality in Europe. Annual Report (QLK5-CT-2001-00345) period 2, July 2002 – June 2003. DG XII Brussels, 293 pp
- Mefyque. (2004) Forest and Timber Quality in Europe – modelling and forecasting yield and quality in Europe. Annual Report (QLK5-CT-2001-00345) period 3, July 2003 – June 2004, 341 pp
- Evans, S.P., Randle, T., Henshall, P. and Taylor, P. (2002). A coupled soil-forest-atmosphere dynamic model for predicting evapo-transpiration (ETp) demands at the plot and landscape scales in the UK. *Report to Scotland and Northern Ireland Forum For Environmental Research (SNIFFER)*

9.3.3 Project publications

At the outset of the project a leaflet was produced outlining the concept of the project and introducing the partners. This leaflet was widely distributed in printed form, and has been available for electronic download from the project web-site. Am electronic copy of the leaflet can be found on the accompanying project CD. (PDF, 272KB)

The Forestry woodchain conference was primarily organised from within this project, though linking to The Compression wood (QLK5-2000-001) and Straight (QLK5-2000-00276) projects. The accepted abstracts were edited to produce a uniform format, printed and bound (173 pp).

Hard copies are available for purchase from Jenny Claridge, Forest Research, Alice Holt Lodge, Farnham, UK, GU10 4LH. An Electronic copy of the publication can be found on the project CD. (6.2 MB)

9.4 Database CD

See chapter 8, and separate CD.

9.5 Models

A number of models and sub-models have been used, developed, further developed, or created during the project. These models are available to interested parties, subject to restrictions governed by the various parent institutes. Many of the models have been published, or are in the process of publication.

The models include; Mefyque-Lite, Forest ETp, Weather generator, Cross-cut, Optimiser, EFISCEN. See also Chapter 5.